

# SMART & GREEN INTERFACES

*CONFERENCE  
PROGRAM AND  
BOOK OF ABSTRACTS*  
4 - 6 May, 2016 *Athens, Greece*



ARISTOTLE UNIVERSITY OF THESSALONIKI



Multiphase Dynamics Group  
Aristotle University of Thessaloniki

[www.sgic2016.com](http://www.sgic2016.com)

© 2016 *Smart and Green Interfaces Conference*

*All rights reserved. No part of this book may be reproduced or transmitted in any form or by any means, electronic, mechanical, photocopying or otherwise, without the prior written permission of the author.*

**PUBLISHER**      *Tziola Publications*

**EDITORIAL  
TEAM**              *Prof. Dr. Thodoris Karapantsios*

**CONTENT  
EDITOR**            *Mr. Dimitrios Ganitis  
Dr. Sotiris Evgenidis*

**INTERIOR  
DESIGN &  
COVER**            *Mr. Evangelos Kokkotzis*

*Thessaloniki April 2016*

*First Edition*

*Printed in Thessaloniki, Greece*

*CONFERENCE  
PROGRAM AND  
BOOK OF ABSTRACTS*  
*4 - 6 May, 2016* *Athens, Greece*

INDEX

PAGES

6-9

PAGES

10-15

PAGES

16-23

SECTION

1

SECTION

2

SECTION

3

FOREWORDS

Foreword Smart and Green Interfaces  
Conference 2016 ..... 8  
Foreword Annual Workshop of MP1106  
COST Action..... 9

GENERAL  
INFORMATION

Organization ..... 12  
Athens Information..... 14  
Cruise Information..... 14  
Top 8 Athens Attractions ..... 15

SCIENTIFIC  
PROGRAM

Invited & Oral Presentations  
1<sup>st</sup> DAY..... 18  
2<sup>nd</sup> DAY..... 19  
3<sup>rd</sup> DAY ..... 20  
Poster Presentations  
1<sup>st</sup> DAY..... 22  
3<sup>rd</sup> DAY ..... 23



SMART & GREEN INTERFACES CONFERENCE 2016

PAGES

24-31

PAGES

32-95

PAGES

96-149

SECTION

4

SECTION

5

SECTION

6

INVITED  
LECTURES

1 <sup>st</sup> DAY .....	26
2 <sup>nd</sup> DAY .....	28
3 <sup>rd</sup> DAY .....	30

ORAL  
PRESENTATIONS

1 <sup>st</sup> DAY	
Hall A .....	34
Bubbles .....	34
Hall B .....	39
Flow related processes .....	39
Hall A .....	43
Droplets on surfaces (1) .....	43
Hall B .....	50
Foams .....	50
Hall A .....	56
Adsorption on surfaces (1) .....	56
Hall B .....	61
New materials .....	61
2 <sup>nd</sup> DAY	
On Board .....	65
Gas handl./Adv. measurements .....	65
Feature lecture .....	70
3 <sup>rd</sup> DAY	
Hall A .....	72
Fluid-solid interactions .....	72
Hall B .....	78
Modified solid surfaces .....	78
Hall A .....	83
Droplets on surfaces (2) .....	83
Hall A .....	89
Adsorption on surfaces (2) .....	89
Hall B .....	93
Thermal processes .....	93

POSTER  
PRESENTATIONS

1 <sup>st</sup> DAY .....	98
Session 1 .....	98
3 <sup>rd</sup> DAY .....	124
Session 2 .....	124



---

SECTION

# 1

---

FOREWORDS

Foreword Smart and Green Interfaces Conference 2016.....	8
Foreword Annual Workshop of MP1106 COST Action .....	9

## FOREWORDS

### *Foreword Smart and Green Interfaces Conference 2016*

Continuing the successful tradition of the three previous Conferences (Prague 2013, Marseille 2014, Belgrade 2015), Athens/Piraeus (Greece) is hosting the 4<sup>th</sup> Smart and Green Interfaces Conference (SGIC 2016). More than 120 scientists from 18 different countries contributed their work to the Conference. Participants came not only from universities and research institutes but also from industry.

The main objective of SGIC 2016 is to display the current status of research on the physics, chemistry, physicochemistry, materials science and engineering of Smart and Green interfaces and relevant applications. Smart are called interfaces that can accomplish a technological task with high efficiency, adaptability and selectivity. Green are called interfaces that are eco-friendly (biodegradable, reusable, more durable, less energy consuming to produce). Food, pharmaceuticals, detergents, health care products, waste treatment, oil extraction are among the Smart and Green Interface applications that are dealt with in a number of presentations.

The conference is organized jointly with the MP1106 COST Action. This gives a broader flavor on the Smart and Green Interfaces subject bringing along colleagues that are involved in the formation, transport, manipulation and coating/protection of interfaces and who usually move at the border line of physical chemistry. Moreover, following the advancement in theoretical and experimental tools, new information is presented on matters such as the role of solid particles in the stability of soft interfaces, liquid encapsulation, spreading/wetting manipulated by external forces, micro/nano fluidics etc. SGIC 2016 expanded more than previous SGIC workshops to audience from the fields of fluid management, dispersed flows and heat transport in situations where interfaces are involved. Liquid penetration in capillaries and porous media, bubbles/drops flow with/without breakage or coalescence, spreading of liquid films and splashing of droplets on complex solids, often under non-isothermal conditions, were among the presented subjects.

The main topics covered by the conference are:

- Bubbles & drops interfaces
- Bubble & drop flow
- Interface related phenomena
- Free surfaces and compliant surfaces
- Complex liquids
- Dispersed systems
- Microfluidics
- Foams, emulsions
- Materials
- Diagnostics & Applications
- Interfaces in bioscience and biotechnology
- Modelling

This wealth of topics promoted the exchange of ideas and knowledge between scientists working on contemporary issues of interfacial phenomena.

We express our gratitude to all participating colleagues for their vivid contribution and we wish them a most fruitful and pleasant stay in Athens/Piraeus.

*The SGIC2016 Organizing Committee  
Athens, May 2016*

*Foreword Annual Workshop of MP1106 COST Action*

Welcome to the final meeting of MP1106 COST Action. After a very busy period of 4 years, full of activities and tasks, MP1106 is about to switch-off engines. More than 450 colleagues, coming from academia and industry, are members of the Action. It has been a pleasure and an honor to chair the Action and to share with its members exciting moments of scientific and networking achievements. The rich record of MP1106 proves beyond doubt that the Action has been a fertile ground for outstanding science, networking and societal accomplishments.

As regards science, MP1106 COST Action has led to:

- a common definition and approach on the fundamentals, materials, diagnostics and technologies related to Smart and Green interfaces applied to Industrial/Environmental/Biomedical Applications.
- identification of current knowledge gaps and detection of ways to overcome existing gaps.
- identification of Thematic Clusters horizontally across the four Working Groups in response to EU/Horizon 2020 Research Calls.

As regards networking, MP1106 COST Action has led to:

- an efficient continuation for interaction and networking both inside of the Action as well as with the external partners of the Action towards Pan-European and multidisciplinary platform to support the realization of the opportunities in the field of Smart and Green interfaces.
- Transfer of knowledge within the partners, exchange of persons, facilities, samples, sharing data and knowledge.
- Establishment of interdisciplinary links between physicists, chemists, material scientists, engineers and mathematicians for manifold approach to complex problems identified within the WGs.
- Development of appropriate specific activities for ESRs.
- Identification of appropriate funding schemes for future joint projects.

As regards society, MP1106 COST Action has led to:

- A successful outreach program towards the general public through a continuously updated website
- Concrete responsibilities and duties within the Action to improve gender balance in science presentations and Short Term Scientific Missions
- Interaction with other research programs: Identification of possible other projects /groups / Actions.

Overall, MP1106 COST Action has been exceptionally effective in:

- coordinating science activities among teams working on fundamental and applied problems on Smart and Green Interfaces
- promoting the dissemination of results and the interaction with other communities
- organizing efforts for future joint training and research projects.
- supporting gender balance and the involvement of Early Stage Researchers

***Thank you for being part of MP1106 COST Action!***

*Thodoris Karapantsios, Professor  
Chair of MP1106 COST Action  
Athens, May 2016*



# 2

---

GENERAL INFORMATION

Organization .....	12
Athens Information.....	14
Cruise Information .....	14
Top 8 Athens Attractions .....	15

# ORGANIZATION

*CHAIR  
OF THE  
ACTION*

*Prof. Dr. Thodoris Karapantsios*

*VICE CHAIR  
OF THE  
ACTION*

*Prof. Libero Liggieri*



SCIENTIFIC  
COMMITTEE

*Thodoris Karapantsios, Aristotle Univ., Thessaloniki, Greece*

*Victoria Dutschke, Univ. Twente, The Netherlands*

*Libero Liggieri, CNR, Genova, Italy*

*Norman McMillan, Drop Technology Ltd., Ireland*

*Reinhard Miller, Max-Planck Institute, Golm, Germany*

*Victor Starov, Univ. Loughborough, United Kingdom*

LOCAL  
ORGANIZING  
COMMITTEE

*Thodoris Karapantsios, School of Chemistry, AUTH*

*Margaritis Kostoglou, School of Chemistry, AUTH*

*John Lioumbas, School of Chemistry, AUTH*

*Maria Petala, School of Chemistry, AUTH*

*Sotiris Evgenidis, School of Chemistry, AUTH*

## GENERAL INFORMATION

# A<sup>THENS</sup> A<sup>INFORMATION</sup>

Athens is the capital and largest city of Greece. It's one of the world's oldest cities, with its recorded history spanning around 3,400 years. Classical Athens was a powerful city-state and a center for the arts, learning and philosophy, home of Plato's Academy and Aristotle's Lyceum.

The history of the city perfectly blends with its modern style, since the city is filled with numerous monuments from the Classical Era, the Byzantine and Ottoman, each and every one perfectly incorporated into the daily lives of its people.

Athens is a city of different aspects. A walk around the famous historic triangle (Plaka, Thission, Psyri) the old neighborhoods, reveal the coexistence of different eras. Old mansions, well-preserved ones and other worn down by time. Luxurious department stores and small intimate shops, fancy restaurants and traditional taverns. All have their place in this city.

# C<sup>RUISE</sup> C<sup>INFORMATION</sup>

Apart from exploring Athens, the capital of Greece, participants have the opportunity to enjoy a cruise through Ydra, Poros and Aigina. There is no better chance for relaxation during the conference than this cruise, which will take you through some of the most picturesque and beautiful islands Greece has to offer, all under the Mediterranean sun.

# 8 TOP ATHENS ATTRactions

## NATIONAL GARDEN

In the heart of Athens, the National Garden provides a green oasis for sunny afternoon trips. The Royal Garden has a private garden for the Royal Palace, which is now the Parliament Building. The Public Garden was established in 1923.

## ACROPOLIS MUSEUM

A main stop on any Athens tour is the New Acropolis Museum, which resides near the base of the hill overlooking the city. Permanent exhibitions here include the Parthenon Frieze, Athena statue, Color the Peplos Kore, Parthenon Gallery and Athena Nike.

## NATIONAL ARCHAEOLOGICAL MUSEUM

For visitors who love art exhibitions, there is no better place to visit in Greece than the National Archaeological Museum. Multiple collections can be found here from contemporary artists all the way back to antiquity. The museum also has a large collection of artwork dating back to the Neolithic Age. Over thirty rooms, sculptures from every century can be viewed including ancient Kouros Egyptian sculptures.

## SYNTAGMA SQUARE

A major point of interest for any traveler to Athens is the Syntagma Square. The most famous aspect of Syntagma is the changing of the guards by the Evzones in front of the Tomb of the Unknown Soldier. The Hellenic Parliament Building is located here as well as various buses, trolleys and tram stops.. It's also the site of various political functions, and it was also at this square that the Military Junta government was overthrown in 1974.

## TEMPLE OF OLYMPIAN ZEUS

The Temple of Olympian Zeus is known as the largest temple in Greece. The massive ancient complex took nearly seven centuries to complete. Building originally began in 515 BC by order of Peisistratos, The temple stands today mostly as a reminder of Greek history, but only 15 of 104 huge columns remain. The columns each rise 17 meters (57 feet) into the air and once surrounded a cella where two large statues were once placed.

## ANCIENT AGORA

Located to the northwest of the Acropolis, the ancient Agora of Athens was once a marketplace and civic center. The people gathered here to browse all kinds of commodities. It was also a place to meet others and talk about politics, business, current events and the nature of the universe and divine. The ancient Greek democracy can actually be traced to this ancient spot. It's a wonderful area to look at the cultural beginnings of Athens.

## PLAKA DISTRICT

One of the most popular tourist attractions in Athens is the Plaka District, which resides under the Acropolis and spreads out to Syntagma. This village is almost like an island within the city, and it's the perfect way to experience authentic Greek culture. The area is quite private and boasts truly unique scenery with several cafes, ancient trees, green leaf canopies and stone walkways.

## PARTHENON

The Parthenon is located on the Acropolis on a hill that overlooks Athens. The temple was built to honor the goddess Athena Parthenos, the patron of Athens, to thank her for protecting the city during the Persian Wars. Originally designed by the famous sculptor Phidias, the Parthenon originally held all kinds of treasures, but the main attraction was a huge statue of Athena that was made out of chryselephantine also known as elephant ivory and gold. The Parthenon dates back to 447 BC, and it was actually built over another temple that is often referred to as the Pre-Parthenon.



# 3

---

SCIENTIFIC PROGRAM

Invited & Oral Presentations	
1 <sup>st</sup> DAY .....	18
2 <sup>nd</sup> DAY .....	19
3 <sup>rd</sup> DAY .....	20
Poster Presentations	
1 <sup>st</sup> DAY .....	22
3 <sup>rd</sup> DAY .....	23

# SCIENTIFIC PROGRAM

Tuesday, May 3th 2016

18:00-20:00 Welcome - Reception / Registration

Wednesday, May 4th 2016

8:00 Registration

9:00-9:10 Welcome - Opening

9:10-10:00 **Miller Reinhard** **Invited Lecture (Chair: L. Liggieri)**  
Adsorption of surfactant and proteins at liquid interfaces – Past, present and future

	<i>Hall A: Bubbles (Chair: H. Kuerten)</i>	<i>Hall B: Flow related processes (Chair: A. Papathanasiou)</i>
10:00-10:15	<b>Jawala Jan</b> A correlation between kinetics of bubble attachment to solids and flotation efficiency	<b>Sosnowski Tomasz</b> New engineering strategies for improvement of drug delivery by aerosol inhalation
10:15-10:30	<b>Oikonomidou Ourania</b> Saturation pressure effect on the size of bubbles formed due to liquid decompression	<b>Palero Virginia</b> Study of mixing in a small-scale model reactor by a Mach-Zehnder interferometer
10:30-10:45	<b>Orvalho Sandra</b> Effect of the approach velocity and bubble size on the critical concentration for coalescence inhibition in electrolyte solutions	<b>Guido Stefano</b> Flow-induced morphology evolution of nano-emulsions
10:45-11:00	<b>Krzac Marcel</b> Influence of bubble wake development on bubble motion in surfactant solutions	<b>Trabi Christophe</b> Capillary penetration into inclined circular glass tubes

11:00-11:30 Coffee break

	<i>Hall A: Droplets on surfaces (1) (Chair: D. Vollmer)</i>	<i>Hall B: Foams (Chair: S. Caserta)</i>
11:30-11:45	<b>Brutin David</b> Evaporative instabilities in sessile drops of ethanol on heated substrates: computer simulations	<b>Langevin Dominique</b> On the use of shear rheology to formulate very stable foams. Example of a lamellar phase containing SDS, hexanol and brine
11:45-12:00	<b>Brabcova Zuzana</b> Axisymmetric spreading of droplets into films using liquid dielectrophoresis	<b>Nastasa Viorel</b> Sclerosing foams assessment in view of their use in sclerotherapy
12:00-12:15	<b>Muradoglu Metin</b> The effects of viscoelasticity on drop impact and spreading on a solid surface	<b>Arjmandi Tash Omid</b> Free drainage of non-Newtonian foams
12:15-12:30	<b>McHale Glen</b> Dewetting dynamics from a non-equilibrium dielectrowetted thin film into a single macroscopic droplet	<b>Pugh Robert</b> Particle Stabilized Three-Phase Foam Systems in the Flotation Process
12:30-12:45	<b>Starov Victor</b> Wetting and spreading: recent developments	<b>Santini Eva</b> Interfacial Properties and Bubble/Drop Coalescence in The Stability of Emulsions and Foams
12:45-13:00	<b>Diddens Christian</b> Modeling the evaporation of sessile multi-component droplets	<b>Haffner Benjamin</b> Stability of foams containing fibres

13:00-14:10 Lunch break

14:10-15:00 **Papathanasiou Athanasios** **Invited Lecture (Chair: T. Gambaryan-Roisman)**  
Modelling of droplet dynamics on complex surfaces

	<i>Hall A: Adsorption on surfaces (1) (Chair: R. Miller)</i>	<i>Hall B: New materials (Chair: V. Koutsos)</i>
15:00-15:15	<b>Arabadzhieva Dimitrinka</b> Two-antennary oligoglycines: Interfacial layer properties on aqueous and solid surfaces	<b>Cabrero-Vilchez Miguel</b> Fabrication of superhydrophobic surfaces on galvanized steel
15:15-15:30	<b>Cristofolini Luigi</b> XPCS and Discrete Fourier Microscopy reveal details on the dynamics of mixed layers formed by hydrophobic/hydrophilic silica nanoparticles in phospholipid films	<b>Ersoz Mustafa</b> Synthesis and functionalization of different forms of graphene for various applications
15:30-15:45	<b>Mileva Elena</b> Aqueous solutions of surfactant mixtures: Hexadecyltrimethylammonium chloride and pentaethylene glycol monododecyl ether	<b>Julia López Alex</b> Encapsulation of phase change materials to obtain novel switchable optical properties
15:45-16:00	<b>Fernandez-Peña Laura</b> Rhamnolipids: a promising alternative to conventional surfactants from polyelectrolyte-surfactant hair-care formulations	<b>Meriç Sureyya</b> Synthesis of magnetite pumice composite and its application in oxidation processes for removal of red dye

16:00-17:00 Poster session 1 / Coffee break

17:00-18:30 Management Committee

# SMART & GREEN INTERFACES CONFERENCE 2016

Thursday, May 5th 2016  
ALL DAY CRUISE / SESSIONS ONBOARD

8:40-9:30	<b>Trybala Anna</b>	<b>Invited Lecture (Chair: D. Langevin)</b> Interactions of foam with porous materials
<i>Gas handling/Advanced measurements</i> (Chair: M. Antoni)		
9:30-9:45	<b>Vollmer Doris</b>	CO <sub>2</sub> capture by superomniphobic membranes
9:45-10:00	<b>Li Puma Gianluca</b>	Ultrafast photochemical transformations of chemical and biological species in microcapillary films photo-reactors
10:00-10:15	<b>Staicu Angela</b>	Studies on the laser induced emission of pendant droplets of dye water solutions containing TiO <sub>2</sub> nanoparticles
10:15-10:30	<b>McMillan Norman</b>	Metrological fundamentals for 'true' nanovolume spectroscopy
10:30-18:00	Visit to islands / Lunch break	
18:00-18:50	<b>Caserta Sergio</b>	<b>Invited Lecture (Chair: M. Pascu)</b> Smart cell dynamics: Phenomenological investigation of cell migration in 2D and 3D substrata
<i>Feature lecture</i> (Chair: M. Pascu)		
18:50-19:10	<b>Balestra Costantino</b>	Oxygen breathing doesn't add benefit compared to whole body vibration on the reduction of post-dive vascular gas emboli
20:30	Gala dinner (Flisvos Marina)	

# SCIENTIFIC PROGRAM

Friday, May 6th 2016

9:10-10:00	<b>Smoukov Stoyan</b>	<b>Invited Lecture (Chair: S. Guido)</b> Unconventional routes to smart materials		
		<i>Hall A: Fluid-solid interactions</i> (Chair: Z. Brabcova)		<i>Hall B: Modified solid surfaces</i> (Chair: M. Ersoz)
10:00-10:15	<b>Liuzzi Roberta</b>	The importance of fluids microstructure in the penetration process for transdermal applications	<b>Stoyanov Simeon</b>	An environmentally benign antimicrobial nanoparticle based on a silver-infused lignin core
10:15-10:30	<b>Gambaryan-Roisman Tatiana</b>	Simultaneous imbibition and evaporation of liquids in model textured substrate	<b>Mirzaeian Mojtaba</b>	Effect of interfacial processes on the electrochemical properties of carbon based electrodes for supercapacitor applications
10:30-10:45	<b>Koutsos Vasileios</b>	Semicrystalline polymers on surfaces: droplets and thin films	<b>Selcuk Huseyin</b>	Copper doping on TiO <sub>2</sub> nanoparticles for development of self-cleaning and anti-bacterial cotton fabric
10:45-11:00	<b>Sicignano Luca</b>	Microfluidics investigation of cluster aggregation in the Buckwald-Hartwig amination reaction	<b>Kiwi John</b>	Self-cleaning processes by polymer/textiles sputtered with semiconductors under sunlight & mild environmental conditions
11:00-11:15	<b>Kumar Abhijeet</b>	Using streaming potential measurements to probe cationic vesicle permeation and deposition on anionic porous substrates	<b>Zhang Zhenyu</b>	Nanotribological properties of biocompatible polyelectrolyte brushes
11:15-11:45	<b>Coffee break</b>			
		<i>Hall A: Droplets on surfaces (2)</i> (Chair: C. Trabi)		<i>Hall B: Cluster meeting (Nanoparticles - Nanostructures)</i> (Chair: M. Ersoz / V. Koutsos)
11:45-12:00	<b>Chamakos Nikolaos</b>	Modeling of droplet mobility on bio-inspired asymmetrically structured substrates		
12:00-12:15	<b>Kalić Karolina</b>	“Kerberos”: A three camera headed (X-Y-Z) centrifugal device for studying liquid spreading on solid substrates under the influence of varying body forces		
12:15-12:30	<b>Rednikov Alexey</b>	Computation of contact angles for perfectly wetting sessile drops evaporating into vapor on substrates of finite thermal conductivity		
12:30-12:45	<b>Pascu Mihail</b>	Modification of wetting properties of phenothiazines water solutions exposed to laser radiation in hypergravity conditions		
12:45-13:00	<b>Perrin Lionel</b>	Effect of silver nanoparticles on the wetting and the evaporation of water sessile droplets for different substrates		
13:00-14:10	<b>Lunch break</b>			
14:10-15:00	<b>Mucic Nenad</b>	<b>Invited Lecture (Chair: E. Mileva)</b> Adsorption of ionic surfactants at water/alkane interfaces		
		<i>Hall A: Adsorption on surfaces (2)</i> (Chair: V. Starov)		<i>Hall B: Thermal processes</i> (Chair: D. Brutin)
15:00-15:15	<b>Mickaël Antoni</b>	Mass transfer and microstructures formation at water paraffin oil interfaces	<b>Khalili Sadaghiani Abdolali</b>	Flow boiling on microstructured aluminum surfaces in high aspect ratio microchannel
15:15-15:30	<b>Basarova Pavlina</b>	Atypical behaviour of aqueous solutions of short-chain alcohols in multi-phase systems	<b>M.C. Vlachou</b>	Flow boiling incipience in macro-channels: Working conditions that maximize heat removal
15:30-15:45	<b>Ritu Ritu</b>	Investigating the mass transfer and microstructures formation at liquid/liquid interfaces using FT-IR imaging spectroscopy	<b>Motezakker Ahmad Reza</b>	Nucleate Pool Boiling Heat Transfer on pHEMA Coated Surfaces
15:45-17:00	Poster session 2 / Coffee break			
17:00-17:30	<b>Closure</b>			



Wednesday, May 4th, 2016 (16:00-17:00)

Europe Foyer: Poster session 1

- 1 Investigating the Physical-Chemistry of Adsorption Layers, Liquid Films, Foams and Emulsions by Microgravity Experiments  
*L. Liggieri, F. Ravera, E. Santini, M. Ferrari, S. Llamas, P. Pandolfini, G. Loglio, R. Miller, J. Kraegel, A. Javadi, M. Karbaschi, V. Kovalchuk, B. Noskov, L. Cristofolini, D. Orsi, D. Clausse, I. Pezron, T. Karapantsios, J. Ferri, Y. Yamashita, M. Schmitt, M. Antoni.*
- 2 A Front-Tracking Method for Direct Numerical Simulation of Evaporation Process in a Multiphase System  
*M. Milieška, R. Kěželis*
- 3 Influence of enzymatic hydrolysis on dilatational properties of pumpkin (*Cucurbita pepo* sp.) seed protein isolate  
*S. Bučko, J. Katona, L. Petrović, R. Miller, N. Mucic*
- 4 Biodegradable aqueous foams based on xanthan and gellan gums  
*M. Krzan I, E. Jarek, H. Petkova, E. Santini, V. Ungalanthan, M. Lofti, A. Javadi, E. Mileva, P. Warszynski, R. Todorov, F. Ravera, L. Liggieri, R. Miller, D. Exerowa*
- 5 Influence of n-alkanol chain length on local and terminal velocities of rising bubbles  
*M. Krzan*
- 6 Kinetics of bubble coalescence at surfaces of different liquids –influence of external disturbances and size of the liquid films formed  
*A. Wiertel, J. Zawala, K. Malysa*
- 7 Influence of enzymatic hydrolysis on functional properties of pumpkin (*Cucurbita pepo* sp.) seed protein isolate  
*S. Bučko, J. Katona, Lj. Popović, L. Petrović, J. Milinković*
- 8 Heat Transfer Coefficient Of An Oscillating Meniscus  
*I. Malavasi, L. Pietrasanta, D. Fioriti, M. Mamei, N. Miche, M. Marengo*
- 9 Interfacial slow dynamics from the micro- to the nanoscale by a combination of real and momentum  
*D. Orsi, L. Liggieri, F. Ravera, L. Cristofolini*
- 10 Comparative Framework for Binder Formulation Development for Inkjet-based Three Dimensional Metal Printing  
*J.K. Ferri, A.D.Cramer, S. Buczek*
- 11 Highly subcooled flow boiling in macro-channels: Effect of channel's height and orientation  
*M.C. Vlachou, J.S. Lioumbas, T.D. Karapantsios*
- 12 Study of coarsening and coalescence for dry foams in 2D  
*A. Cagna, C. Honorez, W. Drenckhan*
- 13 Experimental Determination of Thin Film Drainage Around Single Foam Bubbles  
*A.T. Zamanis, M. Kostoglou, S.P. Evgenidis, T.D. Karapantsios*
- 14 Dynamics of adsorption of ionic surfactants at the water/air interface with hexane vapour in the gas phase  
*T.Kairaliyeva, R. A. Campbell, N. Mucic, A. Javadi, J. Krägel, E.V. Aksenenko, V.B. Fainerman, S.A. Aidarova, R. Miller*
- 15 Determination and comparison of size and stability of Nanobubbles produced by two different generators  
*E.D.Michailidi, R.I.Kosheleva, A.C.Mitropoulos*
- 16 Flow boiling of self-wetting 1- butanol/water mixture in a square microchannel  
*P. Vasileiadou, Khellil Sefiane, T.G. Karayiannis*

## SCIENTIFIC PROGRAM

- 17 VOC free nanoemulsions of aminopropylaminoethylpolysiloxane prepared by phase inversion emulsification with C13 ethoxylated surfactants of various HLB  
*C. G. Koukiotis, G. Kokkinos, T. D. Karapantsios*
- 18 Study of Void Fraction Fluctuations Dependence on Bubble Size through Experimental and Simulated Electrical Signal Analysis  
*S. Evgenidis, M. Kostoglou, T. Karapantsios*
- 19 Velocity of rising air bubbles in aqueous beta-lactoglobulin solutions at different pH and salt concentrations  
*V. Ulaganathan, G. Gochev, C. Gehin-Delval, D.Z. Gunes, M.E. Leser, R. Miller*
- 20 Application of Electrical Resistance Tomography and Differential Pressure Method for Low Void Fraction Values Determination in Bubbly Flow of Sub-millimeter Bubbles  
*S. Evgenidis, P. Zikou, T. Karapantsios*
- 21 Removal of polycyclic aromatic hydrocarbons in aqueous solution by electrochemical oxidation  
*M. Brienza, G. Gallios, E. Vardaka, I. Voinovschi, D. Kupka, M. Vaclavikova*
- 22 Self-assembly by multi-drop evaporation of carbon-nanotube and graphene-oxide-platelets droplets on a glass substrate  
*C.S. Iorio, C. Minetti, Hatim Machrafi*
- 23 Confined tube flow of elastic low viscosity emulsions  
*S. Caserta, V. Preziosi, G. Tomaiuolo, S. Guido*

*Friday, May 6th, 2016 (15:45-17:00)*

*Europe Foyer: Poster session 2*

- 1 The Visualization of Multiphase Plasma Jet During Plasma Processing of Dispersed and Solid Ceramics Materials  
*R. Keželis, M. Milieška, V. Grigaitienė, M. Aikas*
- 2 The Numerical And Experimental Research Of Dynamic And Thermal Properties of In-flight Particles In Plasma-chemical Reactor  
*M. Milieška, R. Keželis*
- 3 Definition of Fundamental Parameters for Modelling of a New Thin-film Photocatalytic Reactor to Remove Sulfamethoxazole Antibiotic  
*C.B. Ozkal, Z. Frontistis, D. Mantzavinos, S. Meric*
- 4 Photocatalytic hydrogen evolution from water by cadmium based photocatalyst  
*M. Ersoz, E. Aslan, I. Hatay Patir, M. Kus*
- 5 Room-temperature Ferromagnetism in Hydrothermally Synthesized Mn<sup>2+</sup> Doped Titania Nanotubes  
*Z. Šaponjić, M. Vranješ, J. Kuljanin Jakovljević, N. Abazović, Z. Konstantinović, A. Pomar, M. Stoiljković, M. Čomor, A. Pavlović*
- 6 Zirconia/ Polyaniline Nanocomposite: Synthesis, Characterization and Applicability as Photocatalyst  
*M.I. Čomor, M.V. Carević, N.D. Abazović, M.B. Radoičić, T.D. Savić*
- 7 Dynamic Surface Activity of the Pulmonary Surfactant (PS) – Graphene Oxide (GO) System  
*T. R. Sosnowski, M. Mazurkiewicz-Pawlicka, A. Malolepszy, L. Stobiński*
- 8 Mass Recovery Kinetics of Heated Carbonated Glass Fabric in Atmosphere with Different Humidity and CO<sub>2</sub> Concentration  
*G. Bajars, E. Pentjuss, A. Lulis, J. Gabrusenoks, J. Balodis*
- 9 Investigation of Electrophoretically Deposited Metal Oxide and Reduced Graphene Oxide Composite as Anode Materials for High Performance Lithium Ion Batteries  
*G. Bajars, K. Kaprans, J. Mateuss, A. Dorondo, G. Kucinskis, J. Kleperis*

- 10 Superabsorbent conducting hydrogel composites produced from Semi-IPN poly(acrylamide-co-maleic acid) with pH sensitivity for Methylene Blue dye removal  
*S. Meriç, B. Tasdelen, D. İz. Çiğçi*
- 11 Silver Loss From Potable Water Consumed In The International Space Station  
*M. Petala, V. Tsiridis, I. Mintsouli, E. Darakas, M. Kostoglou, S. Sotiropoulos, T. D. Karapantsios*
- 12 Crystal growth of biological macromolecules using ultrasonic irradiation  
*E.D. Chrysina, A. Derpogosian, A. Papagiannopoulos, S. Pispas, P. Zoumpoulakis, G. Heropoulos*
- 13 Theoretical considerations and analysis of experiment for a bubble growing on a hot plate during decompression in microgravity  
*M. Kostoglou, T.D. Karapantsios, A. Nedou*
- 14 Amphiphobic coatings for protection in seawater environment  
*F. Cirisano, M. Ferrari, A. Benedetti, L. Liggieri, F. Ravera, E. Santini*
- 15 Hierarchically macro/mesoporous TiO<sub>2</sub> monoliths derived from particle laden foam  
*D. Zabięaj, M. T. Buscaglia, V. Buscaglia, E. Santini, M. Ferrari, L. Liggieri, F. Ravera*
- 16 Fluorine-free Oleophobic coatings deposition and characterization for application in housekeeping  
*A. Plomaritis, I. Tucker, T. D. Karapantsios*
- 17 Fluorapatitenanopowdersynthesed by surfactant-assisted microwave method under isothermal condition  
*V. Stanić, B. K. Adnadjević, S. I. Dimitrijević, M. N. Mitrić, B. Jokić, B. B. Zmejkovski, V. Živković-Radovanović*
- 18 Surface Contribution to Lithium Storage in Anatase TiO<sub>2</sub> Nanotube Arrays  
*N. Cyjetičanin, M. Bratić, D. Jugović, M. Mitrić*
- 19 A prototype carousel-type device for studying boiling in porous matrix at microgravity conditions  
*J. Lioumbas, T. D. Karapantsios*
- 20 Pre-processing Based Approach to Study the Water-Biofilm-Pipe Interface  
*E. Ramos-Martínez, M. Herrera, J. Izquierdo, R. Pérez-García, M. Petala, E. Darakas, V. Tsiridis*
- 21 Development of New Device for Measuring the Thermal Conductivity of Polymeric nanocomposite Materials  
*M. Gannoum, M. Kostoglou, R. Gonzalez-Cinca, T. D. Karapantsios*
- 22 Micro-structured Porous Surfaces for Highly Efficient Flow Boiling Applications  
*C. Argiropoulos, S. Sklari, M. Kostoglou, T. Karapantsios*
- 23 BaTi<sub>1-x</sub>Sn<sub>x</sub>O<sub>3</sub> (x = 0, 0.05 and 0.1) ceramics with improved dielectric properties obtained by sintering in different atmospheres (air and Ar)  
*A. Garaj, S. Marković, N. Cyjetičanin*
- 24 Adsorption in conjunction with SAXS under the influence of a rotational field  
*R.I. kosheleva, E.P. Favvas, T.D Karapantsios, A.Ch. Mitropoulos*



---

SECTION

# 4

---

INVITED LECTURES

1 <sup>st</sup> DAY .....	26
2 <sup>nd</sup> DAY .....	28
3 <sup>rd</sup> DAY .....	30

Adsorption of Surfactant and Proteins at Liquid Interfaces – Past, Present and Future

**Reinhard Müller<sup>1</sup>**, (1)Max Planck Institute of Colloids and Interfaces, 14424 Potsdam/Golm, Germany, [miller@mpikg.mpg.de](mailto:miller@mpikg.mpg.de); in close cooperation with V.B. Fainerman<sup>2</sup>, V.I. Kovalchuk<sup>3</sup>, E.V. Aksenenko<sup>4</sup>, L. Liggieri<sup>5</sup>, F. Ravera<sup>6</sup>, G. Loglio<sup>7</sup>, V. Ulaganathan<sup>8</sup>, T. Kairaliyeva<sup>1,6</sup>, A.A. Sharipova<sup>8</sup>, S.B. Aidarova<sup>8</sup>, N. Mucic<sup>9</sup>, J. Krägel<sup>1</sup>, M. Karbaschi<sup>1,7</sup>, G. Gochev<sup>3,8</sup> and A. Javadi<sup>1,9</sup>, (2) Donetsk Medical University, 16 Ilych Avenue, 83003 Donetsk, Ukraine; (3) Institute of Bio-Colloid Chemistry, Vernadsky str. 42, 03142 Kyiv (Kiev), Ukraine; (4) Institute of Colloid Chemistry and Chemistry of Water, 03680 Kyiv (Kiev), Ukraine; (5) CNR – Institute for Energetics and Interphases, 16149 Genoa, Italy; (6) Kazakh National Technical University, Almaty, Kazakhstan; (7) School of Pharmacy, University of California, San Francisco, 94158, USA; (8) Institute of Physical Chemistry, Bulgarian Academy of Sciences, Sofia, Bulgaria; (9) Chemical Engineering Department, University of Tehran, Tehran, Iran

Surface active agents are an important group of compounds because of their amphiphilicity that makes them adsorb and change the properties of interfaces. A tailored use of such components in respective applications requires accurate knowledge of their adsorption layer properties. In addition to the fundamental thermodynamic parameters of adsorption, the non-equilibrium interfacial properties are very essential, such as the mechanism of adsorption, and the response of such layers to external perturbations, i.e. the dilational visco-elasticity. In many applications it turned out that single surface active compounds are unable to modify the interfacial properties in the required way. Instead of trying to find the super-surfactant that can solve all problems alone, surface scientists started to combine low-molecular weight surfactants with each other or with high molecular weight polymers and proteins in order to optimize systems and technologies.

For many surfactants knowledge on the thermodynamic properties like adsorbed amounts and changes of interfacial tension as a function of bulk concentration is available for quite a while, for example pioneered by people like von Szyszkowski [1] and Frumkin [2]. A quantitative understanding of the adsorption dynamics, however, started much later, mainly with the work of Ward and Tordai in 1946 [3]. Their theory of a diffusion controlled adsorption mechanism is the basis now for almost all models describing the adsorption kinetics of surfactants and proteins at liquid interfaces. Even younger is the theme of the visco-elasticity of interfacial layers, which was introduced in the forties of the 20<sup>th</sup> century by Levich, and names like Lucassen and van den Tempel [4] have to be mentioned here first.

Presently, we can say that there is quite a good knowledge on the thermodynamics, kinetics and relaxation behavior of surfactants but there is still need for a quantitative understanding of proteins and their mixtures with surfactants when adsorbed at water/air and water/oil interfaces.

This contribution tries to give a survey of the history of the theoretical description of the thermodynamics of adsorption, the adsorption mechanisms and the modeling of interfacial relaxations after interfacial external perturbations. In parallel to the theoretical basis the experimental side will be discussed, including dynamic surface and interfacial tensions, as well as studies with oscillating drops and bubbles as methods for measuring the dilational visco-elasticity of liquid interfacial layers. Further experimental methods like interfacial ellipsometry, x-ray and neutron reflection, second harmonic generation or sum frequency generation are only mentioned briefly. In the end a summary of open questions will be presented and their practical relevance discussed.

**References**

- [1] B. von Szyszkowski, Experimentelle Studien über kapillare Eigenschaften der wäßrigen Lösungen von Fettsäuren, *Z. Phys. Chem. (Leipzig)* 64 (1908) 385-414.
- [2] A. Frumkin, *Z.Phys.Chem.Leipzig*, Die Kapillarkurve der höheren Fettsäuren und die Zustandsgleichung der Oberflächenschicht, 116 (1925)466-484.
- [3] A.F.H. Ward and L. Tordai, Time-dependence of boundary tensions of solutions, *J. Phys. Chem.* 14 (1946) 453-461.
- [4] J. Lucassen and M. van den Tempel, Dynamic measurements of dilational properties of a liquid interface, *Chem. Eng. Sci.* 27 (1972) 1283-1291.

---

**Modelling Of Droplet Dynamics On Complex Surfaces**

---

*Athanasios G. Papathanasiou, School of Chemical Engineering, National Technical University of Athens Athens, 15780, Greece, pathan@chemeng.ntua.gr.*

---

We present a continuum level approach for simulating the dynamics of droplets on geometrically patterned surfaces. The proposed scheme provides an efficient way of handling the presence of multiple contact lines, the position and number of which are often unknown *a priori* and may also change dynamically. Interestingly enough, for complex surfaces, we enable the prediction of both static and dynamic contact angle hysteresis, given the specific geometrical characteristics of the substrate, while we are able to demonstrate the increased mobility of droplets in ‘fakir’ state as compared to droplet in Wenzel wetting states in line with previous experimental observations.

The main feature of our approach is that, by formulating the interfacial stress balance augmented with a disjoining pressure term, we enable the computation of multiple and reconfigurable three phase contact lines (TPL) bypassing the tedious implementation of the Young’s contact angle, or boundary conditions of the Cox-Voinov type at each TPL. So far, such computations have been performed utilizing fine scale models, however the required computational power is high, and we could even say prohibitive for droplets with relatively large size.

We focus our study on hydrophobic surfaces and examine the effect of the geometrical characteristics of the solid surface. It is shown that the presence of air inclusions trapped in the micro-structure of a hydrophobic substrate (Cassie–Baxter state) result in the decrease of contact angle hysteresis and in the increase of the droplet migration velocity in agreement with experimental observations for super-hydrophobic surfaces. Moreover, we perform 3D simulations which are in line with the 2D ones regarding the droplet mobility and also indicate that the contact angle hysteresis may be significantly affected by the directionality of the structures with respect to the droplet motion.

---

**Interactions Of Foam With Porous Materials**

---

*A.Trybala, O. Arjmandi-Tash, N. Kovalchuk, V. Starov, Department of Chemical Engineering, Loughborough University, UK, A.Trybala@lboro.ac.uk*

In a number of applications foaming liquids are mixtures of surfactants and polymers. These mixtures frequently show a non-Newtonian power law shear thinning behaviour [1-3]. Surprisingly drainage of foams built up by non-Newtonian liquids does not attract enough attention in spite of wide use of such foams. In a number of applications foams are deposited on porous substrates: hair, skin, textile, sponges and so on, however even the basics of the interaction of Newtonian and non-Newtonian foams with porous materials have never been thoroughly investigated: there is only one publication in the area where a complex interaction of foams with porous substrates was investigated [4].

The current state of drainage of foams built up by non-Newtonian liquids and the studies on drainage kinetics will be presented. It was found [4] that the kinetics of foam drainage on a porous substrate in the case of foam built up by a Newtonian liquid depends on three dimensionless numbers related to the properties of both foam and a porous substrate, and initial liquid volume fraction inside the foam. The result showed that there are three different regimes of the drainage process from foam [4]: (a) rate of imbibition into the porous substrate is faster than the rate of drainage from the foam; (b) a comparable rate of drainage and imbibition; (c) rate of imbibition is slower as compared with the rate of drainage. In the latter case the liquid volume fraction at foam/porous substrate interface reaches maximum limiting value at the moment  $t_m$  and a free liquid layer starts to form on the surface of the porous substrate.

However, in the end, the free liquid layer is sucked by a porous substrate and it completely disappears at the moment  $t_m$ . After that moment again all liquid coming from the foam goes directly into the porous substrate and the liquid volume fraction decreases to its equilibrium value determined by properties of both foam and porous substrate.

**References**

- [1] A. Bureiko, A. Trybala, N. Kovalchuk, V. Starov, *Current applications of foams formed from mixed surfactant–polymer solutions. Adv Colloid Interface Sci*, **222**, 670–677 (2015)
- [2] A. Bureiko, A. Trybala, J. Huang, N. Kovalchuk, V.M. Starov, *Bulk and surface rheology of AculynTM 22 and AculynTM 33 polymeric solutions and kinetics of foam drainage. Colloids&Surfaces A*, **434**, 268-275 (2013)
- [3] A. Bureiko, A. Trybala, J. Huang, N. Kovalchuk, V.M. Starov, *Effects of additives on the foaming properties of Aculyn 22 and Aculyn 33 polymeric solutions. Colloids &Surfaces A*, **460**, 265-271 (2014)
- [4] O. Arjmandi-Tash, N. Kovalchuk, A. Trybala and V. Starov, *Foam drainage placed on a porous substrate. Soft Matter*, **11** (18), 3643-3652 (2015)



**Smart Cell Dynamics:****Phenomenological Investigation of Cell Migration in 2D and 3D Substrata**

*S. Caserta, F. Ascione, S. Guido. Department of Chemical, Materials and Industrial Production Engineering, University of Naples Federico II, P.zzle Tecchio 80, 80125, Naples, Italy, sergio.caserta@unina.it.*

Many physiological and pathological processes, such as inflammation, tissue repair, angiogenesis, tumor growth and invasion, are strongly linked to the dynamic evolution of cell populations, that can be described as active biological soft matter. The current understanding of many mechanisms is still limited and cell dynamic behavior remains a challenging process to study under physiopathologically-relevant conditions *in vitro*. A detailed analysis of these processes requires a rigorous approach to quantitatively analyze cell dynamics and measure cell movement and proliferation indices.

This work is addressed to investigate the dynamic evolution of living cellular systems, from single to collective cell dynamic behavior in 2D and 3D substrata, in a quantitative way. The methodology is based on direct visualization of cell migration assays by live cell imaging using *in-vitro* Time Lapse microscopy, analyzed using image analysis. The technique is based on iterative image acquisition within the sample by means of a motorized video-microscope that is kept in a controlled environment to ensure cell viability thanks to an incubating system.

Different assays, such as single cell random motility assays or Wound Healing assay were used to gain quantitative information about the movement of individual cells, and cell populations, such as cell monolayers or clusters in 2D and 3D. The response of individual cells and groups of cells to the concentration gradient of a chemoattractant was also investigated by using a chemotactic chamber.

The experimental data were interpreted according to mathematical models, based on a transport phenomena approach.

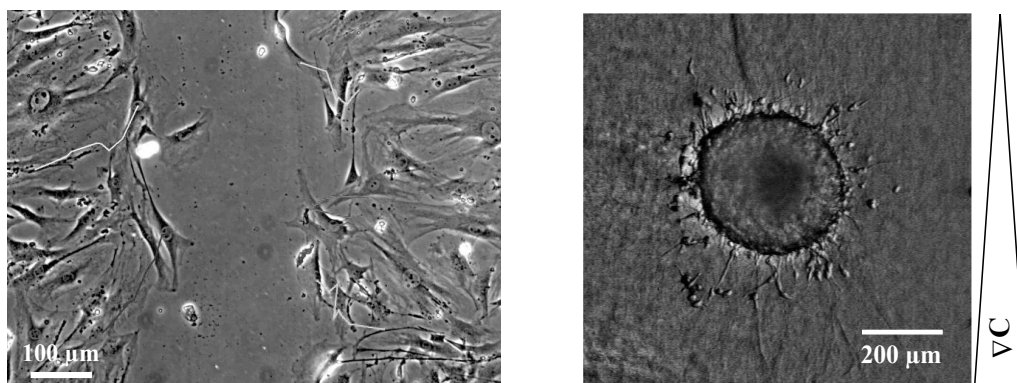


**Figure 1.** Two different examples of directional motion of cell.

Left: During Wound Closure cells move from the dense monolayer toward the nude area, the phenomena can be described according to a reaction-diffusion model.

Right: Cells escape from a tumor spheroid preferentially in the direction of chemoattractant source, external microenvironment can induce morphological instability of tumor aggregates.

**References**

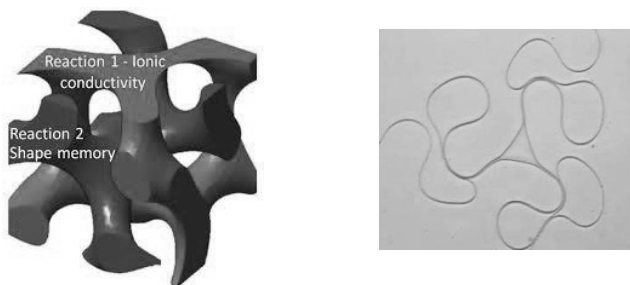
- [1] V. Cristini, H.B. Frieboes, R. Gatenby, S. Caserta, M. Ferrari, J. Sinek, *Clinical Cancer Research*, 11 (2005) 6772.
- [2] A. Vasaturo, S. Caserta, I. Russo, V. Preziosi, C. Ciacci, S. Guido, *PLOS ONE*, 7 (2012) e52251.
- [3] J. Pascal, E.L. Bearer, Z. Wang, E.J. Koay, S.A. Curley, V. Cristini, *Proc Natl Acad Sci U S A*. 110 (2013)
- [4] S. Caserta, S. Campello, G. Tomaiuolo, L. Sabetta, S. Guido, *AIChE Journal* 59 (2013) 4025.
- [5] P.M. Altrock, L.L. Liu, F. Michor, *Nature Reviews Cancer* 15 (2015) 730.
- [6] P.M. Enriquez-Navas, J.W. Wojtkowiak, R. A. Gatenby, *Cancer Research*, 75 (2015) 4675
- [7] H. Ducasse, A. Arnal, M. Vittecoq, S.P. Daoust, B. Ujvari, C. Jacqueline, T. Tissot, P. Ewald, R.A. Gatenby, K.C. King, F. Bonhomme, J. Brodeur, F. Renaud, E. Solary, B. Roche, F. Thomaset, *Evolutionary Applications*, 8 (2015) 527
- [8] *Physical Sciences and Engineering Advances in Life Sciences and Oncology*. P. Janmey, D. Fletcher, S. Gerecht, R. Levine, P. Mallick, O. McCarty, L. Munn, C. Reinhart-King (Eds.), London, Springer, 2016.

Unconventional Routes To Smart Materials

Stoyan K. Smoukov, [sks46@cam.ac.uk](mailto:sks46@cam.ac.uk), Head, Active and Intelligent Materials Lab, University of Cambridge

Current processes for making particles are quite wasteful of energy and material resources. Most complex particles are made in top-down fashion, requiring expensive lithographic and other equipment with relatively low throughput. In addition to the technological pressures for a sustainable, scalable, bottom-up process that can generate regular geometric particles, novel mechanisms of spontaneous symmetry breaking address fundamental questions in materials science, chemistry and physics. Artificial materials exhibiting symmetry breaking, such as dynamic shape-change behaviour, are parsimonious, compared to biological systems, both in terms of number of components and mechanisms. This elegance allows us to study in greater fundamental detail their mechanisms and potential to control such behaviour. Symmetry breaking in living systems is often achieved by reaction-diffusion coupling, but recently nonlinearities in material properties have been shown key to achieving morphogenesis. We explore ways to break symmetry from the macroscopic to the molecular level. We have discovered fundamentally novel mechanisms to direct growth, shape change, and have a vision to develop them in the fields of artificial muscles, adaptive structures, and for bringing insights in the processes of morphogenesis.

We show examples of engineering the symmetry breaking and dynamics for multiple structures and processes, on multiple lengthscales – from nanometers to centimeters. We demonstrate the formation of Janus and other asymmetric particles, which form as a result of coupling of chemical reactions to non-linear mechanical properties of materials[1,2]. We also demonstrate the opposite effects – how mechanical deformations and molecular interactions can help one simplify chemical syntheses[3]. Further, we also demonstrate that even without reactions, the material properties and geometry alone could cause symmetry breaking. We show instabilities and novel behaviors, both static and dynamic in some of the simplest known structures spherical cap and cone shells. Using high speed video, we have captured an intermediate asymmetric quasi-stable state during the inversion of a magnetic spherical cap, the energetics of which was explained by a finite element model [4]. Equilibrium deformations in a conical shell also show symmetry breaking. Upon inversion a circular fold can form 2-, 3-, 4- and 5- sided polygonal shapes.



We combine the geometrical approaches with chemistry to achieve combinatorial multifunctionality. Instead of designing all the desired functions in a single molecule, we use controlled internal phase separation in a material to introduce existing materials with already optimized functions, and interweave them into one. We show how this spatial separation of just 3 phases and 20 functions would lead to over 8000 trifunctional materials. We demonstrate such interpenetrating networks with the separate individual functions, as well as emerging effects.

Finally, we describe molecular mechanisms we have discovered for bottom-up shape change in liquid droplets. It relies only on transformations inside the droplets and, without any external applied fields, is able to generate a number of regular geometric shapes, including octahedra, hexagons, rhomboids, triangles and fibers. We explain the transitions between these shapes and methods to control them in both the liquid and solid state. This scalable process is a molecularly based method for symmetry breaking on various scales.[6] I will outline a number of implications for further fundamental discoveries and for potential applied explorations we are pursuing in symmetry breaking, manufacturing and nanoscience.

References

- [1] Ding T, Baumberg J, Smoukov SK, Harnessing Nonlinear Rubber Swelling for Bulk Synthesis of Anisotropic Hybrid Nanoparticles with Tunable Metal-Polymer Ratios, *J. Mater. Chem. C*, **2**, 8745-8749 (2014) DOI: 10.1039/c4tc01660b
- [2] Wang Y, Ding T, Baumberg J, Smoukov SK, Symmetry Breaking Polymerization: One-Pot Synthesis of Plasmonic Hybrid Janus Nanoparticles, *Nanoscale* **7**, 10344-10349 (2015) DOI: 10.1039/c5nr01999k
- [3] Marshall, JE, Gallagher S, Terentjev EM, Smoukov SK, Anisotropic Colloidal Micromuscles from Liquid Crystal Elastomers, *J. Am. Chem. Soc.*, **136** (1), 474-479 (2014), DOI: 10.1021/ja410930g
- [4] Loukaides E, Seffen KA, Smoukov SK, Magnetic Actuation and Transition Shapes of a Bistable Spherical Cap, *Intl. J. Smart & Nano Mater.* (2015) DOI: 10.1080/19475411.2014.997322
- [5] Khaldi A, Plesse C, Vidal F, Smoukov SK, Designing Smarter Materials with Interpenetrating Polymer Networks, accepted in *Adv. Mater.* **27** (30), 4418-4422 (2015) DOI: 10.1002/adma.201500209
- [6] Denkov N, Tcholakova S, Lesov I, Cholakova D, Smoukov SK, Self-Shaping of Droplets via Formation of Intermediate Rotator Phases upon Cooling, *NATURE* **528**, 392-395 (2015), DOI: 10.1038/nature16189

**Adsorption of Ionic Surfactants at Water/Alkane Interfaces**

*N. Mucic<sup>1,3</sup>, A. Javadi<sup>1,2</sup>, J. Katona<sup>3</sup>, E.V. Aksenenko<sup>4</sup>, V.B. Fainerman<sup>5</sup>, R. Miller<sup>1</sup>. (1) MPI of Colloids and Interfaces, Potsdam, Germany, (2) Chemical Engineering Department, University of Teheran, Teheran, Iran, (3) Faculty of Technology, University of Novi Sad, Novi Sad, Serbia (4) Institute of Colloid Chemistry and Chemistry of Water, Kyiv (Kiev), Ukraine, (5) Donetsk Medical University, Donetsk, Ukraine, mucic@mpikg.mpg.de*

At water/air interfaces surface tension measurements [1], sum frequency spectroscopy, or neutron reflection experiments are very powerful methods to give an accurate idea of the adsorption layer properties, such as adsorbed amount, thickness of the layer, area and orientation of adsorbed molecules. At water/oil interfaces some technical difficulties, such as the decrease of sensitivity of optical methods, are mainly due to the presence of the upper oil phase. The impurities of these oil phases (traces of surface active molecules) and their volatility, which limits the experimental time, are additional critical points.

We have measured the interfacial tension of various ionic model surfactants (sodium dodecyl sulphate SDS, dodecanol C<sub>12</sub>TAB and homologues series of trimethylammonium bromides C<sub>n</sub>TAB, n=10, 12, 14, 16) using the Drop Profile Analysis Tensiometry and the Oscillating Drop and Bubble Analyzer (PAT-1 and ODBA, SINTERFACE Technologies, Berlin). The availability of adsorption kinetics and dilational rheology data depend closely on the choice of the instrument and on the theoretical model for analyzing the data afterwards. ODBA is an excellent tool to measure the dynamic interfacial tension of liquid-liquid interfaces, even when the densities of the two fluids are similar. The shortest adsorption times reached are about 10<sup>-2</sup> s. This limit can be further decreased by a modification of the pressure data recording protocol. Alkane homologous series was used as the oil phases. The obtained kinetic and equilibrium experimental results were fitted with the common theoretical Langmuir and variations of Frumkin adsorption models. A new theoretical model was proposed for the description of the adsorption of surfactants at the aqueous solution/oil (alkane) interface. This theory assumes not only the surfactant adsorption from its aqueous solution, but also the adsorption of alkane molecules.

At the water/alkane interface, calculating the change of C<sub>n</sub>TAB surface concentration and partial molar area as a function of the surfactant bulk concentration it is possible to get information on the adsorption layer structure. The mutual interactions between surfactant molecules can dominate so that the alkane molecules are removed from the surfactant adsorption layer. On the contrary, the surfactant-alkane interactions can be strong enough to let the oil molecules remain in the surfactant adsorption layer.

An SDS diffusion coefficient of  $D = 5 \times 10^{-10} \text{ m}^2/\text{s}$  was obtained at the water-hexane interface, which is not affected by the presence of C<sub>12</sub>OH, in contrast to data observed at the water-air interface [2]. It was possible to estimate the partition coefficient  $K_p = c_o/c_w$  of C<sub>12</sub>OH between water and hexane,  $6.7 \times 10^3$ .

By mixing positively (C<sub>12</sub>TAB) and negatively (SDS) charged ionic surfactants in equimolar solutions, complexes of very high surface activity are formed. When these complexes adsorb at the solution/air and solution/hexane interface the bulk concentration range of the corresponding isotherm is three orders of magnitude lower than for the single surfactants. It was found that the molar area of SDS+C<sub>12</sub>TAB ion pairs is smaller than of the single surfactants due to weaker electrostatic repulsion of the surfactants' polar heads. The complexes are non-ionic and, therefore, at the solution/hexane interface they can transfer across the interface into the hexane phase (partition coefficient  $K_p = 0.32$ ).

From the dynamic interfacial tension curves a significant decrease of the interfacial tension is seen upon releasing the hexane vapour into the atmosphere around the C<sub>n</sub>TAB solution drop, demonstrating the significant increase of surfactants adsorption caused by the presence of hexane molecules. It was found that the co-adsorption of hexane molecules in a surfactant adsorption layer does not significantly depend on the surfactant's surface concentration but rather on the partial hexane vapour pressure. The effect of the surface activity of the studied surfactants and their type (ionic or non-ionic) was found to be of secondary importance.

**Acknowledgements**

This work has been done under support of COST Action MP1106.

**References**

- [1] A.J. Prosser, E.I. Franses, Colloids Surf. A, 178 (2001) 1-40.
- [2] V.B. Fainerman, S.V. Lylyk, E.V. Aksenenko, J.T. Petkov, J. Yorke, R. Miller, Colloids Surf. A, 354 (2010) 8.



## 5

## ORAL PRESENTATIONS

1 <sup>st</sup> DAY	
Hall A.....	34
Bubbles.....	34
Hall B.....	39
Flow related processes.....	39
Hall A.....	43
Droplets on surfaces (1).....	43
Hall B.....	50
Foams.....	50
Hall A.....	56
Adsorption on surfaces (1).....	56
Hall B.....	61
New materials.....	61
2 <sup>nd</sup> DAY	
On Board.....	65
Gas handling/Advanced measurements.....	65
Feature lecture.....	70
3 <sup>rd</sup> DAY	
Hall A.....	72
Fluid-solid interactions.....	72
Hall B.....	78
Modified solid surfaces.....	78
Hall A.....	83
Droplets on surfaces (2).....	83
Hall A.....	89
Adsorption on surfaces (2).....	89
Hall B.....	93
Thermal processes.....	93

## ORAL PRESENTATIONS - 1<sup>st</sup> DAY

	<i>Hall A: Bubbles (Chair: H. Kuerten)</i>	<i>Hall B: Flow related processes (Chair: A. Papathanasiou)</i>
<i>10:00-10:15</i>	<b>Jawala Jan</b> A correlation between kinetics of bubble attachment to solids and flotation efficiency	<b>Sosnowski Tomasz</b> New engineering strategies for improvement of drug delivery by aerosol inhalation
<i>10:15-10:30</i>	<b>Oikonomidou Ourania</b> Saturation pressure effect on the size of bubbles formed due to liquid decompression	<b>Palero Virginia</b> Study of mixing in a small-scale model reactor by a Mach-Zehnder interferometer
<i>10:30-10:45</i>	<b>Orvalho Sandra</b> Effect of the approach velocity and bubble size on the critical concentration for coalescence inhibition in electrolyte solutions	<b>Guido Stefano</b> Flow-induced morphology evolution of nano-emulsions
<i>10:45-11:00</i>	<b>Krzan Marcel</b> Influence of bubble wake development on bubble motion in surfactant solutions	<b>Trabi Christophe</b> Capillary penetration into inclined circular glass tubes

## A Correlation Between Kinetics of Bubble Attachment to Solids and Flotation Efficiency

J. Zawala<sup>1</sup>, P.B. Kowalczyk<sup>2</sup>, D. Kosior<sup>1</sup>, J. Drzymala<sup>2</sup>, K. Malysa<sup>1</sup>. (1) ICSC PAS, ul. Niezapominajek 8 Krakow, Poland [nczawala@cyfronet.pl](mailto:nczawala@cyfronet.pl). (2) Wroclaw UT, Wybrzeze Wyspianskiego 27, Wroclaw, Poland

Frothers are used in flotation systems to enhance degree of the gas dispersion, to ensure formation of a stable froth, to prevent bubble coalescence, to facilitate the three phase contact (TPC) formation and generally to improve flotation recovery. Flotation is a complex process and involves several sub-processes, which have to be taken into account for both quantitative and qualitative characterization. Formation of the bubble-grain aggregates is a necessary condition for flotation separation and it involves the following key steps: (i) collisions of bubbles and grains, (ii) rupture of the intervening liquid films and formation of the three phase (TPC) contacts, and (iii) enlargement of the TPC perimeter and formation of stable bubble-grain aggregates. The rate of many flotation processes can be described by the first order kinetics equation:

$$r = r_{max} \cdot (1 - e^{-kt})$$

where  $r$  is recovery of floating particles,  $r_{max}$  the maximum possible recovery,  $t$  is the flotation time and  $k$  is the 1<sup>st</sup> order kinetics constant. The constant  $k$  depends on efficiencies of collision, attachment and stability of the bubble-particle aggregates ( $E_c$ ,  $E_a$  and  $E_s$ ), respectively. Time-scale of the TPC formation and the bubble attachment to hydrophobic solid surface is of crucial importance for the kinetic of flotation separation process.

The paper presents the results of investigations on kinetics of attachment of a single bubble to a rough hydrophobic solid surface with contact angle greater than 90° (polyterfafluoroethylene - Teflon®) in aqueous solutions of various frothers. The time of the bubble attachment and three-phase contact formation was measured in a model system (liquid column) using by monitoring of a single bubble collision with horizontal solid plate using high-speed camera and image analysis. Results of model experiments were compared with flotation test performed in the Denver type cell, under corresponding conditions. A relationship between time of the TPC formation ( $t_{TPC}$ ) at the bubble/liquid/solid interface and the flotation rate was found. It was observed that at high concentrations of frothers the time of the TPC formation was significantly prolonged and simultaneously the flotation rate was lowered. Moreover, this effect was observed irrespectively of the frothers type (ionic, non-ionic). The decreased flotation rate, measured as 1<sup>st</sup> order rate constant ( $k$ ), correlated well with the increasing the  $t_{TPC}$  values at high frothers concentrations (see Fig.1). These findings indicate that in the case of a highly hydrophobic material such as polyterfafluoroethylene, the high concentrations of frother inhibit the bubble-particle attachment, leading to a decreasing flotation recovery. The obtained results confirm that the air, potentially present at highly hydrophobic solid surfaces, can be a decisive factor in kinetics of the TPC formation. Moreover, obtained results clearly show that, despite the complexity of flotation separation and vast number of sub-processes included in this process, the stability of liquid film separating the bubble and solid surfaces seems to be a factor of crucial importance for the final separation outcome. The single bubble test can be a useful tool for prediction of the flotation response and kinetics of separation process.

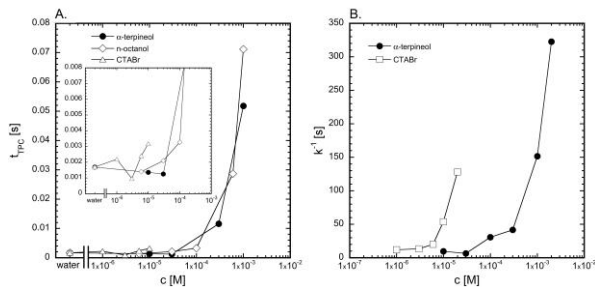


**Figure 1.** Dependencies of the  $t_{TPC}$  values, determined in the single bubble tests (A), and inversed values of the kinetic constant ( $k^{-1}$ ), determined from the flotation tests (B), on concentration of different frothers

### Acknowledgements

The study is related to the activity of the European network action COST MP1106: "Smart and green interfaces - from single bubbles and drops to industrial, environmental and biomedical applications". This work was partially financed by the National Science Centre Research Grant 2012/07/D/ST8/02622 (P.B. Kowalczyk) and 2013/09/D/ST4/03785 (J. Zawala).

---

**Saturation Pressure Effect on the Size of Bubbles Formed due to Liquid Decompression**

---

*O. Oikonomidou<sup>1</sup>, S. Evgenidis<sup>1</sup>, M. Kostoglou<sup>1</sup>, T. D. Karapantsios<sup>1</sup>. (1) Aristotle University of Thessaloniki, University Campus 54124, Thessaloniki, Greece, oikonomid@chem.auth.gr.*

Bubbles formation is widely utilized in potable water and waste water treatment applications for the removal of suspended solid particles. Bubbles rise towards the liquid free surface due to buoyancy effect. During ascension, solid particles attach to bubbles surface and so get separated from the liquid. The efficiency of wastewater flotation strongly depends on bubble size parameter, as the great surface area offered by micro scaled bubbles favors particles attachment and separation [1]. Formation of microbubbles can be achieved when decompressing an air saturated liquid volume through a nozzle, due to desorption of dissolved air. The ability to further control the size distribution of these microbubbles is a very challenging task in flotation. To date the size of bubbles formed during decompression “flow” degassing of liquids has been associated with several parameters such as saturation pressure [1,2], liquid flow rate [2], nozzle geometry [2] and liquid physical properties [1]. However, the effect of saturation pressure on bubbles size remains controversial [2,3].

A new experimental setup has been constructed, Figure 1, to study how saturation pressure affects the final size that bubbles attain due to gas desorption during decompression “flow” degassing. A liquid volume, saturated with gas under high pressure levels, is injected at the bottom of a column containing liquid bulk at atmospheric conditions, by passing through a nozzle. Decompression forces gas to desorb, resulting in bubbles formation and growth. Deionized water containing 0.019% w/w NaCl constitutes the liquid phase and atmospheric air is used as the gas phase. Saturation pressure is the experimental parameter and varies from 200kPa to 500kPa. Bubbles size is measured optically 90cm above the nozzle exit, using a high resolution still digital camera. Optical measurements are taken at different radial positions across the column. Local volumetric gas fraction is determined by applying I-VED, a patented ultra-sensitive electrical impedance technique. Flow conditions within the desorption column are studied using conductivity tracers. Aiming to estimate the total level of degassing during each injection, the gas volume remaining dissolved at the overflown liquid phase is measured using a dissolved oxygen probe. The effect of saturation pressure conditions on bubble size distributions and gas fractions across the desorption column, are presented and discussed.

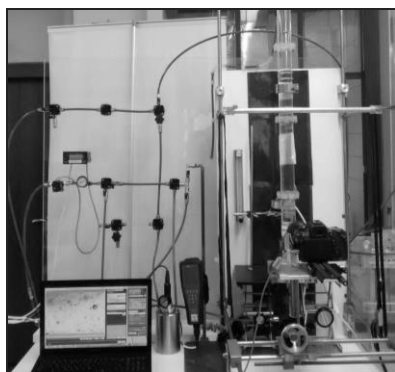


**Figure 1.** Experimental device for studying decompression “flow” degassing of liquids.

**Acknowledgements**

This work was carried out under the project “Bubble dynamics during degassing of liquids” (ESA NPI Project, Contract No. 4000108790/13/NL/PA).

**References**

- [1] A. Vlyssides, S. Mai, E. Barampouti, *Industrial and Engineering Chemistry Research*, 43 (2004) 2775.
- [2] T. Takahashi, T. Miyahara, H. Mochizuki, *Journal of Chemical Engineering of Japan*, 12 (1979) 275.
- [3] R. Rodrigues, J. Rubio, *International Journal of Mineral Processing*, 82 (2007) 1.



## Effect of the Approach Velocity and Bubble Size on the Critical Concentration for Coalescence Inhibition in Electrolyte Solutions

S. Orvalho<sup>1</sup>, P. Stanovský<sup>1</sup>, J. Vejražka<sup>1</sup>, M. Ruzicka<sup>1</sup>. (1) ICPF of the CAS, v.v.i., Rozvojova 2/135, Prague, Czech Republic, orvalho@icpf.cas.cz.

In gas-liquid systems, the interfacial area available for heat and mass transfer plays a key role in the performance of reaction and separation processes. The interfacial area depends on bubble size distribution resulting from the balance between coalescence and breakage of bubbles in the gas-liquid dispersion. The present work will focus on the coalescence of bubbles in solutions of electrolytes. The presence of electrolytes has a dramatic effect on the coalescence of bubbles. Back in the 1971, Lessard and Zieminski [1] introduced the concept of “transition concentration”,  $c_t$ , as the concentration of solute above which coalescence of bubbles is inhibited in more than 50% of contacted pairs of bubbles. Values of  $c_t$  were measured for many systems and theoretical formulas for its prediction can be found in literature. Recently a map of coalescence for 4 mm bubbles in NaCl solutions, without surfactants, was presented by Horn and co-workers [2]. They identified the approach velocity  $V$  and the concentration as the main parameters controlling coalescence. In the present work this map will be analyzed and complemented with new data obtained for different bubble sizes and other two electrolytes (CaCl<sub>2</sub> and Na<sub>2</sub>SO<sub>4</sub>).

The dynamics of bubble coalescence was investigated under well-defined laboratory conditions using a high-speed camera [3]. Each experiment consisted in following the life of two identical bubbles growing at fixed distance, since their emergence till they touch, coalesced or not. The approach velocity between bubbles was investigated in the interval 0.03-30 mm/s. The size of the bubbles investigated was 1 or 1.5 mm. The coalescence efficiency and contact time were evaluated for each set conditions.

Our experiments showed that the transition concentration does depend on the approach velocity and bubble size and that this definition should be carefully used. Also the coalescence map was extended for other bubble sizes and electrolytes.

**Table 1.** Literature values for  $c_t$  and experimental conditions, in NaCl solutions.

Reference	$d_b$ (mm)	$V$ (mm/s)	$c_t$ (M)
[1]	3.6	3	0.175
[4]	?	?	0.145
[5]	2.4	0.1	0.208

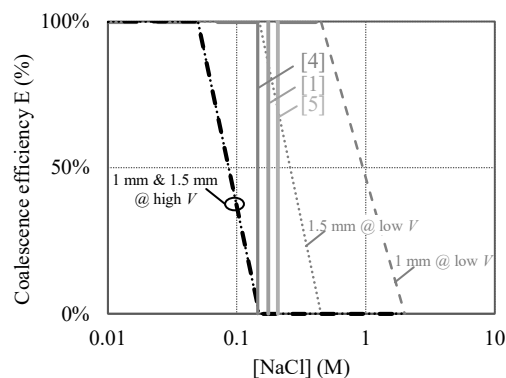


**Figure 1.** Coalescence efficiency in NaCl as function of concentration of electrolyte, showing the effect of the bubble size (1 and 1.5 mm) and approach velocity (low  $V = 4.4$  mm/s and high  $V = 24$  mm/s). Colored lines show  $c_t$  values from literature.

### Acknowledgements

The support of Ministry of Education, Youth and Sports (project LD13018) is gratefully acknowledged.

### References

- [1] R.R Lessard., S.A. Zieminski, *Ind. Eng. Chem. Fund.*, 10 (1971) 260.
- [2] R.G. Horn, L.A. Del Castillo, S. Ohnishi, *Adv. Colloid Interface Sci.*, 168 (2011) 85.
- [3] S. Orvalho, M.C. Ruzicka, G. Olivieri, A. Marzocchella, *Chem. Eng. Sci.*, 134 (2015) 205.
- [4] J. Zahradnik, M. Fialova, F. Kastanek, K.D. Green, N.H. Thomas, *Chem. Eng. Res. Des.*, 73 (1995) 341.
- [5] H.K. Christenson, R.E. Bowen, J.A. Carlton, J.R.M. Denne, Y. Lu, *J. Phys. Chem. C*, 112 (2008) 794.

---

**Influence of bubble wake development on bubble motion in surfactant solutions**

---

*M. Krzan, J. Haber Institute of Catalysis and Surface Chemistry PAS, Cracow, Poland, nckrzan@cyf-kr.edu.pl*

Description of the bubbles motion is a key problem that has a bearing on a wide range of application from froth flotation to biotechnology and chemical engineering. Due to complex nature of bubble motion there still doesn't exist any general theory describing motion of the bubbles at high Reynolds numbers. We all agree that presence of surface active substances affects (diminishes) strongly velocity of the rising bubble. Together with Frumkin-Levich theories the viscous drag exerted by continuous medium on the rising bubble surface causes uneven distribution of the surfactant molecules adsorbed, with significantly lowered adsorption coverage at the upstream pole of the rising bubble. The uneven adsorption coverage means arising of the surface tension gradient over the bubble surface, which retards the bubble surface fluidity and in a consequence the bubble velocity is lowered. The process is generally known as a Marangoni effect or Dynamic Adsorption Layer formation.

However, till today exist no direct experimental evidence of Dynamic Adsorption Layer formation. Therefore in this paper I propose new innovative method, which allow us to visualize the processes occurring in the wake of the bubble. In my experiments I used the mixture of CTAB and special blue dye (methylene blue). Thanks for this the evolution of wake, its size and shape could be studied in detail.

I found that the size of the wake increases gradually with the CTAB solution concentration and with the distance from the capillary. It was also evident that the wake is created by the solution shifted probably by the separation point from the boundary layer. Moreover, in the case of highest CTAB concentrations the size of wake was ca. 3 times larger than the volume of the rising bubble. Therefore it is clear that the hydrodynamic drag caused by the wake should also be considered during the analysis of free rising bubble experiments.

I also confirmed that the zig-zag path of the motion is strictly connected with the turbulences in the wake region. Together with the hydrodynamic rules such turbulences (, in high Reynolds number) are caused by the flow separation. I believe that it ultimately confirm the assumptions of the Frumkin-Levich theory. In my opinion, the boundary layer immobilization caused so huge hydrodynamic drag that in the result flow separation happen. However, in contrary for the classical understanding of the theory, I believe that we observe the periodic (cyclic) formation and destroying of the Dynamic Adsorption Layer. The process periodically happened during bubble acceleration, deceleration and in the motion with the zig-zag path.

Finally, I proved that in the case of high surfactant solution the whole bubble boundary layer rotate (and the vectors of the rotation varied with dependence of the surfactant concentration). Rotations caused characteristic shape of the wake. It could be assume that rotation are responsible for faster motion of the bubbles - relatively to the medium concentrated surfactant solutions. But it must be pointed, that similar effect was never predicted before by any theory.

**Acknowledgements:**

*Financial support from Polish National Scientific Centre (grant no. 2011/01/ST8/03717) is gratefully acknowledged. Part of this work has been also supported by the research and/or staff mobility actions COST MP1106, COST CM1101 and European Union Erasmus+ program (project number: 2014-1-PL01-KA103-000225).*

**New engineering strategies for improvement of drug delivery by aerosol inhalation**

*T. R. Sosnowski, Faculty of Chemical and Process Engineering, Warsaw University of Technology, Waryńskiego 1, Warsaw, Poland, t.sosnowski@ichip.pw.edu.pl.*

This work summarizes the main directions and achievements of research done during last few years, mostly under umbrella of COST Actions MP1106 "Smart and green interfaces" and P21 "Physics of droplets", which were focused on aerosol systems considered as carriers of inhaled medicines to the respiratory system. Several engineering aspects have been analyzed for that time both theoretically (mainly by CFD computations) and experimentally (by in vitro physicochemical modeling):

- improvement of powder resuspension and aerosol generation by airflow turbulization, focusing or fluctuations (intermittence) [1-3],
- dynamics of aerosol particles and their interactions with non-stationary flow of air during breathing cycle [4-6],
- influence of liquid properties (surface tension and viscosity) on the quality of aerosol produced by atomization (nebulization) [7-9],
- new types of inhalable medicinal aerosols and drug carriers - preparation and aerosolization [10-12],
- influence of particle properties on surface activity of the lung surfactant system [13-17],
- electronic cigarette as a novel inhalation device [18,19],
- characterization and optimization of nasal aerosol products [20],
- application of aerosol delivery systems in neonatology [21].

All mentioned issues are strongly related to dispersed systems, surface forces and interactions with interfaces, so they are embedded in the main objectives of MP1106 Action and of the earlier P21 Action. Author participation in these COST initiatives allowed to cooperate and interact with the scientists from different countries who represented different disciplines, which led to the positive outcome regarding the development of knowledge and the enhancement of practical importance of obtained scientific results.

**Acknowledgements**

Work supported by National Centre for Science of Poland – grant No. 2014/13/B/ST8/00808. Work done under umbrella of the COST Action MP1106.

**References**

- [1] J. Gac, T.R. Sosnowski, L. Gradoń, *J. Aerosol Sci.* 39 (2008)113.
- [2] A. Moskal, T.R. Sosnowski, *In: Respiratory Drug Delivery 2008*, R.N. Dalby (Ed.), River Grove, USA, Davis Healthcare Publ., 2008, 969.
- [3] T.R. Sosnowski, K. Giżyńska, Ł. Żywczyk. *Coll. Surfaces A: Physicochem. Eng. Aspects* 441 (2014) 905.
- [4] T.R. Sosnowski, A. Moskal, L. Gradoń, *Ann. Occup. Hyg.* 51 (2007) 19.
- [5] T.R. Sosnowski, A. Moskal, *Chem. Process Eng.* 30 (2009) 545.
- [6] A. Moskal, T.R. Sosnowski, L. Gradoń, *In: Environmental and medical aerosol nanoparticles. Inhalation and health effects*, J.C.M. Marijnissen, L. Gradoń (Eds.), Dordrecht, Springer, 2010, 113.
- [7] T.R. Sosnowski, *Abstracts of COST P21 MC&WG's Conference, Bucharest, Romania, 2009*, 54.
- [8] J. Bąk, T.R. Sosnowski, *Abstracts of COST P21 Final Meeting, Physics of droplets, Borovets, Bulgaria, 2010*, P21.
- [9] L. Broniarz-Press, T.R. Sosnowski, M. Matuszak, M. Ochowiak, K. Jabłczyńska, *Int. J. Pharmaceut.* 485 (2015) 41.
- [10] T.R. Sosnowski, A. Kurowska, B. Butruk, K. Jabłczyńska, *Chem. Eng. Transact.* 32 (2013) 2257.
- [11] M. Odziomek, T.R. Sosnowski, L. Gradoń, *Int J. Pharmaceut.* 433 (2012) 51.
- [12] K. Jabłczyńska, M. Janczewska, A. Kulikowska, T.R. Sosnowski, *Int J. Polymer Sci.* 2015 (2015) 763020.
- [13] T.R. Sosnowski, M. Koliński, L. Gradoń, *J. Biomedical Nanotechnol.* 8 (2012) 818.
- [14] D. Kondej, T.R. Sosnowski, *Inhalation Toxicol.* 25 (2013) 77.
- [15] T.R. Sosnowski, *J. Nanosci. Nanotechnol.* 15 (2015) 3476.
- [16] K. Kramek-Romanowska, M. Odziomek, T.R. Sosnowski, *Coll. Surf. A: Physicochem. Eng. Asp.* 480 (2015) 149.
- [17] D. Kondej, T.R. Sosnowski, *Env. Sci. Pollut. Res.* 23 (2016) 4660.
- [18] T.R. Sosnowski, A. Piela, *Materials of "Multiphase flow with/without phase change" COST Action MP1106, Zaragoza, Spain, 2013*,15.
- [19] T.R. Sosnowski, K. Kramek-Romanowska, *J Aerosol Med. Pulm. Drug. Del.* – accepted (2016), DOI: 10.1089/jamp.2015.1268
- [20] P. Rapięjko, T.R. Sosnowski, J. Sova, D. Jurkiewicz, *Otolarygol. Pol.* 69 (2015) 30.
- [21] J. Mazela, K. Chmura, M. Kulza, C. Henderson, T.J. Gregory, A. Moskal, T.R. Sosnowski, L. Kramer, M. Keszler, *J. Aerosol Med. Pulm. Drug. Del.* 27 (2014) 58.

### Study of mixing in a small-scale model reactor by a Mach-Zehnder interferometer

V. Palero<sup>1</sup>, N. Andrés<sup>1</sup>, M. P. Arroyo<sup>1</sup>, I. Sancho<sup>2</sup>, A. Verme<sup>2</sup>, J. Pallarés<sup>2</sup> (1) Instituto de Investigación en Ingeniería de Aragón (I3A), Universidad de Zaragoza, Pedro Cerbuna 12, 50009 Zaragoza, Spain, palero@unizar.es (2) Departamento de Ingeniería Mecánica, Universitat Rovira i Virgili, Campus Sescelades, Av. Països Catalans, 26, 43007Tarragona, Spain.

The objective of this work is to study the mixing in a small scale model of a reactor with a volumetric reaction at high Schmidt numbers, as the ones that can be found, for example, in many liquid phase chemical reactors. In this case the mass transfer occurs in a fluid/fluid interface. Numerical and experimental data obtained in a cylindrical reactor will be compared.

The flow is contained in a cylindrical reactor with an inner diameter of 8 cm. Its top wall rotates thanks to an electronically controlled DC motor operating at angular velocities between

$\Omega = 5$  and 25 rad/s. These angular velocities correspond to a Reynolds number between 1000 and 2300. The aspect ratio of the cavity is set to  $H/R = 2$ .

The chemical reaction considered is a fast irreversible neutralization acid-base reaction. The reaction constant ( $K$ ) is of order  $10^8$  m<sup>3</sup>/mol·s and the concentration of the Acetic Acid ( $A$ ) and Ammonium Hydroxide ( $B$ ) are, respectively, 0.1 M and 0.01 M. The base solution ( $B$ ) is initially inside the cylindrical cavity. The acid solution ( $A$ ) is introduced in the cavity through the bottom inlet of 3 mm of diameter with a syringe pump (CHEMYX Fusion 100). The fluid is a water-glycerine (60% v/v glycerine) solution of acid and base with kinematic viscosity  $\nu \sim 10^{-5}$  m<sup>2</sup>/s and density  $\rho \sim 1100$  kg/m<sup>3</sup>.

The three dimensional flow structure at different Re has been analyzed with a MachZehnder interferometer. This interferometer (Figure 1) is particularly useful for the analysis of mixtures which components are transparent and have different refractive index.

The light from a solid state laser ( $\lambda = 532$  nm) was divided in two beams: the reference and the object beams. The object beam was expanded to illuminate an area of 65x65 mm<sup>2</sup>. This object beam travels through the reactor and a rough surface which is imaged onto the digital sensor. The laser light scattered by the surface is combined with the smooth reference beam and their interference is recorded on the sensor. Phase difference maps are obtained by subtracting the phases reconstructed from two interferograms recorded at two different time instants. In these experiments the phase differences are directly related to optical path length changes produced by refractive index changes along the beam path.

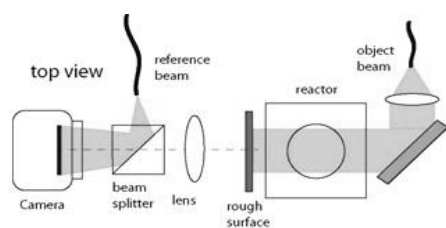


**Figure 1.** Schematic drawing of a Mach-Zehnder interferometer



**Figure 2.** Flow three dimensional structure obtained from the interferograms.

Figure 2 shows an example of the 3D structures obtained from the analysis of two interferograms recorded at  $Re = 2300$ . It can be seen that the liquid introduced from the bottom of the cylindrical cavity has a different refractive index and is moving up following a helical path, while mixing with the liquid inside the cavity. This structure agrees qualitatively with the numerical simulations. Quantitative data are expected to be obtained from the interferograms at different Re.

#### Acknowledgements

Authors thank Spanish Ministerio de Economía y Competitividad and European Commission FEDER program (projects CTQ2013-46799-C2-1-P and CTQ2013-46799-C2-2-P) and Gobierno de Aragón (Laser Optical Technology – T76-research group) for financial support. The support of the COST Action MP1106 is also acknowledged.

---

**Flow-Induced Morphology Evolution of Nanoemulsions**

---

*V. Preziosi<sup>1</sup>, A. Perazzo<sup>1\*</sup>, S. Guido<sup>1,2</sup>. (1) Dipartimento di Ingegneria chimica, dei Materiali e della Produzione Industriale, Università di Napoli "Federico II", 80125 Napoli, Italy, steguido@unina.it. (2) CEINGE Advanced Biotechnologies, Napoli, Italy. \*) Current address: Princeton University, Mechanical and Aerospace Engineering Department, USA*

Microstructured emulsions are often exploited as drug delivery systems, in particular for dermal delivery [1]. Such mesophases are characterized by both viscous and solid-like properties, and can be obtained by slow addition of water into an agitated oil/surfactant solution at fixed temperature. Surfactants hydration may lead to sponge, lamellar, cubic or hexagonal arrangements. Such bi-continuous surfactants solutions show highly viscoelastic behavior and may display also some features typical of lyotropic liquid crystalline phases. These systems show a continuous interplay between viscoelastic phase separation and surfactants self-organization, thus displaying a variety of morphologies.

This work is focused on flow-induced morphology evolution of the bicontinuous phases of a system composed of mineral oil, two non-ionic surfactants (one hydrophilic and one hydrophobic) and distilled water. During all the experiments, temperature was kept constant at room temperature. The already mentioned "phase inversion composition" method, i.e., dropwise addition of water to the oil-surfactant mixture, was exploited to obtain bicontinuous structures. To outline emulsion morphology development, confocal microscopy and rheological measurements have been exploited.

Rheological measurements probed the increased viscoelasticity induced by water addition up to the point of bicontinuous phase formation. Confocal microscopy revealed the formation of complex structures at the microscale, where a slow phase separation is initially driven by system viscoelasticity, likely due to a strong coupling between highly viscoelastic behaviour and liquid-crystalline mesophases.

***Acknowledgements***

This work has been done under the umbrella of COST MP1106 Smart and Green interfaces for biomedical and industrial applications.

***References***

- [1] Y. Iwashita, H. Tanaka, *Nature materials*, 5(2) (2006), 147.

Capillary Penetration into Inclined Circular Glass Tubes

*Christophe L. Trabi<sup>1</sup>, F. Fouzia Ouali<sup>1</sup>, Glen McHale<sup>2</sup>, Haadi Javed<sup>1</sup>, Robert H. Morris<sup>1</sup>, and Michael I. Newton. (1) School of Science and Technology, Nottingham Trent University, Clifton Lane, Nottingham NG11 8NS, U.K., christophe.trabi@ntu.ac.uk. (2) Faculty of Engineering & Environment, Northumbria University, Ellison Place, Newcastle upon Tyne NE1 8ST, U.K..*

The spontaneous penetration of a wetting liquid into a vertical tube against the force of gravity and the imbibition of the same liquid into a horizontal tube (or channel) are both driven by capillary forces and described by the same fundamental equations. However, there have been few experimental studies of the transition from one orientation to the other. We report systematic measurements of capillary penetration of polydimethylsiloxane oils of viscosities 9.6, 19.2, and 48.0 mPa·s into glass capillary tubes. We first report the effect of tube radii  $R$  between 140 and 675  $\mu\text{m}$  on the dynamics of spontaneous imbibition. We show that the data can be fitted using the exact numerical solution to the governing equations and that these are similar to fits using the analytical viscogravitational approximation. However, larger diameter tubes show a rate of penetration slower than expected using an equilibrium contact angle and the known value of liquid viscosity. To account for the slowness, an increase in viscosity by a factor  $(\eta/\rho)_{\text{scaling}}$  is needed. We show full agreement with theory requires the ratio  $R/\kappa^{-1} \sim 0.1$  or less, where  $\kappa^{-1}$  is the capillary length. In addition, we propose an experimental method that enables the determination of the dynamic contact angle during imbibition, which gives values that agree with the literature values. We then report measurements of dynamic penetration into the tubes of  $R = 190$  and  $650 \mu\text{m}$  for a range of inclination angles to the horizontal,  $\phi$ , from  $5$  to  $90^\circ$ . We show that capillary penetration can still be fitted using the viscogravitational solution, rather than the Bosanquet solution which describes imbibition without gravity, even for inclination angles as low as  $10^\circ$ . Moreover, at these low angles, the effect of the tube radius is found to diminish and this appears to relate to an effective capillary length,  $\kappa^{-1}(\phi) = (\gamma_{LV}/\rho g \sin \phi)^{1/2}$ .

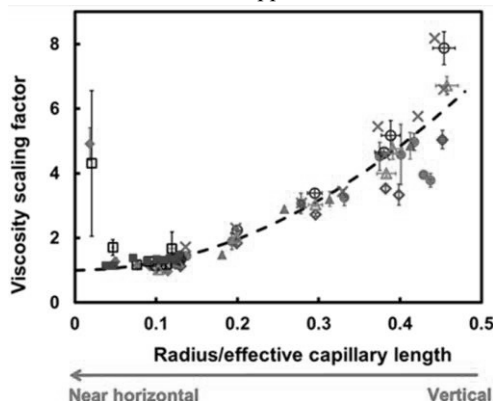


**Figure 1.** Dependence of the scaling factor  $\text{ascaling} = (\eta/\rho)_{\text{scaling}}$  on the effective  $R/\kappa^{-1}(\phi)$  ( $5^\circ \leq \phi \leq 90^\circ$ ) in tilted tubes with radius  $R = 190 \mu\text{m}$  (dark teal  $\blacklozenge$ ,  $\eta = 9.6 \text{ mPa}\cdot\text{s}$ ; black  $\square$ ,  $\eta = 19.2 \text{ mPa}\cdot\text{s}$ ; dark blue  $\blacksquare$ ,  $\eta = 48.0 \text{ mPa}\cdot\text{s}$ ) and  $R = 650 \mu\text{m}$  (red  $\bullet$ ,  $\eta = 9.6 \text{ mPa}\cdot\text{s}$ ; light blue  $\times$ ,  $\eta = 19.2 \text{ mPa}\cdot\text{s}$ ; green  $\blacktriangle$ ,  $\eta = 48.0 \text{ mPa}\cdot\text{s}$ ).

**Acknowledgements**

The authors acknowledge financial assistance from the U.K. Engineering and Physical Sciences Research Council (Grant EP/E063489/1). H.J. would like to acknowledge Nottingham Trent University for financial support. The authors would also like to thank Dr. David Fairhurst for his help with the viscosity measurements

**References**

- [1] Schoelkopf, J.; Gane, P. A. C.; Ridgway, C. J.; Matthews, G. P. Practical observation of deviation from Lucas – Washburn scaling in porous media. *Colloids Surf., A* 2002, 206, 445–454.
- [2] Brody, J. P.; Yager, P.; Goldstein, R. E.; Austin, R. H. Biotechnology at low Reynolds numbers. *Biophys. J.* 1996, 71, 3430–3441
- [3] Marmur, A.; Cohen, R. D. Characterization of porous media by the kinetics of liquid penetration: The vertical capillaries model. *J. Colloid Interface Sci.* 1997, 189, 299–304.
- [4] Lucas, R. *Colloid Polym. Sci.* 1918, 23, 15–22.
- [5] Washburn, E. W. The dynamics of capillary flow. *Phys. Rev.* 1921, 17, 273–283.
- [6] Bosanquet, C. H. On the flow of liquids into capillary tubes. *Philos. Mag. Ser. 6* 1923, 45, 525–53.

## HALL A - DROPLETS ON SURFACES (1)

	<i>Hall A: Droplets on surfaces (1)</i> <i>(Chair: D. Vollmer)</i>	<i>Hall B: Foams</i> <i>(Chair: S. Caserta)</i>
<i>11:30-11:45</i>	<b>Brutin David</b> Evaporative instabilities in sessile drops of ethanol on heated substrates: computer simulations	<b>Langevin Dominique</b> On the use of shear rheology to formulate very stable foams. Example of a lamellar phase containing SDS, hexanol and brine
<i>11:45-12:00</i>	<b>Brabcova Zuzana</b> Axisymmetric spreading of droplets into films using liquid dielectrophoresis	<b>Nastasa Viorel</b> Sclerosing foams assessment in view of their use in sclerotherapy
<i>12:00-12:15</i>	<b>Muradoglu Metin</b> The effects of viscoelasticity on drop impact and spreading on a solid surface	<b>Arjmandi Tash Omid</b> Free drainage of non-Newtonian foams
<i>12:15-12:30</i>	<b>McHale Glen</b> Dewetting dynamics from a non-equilibrium dielectrowetted thin film into a single macroscopic droplet	<b>Pugh Robert</b> Particle Stabilized Three-Phase Foam Systems in the Flotation Process
<i>12:30-12:45</i>	<b>Starov Victor</b> Wetting and spreading: recent developments	<b>Santini Eva</b> Interfacial Properties and Bubble/Drop Coalescence in The Stability of Emulsions and Foams
<i>12:45-13:00</i>	<b>Diddens Christian</b> Modeling the evaporation of sessile multi-component droplets	<b>Haffner Benjamin</b> Stability of foams containing fibres

---

**Evaporative Instabilities In Sessile Drops Of Ethanol On Heated Substrates: Computer Simulations**

---

*S. Semenov, F. Carle, M. Medale, D. Brutin. Aix-Marseille Université, IUSTI UMR 7343 AMU/CNRS, 13453 Marseille, France, [david.brutin@univ-amu.fr](mailto:david.brutin@univ-amu.fr)*

Evaporating sessile drops of simple and complex fluids are widely encountered in nature and have a great diversity of actual and potential applications. To name some of them: heat exchangers, patterns of nanoparticles deposition from evaporation of sessile drops (coffee-ring effect), spraying of herbicides and pesticides on hydrophobic leaves, inkjet printing, microlens manufacturing, biological tissue engineering and other biomedical applications (e.g. blood analysis) and surfactant replacement therapy. Due to a wide range of applications, sessile drops have been the subject of extensive experimental and theoretical studies, and still remain an interesting problem from both scientific and industrial points of view.

Our current research is focused on thermal Marangoni instabilities in sessile ethanol droplets, which develop spontaneously during evaporation. One distinctive type of these thermo-capillary instabilities is called hydrothermal waves (HTW). Conventional HTW are observed in thin liquid layers whose surface is subject to a lateral temperature gradient. In sessile droplets, however, the HTW are driven by the process of evaporation which generates these temperature gradients naturally. These instabilities have been observed in droplets of volatile liquids (ethanol, methanol, FC-72) on heated substrates by few researchers. The ultimate aim of current research is to achieve both qualitative and quantitative agreement between computer simulations and experiments. Achieving the first one would require a 3D numerical modelling, as the flow observed in drops is essentially three-dimensional. Meanwhile 2D axisymmetric modelling is quite sufficient for the quantitative validation, because the most appropriate for that purpose and experimentally measurable quantity is the droplet's evaporation rate, which is weakly influenced by the 3D flow pattern inside a droplet. The present work is dedicated to the quantitative validation and, therefore, is limited to 2D axisymmetric numerical models, which take into account all relevant processes of heat and mass transfer, essential for the achievement of quantitative agreement with experiments.

***Acknowledgements***

We would like to acknowledge the financial support of CNES (Centre National d'Etudes Spatiales) research grant for post-doctorates and parabolic flights experimentation.



## Axisymmetric Spreading Of Droplets Into Films Using Liquid Dielectrophoresis

Z. Brabcova<sup>1</sup>, G. McHale<sup>1</sup>, G.G. Wells<sup>1</sup>, C.V. Brown<sup>2</sup>, M. I. Newton<sup>2</sup>, A.M.J. Edwards<sup>2</sup>, (1) Smart Surfaces & Materials Laboratory, Northumbria University, Newcastle upon Tyne, UK, z.brabcova@northumbria.ac.uk  
(2) School of Science & Technology, Nottingham Trent University, Nottingham, UK

The wetting of solid surfaces is important for a wide range of disciplines and applications such as creating thin films, coating of surfaces and adhesion, and droplet deposition and control. There are many methods in which to modify the wetting, all based on altering the energy balance between the solid, liquid and vapour phases. Electrostatic fields can alter how effectively a liquid wets a solid surface with the most common example being electrowetting (change in a solid-electrolyte contact angle) [1,2]. A critical aspect of this method is the reversible increase of hydrophilicity of a solid surface and reduction of the contact angle of the droplet without altering the surface chemistry or the liquid's materials properties. However, liquids of interest need to be conducting, an electrode must be in direct contact with the liquid, and the contact angle displays a minimum saturation value thereby limiting the range of applicability of electrowetting. Recently, it has been shown how an interface localized form of liquid dielectrophoresis (DEP), which moves dielectric liquid to regions where non-uniform fields are high [3], can be used to create spreading and superspreading of droplets in air [4,5] or a second liquid [6]. This is described as dielectrowetting and theoretically obeys a similar equation to that for electrowetting. This has been confirmed experimentally in a non-axisymmetric stripe droplet form using parallel interdigitated electrodes (IDEs) [4]. The decaying non-uniform electric field created above the IDEs on which the droplet sits has an associated liquid dielectrophoresis energy, which changes the energy balance, thus giving a voltage controlled contact angle. However, the periodic IDEs provide a small periodic energy barrier, thus preventing spreading across the electrodes. To develop the concept of dielectrowetting towards the spreading of an axisymmetric droplet when viewed from above, we have developed a four arm spiral electrode format activated by AC voltages with 0°, 90°, 180° and 270° phases. This achieves complete and reversible control from an axisymmetric droplet state to a circular film state. As an example, Fig. 1 shows the spreading of a droplet of glycerol on a hydrophobic substrate. The glass substrate has equally spaced gold electrodes of 80  $\mu\text{m}$  capped by 1  $\mu\text{m}$  of SU-8 photoresist. A 2 kHz sinusoidal voltage of amplitude 0 to 215 V (rms) was generated and split into four signals each successively phase shifted by 90° and these were applied to the four interlaced spiral electrodes.

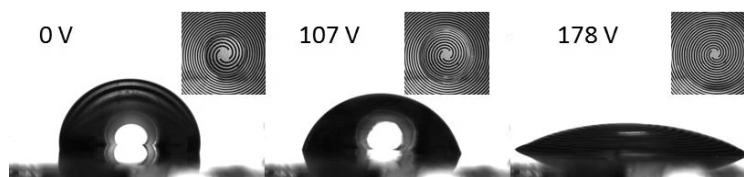


Figure 1. Evolution of the side profile of a droplet as a result of the applied voltages (Insets: Top views).

We have shown how liquid dielectrophoresis can be used in combination with spiral electrode designs and phase shifted signals to achieve reversible axisymmetric spreading of a droplet to a film state. Our results suggest that this type of dielectrowetting can be combined with superoleophobicity to create control of non-aqueous droplets across the full contact angle range whilst maintaining a circular droplet shape.

#### Acknowledgements

The work was performed under the umbrella of COST Action MP1106 (Smart and Green Interfaces) and financially supported by EPSRC grants (EP/K014803/1 and EP/K015192/1).

#### References

- [1] B. Berge, *C. R. Acad. Sci. Ser. II* 317 (1993).
- [2] F. Mugele, J.C. Baret, *J. Phys. Condens. Matt.* 17 (2005).
- [3] M. Gunji, M. Washizu, M.J. Feldman, *J. Appl. Phys.* 89 (2001).
- [4] G. McHale, C.V. Brown, M.I. Newton, G.G. Wells, N. Sampara, *Phys. Rev. Lett.* 107 (2011).
- [5] G. McHale, C.V. Brown, N. Sampara, *Nat. Commun.*, 4 (2013).
- [6] C.V. Brown, G. McHale, C.L. Trabi, *Langmuir* 31 (2015).

**The Effects of Viscoelasticity on Drop Impact and Spreading on a Solid Surface**

M. Muradoglu, D. Izbassarov, Koc University, Istanbul, Turkey. muradoglu@ku.edu.tr.

The effects of viscoelasticity on drop impact and spreading on a flat solid surface are studied computationally using a finite-difference/front-tracking method. The FENE-CR model is used to account for the fluid viscoelasticity. We fully account for the effects of surface tension and treat the partially wetting cases with a dynamic contact angle. The Navier-Stokes and the viscoelastic model equations are solved in the entire computational domain using a front-tracking method [3,4]. The fluid viscoelasticity is characterized by the Weissenberg number ( $Wi$ ), the concentration parameter defined as the ratio of polymeric viscosity to solvent viscosity ( $c$ ) and the extensibility parameter ( $L^2$ ). We first examined the effects of drop viscoelasticity without the polymer-induced contact angle hysteresis. It is found that viscoelasticity favors advancement of contact line during the spreading phase leading to a slight increase in the maximum spreading in agreement with the experimental observations of Huh et al. [2]. However, in contrast with the well-known anti-rebound effects of polymeric additives, the viscoelasticity is found to enhance the tendency of the drop rebound in the receding phase. These results suggest that the antirebound effects are mainly due to the polymer-induced modification of wetting properties of the substrate rather than the change in the material properties of the drop fluid. To remedy this deficiency, we propose a model that mimics the hysteresis of the contact angle observed experimentally by Bertola and Wang [1]. The simulations with the contact line hysteresis result in good qualitative agreement with the experimental observations [1] supporting the hypothesis that the anti-rebound effect is mainly due to the modification of surface wetting properties by the deposited polymer molecules rather than the drop viscoelasticity. Although the emphasis is placed on the effects of the viscoelasticity, further simulations are also carried out to examine the effects of the Weber number ( $We$ ), the Reynolds number ( $Re$ ) and the equilibrium contact angle ( $\theta_e$ ).

Sample results are shown in Fig. (1). The effects of viscoelasticity characterized by Weissenberg number are demonstrated on the left hand side of Fig. (1) where no contact angle hysteresis is taken into account. As seen,  $Wi$  enhances the tendency of drop to rebound in this case. When the contact angle hysteresis is taken into account, however, the drop rebound is completely avoided and the results are in qualitative agreement with the experimental observations of Bertola and Wang [1] as shown on the right hand side of Fig. (1).

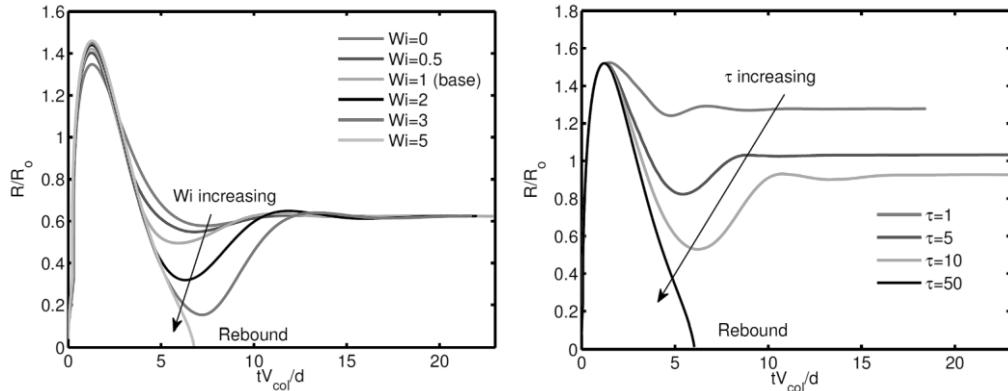


**Figure 1.** (Left) Effects of the Weissenberg number on droplet impact and spreading in the absence of substrate hysteresis. Time evolution of the spread factor is plotted for various values of  $Wi$  in the range  $0 \leq Wi \leq 5$ . ( $Re = 35; We = 30; L^2 = 225, c = 1.27$  and  $\theta_e = 145^\circ$ ). (Right) Effects of the nondimensional deposition time scale ( $\tau$ ) on the droplet impact and spreading in the range  $0 \leq \tau \leq 50$ . ( $Re = 75; We = 30; Wi = 1; L^2 = 225; c = 0.075; \theta_e = 145^\circ$  and  $\theta_s = 90^\circ$ ).

**Acknowledgements**

This work is supported by the Scientific and Technical Research Council of Turkey (TUBITAK), Grant No. 112M181 and by the COST Action MP1106.

**References**

- [1] V. Bertola and M. Wang, Colloids and Surfaces A: Physicochem. Eng. Aspects 481, (2015) 600.
- [2] H.K. Huh, S. Jung, K.W. Seo, and S.J. Lee, Microfluid. Nanofluid. 18, (2015) 1221.
- [3] D. Izbassarov and M. Muradoglu, J. Non-Newt. Fluid Mech. 223, 122 (2015) 122.
- [4] S.O. Unverdi and G. Tryggvason, J. Comput. Phys. 100(1), (1992) 25.

---

**Dewetting Dynamics From A Non-Equilibrium Dielectrowetted Thin Film Into A Single Macroscopic Droplet**

---

**G. McHale**<sup>1</sup>, **R. Ledesma-Aguilar**<sup>1</sup>, **C.V. Brown**<sup>2</sup>, **M. I. Newton**<sup>2</sup>, **A.M.J. Edwards**<sup>2</sup>, (1) *Smart Surfaces & Materials Laboratory, Northumbria University, Newcastle upon Tyne, UK, glen.mchale@northumbria.ac.uk*  
(2) *School of Science & Technology, Nottingham Trent University, Nottingham, UK*

In recent work we have shown how liquid dielectrophoresis (L-DEP) [1] can be transformed into an interface localized effect which can control the equilibrium contact angle of an isotropic sessile droplet in a similar manner to electrowetting [2], but avoiding contact angle saturation [3,4]. Even on usually nonwetting surfaces our L-DEP techniques can use electric fields to force droplet wetting and drive spreading to create thin films of liquid. By abruptly removing the electric field we are provided with a unique opportunity to observe and accurately measure the dynamic surface evolution during de-wetting from a variety of user-defined different initial wetting shapes back towards the spherical cap high contact angle equilibrium state. We will show how our techniques can be used to mimic natural de-wetting phenomena, such as droplet rebound shapes, allowing controlled and detailed study for the first time of the different dewetting morphologies that occur at different timescales. We complement our experimental observations with Lattice-Boltzmann simulations and theoretical calculations to reveal the underlying principles of the dewetting from a film into a macroscopic droplet. Our new experimental technique is also able induce dewetting from novel initial droplet and film morphologies that would not normally be observed in nature.

**Acknowledgements**

The work was performed under the umbrella of COST Action MP1106 (Smart and Green Interfaces) and financially supported by EPSRC grants (EP/K014803/1 and EP/K015192/1).

**References**

- [1] M. Gunji, M. Washizu, M.J. Feldman, *J. Appl. Phys.* 89, 1441-1448 (2001).
- [2] F. Mugele, J.C. Baret, *J. Phys. Condens. Matt.* 17, R705-R774 (2005).
- [3] G. McHale, C.V. Brown, M.I. Newton, G.G. Wells, and N. Sampara, *Phys. Rev. Lett.* 107, 186101 (2011).
- [4] G. McHale, C.V. Brown, N. Sampara, *Nat. Commun.* 4, 1605 (2013).

**Wetting And Spreading: Recent Developments**

*V Starov<sup>1</sup>, O Arjmandi-Tash<sup>1</sup>, N Kovalchuk<sup>1</sup>, I Kuchin<sup>2</sup>, A Trybala<sup>1</sup>. (1) Department of Chemical Engineering, Loughborough University, Loughborough, LE11 3TU, UK. (2) Institute of Physical Chemistry and Electrochemistry, Russian Academy of Sciences, Leninsky pr, 31/4, Moscow, 119071, Russia [V.M.Starov@lboro.ac.uk](mailto:V.M.Starov@lboro.ac.uk)*

Current developments in kinetics of wetting and spreading are presented in the following areas: (1) contact angle hysteresis on smooth homogeneous substrates, (2) kinetics of spreading of surfactants solutions over hydrophobic substrates and (3) kinetics of spreading of non-Newtonian liquids (blood) over porous substrates.

It has been shown that hysteresis contact angles (both static advancing and static receding) on smooth homogeneous surfaces can be calculated based on disjoining/conjoining isotherm. It is shown that both hysteresis contact angles depend on droplet or capillary size. It is shown that the receding contact angles are much closer to the equilibrium contact angles than the advancing contact angle [1,2].

Special features of spreading of fluorosurfactant aqueous solutions are investigated. Available data on the adsorption of fluorosurfactants on liquid/vapour, solid/liquid and solid/vapour interfaces are discussed in comparison to those of hydrocarbon surfactants [3]. The spreading behaviour of aqueous solutions of mixture of two surfactants sodium 1-decane sulfonate and dodecyltrimethylammonium bromide is investigated on hydrophobic substrates. The solutions demonstrate rapid complete wetting on polyethylene film and only partial wetting on silanized glass. An interesting phenomenon was observed - a transition from complete to partial wetting, that is, a droplet of freshly prepared mixture first spreads completely but after some time the solution assembles into the droplet again [4]. Additional kinetics of spreading of mixed solutions of cationic and anionic surfactants over highly hydrophobic substrate such as polyethylene is also investigated. It is shown that due to synergetic effect these solutions can wet hydrophobic substrates nearly as effectively as solutions of trisiloxane superspreader [5]. A comparison of the kinetics of spreading of aqueous solutions of different surfactant solutions and their short time adsorption kinetics at the water/air interface has shown that the surfactant which adsorbs slower provides a higher spreading rate [6].

Spreading of small drops of blood, which is a power law shear thinning non-Newtonian liquid, over a dry porous layer is investigated from both theoretical and experimental points of view. A system of two differential equations is derived, which describes the time evolution of radii of both the drop base and the wetted region inside the porous medium. The system of equations does not include any fitting parameters. The predicted time evolutions of both radii are compared with experimental data published earlier.

The predicted theoretical relationships are three universal curves accounting satisfactorily for the experimental data [7].

**Acknowledgement.**

This research was supported by CoWet ITN, EU; EPSRC, UK; MAP EVAPORATION, European Space Agency; COST MP1106, EU; Proctor & Gamble, USA

**References**

- I. Kuchin, V. Starov. *Langmuir*, 2015, 31, 5345.
- I. Kuchin, V. Starov. *Langmuir*, 2016. Submitted.
- N. Kovalchuk, A. Trybala, V. Starov, O. Matar. *Adv Colloid Interface Sci*, 2014, 210, 65.
- N.M. Kovalchuk, A. Barton, A. Trybala, V. Starov. *Colloids Interface Sci Communications*, 2014, 1, 1.
- N.M. Kovalchuk, A. Barton, A. Trybala, V. Starov. *J Colloid Interface Sci*. 2015, 459, 250.
- N. Kovalchuk, A. Trybala, F. Mahdi, V. Starov. *Colloids & Surfaces A*, 2016, In press.
- T. Chao, O. Arjmandi-Tash, D. Das, V. Starov. *J Colloid Interface Sci*, 2015, 446, 218.

**Modeling the Evaporation of Sessile Multi-Component Droplets**

*C.Diddens<sup>1</sup>, J.G.M. Kuerten<sup>1,2</sup>, C.M.W. van der Geld<sup>1</sup>, H.M.A. Wijshoff<sup>3</sup>* (1) Department of Mechanical Engineering, Eindhoven University of Technology, P.O. Box 513, 5600 MB Eindhoven, The Netherlands, C.Diddens@tue.nl. (2) Faculty EEMCS, University of Twente, P.O. Box 217, 7500 AE Enschede, The Netherlands. (3) Océ-Technologies B.V., P.O. Box 101, 5900 MA Venlo, The Netherlands.

The evaporation of a sessile droplet is a ubiquitous phenomenon, which is of utmost relevance in a plethora of applications ranging from ink-jet printing over spray cooling and coatings to medical and biological deposition methods.

Since the typical liquids used in these applications are usually multi-component mixtures of solvents, cosolvents and surfactants, a detailed understanding of the evaporation, flow and deposition dynamics of sessile multi-components droplets is an essential step to improve these technologies in terms of costs, speed and quality.

We have developed a numerical model for the evaporation of a sessile multi-component droplet [1]. In order to reduce the computational effort, we use a generalized axisymmetric lubrication approximation and combine it with volume-of-fluid, boundary integral and multi-grid methods. Furthermore, we validated the appropriateness of our lubrication theory by comparing it with full finite element simulations. We use experimental data to accurately incorporate the composition-dependence of the mixture properties, i.e. mass density, viscosity, surface tension, diffusivity and activity.

As representative mixtures, we investigate the evaporation of binary water-ethanol and water-glycerol droplets (cf. Figure 1). In both cases, the more volatile component predominantly evaporates near the rim of the droplet. This leads to a compositional gradient along the liquid-air interface which induces a Marangoni flow. In the case of ethanol-water droplets, the Marangoni flow continually replenishes the more volatile ethanol at the interface. As a result, ethanol evaporates in the first regime, leaving a slowly evaporating pure water droplet behind. For water-glycerol droplets, however, the Marangoni flow is inhibited by the vast increase of viscosity, so that a residual amount of water is entrapped by a non-volatile viscous glycerol shell.

We also take solute colloidal particles and their deposition to the substrate into account and show how the Marangoni flow can be utilized to tailor the resulting deposition pattern after drying.

Furthermore, with particular relevance for ink-jet printing, we also investigate the drying of binary droplets on porous substrates, e.g. on paper. Due to the coupled dynamics of preferential evaporation, composition-dependent properties and the absorption process, it is possible that an ink droplet effectively dries faster at lower evaporation rates.

In conclusion, we have developed a versatile numerical tool to investigate the complicated interplay of evaporation, multi-component flow and possibly absorption during the drying of a mixture droplet. By tuning the initial composition and the ambient conditions, we are able to give predictions that can help to optimize all afore-mentioned applications which base on the evaporation of multi-component droplets.

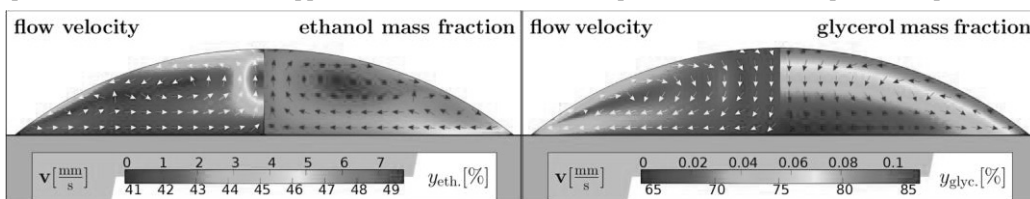


**Figure 1.** snapshots of an evaporating sessile 100 nL water-ethanol droplet (left) and a water-glycerol droplet (right).

**Acknowledgements**

This research is supported by the Dutch Technology Foundation STW and by Océ – A Canon Company. This work has been done under the umbrella of COST Action MP1106.

**References**

[1] C. Diddens, J.G.M. Kuerten, C.M.W van der Geld, H.M.A. Wijshoff, submitted, 2016

## On The Use Of Shear Rheology To Formulate Very Stable Foams. Example Of A Lamellar Phase Containing SDS, Hexanol And Brine.

Z. Briceño-Ahumada<sup>1,2</sup>, A. Soltero-Martínez<sup>3</sup>, A. Maldonado<sup>4</sup>, M. Impéror-Clerc<sup>1</sup>, **D. Langevin**<sup>1</sup>. (1) Laboratoire de Physique des Solides, Université Paris Sud, Orsay, France. (2) Departamento de Investigación en Polímeros y Materiales de la Universidad de Sonora, Hermosillo, México. (3) Departamento de Ingeniería Química de la Universidad de Guadalajara, Guadalajara, México, dominique.langevin@u-psud.fr.

The stability of foams made with sponge phases ( $L_3$  phases) and lamellar phases ( $L_\alpha$  phases), both containing surfactant bilayers, has been investigated and correlated with rheological characterisations of the bulk bilayer phases.

The foams made with lamellar phases are extremely stable (figure 1). The stability is mainly due to the high viscosity of the foaming solution, which slows down gravity drainage. Moreover, the foams start draining only when the buoyancy stress overcomes the yield stress of the  $L_\alpha$  phase. The bubble growth associated to gas transfer is unusual: it follows a power law with an exponent smaller than those corresponding to Ostwald ripening (wet foams) and to coarsening (dry foams).

In the system studied and at the difference of other systems described in the literature [1], the stability does not originate from the presence of multilamellar vesicles acting as particles at the bubble surfaces. We performed rheology experiments coupled with Small Angle X-ray Scattering (rheo-SAXS) using synchrotron radiation. We showed in this way that multilamellar vesicles are formed above a critical shear rate, but that they disappear rapidly once shearing is stopped.

The foams made with sponge phases are in turn very unstable, even less stable than pure surfactant foams. We conjecture that because the surfactant bilayers in the sponge phase have a negative Gaussian curvature, bubble coalescence could be facilitated.

More details on the foam work can be found in [2].

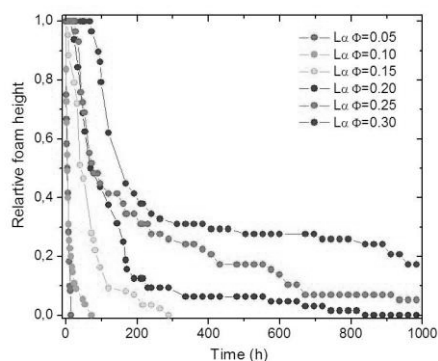


**Figure 1.** Foam height (relative to height at time  $t=0$ ) versus time for lamellar phases with different bilayer fractions  $\Phi$ .

### Acknowledgements

We acknowledge fruitful discussions concerning the foam topic with our COST partners.

### References:

- [1] S.E. Friberg, C. Solans, *Langmuir*, 2 (1986) 121-126. L.K. Shrestha, E. Saito, R.G. Shrestha, H. Kato, Y. Takase, K. Aramaki, *Colloids Surfaces A* 293 (2007) 262-271  
 [2] Z. Briceño-Ahumada, A. Maldonado, M. Impéror-Clerc, D. Langevin, *Soft Matter*, 12 (2016) 1459

---

**Sclerosing Foams Assessment In View Of Their Use In Sclerotherapy**


---

*V.Nastasa<sup>1</sup>, K.Samaras<sup>2</sup>, Ch. Ampatzidis<sup>2</sup>, T.D. Karapantsios<sup>2</sup>, M. A. Trelles<sup>3</sup>, J. Moreno-Moraga<sup>4</sup>, A. Smarandache<sup>1</sup>, M.L.Pascu<sup>1</sup>. (1) National Institute for Laser Plasma and Radiation Physics, Bucharest, Romania, viorel.nastasa@inflpr.ro (2) Aristotle University of Thessaloniki, Faculty of Chemistry, Thessaloniki, Greece (3) Instituto Médico Vilafortuny/FUNDACION ANTONI DE GIMBERNAT, Cambrils, Spain (4) Instituto Médico Láser, Madrid, Spain.*

Foam sclerotherapy is a widely used method to treat varicose veins disease. It is easy to use and apply, it is affordable and its efficiency depends on foam stability upon injection [1].

Since sclerotherapy is applied in a medical doctor's office, one of the most employed methods to generate foam is based on Tessari technique which uses two syringes connected through a three way stopcock to mix the sclerosing liquid and air (atmospheric air, N<sub>2</sub>, etc.) at a certain ratio. Finally, the produced foam exits through a small orifice (~ 2mm) at the output of a three-way valve.

The present work shows results regarding the factors that may influence foam stability (liquid to air ratio, type of connector, syringe diameter, number of pumping cycles, etc.) of a commonly used sclerosing agent, namely Polidocanol (POL). Furthermore, an effort is made to evaluate the effect of adding different substances on the stability of Polidocanol foams (0.5% v/v) by altering the surface tension and/or the bulk and interfacial rheological properties of the fluids. It is shown that addition of small concentrations of nonionic surfactants can increase foam stability with just a very small variation of the mean bubbles size.

This study is actually conducted to evaluate the effect of different rheology or surface tension modifier substances on the stability of foams generated by Tessari technique for POL. It is observed that addition of concentrations up to 10% v/v of Glycerin and Tween 80 leads to an increase in foam stability (~3 times the stability of simple POL foam) with no visible variation of bubble size distribution. However, the addition of Xanthan gum at a concentration of 0.42% w/v leads to an increase of foam stability of almost 47 times with respect to that obtained for POL with no other added substance.

One of the reasons for the increased stability of this mixture is represented by the shear-thinning (non-Newtonian) behavior of Xanthan gum that presents a small viscosity during the mixing process and becomes very viscous after the mixing is stopped. This behavior is also responsible for the small variation of bubble size distribution.

At the same time, interfacial dilatational rheological measurements of the POL/Xanthan gum mixture confirm that a modification of the visco-elastic behavior appears after the addition of Xanthan gum to POL 0.5% solution that leads to a decrease of  $|E|$  values [2].

The sclerosing foams are also investigated through optical means to assess the foam stability, composition and the effect of IR laser beams on the foam efficiency in treating varicose veins disease [3].

#### **Acknowledgements**

Acknowledgements: The research was funded by CNCS-UEFISCDI - project numbers PN1647/2016, PN-II-ID-PCE-2011-3-0922 and by COST network MP1106.

#### **References**

- [1] M.L. Pascu, Adriana Smarandache, M. Boni, Jette Kristiansen, V. Nastasa, I. R. Andrei, Spectral properties of laser irradiated sclerosing foams, Romanian Reports in Physics, Vol. 67, No. 4, P. 1480–1490, 2015.
- [2] V.Nastasa, K.Samaras, Ch. Ampatzidis, T.D. Karapantsios, M. A. Trelles, J. Moreno-Moraga, A. Smarandache, M.L.Pascu, Properties of Polidocanol foam in view of its use in sclerotherapy, Int J Pharm, Volume 478, Issue 2, 30, Pages 588–596, 2015
- [3] A. Smarandache, J. Moreno-Moraga, M. Treles, V. Nastasa, M.L. Pascu, Study of Commercial Grade Aetoxisclerol by Optical Means, in View of Its Use in Varicose Vein Treatment, AIP Conf. Proc. 1364, 117, 2011

Free drainage of non-Newtonian foams

O. Arjmandi-Tash, A. Trybala, F.M. Mahdi, V. Starov Department of Chemical Engineering, Loughborough University, UK.

Foams are multiphase colloidal systems, which are formed by trapping a gas in a continuous phase (a liquid or a solid). A flow of liquid in between the gas bubbles through Plateau borders, nodes and films in foam driven by capillarity and/or gravity is referred to as drainage. The drainage equations in the case of Newtonian liquids have been solved numerically and/or analytically in different prototype situations including free, forced, and pulsed drainage. A recently proposed type of these situations is foam drainage placed on a porous substrate [1,2] where foam is in contact with a porous substrate and the presence of unsaturated pores inside the porous layer results in an imbibition of liquid from foam into the unsaturated pores.

Foams are conventionally stabilised by surfactants; however, polymers (polyelectrolytes) grow in popularity during the last decade as alternative stabilising additives to foaming solutions. In our previous Study [3,4] the influence of rheology of commercially available polymers Aculyn™22 (A22) and Aculyn™33 (A33) on foam drainage was investigated experimentally and the results of the properties modification (polymer type, concentration, mixtures, salt and iso-propanol addition) of A22 and A33 polymeric solutions were presented. Here a theory of foam drainage is presented for the non-Newtonian polymeric solutions in the case of free drainage and its results are compared with experimental data.

The deduced dimensionless equations are solved using finite element method with appropriate boundary conditions. The numerical simulations show that the decrease in the foam height and liquid content is very fast in the very beginning of the drainage; however, it reaches a steady state at long times (Fig. 1). Under the assumption of rigid surface of the Plateau border, the predicted values of the time evolution of the foam height and liquid content are in good agreement with the measured experimental data for lowly viscous polymeric solutions. However, in the case of highly viscous solutions an interfacial mobility at the surface of the Plateau border has to be taken into account.

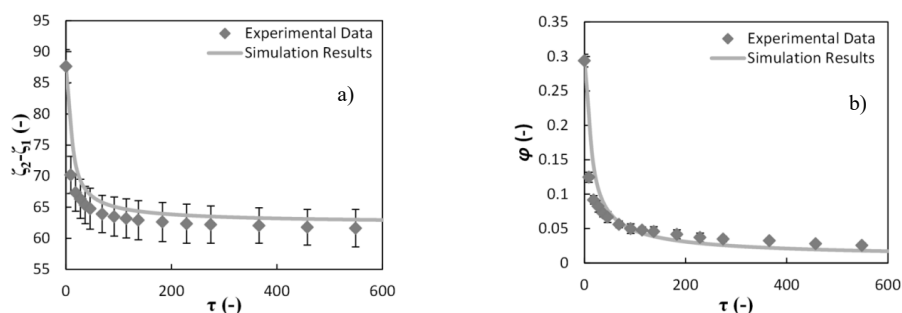


Figure 1. Comparison of the predicted and experimental time evolution of a) the height of the foam,  $\zeta_2 - \zeta_1$ , and b) the average liquid volume fraction along the foam height,  $\phi$ , for A33\_1.0% solution

References

[1] O. Arjmandi-Tash, N. Kovalchuk, A. Trybala and V. Starov, Foam drainage placed on a porous substrate, *Soft matter* **11**, 3643-3652 (2015).  
 [2] A. Bureiko, O. Arjmandi-Tash, N. Kovalchuk, A. Trybala and V. Starov, Interaction of foam with a porous medium: theory and calculations, *EPJ ST* **224**, 459-471 (2015).  
 [3] A. Bureiko, A. Trybala, J. Huang, N. Kovalchuk, and V. Starov, Bulk and surface rheology of Aculyn™ 22 and Aculyn™ 33 polymeric solutions and kinetics of foam drainage, *Colloids Surf., A* **434**, 268-275 (2013).  
 [4] A. Bureiko, A. Trybala, J. Huang, N. Kovalchuk, and V. Starov, Effects of Additives on the Foaming Properties of Aculyn 22 and Aculyn 33 Polymeric Solutions, *Colloids Surf., A* **460**, 265-271 (2014).



---

**Particle Stabilized Three-Phase Foam Systems in the Flotation Process**

---

*R. J. Pugh, School of Science and Technology, Nottingham Trent University, Clifton Lane, Nottingham, United Kingdom bobpugh42@gmail.com*

The froth flotation process has a long history and today has widespread applications. Essentially the traditional process involved the selective attachment of finely dispersed mineral particles to air bubbles which rise to the top of a flotation cell to produce a 3-phase froth. The particle rich froth systems is then removed to release the particles. Essential the capture of particles and the characteristics of the froth (the foamability or foam generation, the foam stability, bubble size, rheological properties) are controlled by surface active chemical additives which give the particles a critical degree of hydrophobicity and these factor plays an extremely important role in determining the efficiency of the process. Most of the early development work used a trial and error approach but today with insight it is possible to explain the interaction between the different additives and the particles. In these talk research in the interaction of particles at the air/solution interface in froth flotation is presented particular with respect to different types of flotation systems. As well as traditional mineral flotation which involves the recovery of valuable minerals, we present results obtained both on the recycling of plastics and de inking flotation.

**References**

- [1] Examination of NaCl and MIBC as Bubble Coalescence Inhibitor in Relation to Froth Flotation, G. Bournival, R. J. Pugh and S. Ata, *Minerals Engineering*, 25 47-53, (2012)
- [2] The Role of Particles in Stabilising Foams and Emulsions, T. N. Hunter, R. J. Pugh, G.V. Frank and G.J. Jameson *Adv. Colloid Interface Sci* 137, 57-81 (2008).
- [3] Non-ionic Surfactant interactions with Hydrophobic Nanoparticles Impact on Foam Stability, T. Hunter, E.J. Wanless., G. J. Jameson., and R.J. Pugh, *Colloids Surf. A* 347, 81-89, (2009)
- [4] Collection and Attachment of Particles by Air-Bubbles in the Froth Flotation, Nguyen AV, R. J. Pugh and G.J. Jameson. In "Colloidal Particles at Liquid Interfaces", Cambridge University Press, Cambridge, UK, Edits: B.P. Binks and T.S. Horozov, 328-383 (2006)

---

**Interfacial Properties and Bubble/Drop Coalescence in The Stability of Emulsions and Foams**

---

*E. Santini<sup>1</sup>, F. Ravera<sup>1</sup>, S. Llamas<sup>1</sup>, L. Cristofolini<sup>1,2</sup>, D. Orsi<sup>2</sup>, L. Liggieri<sup>1(1)</sup> CNR – Istituto per l'Energetica e le Interfasi, via de Marini 6, 16149 Genova, Italy; [e.santini@ge.ieni.cnr.it](mailto:e.santini@ge.ieni.cnr.it) (2) Università di Parma – Dipartimento di Fisica e Scienze della Terra, Parco Area delle Scienze, 7/A 43124 Parma, Italy.*

We report a study on the stability of emulsions and foams in relation to the coalescence of single bubble/drops and to the interfacial properties of the corresponding liquid interfaces.

The investigated systems are foams stabilised by complexes of silica nanoparticles (SNP) and palmitic acid dispersed in the aqueous phase, and emulsions of aqueous SNP dispersion in hexane solution of palmitic acid. The latter are particularly interesting because stabilized by complexes, which form directly at the liquid-liquid interface due to the interaction of NPs and surfactant.

For the proposed formulations, we have investigated the dynamic interfacial/surface tensions and interfacial dilational rheology by dynamic tensiometry, the coalescence features by a drop-drop micromanipulator and the stability of the corresponding emulsions and foams both by direct observations and by Diffusion Wave Spectroscopy.

The study provides interesting results about the processes involved in the destabilisation of emulsions and foams.

These results can be useful to address the utilisation of emulsions and foams as smart platforms for the assembling of new nanomaterials or in the design advanced chemical processing devices (ex. liquid-liquid extraction).

**Acknowledgements**

The work was undertaken under the umbrella of the COST action MP1106 and partially supported by the European Space Agency within the projects “Particle Stabilized Emulsions-PASTA” and “Soft Matter Dynamics” and by the Italian Space Agency (contract n. 2013-028-R.0.).

Stability Of Foams Containing Fibres

Benjamin Haffner<sup>1</sup>, Friedrich F. Dunne<sup>1</sup>, Stefan Hutzler<sup>1</sup>. (1) School of Physics, Trinity College Dublin, The University of Dublin, Ireland

The pulp and paper industry contributes more than 1% to the worldwide energy consumption [1]. The use of foams instead of water in the paper production process reduces the use of water considerably. It also offers a further control parameter, namely average bubble size, for obtaining more uniform paper density and renders possible the use of longer fibres for novel products. However, few studies are dedicated to the effect that the inclusion of fibres have on foam properties [2].

We have the stability of such foams by carrying out free drainage experiments on foams produced with a protocol which mimics that used in industry [2]. A surfactant solution containing paper fibres (average length 2.3 mm, diameter 35  $\mu\text{m}$ ), in concentrations below 2%) is agitated mechanically to form a foam with average bubble diameter between 150 and 220  $\mu\text{m}$ . The foam is then allowed to drain under gravity and we monitor the volume of drained liquid as a function of time for different fibre concentrations and bubble sizes.

Our experiments show that foam drainage is considerably slowed down with increasing fibre content. This is due to a combination of different effects.

We find that the average bubble size decreases with increasing fibre content. This decreases the rate of drainage according to standard foam drainage theory and indeed all our data (for different fibre concentrations, and thus average bubble sizes) is well described by our numerical solutions of the foam drainage equation [3] for up to about ten minutes when foam coarsening becomes noticeable. From monitoring bubble sizes we find that coarsening is slowed down with increasing fibre concentration. We believe the reason for this to be the pinning of foam films to the fibres, similar to the observed slow-down of coarsening in 2d foam experiments in the presence of pinning centres [4]. The reduced coarsening in foams with a higher fibre content is a further reason why such foams drain slower, foams with smaller bubbles contain more liquid in equilibrium under gravity.

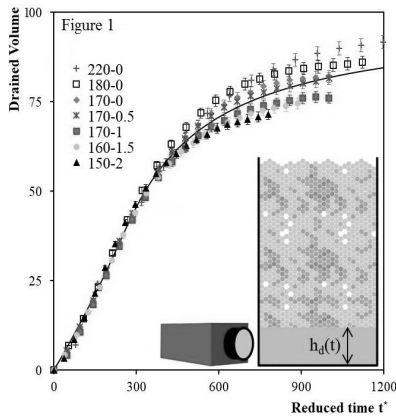


Figure 1: Drained volume (ml) as a function of reduced time  $t^* = t (R_{32}/\lambda)^2$  ( $R_{32}$  Sauter mean diameter,  $\lambda$  capillary length). All data collapses as long as coarsening is negligible. (Legend: Bubble Diameter-Fibre Concentration. Solid line: Simulation.)

**Acknowledgements:** Science Foundation Ireland (13/IA/1926). MPNS COST Actions MP1106 ‘Smart and green interfaces’ and MP1305 ‘Flowing matter’. European Space Agency: MAP Metalfoam (AO-99-075), Soft Matter Dynamics (AO-09-943+99-108+09-813).

- [1] Lundell, F., Söderberg, L.D. and Alfredsson, P.H., 2011. Fluid mechanics of papermaking. Annual Review of Fluid Mechanics, 43, pp.195-217.
- [2] Al-Qararah, A.M., Hjelt, T., Koponen, A., Harlin, A. and Ketoja, J.A., 2013. Bubble size and air content of wet fibre foams in axial mixing with macro-instabilities. Colloids and Surfaces A: Physicochemical and Engineering Aspects, 436, pp.1130-1139.
- [3] Weaire, D.L. and Hutzler, S., 2001. The physics of foams. Oxford University Press.
- [4] Krichevsky, O. and Stavans, J., 1992. Coarsening of two-dimensional soap froths in the presence of pinning centers. Physical Review B, 46(17), p.10579.

## ORAL PRESENTATIONS - 1<sup>st</sup> DAY

<i>Hall A: Adsorption on surfaces (1)</i> <i>(Chair: R. Miller)</i>		<i>Hall B: New materials</i> <i>(Chair: V. Koutsos)</i>	
<i>15:00-15:15</i>	<b>Arabadzhieva Dimitrinka</b>	Two-antennary oligoglycines: Interfacial layer properties on aqueous and solid surfaces	<b>Cabrerizo-Vilchez Miguel</b>
<i>15:15-15:30</i>	<b>Cristofolini Luigi</b>	XPCS and Discrete Fourier Microscopy reveal details on the dynamics of mixed layers formed by hydrophobic/hydrophilic silica nanoparticles in phospholipid films	<b>Ersöz Mustafa</b>
<i>15:30-15:45</i>	<b>Mileva Elena</b>	Aqueous solutions of surfactant mixtures: Hexadecyltrimethylammonium chloride and pentaethylene glycol monododecyl ether	<b>Julià López Àlex</b>
<i>15:45-16:00</i>	<b>Fernandez-Peña Laura</b>	Rhamnolipids: a promising alternative to conventional surfactants from polyelectrolyte-surfactant hair-care formulations	<b>Meriç Sureyya</b>

**Two-antennary Oligoglycines: Interfacial Layer Properties on Aqueous and Solid Surfaces**

*D. Arabadzhieva<sup>1</sup>, St. Stoyanov<sup>1</sup>, E. Mileva<sup>1</sup>, M. Mirzaeian<sup>2</sup>, A. A. Ogwu<sup>2</sup>, Qaisar Abbas<sup>2</sup>. (1) Institute of Physical Chemistry, BAS, "Acad.G.Bonchev" Str., bl.11, Sofia 1113, Bulgaria, dimi@ipc.bas.bg. (2) School of Engineering and Computing, University of the West of Scotland, Paisley, PA1 2BE, Scotland, UK*

A new class of synthetic antennary oligoglycines is investigated. These novel types of self-assembling molecules contain several oligoglycine units [1]. Here the study is focused on the two-antennary oligoglycine (T2). T2 are known to build supramolecular structures on mica surfaces [1]. Insofar that their molecules have well-defined hydrophilic and hydrophobic portions, a possibility of self-assembly at the air/solution interface and/or in the solution bulk might also be expected.

In the present research we have studied the surface properties of aqueous solutions of  $C_8H_{16}$  ( $-CH_2-NH-Gly_3)_2 \cdot 2HCl$  (T2 with a  $C_8H_{16}$  spacer chain (C8-T2)) on air/solution interface, on glass plates and on activated carbon electrodes as shown in Figure 1. The experiments are performed at two and twenty four hours after preparation of the solutions. During the experiments the temperature is strictly kept at  $20^\circ C \pm 0.1^\circ C$ , the pH and the conductivity of the system are also tracked. Dynamic, equilibrium and rheological properties of the adsorption layers are studied by Profile Analysis Tensiometry. The investigated concentration range is  $1 \times 10^{-5} M$  to  $1 \times 10^{-3} M$  C8-T2. To study the surface properties of C8-T2 solutions in more details one specific C8-T2 concentration is selected, and electrolyte is added (NaCl,  $1 \times 10^{-3} M$  to  $1 \times 10^{-1} M$ ). The basic result indicates that the plot of the equilibrium surface tension against the electrolyte concentration passes through a minimum. The surface dilation rheology for the same system shows that the dilatational elasticity passes through a maximum. Drainage kinetics and stability of foam films from aqueous solutions of C8-T2 are studied by the microinterferometric method of Scheludko-Exerowa.

Contact angle measurements are performed using computer controlled KSV instrument CAM 200, Optical Contact Angle Meter (goniometer system). Activated carbons (ACs), used in this study are prepared at different activation temperatures according to the procedure reported in [2]. The results show that fixing a layer of C8-T2 on the surface of electrodes fabricated from these carbons improves their hydrophilicity and their affinity toward aqueous electrolytes.

The properties of the obtained nanoaggregates have a considerable potential for the design and preparation of nanotransporters for various active agents in aqueous media, e.g. nanocarriers towards solid or fluid interface, in purification procedures aimed at the removal of biological impurities from natural or waste waters; for the surface modification of carbon electrodes used in electrochemical energy storage devices by lowering electrode/electrolyte contact resistances; and for many other applications.

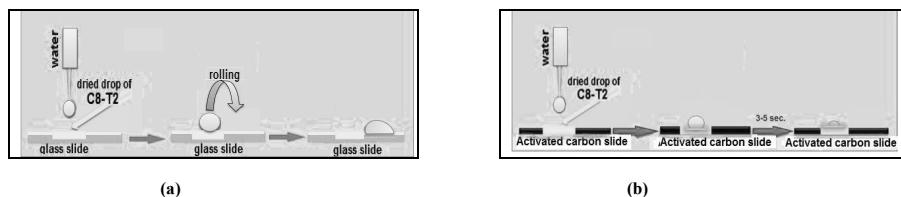


Fig. 1. A water droplet on a glass slide (a) and on an activated carbon electrode (b), both pretreated with C8-T2.

**Acknowledgements**

The studies are performed under the umbrella of COST Action MP1106 "Smart and green interfaces – from single bubbles and drops to industrial, environmental and biomedical applications" (SGI).

**References**

- [1] N. V. Bovin, A. B. Tuzikov, A. A. Chinarev, *Nanotechnologies in Russia*, 3 (2008) 291.
- [2] M. Mirzaeian, P. J. Hall, *Journal of Power Sources*, 195 (2010) 6817.

**XPCS And Discrete Fourier Microscopy Reveal Details On The Dynamics Of Mixed Layers Formed By Hydrophobic/ Hydrophilic Silica Nanoparticles In Phospholipid Films**

*Luigi Cristofolini<sup>1,2</sup>, Davide Orsi<sup>1</sup>, Libero Liggieri<sup>2</sup>, Francesca Ravera<sup>2</sup> (1) Dipartimento di Fisica e Scienze della Terra, Università degli Studi di Parma, Parma, Italy (2) Consiglio Nazionale delle Ricerche - Istituto per l'Energetica e le Interfasi, U.O.S. Genova (Italy) [luigi.cristofolini@unipr.it](mailto:luigi.cristofolini@unipr.it)*

We present here a detailed study on the dynamics of the complex systems formed when Silica nanoparticles (SiNP) are trapped into phospholipid monolayers. We speculate how these findings may impact in drug deliver: SiNP of different philicity are used in drug delivery platforms to improve the stability and control the release rate of drugs. The fine-tuning of these systems requires detailed understanding of their dynamics. Recent X-ray reflectivity experiments [1] demonstrated opposite structural effects of hydrophobic / hydrophilic SiNP on phospholipids: hydrophilic SiNP stabilize the liquid-condensed phospholipid domains, while hydrophobic SiNP induce the formation of a highly ramified structure. While these structural effects are understood, much less is known about the effects on the dynamics of these layers, which in turn determine molecular diffusivity and the possibility of drug release.

We combined Grazing Incidence X-ray Photon Correlation Spectroscopy (XPCS) with microscopy tracking, and Epifluorescence Discrete Fourier Microscopy to cover a broad temporal and Q-range. In this way we characterized the dynamics of mixed Langmuir layers made of phospholipid (DPPC) and hydrophobic/hydrophilic SiNP (Fig. 1). In phopsholipid/ hydrophilic SiNP layers we find – upon compression- a transition from Brownian diffusion to an arrested glassy phase of repulsive disks [2]. On the contrary, in phopsholipid/ hydrophobic SiNP layers we obtain evidence for the onset of an arrested state characterized by intermittent stress-relaxation rearrangement events, corresponding to a 2D gel network dominated by attractive interactions [3]. We believe that this information shall help the development of new, highly refined drug-delivery platforms.

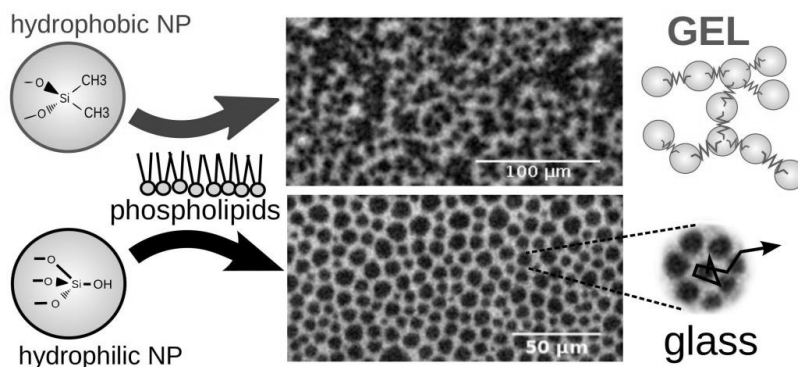


**Figure 1.** Artist's impression of the effects of Silica NP of different philicity interacting with phospholipid monolayers

**References**

- [1] Bulpett et al., *Soft Matter* 11, 8789 (2015)
- [2] D. Orsi, et al., *Scientific Reports*, 5, 19730 (2015)
- [3] D. Orsi, et al., submitted (2016)

**Aqueous Solutions of Surfactant Mixtures: Hexadecyltrimethylammonium Chloride and Pentaethylene Glycol Monododecyl Ether**

*E. Mileva, D. Arabadzhieva, P. Tchoukov, St. Stoyanov Institute of Physical Chemistry, Bulgarian Academy of Sciences, "Acad. G. Bonchev" Str. Bl. 11, 1113 Sofia, Bulgaria, [mileva@ipc.bas.bg](mailto:mileva@ipc.bas.bg).*

Previous research revealed the important role that the properties of adsorption layers play for thin film drainage and stability [1-3]. These studies were focused exclusively on single surfactant systems with commonly used anionic (SDS), cationic (CTACl) and nonionic surfactants ( $C_nE_m$ ). Here we provide a comparative study of interfacial and film properties of aqueous solutions of mixtures of the cationic surfactant hexadecyltrimethylammonium chloride (CTACl) and the nonionic surfactant pentaethyleneglycol-monododecyl ether ( $C_{12}E_5$ ) at ratio 1:1 (mol:mol), in the presence of 0.1 mol/l sodium chloride (NaCl). The equilibrium surface tension isotherms for the mixed system (CTACl/ $C_{12}E_5$ ) show lower interfacial tension values for equal total concentration of surfactant compared to the single surfactant cases. Profound increase in the magnitude of dilatational elasticity is observed, as well and the maximum is shifted towards lower concentrations as compared to single surfactants systems. The critical micelle concentration for the mixed system is  $2.0 \times 10^{-5}$  mol/l, a lower value as compared to  $7.0 \times 10^{-5}$  mol/l for CTACl and  $6.2 \times 10^{-5}$  mol/l for  $C_{12}E_5$ . The reported results underline the importance of interfacial adsorption layers and suggest significant benefits of using mixed surfactant systems in the design of aqueous formulations for various applications.

**Acknowledgements**

The investigation was performed under the umbrella of COST Action MP1106.

**References**

- [1] E. Mileva, P. Tchoukov, , *Chapter 8 in Colloid Stability: The Role of Surface Forces, part I, vol. 1. (ed. Th. Tadros), Wiley-VCH, UK, 2007.*
- [2] D. Arabadzhieva, E. Mileva, P. Tchoukov, R. Miller, F. Ravera, L. Liggieri, *Colloids Surf. A*, 392 ( 2011) 233.
- [3] D. Arabadzhieva, P. Tchoukov, B. Soklev, E. Mileva, , *Colloids Surf. A*, 460 (2014) 28.

---

**Rhamnolipids: a promising alternative to conventional surfactants from polyelectrolyte–surfactant hair-care formulations**

---

Laura Fernández-Peña<sup>1</sup>, Sara Llamas<sup>1</sup>, Eduardo Guzmán<sup>1</sup>, Francisco Ortega<sup>1</sup>, Ramón G. Rubio<sup>1,2</sup>.

<sup>1</sup> Departamento de Química Física I. Universidad Complutense de Madrid, Ciudad Universitaria s/n, 28040-Madrid, Spain, <sup>2</sup> Instituto Pluridisciplinar, Universidad Complutense, Av. Juan XIII, 2. 28040-Madrid  
laura.fernandez.pena@ucm.es.

The use of polymer-surfactant mixtures is interesting for development cosmetic hair-conditioner formulations [1,2]. Nowadays, the new European Legislation (REACH) advises to replace polycations and anionic surfactants by other of natural origin. This work is a first step towards the substitution of anionic surfactants, thus we have studied mixtures of a classical polycation, poly(diallyl-dimethylammonium chloride), with natural surfactants (rhamnolipids) that are biodegradable and have lower toxicity. This study has focused both in the bulk properties of the polymer-surfactant complexes and on the adsorption of the bulk complexes onto negatively charged surfaces mimicking the surface of hair fibres. Furthermore, they can be produced at industrial scale using biotechnological procedures. We have measured  $\zeta$  potential and size distribution of the complexes formed by the polycation and the surfactant. Both characteristics are related to their ability to adsorb onto solid surface. The adsorption on the solid substrate has been studied by two complementary techniques: Ellipsometry and Dissipative Quartz Crystal Microbalance (D-QCM). The information contained on the adsorption results provides insights on the conditioning effects and lubrication (water content) of the polymer-surfactant mixtures. The topography of the layer obtained by Atomic Force Microscopy (AFM) allows us to obtain further insights on the conditioning performance of the formulation. In general the amount of adsorbed polyelectrolyte – rhamnolipid complexes onto the negatively charged surface has been found to be higher than for typical anionic surfactants. This has allowed us to conclude that the use of these new surfactants are good choices for designing new conditioner formulations with enhanced properties in relation to conventional one.

Four different mixtures containing rhamnolipids with different hydrophobicity were studied, and the results have shown that the mixtures containing the most hydrophobic surfactants present the best performance for conditioning purposes, being even better than conventional formulations including classical surfactants [3].

**Acknowledgements**

This work was funded by L'Oréal S.A., by MINECO under grants FIS-2012 -38231-C02-01 and FIS 2014-62005-EXP, by EU under Marie Curie ITN CoWet, and performed in the framework of the COST Actions CM-1101 and MP-1106.

**References**

- [1] S. Llamas, E. Guzmán, F. Ortega, N. Baghdadli, C. Cazeneuve, R.G. Rubio, G.S. Luengo, *Adv. Colloid Interface Sci.*, 222 (2015) 461.
- [2] E. Guzmán, S. Llamas, A. Maestro, L. Fernández-Peña, A. Akanno, R. Miller, F. Ortega, R.G. Rubio, *Adv. Colloid Interface Sci.*, in press (2016) doi:10.1016/j.cis.2015.11.001
- [3] S. Llamas, E. Guzmán, N. Baghdadli, F. Ortega, C. Cazeneuve, R.G. Rubio, G.S. Luengo, *Colloids Surf. A*, in press (2016) doi:10.1016/j.colsurfa.2016.03.003.



---

**Investigating the Physical-Chemistry of Adsorption Layers, Liquid Films, Foams and Emulsions by Microgravity Experiments**

---

*L. Liggieri<sup>1</sup>, F. Ravera<sup>1</sup>, E. Santini<sup>1</sup>, M. Ferrari, S. Llamas<sup>1</sup>, P. Pandolfini<sup>1</sup>, G. Loglio<sup>1</sup>, R. Miller<sup>2</sup>, J. Kraege<sup>3</sup>, A. Javadi<sup>2</sup>, M. Karbaschi<sup>2</sup>, V. Kovalchuk<sup>3</sup>, B. Noskov<sup>4</sup>, L. Cristofolini<sup>5</sup>, D. Orsi<sup>5</sup>, D. Clause<sup>6</sup>, I. Pezron<sup>6</sup>, T. Karapantsios<sup>7</sup>, J. Ferri<sup>8</sup>, Y. Yamashita<sup>9</sup>, M. Schmitt<sup>10</sup>, M. Antoni<sup>10</sup>. (1) CNR-Istituto per l'Energetica e le Interfasi, Genova, Italy, [Liggieri@ge.ieni.cnr.it](mailto:Liggieri@ge.ieni.cnr.it). (2)Max-Planck Inst. fur Kolloid und Grenzflaechenforschung, Potsdam/Golm, Germany. (3) Institute of Bio-Colloid Chemistry, Kiev, Ukraine. (4) St. Petersburg State University, Dept. of Colloid Chemistry, Russian Federation. (5) Università di Parma, Dipartimento di Fisica e Scienze della Terra, Italy. (6) Université de Technologie de Compiègne, France. (6) School of Chemistry, Aristotle University of Thessaloniki, Greece. (8) Lafayette College, Easton PA, USA. (9) Faculty of Pharmacy Chiba Institute of Science, Japan. (10) Aix-Marseille Université, CNRS MADIREL – France.*

Metals are ubiquitous as base materials in many different structures and equipments. The design of durable superhydrophobic coatings for metal surfaces is being a subject of interest and research. Galvanized steel is one of the most used metallic materials as part of the components of automobiles, building structures, roofing, etc. In spite of its wide number of applications, galvanized steel has been scarcely modified to reach superhydrophobicity. The main reason for this lack is that galvanized steel is a zinc-coated steel surface and most of the strategies to prepare superhydrophobic coatings on metal substrates produce a partial removal of the surface material. In this paper, we propose a two-step texturization process followed by a fluoropolymer deposition as non-invasive strategy to produce water repellent surfaces on galvanized steel. Contact angle hysteresis measurements were used to study the wettability properties of the substrates employed and confocal microscopy and FE-SEM techniques were used to analyze the topographic features of the substrates.

---

**Synthesis And Functionalization Of Different Forms Of Graphene For Various Applications**

---

*M. Karaman<sup>1,2</sup>, E. Citak<sup>2</sup>, M. ERSOZ<sup>2,3</sup>. (1) Selcuk University, Faculty of Engineering, Department of Chemical Engineering, 42075, Konya, Turkey, (2) Selcuk University, Advanced Technology Research and Application Center, 42075, Konya, Turkey, (3) Selcuk University, Faculty of Science, Department of Chemistry, 42075 Konya, Turkey, merso@selcuk.edu.tr.*

Graphene is the state of carbon atoms aligned in a hexagonal structure. Graphene exhibits exceptional electronic and physical properties which make graphene a desired material for many applications including energy storage, nanoelectronics, biosensors, gas storage devices and medicine. Graphene can be synthesized in various ways and on different substrates. Here, the synthesis and functionalization of different forms of graphene and their applications for various sectors will be summarised.

In Selcuk University, Advanced Technology Research and Application Center (ILTEK) laboratory, two different forms of graphene are synthesized. Thin films of few layer graphene on silicone surfaces are prepared by using catalytic chemical vapour deposition (CVD) process and other forms as graphene flakes is prepared by using Hummer's method. In this method, reduced graphene oxide or few layer graphene can be produced in powder form.

In CVD synthesis of graphene usually nickel and copper foils are used as catalytic substrates. Compared with commonly used volatile carbon sources such as methane and ethylene, alcohol precursors in liquid form are safer and easy to use. In our laboratory, graphene is being synthesized by low-pressure CVD method using different carbon sources including both volatile (acetylene) and non-volatile (methanol, ethanol, 2-propanol, etc.) ones. Copper foil (25µm thick) is used as substrate, which at the same time, acts as catalyst for graphene growth. The reactor is a pressure controlled cylindrical quartz tube placed in a tube furnace. The effects of precursor type, deposition conditions and process time on the quality and thickness of graphene layers are investigated. After each deposition, as-deposited graphene layer on copper substrates are transferred to silicon wafers (100, p-doped). Chemical structures and the surface morphologies of the synthesized graphene films are investigated using Raman and SEM analyses.

For many industrial applications, functionalization and/or patterning of graphene is of great importance. For example; the absence of energy band gap in pure graphene is an important disadvantage in electronics applications. It is proposed that it will be possible to overcome this disadvantage by patterning graphene at sub-20nm scale in order to obtain semiconductor graphene with the appropriate energy band gap. In our laboratory, we are studying on the patterning of CVD synthesized graphene using phase separation of block copolymers (BCP) with specific geometrical arrangement. Important outcomes of this study are going to be the formation of BCP films on graphene in desired dimensions, obtaining phase separation, selective etching of formed BCP films and building graphene nanosequences in certain dimensions for the development of graphene based functional structures for applications in electronics industry.

For the preparation of nano-composites using graphene as nano-filler, the surface of graphene should be modified. For example, the production of transparent conductive graphene films for touch screens, smart windows and other applications, and the dispersion and adhesion of graphene to polymers can be enhanced by the control of surface chemistry of graphene. However, modification of graphene is not easy because of the high energy barriers need to be overcome due to interlayer conjugation and van der Waal forces. In ILTEK laboratory, the rotating-plasma technique is used to change the surface chemistry of graphene. For example, we are able to make the hydrophobic and hydrophilic modification of graphene powders is also able to make by the given method easily, which will open up many more application areas for graphene in composite industry.

**Acknowledgements**

The authors would like to thank the Scientific and Technological Research Council of Turkey (TUBITAK Grant Number 114Z934) for the financial support of this research.

## Encapsulation Of Phase Change Materials To Obtain Novel Switchable Optical Properties

. A.Julià, C.Roscini, D.Ruiz-Molina. (1) ICN2, Passatge Sant Lluís 14 Cornellà de Llobregat, Spain, alex.julia.lolrol@gmail.com

Phase change materials (PCM) are substances that can reversibly change from solid to liquid upon temperature variation. This transition is accompanied by the storage and release of large amounts of heat. These properties make these materials very interesting mainly for their promising benefits in different applications such as energy storage<sup>1</sup> and smart building insulation<sup>2</sup>. However, the phase transition of the PCMs is potentially exploitable also to reversibly tune the optical properties of dispersed dyes that behave differently in the solid and in the liquid phase of the PCM. So far, the only well-known example of temperature dependent optically active systems based on PCM is given by the commercially available thermochromic materials<sup>3</sup>.

Thermochromism is defined as the reversible colour change induced by temperature variations. There are different ways to obtain thermochromic materials<sup>4</sup>. Most of the commercial ones are composed by a pH-sensitive dye (halochromic dye which reversibly isomerizes between a coloured and non-coloured form when subjected to pH changes) dispersed in a PCM matrix. The solid-liquid transition allows or prevents the acid-base reaction between the dye and the PCM (if acidic paraffin) or an acid (colour developer) also dispersed in the matrix. The melting point of the PCM controls the temperature at which the acid-base reaction takes place and therefore the temperature at which the colour change is produced.

To make the thermochromic system functional and reversible, its components must be confined in the same microambient and the mixing with external components (e.g. polymeric matrix) should be avoided. A solution that allows to achieve these conditions is the micro/nanoencapsulation, which gives different advantages: (i) prevents the leakage of the PCM during the phase transition (ii) allows the integration in polymeric materials (iii) permits to preserve the mechanical properties of the material where the capsules are embedded in and (iv) reduces the reactivity with the surrounding media.

In the literature several methods to encapsulate particles, oil droplets or PCMs with polymeric materials, are described.<sup>5</sup> Among all of them, the emulsion-solvent evaporation method is characterized by the absence of chemical reactions in the encapsulation procedure.<sup>6</sup> This is an important advantage, especially in those cases where optically active materials (dyes) need to be encapsulated. These dyes generally possess many functional groups and, therefore, can easily undergo degradation in encapsulation processes involving chemical reactions. This micro/nanoencapsulation process involves a previous formation of oil in water (O/W) emulsion by mixing energetically an organic phase with an aqueous phase. The organic phase is made by a preformed polymer, the organic dye, the PCM and an organic solvent, while the water phase by the surfactant, which avoids the coalescence of the formed droplets. The size of the oil droplets determines the final size of the capsules. The emulsification method is one of the most important factors that determine the size of the emulsion droplets and generally, the higher the applied energy to prepare the emulsion (speed of stirring, method of homogenization, etc.), the smaller are the droplets. After the emulsion formation, the solvent is evaporated and the precipitation of the polymer around the droplets is induced, yielding the final core-shell microcapsules. The Nanosfun group has gained lots of experience in tuning the experimental conditions to obtain core-shell polymeric capsules for industrial applications<sup>6</sup>, from the micro to the nanoscale, applying different emulsification methods, such as magnetic stirring, high-share or ultrasonic homogenization.

In this presentation I will show the development and the optimization of a versatile, easy and scalable synthesis of impermeable, core-shell micro and nanocapsules of PCMs of different nature (hydrocarbon, acidic, etc.) using the emulsion-solvent evaporation method. It will be also showed how these capsules could be used to encapsulate specific dyes to yield temperature switchable optically active materials based on the reversible PCM transition.

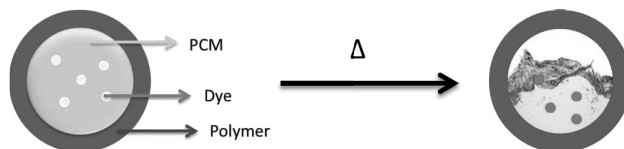


**Figure 1:** Schematic representation of the behaviour of the capsules when the temperature is increased above the melting point of the PCM

[1] A. Barba, M. Spiga *Sol Energy* 2003, 74, 141–148

[2] Y. Zhang, G. Zhou, K. Lin, Q. Zhang, H. Di *Build Environ* 2007, 42, 2197–2209

[3] M.A.White, M. LeBlanc *J. Chem. Educ.* 1999,76, 1201-1205

[4]A. Seeboth, D. Löttsch, R. Ruhmann, O. Muehling *Chem. Rev.* 2014, 114, 3037–3068

[5] A. Jamekhorshid, S. M. Sadrameli, M. Farid *Renew. Sust. Energy Rev.* 2014, 31, 531-542

[6] S. Freitas, HP. Merkle, B. Gander *J. Control Release* 2005, 102, 313-332

[7] N.Vázquez-Mera, C.Roscini, D.Ruiz-Molina *Adv. Opt. Mater.* 2013, 1, 631-636

## Synthesis of Magnetite Pumice Composite and Its Application in Oxidation Processes for Remazole Red Dye Removal

D.I. Çiğci<sup>1\*</sup>, Sureyya Meriç<sup>1</sup>. (1) Department of Environmental Engineering, Çorlu Faculty of Engineering, Namık Kemal University, Çorlu 59860- Tekirdağ, Turkey. (\*) [dicigci@nku.edu.tr](mailto:dicigci@nku.edu.tr); [smeric@nku.edu.tr](mailto:smeric@nku.edu.tr)

Azo dyes which are one of the most widely used in textile industry are mainly characterized by azo linkages and aromatic structure [1]. However, this azo dye containing textile wastewater is not treated with biological treatment and become a significant problem in the environment [2]. Color containing wastewater can be treated with adsorption and advanced oxidation process [3]. Pumice is highly porous materials and could be used as adsorbent or catalyst for removing most of dyes and metal [4].

The main objective of this study is to evaluate the oxidation of an azo dye from aqueous solution using magnetite pumice in the absence and presence of H<sub>2</sub>O<sub>2</sub>. Remazol Red (RR) was chosen as a dye pollutant often used in the textile industry. The effect of initial parameters such as dye concentration, pH, concentrations of H<sub>2</sub>O<sub>2</sub> and magnetite pumice on the removal of azo dye were investigated.

Pumice (particle size <0.125 mm) was provided from Nevşehir, Turkey. In the synthesis of magnetic pumice, FeSO<sub>4</sub>.6H<sub>2</sub>O and FeCl<sub>3</sub>.6H<sub>2</sub>O was first dissolved in 200 mL distilled water with the molar ratio of Fe<sup>3+</sup> to Fe<sup>2+</sup> to be 2 in the solution. Pumice was added to solution with the weight ratio between pumice and iron to be 10. The pH of the solution was adjusted to 9.5 adding 6 N NaOH and while the solution was ultrasonicated for 15 min and mixed for 1 h at 70°C. 5 mL of 30% v/v ammonia solution was added and left at room temperature for 24 h. After pumice adsorbed magnetite iron particles, solution was rinsed several times using distilled water. Latter magnetite pumice was dried at 105°C for 24 h.

Synthesized magnetite pumice and pure pumice were submitted to analyses before and after used scanning electron microscopy (SEM)-energy dispersive X-ray analyzer (EDX) and fourier transform infrared spectroscopy (FTIR) methods before and after experiments.

Batch adsorption experiments were conducted in 100 mL flasks with active volumes of 50 mL that were placed on a rotary shaker (Biosan PSU-10i) at 200 rpm speed and at room temperature. The pH was adjusted to the desired values using 1 N HNO<sub>3</sub> and 1 N NaOH. Samples were taken at a given time intervals during the reaction and centrifuged at 4000 rpm for 5 min. After that the supernatant was analyzed using UV spectrophotometer (Schimadzu UV-2401 PC instrument) at 540 nm. In the oxidation experiments, concentrations of RR concentration, magnetite pumice and pumice alone and H<sub>2</sub>O<sub>2</sub> were ranged in 50-250 ppm, 0.2-10 g/L and 1-5 mM respectively while the initial pH was varied from 2 to 11. Removal efficiency was mainly defined by the removal of maximum absorbance at 540 nm. Demineralization was monitored by TOC (Shimadzu, TOC-L CPH/CPN, SSM 5000A).

According to EDX analysis, pumice mainly contains 60.4% O, 28.3% Si, 6.6% Al, 1.5% K, 2.9% Na and 0.3% Fe [5]. The oxidation efficiency of RR was also drastically higher in magnetite pumice system compared to the pumice alone one in the presence of H<sub>2</sub>O<sub>2</sub>. Furthermore, even adding 1 mM H<sub>2</sub>O<sub>2</sub>, RR removal was 84.2% with magnetite pumice. The removal of RR increased from 72.3% to 90% using magnetite pumice and pure pumice of 0.25 g/L respectively in the presence of 3 mM H<sub>2</sub>O<sub>2</sub> after 2 h oxidation.

The pH, H<sub>2</sub>O<sub>2</sub> and pumice dosage were found to influence the dye removal in oxidation system as indicated by the variation in kinetics. Maximum removal of RR was obtained in the magnetite pumice/H<sub>2</sub>O<sub>2</sub> system at pH 3 as it has been known to be optimum pH in the Fenton based processes [6]. It can be concluded that magnetite pumice composite is a promising and effective as well as low-cost adsorbent and catalyst to remove RR dye from aqueous solution.

### Acknowledgements

This work has been done under the umbrella of COST Action MP1106 and was finally supported by NKU Research Funding Project (NKUBAP.00.17.AR.14.17). Authors acknowledge MSc. Bülent Birden and Soylu L.T.D. for their kind favour to provide pumice.

### References

- [1] S. Karaca, A. Gürses, Ö. Açışlı, A. Hassani, M. Kırınşan, K. Yıkılmaz, *Desalination and Water Treatment*, 51:13-15 (2013) 2726.
- [2] N. Dizge, C. Aydiner, E. Demirbas, M. Kobya, S. Kara, *Journal of Hazardous Materials*, 150:3 (2008) 737.
- [3] N. Azbar, T. Yonar, K. Kestioglu, *Chemosphere* 55:1 (2004) 35.
- [4] M. Kitis, E. Karakaya, N.O. Yigit, G. Civelekoglu, A. Akcil, *Water Research* 39:8 (2005) 1652.
- [5] D.I. Cıfci, S. Meric. *Advances in Environmental Research*, 5:1 (2016) 37.
- [6] A. Babuponnusami, K Muthukumar, *Journal of Environmental Chemical Engineering*, 2:1 (2014) 557.

*Gas handling/Advanced measurements*  
(Chair: M. Antoni)

9:30-9:45	<b>Vollmer</b>	CO <sup>2</sup> capture by superomniphobic membranes
9:45-10:00	<b>Li Puma</b> <b>Gianluca</b>	Ultrafast photochemical transformations of chemical and biological species in microcapillary films photoreactors
10:00-10:15	<b>Staicu</b> <b>Angela</b>	Studies on the laser induced emission of pendant droplets of dye water solutions containing TiO <sub>2</sub> nanoparticles
10:15-10:30	<b>McMillan</b> <b>Norman</b>	Metrological fundamentals for 'true' nanovolume spectroscopy

**CO<sub>2</sub> capturing by robust superomniphobic membranes**

*Doris Vollmer, Florian Geyer, Clarissa Schönecker, Hans-Jürgen Butt Max Planck Institute for Polymer Research, Ackermannweg 10, 55128 Mainz, Germany, vollmerd@mpip-mainz.mpg.de*

Limiting carbon dioxide (CO<sub>2</sub>) emission into the atmosphere to reduce global warming is a major challenge of our times. However, CO<sub>2</sub> capture is at present highly energy consuming and more efficient techniques are required. We develop superomniphobic membranes for enhanced CO<sub>2</sub> absorption. A unique feature of superomniphobic membranes is that the CO<sub>2</sub> capturing solution stays on the topmost part of the membrane, preventing the wetting of the membrane. Wetting would greatly reduce the absorption efficiency. To fabricate mechanically and chemically robust superomniphobic membranes, we coated polyester fabrics with nanofilaments. The uptake of CO<sub>2</sub> in the capturing medium - here a concentrated N-methyldiethanolamine (MDEA) solution - was monitored by infrared spectroscopy. The CO<sub>2</sub> capture rate was enhanced by more than 20% compared to state-of-the-art commercial membranes and showed no decay within 50 hours. We anticipate that this finding will guide the development of the next generation of highly-efficient gas contactor membranes.

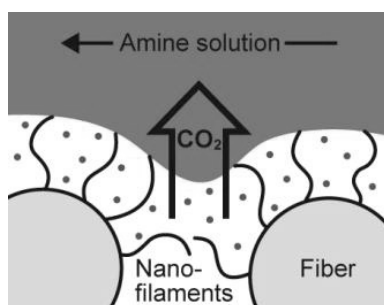


**Figure 1.** Capturing of carbon dioxide

**Acknowledgements**

This work was supported by the ERC advanced grant 340391-SUPRO and the COST action 1106.

**References**

[1] M. Paven *et al.*, Super liquid-repellent gas membranes for carbon dioxide capture and heart-lung machines. *Nature Communications* 4, (2013).

**Ultrafast Photochemical Transformations of Chemical and Biological Species in Microcapillary Films Photoreactors**

*Gianluca LI PUMA\* and Nuno M. REIS Environmental Nanocatalysis & Photoreaction Engineering, Department of Chemical Engineering, Loughborough University, Loughborough LE11 3TU, United Kingdom. Emails: g.lipuma@lboro.ac.uk; n.m.reis@lboro.ac.uk*

A disruptive microfluidics platform technology for extremely fast and efficient phototransformation of chemical and biological species is presented<sup>1</sup>. This is based on the fabrication of fluoropolymer microcapillary films (MCF) which are fully transparent to the entire spectrum of incident light, from the visible to the UVC. The unique fluid-dynamics and optical properties of the MCF makes it ideal for exploring the phototransformation of ECs and controlled substances, for the identification of transformation by-products and for the formulation of reaction mechanisms, particularly from very small volumes of highly-priced chemical compounds.

Six unique properties are exemplified in the MCF: (i) The MCF is fully transparent to visible and UV radiation, including UVC; (ii) The flat surface of the film (Fig. 1b) combined with the excellent optical transparency and low refractive index of fluoropolymers allows the irradiation of the entire volume of the fluid flowing in the microcapillaries with straight incident photon rays, without wall refraction effects (such effect is not realized in glass/quartz tubular photoreactors); (iii) The small capillary diameters permit operation under low optical thicknesses (less than 0.1) with uniform irradiance of the flowing fluid (even for fluids that in conventional reactors appear to be opaque) and the capillary diameters can be fine-tuned to the incident light and its penetration depth; (iv) Fluid behaviour approaches the plug flow regime allowing a tight fluid residence time distribution at the reactor exit, and in consequence (in conjunction with (iii)), high reactants conversions and high products yield and selectivity; (v) The small capillary volumes results in extremely rapid photo-transformations of substrates which are complete in a matter of seconds, a result until now not attainable in other practical photoreactors; (vi) The flexible nature of the MCF make it easily scalable. We demonstrate these capabilities with a range of applications, including the fast photoinactivation of a highly contagious enveloped Herpes HSV-1 virus particles<sup>2</sup>, the fast decolourization of a dye and the photodegradation of contaminants of emerging concern including a pharmaceutical compound (diclofenac) and a class I drug metabolite (benzoylecgonine)<sup>3,4</sup>.

Microstructured reactors and microphotoreactors have been shown in literature to perform photochemical transformations and to outperform classical photoreactor designs, but none of them could accomplish collectively the six unique properties of the MCF photoreaction system described here.

**References**

- [1] Reis, N. M., Li Puma, G., *A novel microfluidic approach for extremely fast and efficient photochemical transformations in fluoropolymer microcapillary films*, *Chem. Commun.* 51 (2015) 8414-8417.
- [2] Ren, Y.; Crump, C.M.; Mackley, M.M.; Li Puma, G.; Reis, N.M. *Photo inactivation of virus particles in microfluidic capillary systems*. *Biotechnology & Bioengineering*, 2016, DOI: 10.1002/bit.25912.
- [3] Russo, D., Spasiano, D., Vaccaro, M., Cochran, K.H., Richardson, S., Andreozzi, R., Li Puma, G., Reis, N.M., Marotta, R., *Investigation on the removal of the major cocaine metabolite (benzoylecgonine) in water matrices by UV254/H<sub>2</sub>O<sub>2</sub> process by using a flow microcapillary film array photoreactor as an efficient experimental tool* *Water Res.*, 89, (2016) 375-383.
- [4] Russo, D., Spasiano, D., Vaccaro, M., Andreozzi, R., Li Puma, G., Reis, N.M., Marotta, R., 2016, 'Direct photolysis of benzoylecgonine under UV irradiation at 254 nm in a continuous flow microcapillary film (MCF) array photoreactor' *Chem. Eng. J.*, 284, pp. 243-250

### Studies on the laser induced emission of pendant droplets of dye water solutions containing TiO<sub>2</sub> nanoparticles

*A. Staicu<sup>1</sup>, M. Boni<sup>1,2</sup>, I. R. Andrei<sup>1</sup>, A. Smarandache<sup>1</sup>, V. Nastasa<sup>1</sup>, Z. Saponjic<sup>3</sup>, M.L. Pascu<sup>1,2</sup>, (1) National Institute for Laser, Plasma and Radiation Physics, Laser Department, Magurele, Romania, (2) Faculty of Physics, University of Bucharest, Magurele, Romania, (3) Vinča Institute of Nuclear Sciences, Department of Radiation Chemistry and Physics, Belgrad, Serbia, angela.staicu@inflpr.ro*

Studies on the emission spectra of microdroplets containing Rh6G solutions in water doped with TiO<sub>2</sub> nanoparticles are here presented. The excitation is made by the second harmonic of a pulsed Nd:YAG laser at 532 nm, pulse duration at half maximum 6ns, energy varied between 6-10mJ. The laser induced emission spectra are analyzed function of TiO<sub>2</sub> concentration, and laser pumping energy. The comparison between emission spectra for pendant droplets containing TiO<sub>2</sub> nanoparticles with respect to the case of Rh6G water solutions droplets pumped in the same conditions is made. In Fig. 1, the emission spectra for excitation energy of 8mJ are shown for pendant droplets of R6G water solutions at  $5 \times 10^{-4}$  M containing TiO<sub>2</sub> nanoparticles at a) 0, b)  $10^{11}$  part/cm<sup>3</sup>, c)  $10^{12}$  part/cm<sup>3</sup> number density. A very interesting behavior of the spectra can be noticed when the TiO<sub>2</sub> number density is  $10^{11}$  part/cm<sup>3</sup>: beside a fluorescence peak placed at longer wavelength (the spectral range 595.3 -599.7 nm), two other bands appear at shorter wavelength and these have quite a strong intensity variation from pulse to pulse.

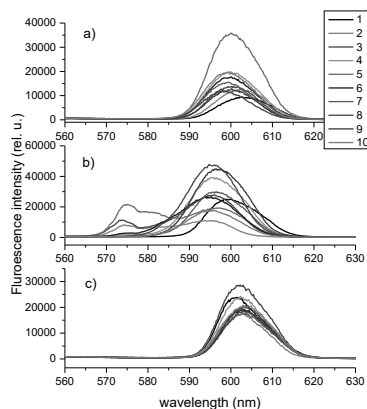


**Figure 1.** LIF spectra of pendant droplets of R6G water solutions at  $5 \times 10^{-4}$  M containing TiO<sub>2</sub> nanoparticles at a) 0, b)  $10^{11}$  part/cm<sup>3</sup>, c)  $10^{12}$  part/cm<sup>3</sup> number density. Excitation at 532 nm, energy 8 mJ

It was observed that the presence in the droplet dye solution of TiO<sub>2</sub> nanoparticles induces emission spectra modifications depending on nanoparticles number density and pumping energy. It can be noted that a concentration of  $10^{11}$  part/cm<sup>3</sup> nanoparticles favors the formation of two other emission bands that are shifted to the blue with respect to the main band. The increase with one order of magnitude of the TiO<sub>2</sub> number density produces the disappearance of these bands, regardless the pumping energy. The main emission band (the one placed at longer wavelength) has first a shift to the blue and then to the red with the increase of nanoparticles concentration. All of these behaviors suggest that the TiO<sub>2</sub> nanoparticles addition to dye droplet solutions has an influence on the emission spectra which can be modulated by varying nanoparticles concentration and pumping energy.

#### Acknowledgements

This work was supported by ANCSI through project number NUCLEU project PN1647/2016 and by the COST Action MP1106 "Smart and green interfaces - from single bubbles and drops to industrial, environmental and biomedical applications (SGI).



**Metrological Fundamentals for 'true' Nanovolume Spectroscopy**

*Norman McMillan, Drop Technology, Tallaght Business Park, Dublin 24, [mcmillan@itcarlow.ie](mailto:mcmillan@itcarlow.ie)*

This study looks at the issue of traceability and other metrological issues for nanovolume spectroscopy giving special consideration to measurements that are below the optical diffraction limit. The author in pioneering nanovolume spectroscopy has confronted the instrumental limitations related to fundamental sample volume for quantitative measurements while attempting to address the technological limitations of the various patented commercial approaches for quantitative spectroscopy on such small micro-volume drop-samples. Despite a marketing coup of using the name nanodrop and notwithstanding the incredible success of this technology's commercialisation which leading position in the laboratory instrument market, none of the products delivering spectra and quantitative measurements on such samples as DNA are truly a nanoscience, quite simply, because the sample volumes are actually microvolumes. It is clear that fundamental spectroscopic and related metrological issues arise when spectroscopy moves below the diffraction limit and the impassable 'concrete wall' for methods based on the Beer Lambert law which presents the real theoretical challenge in front of spectroscopy as the sensitivity of optical detectors make their inexorable advances. The measurement problems are explained and the issue of traceability for nanovolume spectroscopy is addressed. The first approach via the well-established and routine use of traceable standards, the second, via traceability established from the theory to the fundamental optical standards such as Planck's constant. The need then arises directly from the development of this new approach for the traceability of software within these instruments; software traceability is of course a relatively new concern for industries such as the pharmaceutical sector facing the regulatory demands for human health products. The surprising conclusion is that theoretical traceability has revealed a new complex of related and connected metrological issues. It is explained that the technological platform employed for investigating these issues requires a unique theoretically secure methodology underpinning an optimised experimental set-up possessing the sensitivity required to experimentally explore these new metrological questions.

ORAL PRESENTATIONS - 2<sup>nd</sup> DAY

*Feature lecture*  
*(Chair: M. Pascu)*

18:50-19:10

**Balestra** Oxygen breathing doesn't add benefit compared to whole body vibration on  
**Costantino** the reduction of post-dive vascular gas emboli

---

**Oxygen Breathing Doesn't Add Benefit Compared To Whole Body Vibration On The Reduction Of Post-Dive Vascular Gas Emboli**

---

Costantino Balestra<sup>1,3</sup> Sigrid Theunissen<sup>1,1</sup> Haute Ecole Paul-Henri Spaak, Environmental, Occupational & Ageing Physiology Lab., Brussels, Belgium 2 DAN Europe Research, Brussels, Belgium

**Introduction**

In this study a « frame-based » counting method was used to compare the effect of three different pre-dive conditioning on post dive vascular gas emboli (VGE). The three pre-conditioning were 100% normobaric oxygen breathing (Oxygen) by mean of a demand valve regulator, a whole body vibration (Vibration) and the combination of normobaric oxygen breathing and whole body vibration (Oxygen + Vibration).

**Materials and Methods**

Six experienced divers (6 men, 38 ± 5 years old) who consistently showed bubbles post-dive on echocardiograms (repeated control dives at least 3 times) underwent several controlled, standardized, deep pool SCUBA dive (33m, 20min in 33°C) at least one week apart with the different pre-conditioning. Each preconditioning took place 2 h pre-dive and lasted 30 min VGE were counted according to the method described by Germonpre et al in 2014.

**Results**

Each subject acted has its own control and results are expressed as % of individual baseline value. A significant reduction in post dive VGE was observed after Oxygen pre-conditioning (76 ± 18 % of control dive), Oxygen + Vibration pre-conditioning (44 ± 23 %) and Vibration pre-conditioning (15 ± 13 %). Post dive VGE was significantly smaller with Vibration preconditionings compared to Oxygen + Vibration pre-conditioning. Post dive VGE was significantly smaller with Oxygen + Vibration pre-conditionings compared to Oxygen alone pre-conditioning.

**Conclusions**

All three pre-conditioning reduce the VGE. Vibration pre-conditioning is more efficient than Oxygen + Vibration pre-conditioning which is more efficient than Oxygen alone preconditioning.

**References**

Germonpre P, Papadopoulou V, Hemelryck W, Obeid G, Lafere P, Eckersley RJ, Tang MX & Balestra C. (2014). The use of portable 2D echocardiography and 'frame-based' bubble counting as a tool to evaluate diving decompression stress. *Diving Hyperb Med* **44**, 5-13.

Balestra C, Blatteau J, Gempp E & Rozloznik M. (2014). Preconditioning as a tool to improve diving safety. In *The science of Diving : Things you instructor never told you*, ed. Balestra C & Germonpre P, pp. 160-180. Lambert Academic Press, Germany.

## ORAL PRESENTATIONS - 3<sup>rd</sup> DAY

<i>Hall A: Fluid-solid interactions</i> (Chair: Z. Brabcova)		<i>Hall B: Modified solid surfaces</i> (Chair: M. Ersoz)	
10:00-10:15	<b>Liuzzi Roberta</b>	The importance of fluids microstructure in the penetration process for transdermal applications	<b>Stoyanov Simeon</b>
10:15-10:30	<b>Gambaryan-Roisman Tatiana</b>	Simultaneous imbibition and evaporation of liquids in model textured substrate	<b>Mirzaeian Mojtaba</b>
10:30-10:45	<b>Koutsos Vasilcios</b>	Semicrystalline polymers on surfaces: droplets and thin films	<b>Selcuk Huseyin</b>
10:45-11:00	<b>Sicignano Luca</b>	Microfluidics investigation of cluster aggregation in the Buckwald-Hartwig amination reaction	<b>Kiwi John</b>
11:00-11:15	<b>Kumar Abhijeet</b>	Using streaming potential measurements to probe cationic vesicle permeation and deposition on anionic porous substrates	<b>Zhang Zhenyu</b>
			An environmentally benign antimicrobial nanoparticle based on a silver-infused lignin core
			Effect of interfacial processes on the electrochemical properties of carbon based electrodes for supercapacitor applications
			Copper doping on TiO <sub>2</sub> nanoparticles for development of self-cleaning and anti-bacterial cotton fabric
			Self-cleaning processes by polymer/textiles sputtered with semiconductors under sunlight & mild environmental conditions
			Nanotribological properties of biocompatible polyzwitterionic brushes

### The Importance of Fluids Microstructure in the Penetration Process for Transdermal Applications

R. Liuzzi<sup>1,2</sup>, A. Carciati<sup>1,2</sup>, V. Preziosi<sup>1</sup>, S. Caserta<sup>1,2</sup>, S. Guido<sup>1,2</sup>. (1) Department of Chemical, Materials and Production Engineering, University of Naples "Federico II", P.zze Tecchio 80, 80125 Naples, roberta.liuzzi@unina.it (2) CEINGE-Advanced Biotechnologies, Via Sergio Pansini 5, 80131 Naples, Italy

Interaction of microstructured fluids with skin is ubiquitous in everyday life from the application of cosmetics and drugs to personal care. Skin has a complex structure, where the outer layer, the stratum corneum (SC), acts as the main barrier against the entry of external molecules carried by different formulations, generally based on emulsions [1]. Formulations microstructure plays a key role in the penetration process through the SC and can be strongly influenced by emulsification processing, or even by the stress induced during topical application of the product [2]. The effective interaction mechanisms between multiphase fluids and SC is a topic of notable interest and not fully elucidated. The focus of this work is to propose an innovative methodology to investigate the penetration of different compounds through the SC by time-lapse confocal laser scanning microscopy (CLSM) and images analysis. To this aim, we have used an agarose gel as a model system. Localization of the permeating molecule in the gel is possible by properly staining one or more emulsion components with specific dyes or antibodies. Data obtained from diffusion experiments of labeled solutions and emulsions are fitted with a solution of Fick's law, in order to estimate the diffusion coefficient of each molecule. This approach allows to investigate the transport behavior of different formulations, based on their own properties and molecular affinity with the matrix in which they diffuse. The results demonstrate the higher affinity of the water solutions for agarose gels, whereas oil solutions hardly penetrate. Oil-in-water (O/W) emulsions act as penetration enhancer, as also reported in literature. The proposed method can be applied to investigate the effectiveness of transdermal drug delivery as a function of skin morphology, which is directly related to age and body site.

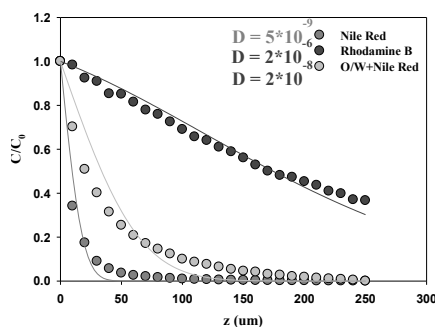


**Figure 1.** Normalized concentrations as function of penetration depth in 2% agarose gel of water and rhodamine (blue), oil and Nile Red (red) solutions and O/W emulsion with Nile Red (gray). Solid lines represent the fit with Fick's solution.

#### References

- [1] R. Liuzzi, A. Carciati, S. Guido, S. Caserta, *Colloids and Surfaces B: Biointerfaces*, 139 (2016) 294-305.
- [2] W. Naoui, M. A. Bolzinger, B. Fenet, J. Pelletier, J.-P. Valour, R. Kalfat, Y. Chevalier, *Pharmaceutical research*, 28 (2011) 1683-1695.

---

**Simultaneous Imbibition and Evaporation of Liquids in Model Textured Substrate**

---

*T. Gambaryan-Roisman, Institute of Technical Thermodynamics and Center of Smart Interfaces, Darmstadt, Germany, [gatiana@itd.tu-darmstadt.de](mailto:gatiana@itd.tu-darmstadt.de).*

Imbibition of volatile liquids on textured surfaces and in porous layers governs heat and mass transport in natural phenomena and in technological applications, including thermal management of electronic devices and ink-jet printing. These processes are responsible for significant improvement of cooling efficiency during drop impact cooling [1] and flow boiling [2] if the surfaces to be cooled are covered by highly porous nanofiber layers.

Prediction of imbibition rate in textured substrates and porous layers, especially in the presence of evaporation, is a very complicated task. The existent imbibition theory for porous media relies on the known capillary pressure and the material permeability and is only applicable for the cases where the imbibition front separates a completely saturated region from a completely dry region. The hydrodynamics and transport processes during imbibition on textured surfaces and porous layers are substantially more complicated and are not completely understood.

In this work a simultaneous imbibition and evaporation in a model textured substrate are described theoretically and numerically. A typical element of the model system is a single groove, along which the liquid flows under the action of capillary pressure gradient. The shape of the cross-section area occupied by the liquid varies along the groove. The shape of the liquid-gas interface and the imbibition rate are determined by the groove geometry, the properties of the liquid, the substrate wettability and the temperature. If the supply of the liquid in reservoir is finite, the initial increasing of the wetted groove length is followed by the decreasing of the wetted length, and the maximal wetted length decreases with increasing of substrate temperature. This trend agrees with the available experimental results on imbibition into porous layers [1].

The presented model is a new step towards development of a general model for prediction of simultaneous imbibition and evaporation on real textured surfaces and porous layers.

**Acknowledgements**

The study has been performed in the framework of the Marie Curie Initial Training Network “Complex Wetting Phenomena” (CoWet), Grant Agreement no. 607861.

**References**

- [1] C.M. Weickgenannt, Y. Zhang, A.N. Lembach, I.V. Roisman, T. Gambaryan-Roisman, A.L. Yarin, C. Tropea, *Phys. Rev. E*, 83 (2011) 036305.
- [2] M. Freystein, F. Kolberg, L. Spiegel, S. Sinha-Ray, R.P. Sahu, A.L. Yarin, T. Gambaryan-Roisman, P. Stephan, *Int. J. Heat Mass Transf.*, 93 (2016) 827.

## Semicrystalline Polymers on Surfaces: Droplets and Thin Films

V. Koutsos. Institute for Materials and Processes, School of Engineering, The University of Edinburgh, King's Buildings, Edinburgh EH9 3FB, United Kingdom, [vasileios.koutsos@ed.ac.uk](mailto:vasileios.koutsos@ed.ac.uk).

Semicrystalline polymers (which display both crystalline and amorphous regions) have a wide range of technological applications in chemical and materials industry. Polyethylene oxide (PEO) is a semicrystalline polymer with important biomedical applications due to its biocompatibility [1] and water solubility [2]. It can be used as a model system to study polymer crystallization in confined spaces and provides opportunities for environmentally-friendly fabrication, based on self-assembly, of advanced (and potentially 'smart') thin films and structures at several scales.

We used drying droplets of PEO solutions (several molecular weights of PEO) to study in some depth the pinning/de-pinning transition which is a determining factor for the final morphology of the deposit. It is well-known that this process can lead to pillar formation under specific conditions [3-5].

We report on the drying process of sessile droplets of aqueous PEO solutions studied by contact angle analysis [6]. Liquid samples were prepared with the same initial concentration of four different molecular weights of PEO. Droplets with initial volumes between 1  $\mu\text{L}$  and 5  $\mu\text{L}$  were left to evaporate while temperature, pressure and relative humidity were kept constant. Residues were formed with either a disk-like puddle or a distinctive tall conical pillar shape. This occurred following a four-stage deposition process: pinned drying, during which the contact line is stationary; pseudo-dewetting, where precipitation is induced by the receding contact line; bootstrap building, during which the liquid droplet is lifted upon freshly-precipitated solid; and late drying.

Contact angle analysis allowed us to monitor all stages during drying and consider transitions between stages for different molecular weights. We illustrate the mechanisms taking place during the crucial stages of pinning and depinning, revealing the effect of adhesion and contact line friction for high molecular weights and its influence on the final morphology of the dried PEO solute. To this end, we performed PEO solution droplet evaporation on PEO films demonstrating the importance of interfacial interaction phenomena. We argue that for high molecular weights the results are compatible with a pinning mechanism based on the inter-digitation of the loops and tails of an adsorbed polymer layer with the polymer gel network inside the droplet that forms as water evaporates (Figure 1).

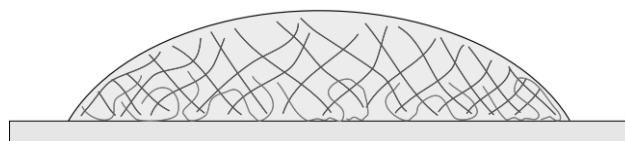


Figure 1. Adsorbed chains interdigitate into the polymer network in the droplet formed as water evaporates.

We also present an atomic force microscopy (AFM) study of the nano/microstructure morphology of pure PEO thin films spin cast on mica from aqueous solutions. Then, we continue with a comprehensive investigation [7] of a series of amphiphilic poly(isoprene-*b*-ethylene oxide) diblock copolymer thin films (with various block fractions) fabricated in the same manner. We show the crucial effect of the PEO crystallization in determining the morphology of the self-assembled structures.

#### References

- [1] V. A. Liu, W. E. Jastromb, S. N. Bhatia, *Journal of Biomedical Materials Research*, 60 (2002) 126.
- [2] E. E. Dormidontova, *Macromolecules*, 35 (2001) 987.
- [3] D. Willmer, K. A. Baldwin, C. Kwartnik, D. J. Fairhurst, *Physical Chemistry Chemical Physics*, 12 (2010) 3998.
- [4] K. A. Baldwin, M. Granjard, D. I. Willmer, K. Sefiane, D. J. Fairhurst, *Soft Matter*, 7 (2011) 7819.
- [5] K. A. Baldwin, D. J. Fairhurst, *Colloids and Surfaces A: Physicochemical and Engineering Aspects*, 441 (2014) 867
- [6] D. Mamalis, V. Koutsos, K. Sefiane, A. Kagkoura, M. Kalloudis, M. E. R. Shanahan, *Langmuir*, 31 (2015) 5908
- [7] M. Kalloudis, E. Glynos, S. Pispas, J. Walker, V. Koutsos, *Langmuir*, 29 (2013) 2339

**Microfluidics Investigation Of Cluster Aggregation In The Buckwald-Hartwig Ammination Reaction**

*Luca Sicignano<sup>1,2</sup>, Giovanna Tomaiuolo<sup>1,2</sup>, Stefano Guido<sup>1,2</sup>. (1) Department of Chemical, Materials and Production Engineering, University of Naples "Federico II", P.zze Tecchio 80, 80125 Naples, luca.sicignano@unina.it Address, (2) CEINGE-Advanced Biotechnologies, Via Sergio Pansini 5, 80131 Naples, Italy.*

Several applications, ranging from petrochemical industry to pharmaceutical processes, involve the use of microfluidics in order to manipulate and study heterogeneous systems under flow<sup>1</sup>. Microfluidics presents many advantages including lower flow rate compared to traditional batches, higher speed of heat and mass transfer, lower waste production and lower costs and operational safety. The main drawbacks to take into account are the lower degree mixing due to the laminar flow conditions typical of microfluidics and solids handling which may lead to clogging<sup>2</sup>. Here, we focus on the Buckwald-Hartwig reaction, widely used in pharmaceutical field for the production of aromatic amines, and recently studied with a microfluidics approach<sup>3</sup>. The aim of this work is to propose an innovative method to investigate the Buckwald-Hartwig reaction and the ensuing kinetics of undesired clusters aggregation (a problem that has not been investigated in the literature) by using a combination of microfluidics and microscopy techniques. Four syringe pumps have been connected to a microreactor made by a stainless steel tube with an inner diameter of 2mm and length of 70cm, at 50°C, where the reaction was run. The microreactor was in turn connected to a glass chip of rectangular shape with micrometric dimensions. Reaction has been followed under an optical microscope equipped with a high-speed camera. Concentration of the product of reaction has been estimated by gas-chromatography and images of cluster formation have been analysed with a commercial software. It was found that cluster aggregation and shape is strongly influenced by the flow rate. In conclusion, this microfluidics setup can be a valid tool to improve drug development and to understand the kinetics of cluster aggregation.

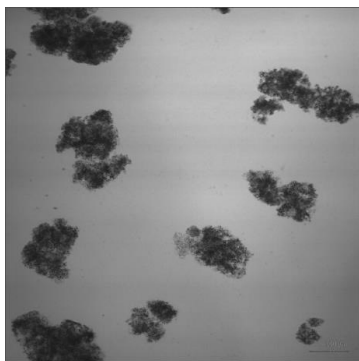


**Figure 1.** Representative image of cluster at 10min.

**References**

- [1] C. Wiles and P. Watts, *Green Chemistry*, 2012, 14, 38-54.
- [2] T. Gudipaty, M. T. Stamm, L. S. Cheung, L. Jiang and Y. Zohar, *Microfluidics and nanofluidics*, 2011, 10, 661-669.
- [3] A. Perazzo, G. Tomaiuolo, L. Sicignano, G. Toscano, R. Meadows, S. Nolan and S. Guido, *RSC Advances*, 2015, 5, 63786-63792.



### Using streaming potential measurements to probe cationic vesicle permeation and deposition on anionic porous substrates

*Abhijeet Kumar<sup>a,b</sup>, Jochen Kleinen<sup>b</sup>, Joachim Venzmer<sup>b</sup>, Tatiana Gambaryan-Roisman<sup>a</sup>,<sup>a</sup> Institute of Technical Thermodynamics & Center of Smart Interfaces, TU Darmstadt, Germany, <sup>b</sup> Research Interfacial Technology, Evonik Nutrition & Care GmbH, Essen, Germany*

Cationic vesicles are important ingredients in personal care, homecare [1], and drug delivery formulations [2] where they are used as vehicles to transport active ingredients to target surfaces. Most of these target surfaces such as textile, hair, and skin have a porous structure. Depending upon the purpose of the formulation, an effective performance requires either low permeation (example: fabric softening) or high permeation (example: drug delivery to skin) of vesicles into the porous substrate. It is thus critical to have a good understanding of the mechanisms which govern the permeation of cationic vesicles into porous substrates.

In this work, we study the interaction of dispersions of cationic vesicle with anionic cotton yarns. The interaction involves simultaneous diffusive transport of the vesicles into the porous substrate, and deposition of vesicles on cotton fibers constituting the yarns. A novel streaming potential method is implemented which enables the post-treatment characterization of the distribution of deposition on external surfaces and the inside of the porous structure. The measurement conditions are optimized to attain the best possible performance of the technique.

Two different types of cationic vesicles, composed of chemically similar lipids, but with contrasting lipid bilayer phase behavior are used. It is identified that the distribution of vesicle deposition across the porous substrate is significantly different for the two vesicle types, with vesicles composed of solid-gel phase bilayers permeating to much lower depths than vesicles composed of liquid-crystalline phase bilayers. The findings can be helpful in designing better performing formulations for a variety of applications.

#### References

- [1] Venzmer, J. Hairs, Cars, Textiles: In Quats We Care, SOFW-Journal, 136-3 (2010), 62-71
- [2] Cevc, G. , Lipid vesicles and other colloids as drug carriers on the skin, Advanced Drug Delivery Reviews 56 (2004) 675–711

---

**An Environmentally Benign Antimicrobial Nanoparticle Based On A Silver-Infused Lignin Core**

---

Alexander P. Richter, Joseph S. Brown<sup>1</sup>, Bhuvnesh Bharti<sup>1</sup>, Amy Wang<sup>2</sup>, Sumit Gangwal<sup>2</sup>, Keith Houck<sup>2</sup>, Elaine A. Cohen Hubal<sup>2</sup>, Vesselin N. Paunov<sup>3</sup>, **Simeon D. Stoyanov**<sup>4,5</sup> and Orlin D. Velev<sup>1</sup>. (1)Department of Chemical and Biomolecular Engineering, North Carolina State University, Raleigh, North Carolina 27695, USA. (2) United States Environmental Protection Agency, Office of Research and Development, RTP, North Carolina 27711, USA. (3) Surfactant and Colloid Group, Department of Chemistry, University of Hull, Hull HU6 7RX, UK. (4) Physical Chemistry and Soft Matter, Wageningen University, Wageningen, the Netherlands, Simeon.Stoyanov@unilever.com. (5) Department of Mechanical Engineering, University College London, Torrington Place, London WC1E 7JE, UK.

Silver nanoparticles have antibacterial properties, but their use has been a cause for concern because they persist in the environment. Here, we show that lignin nanoparticles infused with silver ions and coated with a cationic polyelectrolyte layer form a biodegradable and green alternative to silver nanoparticles. The polyelectrolyte layer promotes the adhesion of the particles to bacterial cell membranes and, together with silver ions, can kill a broad spectrum of bacteria, including *Escherichia coli*, *Pseudomonas aeruginosa* and quaternary-amine-resistant *Ralstonia sp.* Ion depletion studies have shown that the bioactivity of these nanoparticles is time-limited because of the desorption of silver ions. High-throughput bioactivity screening did not reveal increased toxicity of the particles when compared to an equivalent mass of metallic silver nanoparticles or silver nitrate solution. Our results demonstrate that the application of green chemistry principles may allow the synthesis of nanoparticles with biodegradable cores that have higher antimicrobial activity and smaller environmental impact than metallic silver nanoparticles.

**Effect of Interfacial Processes on the Electrochemical Properties of Carbon Based Electrodes for Supercapacitor Applications**

M. Mirzaeian<sup>1</sup>, Q. Abbas<sup>1</sup>, A. A. Ogwu<sup>1</sup>, E. Mileva<sup>2</sup>, D. Arabadzhieva<sup>2</sup>, S. Aidarova<sup>3</sup>.

(1) School of Engineering & Computing, University of the West of Scotland, Paisley, PA1 2BE, UK,

mojtaba.mirzaeian@uws.ac.uk

(2) Institute of Physical Chemistry, BAS, "Acad.G.Bonchev" Str., bl.11, Sofia 1113, Bulgaria.

(3) Kazakh National Research Technical University, 22a Satpaev Street, 050013, Almaty, Kazakhstan.

Due to their coexisting larger power and energy densities electrochemical capacitors (ECs) will play a vital role in continuously increasing global demand on electrical energy [1]. As a result, breakthroughs in novel functional electrode materials which allow the development of high performance ECs with high energy and power densities to meet our future energy demands become indispensable.

Owing to their low cost, ease of production in large scale and also simplicity in the control of their porosity during the synthesis process, activated carbon aerogels obtained by the carbonization and activation of resorcinol formaldehyde gels are widely used for supercapacitor applications [2].

Several parameters influence the performance of these carbons when used as electroactive materials for supercapacitors. In this study composite electrodes based on these porous activated carbons are fabricated and their wettability by different electrolytes (Figure 1) and also diffusion of electrolytes into their porous structure are investigated by scanning electron microscopy (SEM) and contact angle measurements.

Electrochemical impedance spectroscopy (EIS) measurements are also used to further study the interfacial changes occurring on the internal surface of electrodes during charge/discharge processes and understand the effect of electrode's porous, structural and surface characteristics on the electrode/electrolyte contact resistance in an electrochemical capacitor.

The results show that the cell's charge-transfer resistance decreases with increasing electrode's pore size as a result of increase in ionic conducting paths within the electrode structure. The *in-situ* electrochemical impedance spectroscopy of the electrodes showed that the interfacial resistance of the electrode,  $R_{int}$ , passes through a minimum at an optimum pore size in the range of 4-6 nm. Electrodes with pores size smaller than this range showed high interfacial resistances due to the high volume of inaccessible micropores contained within their structure. For electrodes with pore sizes above the optimum range, 'pore flooding' and decrease in the electrode conductivity result in increase in the interfacial resistances. These results are further confirmed by the correlation of SEM and contact angle measurements data with EIS measurement results and electrodes porous and surface properties.

The results of FTIR and contact angle measurements also show that nitrogen doping improves electrode/electrolyte contacts improving charge transfer and storage on the electrodes. This is in addition to increase in the specific capacitance due to a greater amount of charge displaced at nitrogen sites during the charge-discharge process, coupled with enhanced electron conductivity through the carbon matrix [3].

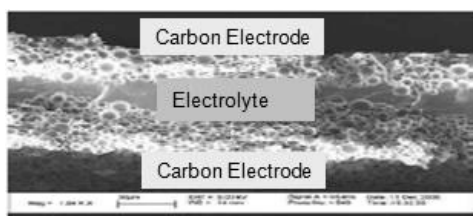


Figure 1. SEM image of electrode/electrolyte contact

**Acknowledgements**

This work has been performed under the umbrella of COST Action MP1106.

**References**

- [1] C. Zhong, Y. Deng, W. Hu, J. Qia, L. Zhangd, J. Zhang, *Chem. Soc. Rev.*, 44 (2015) 7484.
- [2] M. Mirzaeian, P. J. Hall, *J. Mater. Sci.*, 44 (2009) 2705.
- [3] B. Li, F. Dai, Q. Xiao, L. Yang, J. Shen, C. Zhang, M. Cai, *Energy Environ. Sci.*, 9 (2016) 102.

## Copper Doping on TiO<sub>2</sub> Nanoparticles for Development of Self-Cleaning and Anti-Bacterial Cotton Fabric

M.I. Aydın<sup>1</sup>, B. Yüzer<sup>1</sup>, H. Selçuk<sup>1</sup> (1) Department of Environmental Engineering, Faculty of Engineering, Istanbul University, Avcılar, Istanbul, Turkey

The performance of a photocatalytic film depends on the structural, optical and morphological properties of particles [1]. Nature of particles in a solution and on the substrate surface is one of the important points to get an efficient film. Doping TiO<sub>2</sub> with metals ions has been demonstrated as an effective method to enhance its photocatalytic/self-cleaning properties [2]. In this study, Cu-doped TiO<sub>2</sub> sol-gel was coated on the cotton textile surface under different conditions to develop antibacterial cotton textile. Antibacterial performance of modified textile was determined against *E. coli* and *S. aureus* bacteria.

TiO<sub>2</sub> NPs are prepared by sol-gel method using Titanium isopropoxide (TTIP) as described in the literature [3].

Sol-gel methods were performed under different Cu(II) concentrations to investigate dose-response relationship of Cu-Doping with antibacterial and self-cleaning properties of textile fabric.

Dipping method was used to coat both fabrics and titanium foils. After drying at the room temperature, coated substrates are heated between 70-400°C in a furnace for calcination of the film. As textile fabric is a thermally sensitive surface, coated cotton fabrics are heated between 25-100°C to activate nanofilm.

Calcined foil electrodes are used for the determination of photocatalytic (PC) and photoelectrocatalytic (PEC) properties of Cu-doped TiO<sub>2</sub> nanofilms.

Zeta potential, particle size, UV-Vis wavelength scan, XRF, XRD, SEM are measured to evaluate structural, morphological and optical properties of Cu-Doped nanofilms.

Metallization of semi-conductors occurs with increasing of the metal dose. This causes reduced photocurrent values and blocks the photocatalytic properties of TiO<sub>2</sub>. In this study, it is observed that photocurrent still observable at %3 Cu dose (Figure 1). In conclusion, modified surface still suitable self-cleaning function. Otherwise increasing Cu dose also increased anti-bacterial properties of cotton fabric (Figure 2).

UV-Vis analyses exhibit that Cu-Doping changes light absorption range of TiO<sub>2</sub>. Colour of the Cu-Doped NPs was observed to be light yellow, thus coating with Cu-Doped TiO<sub>2</sub> NPs results no colour change on the yellow cotton fabrics. Color of the TiO<sub>2</sub> NPs are important for textile industry as the colour change is not acceptable for commercial textile products.

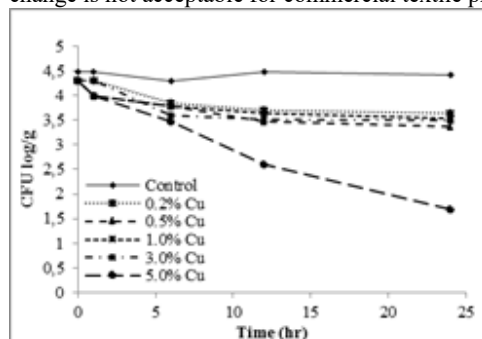


Figure 1. PEC properties of TiO<sub>2</sub> NPs with different Cu doses.

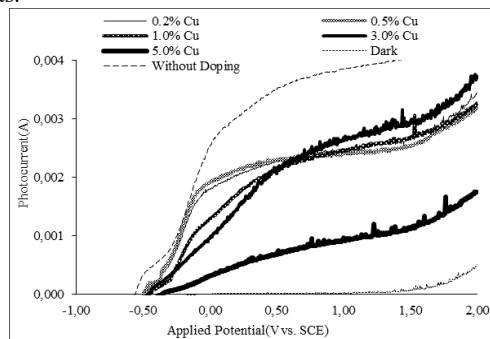


Figure 2. Anti-bacterial property of Cu-Doped TiO<sub>2</sub> NP coated fabrics

### Acknowledgements

This work has been done with the support of The Scientific and Technological Research Council of Turkey (TÜBİTAK), Project Number 108M211.

### References

- [1] T. Yuranova, A.G Rincon, C. Pulgarin, D. Laub, N. Xantopoulos, H.-J. Mathieu, J. Kiwi, *Journal of Photochemistry and Photobiology A: Chemistry*, 181:2-3 (2006) 363-369.
- [2] H. Selçuk, W. Zaltner, J.J. Sene, M. Bekbolet, M.A. Anderson, *Journal of Applied Electrochemistry*, 34:6 (2004) 653-658.
- [3] A. Atyaoui, L. Bousselmi, H. Cachet, et al. *J. Photoch. Photobio. A*, 224 (2011) 71-79.

**Self-Cleaning Processes by Polymer/Textiles Sputtered with Semiconductors under Sunlight & Mild Environmental Conditions**

*John Kiwi, Sami Rtimi, Cesar Pulgarin - Ecole Polytechnique Fédérale de Lausanne, EPFLSB-ISIC-GPAO, Station 6, CH-1015, Lausanne, Switzerland, john.kiwi@epfl.ch*

During the last few years work on self-cleaning of commercial thin and flexible polymers as polyethylene and artificial fiber based textiles like polyester has gained increased attention. The modification of polymers/textiles by nano-particulate uniform, adhesive, robust and stable films that will self-clean the substrate surfaces in acceptable times is a subject of current research. The self-cleaning should proceed in a repetitive way under low intensity sunlight using air ( $O_2$ ) and  $H_2O$ . This avoids the expense related to the present commercial cleaning processes requiring materials, facilities, labor and energy costs.

Polyethylene- $TiO_2$  (PE- $TiO_2$ ) transparent, non-scattering uniform sputtered films have been deposited on RF-pretreated PE. They have shown to be effective in the discoloration of methylene blue (MB) taking as probe under low intensity sunlight irradiation. RF-pretreatment increasing the surface bonding sites allowed the grafting of enough  $TiO_2$  on the PE surface. The transformation of the hydrophobic to hydrophilic site occurred concomitant to MB discoloration under light and reverse photo-switching was observed in the dark taking longer times. Evidence for the interfacial charge transfer (IFCT) between MB and  $TiO_2$  is described taking into account the relative positions of the  $TiO_2$  and MB potential band energies. This allows suggesting a self-cleaning mechanism in Figure 1. The MB discoloration occurred within 120 min [1].

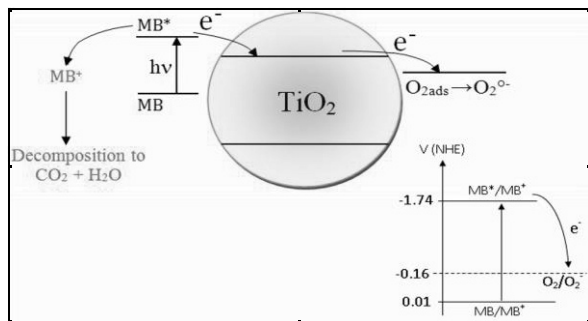


**Figure 1.** Schematic discoloration mechanism of MB on PE- $TiO_2$  films induced by low intensity sunlight.

To accelerate the MB-degradation kinetics, adhesive  $TiO_2$ - $ZrO_2$  films were co-sputtered on polyester (PES) and later decorated with ppb amounts of Cu. The  $TiO_2$ - $ZrO_2$  films discolored the MB under sunlight within 60-90 min.  $Ti_2ZrO_2$ -Cu films on PES discolored the MB within 30 min. The microstructure of the  $TiO_2$ - $ZrO_2$  is still a controversial subject and the ppb amounts sputtered of Cu improved the optical absorption of the  $TiO_2$ - $ZrO_2$  films providing intra-gap states for the transition of the hole from the vb to the cb in the  $TiO_2$ . The band gap of the  $TiO_2$ - $ZrO_2$ -Cu (2.25 eV) films were determined to be smaller compared to  $TiO_2$  (3.1 eV) and  $TiO_2$ - $ZrO_2$  (2.47 eV) by Tauc's method. An IFCT mechanism is suggested discussing the interaction of MB and  $TiO_2$ - $ZrO_2$ -Cu and the possible position of the Cu intra-gap states [2].

**Acknowledgements**

We wish to thank the EPFL and the EC7th Limpid FP project (Grant No 3101177) for financial support and the COST Action MP1106 for interactive discussions.

**References**

- [1] S. Rtimi, C. Pulgarin, R. Sanjines, J. Kiwi, *Appl. Cat B*, 162 (2015) 236 [2]  
 S. Rtimi, C. Pulgarin, R. Sanjines, J. Kiwi, *Appl. Cat B*, 180 (2016) 648

## Nanotribological Properties of Biocompatible Polyzwitterionic Brushes

Zhenyu J. Zhang,<sup>1,\*</sup> Mark Moxey,<sup>1</sup> Abdullah Alswieleh,<sup>1</sup> Andrew J. Morse,<sup>1</sup> Steven P. Armes,<sup>1</sup> Andrew L. Lewis,<sup>2</sup> Mark Geoghegan,<sup>3</sup> and Graham J. Leggett<sup>1</sup> (1) Department of Chemistry, University of Sheffield, Brook Hill, Sheffield, S3 7HF, UK, [z.j.zhang@bham.ac.uk](mailto:z.j.zhang@bham.ac.uk) (2) Biocompatibles UK Ltd., Chapman House, Farnham Business Park, Weydon Lane, Farnham, Surrey, GU9 8QL, UK, and (3) Department of Physics & Astronomy, University of Sheffield, Sheffield S3 7RH, UK \* Present address: School of Chemical Engineering, University of Birmingham, Birmingham B15 2TT, UK

## BACKGROUND:

Polymer brushes are an important smart coating in many applications due to their ability to modify surface properties and enhance biocompatibility. The frictional properties of polymer brushes is of great interest because they can act as lubricants in good solvent conditions.

## OBJECTIVES:

We intend to measure the nanotribological properties of polymer brushes to examine their potential as smart surface coating upon exposure to external stimuli.

## METHODS:

Friction force microscopy (FFM), a variant of Scanning Probe Microscopy (SPM), has been introduced to quantitatively examine the mechanical properties of surface grown zwitterionic polymer brushes: poly(2-(methacryloyloxy)ethyl phosphorylcholine) (PMPC).

## RESULTS &amp; CONCLUSION

## 1. Effect of molecular weight and solvent on the frictional properties

In a good solvent, it was found that the coefficient of friction ( $\mu$ ) decreased with increasing film thickness. We conclude that the amount of bound solvent increases as the brush length increases, causing the osmotic pressure to increase and yielding a reduced tendency for the brush layer to deform under applied load [1,2]. When measured in a series of alcohol/water mixtures, a significant increase in  $\mu$  was observed for ethanol/water mixtures at a volume fraction of 90%. This is attributed to brush collapse due to cosolvency, leading to loss of hydration of the brush chains and hence substantially reduced lubrication (Figure 1). Such a result is in agreement with recent ellipsometric studies of PMPC brushes [3]. FFM has also been used to demonstrate that PMPC brushes exhibit different frictional properties depending on the medium (methanol, ethanol, 2-propanol, and water) in which the measurement was made.

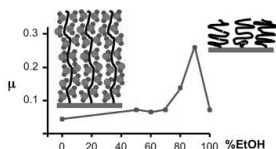


Figure 1. Frictional coefficient of surface grafted PMPC brush changes as a function of ethanol fraction.

## 2. Frictional properties as a function of structure and density of polymer brushes

To develop design principles for the construction of molecular objects at the nanometre scale, photolithography was utilized to facilitate the growth of polymer brushes that are patterned on different length scales. Structures were formed on surfaces that exhibited varying densities of initiator sites. Using AFM, it was possible to measure the effect of the initiator density on both the heights and the frictional properties of the resulting nanostructured brushes. The coefficient of friction was found to decline as the brush height increased, with a smooth variation in both parameters being observed as a function of the density of initiator sites [4].

## References

- [1] Z. Zhang, A. J. Morse, S. P. Armes, A. L. Lewis, M. Geoghegan, and G. J. Leggett, *Langmuir* 27, 2514 (2011)
- [2] Z. Zhang, A. J. Morse, S. P. Armes, A. L. Lewis, M. Geoghegan, and G. J. Leggett, *Langmuir* 29, 10684 (2013)
- [3] S. Edmondson, N. T. Nguyen, A. L. Lewis, and S. P. Armes, *Langmuir* 26, 7216 (2010)
- [4] Z. Zhang, M. Moxey, A. Alswieleh, S. P. Armes, A. L. Lewis, M. Geoghegan, and G. J. Leggett *To be submitted*

## HALL A - DROPLETS ON SURFACES (2)

*Hall A: Droplets on surfaces (2)*  
*(Chair: C. Trabi)*

<i>11:45-12:00</i>	<b>Chamakos Nikolaos</b>	Modeling of droplet mobility on bio-inspired asymmetrically structured substrates
<i>12:00-12:15</i>	<b>Kalić Karolina</b>	“Kerberos”: A three camera headed (X-Y-Z) centrifugal device for studying liquid spreading on solid substrates under the influence of varying body forces
<i>12:15-12:30</i>	<b>Rednikov Alexey</b>	Computation of contact angles for perfectly wetting sessile drops evaporating into vapor on substrates of finite thermal conductivity
<i>12:30-12:45</i>	<b>Pascu Mihail</b>	Modification of wetting properties of phenothiazines water solutions exposed to laser radiation in hypergravity conditions
<i>12:45-13:00</i>	<b>Perrin Lionel</b>	Effect of silver nanoparticles on the wetting and the evaporation of water sessile droplets for different substrates

**Modeling of Droplet Mobility on Bio-inspired Asymmetrically Structured Substrates**

*Nikolaos T. Chamakos<sup>1</sup>, George Karapetsas<sup>1</sup> and Athanasios G. Papathanasiou<sup>1</sup>. (1) School of Chemical Engineering, National Technical University of Athens, 15780, Greece, [nhamakos@mail.ntua.gr](mailto:nhamakos@mail.ntua.gr)*

Nature abounds with micro- and nano-structured advanced functional surfaces, featuring fascinating or even enviable properties. In particular, the asymmetrically structured wings of the Morpho aega butterfly have the ability to keep water droplets away from its body, providing flying stability [1]. Similar paradigms of functional surfaces, which facilitate uni-directional droplet transport, have also recently discovered on the skin of the bonnethead shark, on the silk of cribellate spider, etc.

The above characteristics have attracted considerable scientific interest over the last years due to their potential use for passive directional droplet transfer in modern miniaturized devices (e.g. lab-on-a-chip) [2]. In particular, aiming to design substrates with controllable wetting properties, researchers have focused on investigating the effect of the roughness asymmetry on the dynamic behavior of impinging droplets. Such a study is however hindered by the limited capabilities of the conventional modeling approaches for predicting the droplet dynamics on complex substrates. The above limitation originates from the contentious issue of imposing a boundary condition at the contact line (where the three different phases, liquid-solid-ambient meet), when using continuum-level approaches. In particular, an *a priori* unknown number of contact lines can be formed due the presence of air inclusions trapped in the structure of the solid surface.

In this work we use a recently proposed continuum level scheme [3, 4] for modeling the dynamics of droplets on asymmetrically patterned substrates. The efficiency of our formulation is attributed to the fact that the dynamic contact angle is not imposed explicitly but implicitly emerges as a result of the liquid/solid micro-scale interactions, capillary pressure and viscous stresses at the contact line. The absence of the explicit implementation of the contact angle boundary condition renders our model particularly powerful in cases where the droplet forms reconfigurable three-phase contact lines (e.g. droplet motion on a structured solid surface).

By carrying out detailed simulations, we predict droplet sliding velocities and contact angle hysteresis, and their dependence on the surface corrugations tilt (the source of asymmetry) (Figure 1a). We also examine cases where the droplet displacement is induced by forced vibrations of the solid substrate (Figure 1b). In the latter case, we predict migration velocities and resonance frequencies for maximizing speed, for vertical or horizontal solid surface vibrations.

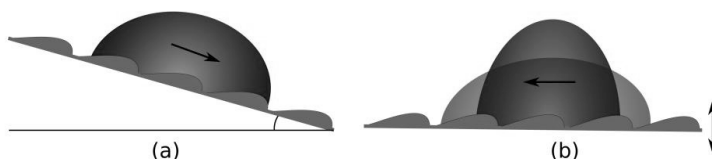


**Figure 1.** Schematic of a droplet moving (a) on an inclined and (b) on a vertically vibrated asymmetrically structured solid surface.

**Acknowledgements**

The authors kindly acknowledge funding from the European Research Council under the Europeans Community’s Seventh Framework Programme (FP7/2007-2013)/ERC grant agreement no. [240710].

**References**

- [1] Y. Zheng, X. Gao and L. Jiang, *Soft Matter*, 3 (2007) 178–182.
- [2] Y. Temiz, R. D. Lovchik, G. V. Kaigala and E. Delamarche, *Microelectronic Engineering*, 132 (2015) 156–175.
- [3] N. T. Chamakos, M. E. Kavousanakis, A. G. Boudouvis and A. G. Papathanasiou, *Physics of Fluids*, 28 (2016) 022105.
- [4] G. Karapetsas, N. T. Chamakos and A. G. Papathanasiou, *Journal of Physics: Condensed Matter*, 28 (2016) 085101.



---

**“Kerberos”: A three camera headed (X-Y-Z) centrifugal device for studying liquid spreading on solid substrates under the influence of varying body forces**


---

K. Kalić<sup>1</sup>, S. Evgenidis<sup>1</sup>, M. Kostoglou<sup>1</sup>, T. Karapantsios<sup>1</sup>, Aristotle University of Thessaloniki, Thessaloniki 54124  
 Aristotle University of Thessaloniki, Thessaloniki, Greece, Division of Chemical Technology, karolinak@chem.auth.gr

Wetting behavior of liquids in contact with solid substrates plays an important role in different industrial processes. In many of these processes external forces are applied to a liquid, and in this case, the proper term to describe the process is either forced wetting or spreading. Until now, the tilted plate method has been used extensively [1] to identify the force necessary to move a liquid droplet on a solid surface, to measure contact angles as well as to monitor changes of contact line and droplet shape evolution. The above quantities have been customary used to characterize spreading properties of a liquid on a solid surface. There have been several experiments where, as external force, centrifugal force was applied on a droplet [2 – 4]. By varying the tilt angle of the solid surface with respect to the direction of the centrifugal force, the latter decomposes to a variety of combinations of normal and tangential components as regards to the main axis of symmetry of a droplet lying on a surface.

In this work, different tilted plate and centrifugal force experiments are reviewed first. The review of theoretical work indicated that there is a serious controversy between attempts to correlate these experiments with theory [4]. Due to this controversy and the lack of good quality data to solve it, the need for a new experimental measurements and a new theory arises.

The ability to control the magnitude and orientation of external forces would offer new opportunities in understanding liquid spreading dynamics. On this account, a new centrifugal device has been developed, Figure 1, that allows experiments with independent control of normal and tangential forces acting on a droplet that stands initially still on a surface.

This innovative technique allows experiments with droplets on plain surfaces, but also with droplets on morphologically complex surfaces including porous substrates. A simplified 2D theoretical approach has been developed for designing experiments that can assess these controversial matters. Furthermore, detailed 3D computations are on the way for describing the equilibrium state of a droplet (3D shape and conditions to start sliding). An overview of the new device and the suggested theoretical approach is outlined.

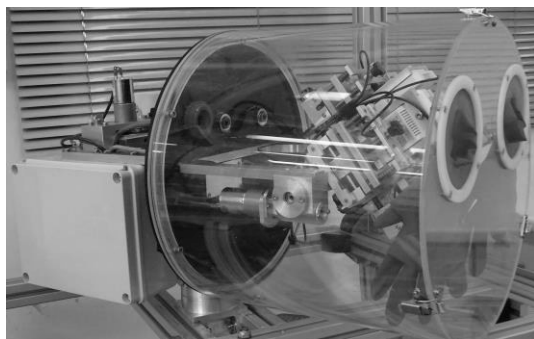


**Figure 1.** Experimental part of the device (rotating unit)

#### Acknowledgements

Authors would like to thank Mr Triantafyllos Tsilipiras and Mr Ilias Papianos for their help in developing Kerberos. This work was done in the framework of the Marie Curie Initial Training Network “Complex wetting Phenomena” (CoWet), Grant Agreement no. 607861.

#### References

- [1] A.I. ElSherbini, A.M. Jacobi, *Journal of Colloid and Interface Science* 273 (2004) 556.
- [2] C. W. Gestrland, A. N. Gent, *Journal of Colloid and Interface Science* 138 (1990) 431.
- [3] M. Higashine, K. Katoh, T. Wakimoto, T. Azuma, *Journal of the Japanese Society for Experimental Mechanics* 8 (2008) 49.
- [4] R.Tadmor, P. Bakadur, A. Leh, H. E. N’guessan, R. Jaini, L. Dang, *Physical Review Letters* 103 (2009) 266101.

**Computation Of Contact Angles For Perfectly Wetting Sessile Drops Evaporating Into Vapor On Substrates Of Finite Thermal Conductivity**

A. Rednikov, P. Colinet, TTPs Laboratory, Université Libre de Bruxelles, 50 Av. F.D. Roosevelt, CP. 165/67, 1050 Brussels, Belgium, aredniko@ulb.ac.be

The present theoretical and parametric study deals with evaporation of a sessile droplet of a one-component liquid into its pure vapor from a massive superheated solid substrate (Figure 1 left), a configuration originally and thoroughly studied in [1]. However, unlike [1] where the contact angles  $\theta$  were given (viz. the Young's angles), here the liquid is assumed to be perfectly wetting (i.e. zero Young's angles). In these circumstances, finite apparent contact angles  $\theta$  are due to evaporation itself [2], hence a non-trivial feedback within the overall configuration since the evaporation rates in turn depend on  $\theta$ . On the other hand, the values of  $\theta$  obtained here typically prove to be sufficiently small, which is made use of in the developed analysis (lubrication hypothesis for the droplet shape).

The evaporation-induced apparent contact angles are established in a small vicinity of the contact line, referred to as the "microregion", where macroscopic contact-line singularities (here first of all the divergence of the evaporation flux) are regularized by means of certain microphysics effects. In the present study, a regularization based solely on the Kelvin effect (curvature dependence of the saturation conditions) is assumed [2].

Two distinguished cases are established. In the first one (I), which takes place for not so large ratios of the solid-to-liquid thermal conductivities, temperature gradients in the substrate are essential already at the scale of the microregion, not to mention the scale of the droplet as a whole. In this case, a new model of evaporation-induced contact angles is developed, which proves to have similar mathematical features with the one for a diffusion-limited evaporation into an inert-gas atmosphere recently considered by the present authors. The other distinguished case (II), taking place for sufficiently large thermal conductivity ratios, corresponds to local substrate isothermia within the microregion, yet still with essential global temperature variations at the droplet scale. In this case, the model for evaporation-induced contact angles is a standard one [2], while the novelty consists in a newly developed asymptotic (multiscale) approach to account for the microregion influence on the global temperature field. At last, the limit of a globally isothermal substrate ensues from this latter case as the thermal conductivity ratio tends to infinity.

Mathematically, the problems and sub-problems treated here are quasi-steady and based upon the lubrication film equation coupled with the heat conduction (Laplace) equation in the solid substrate, whose solutions are obtained numerically whenever necessary. Some results are shown in Figure 1 (right).

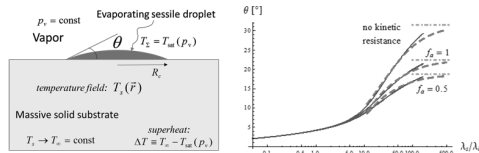


**Figure 1.** (Left) Configuration studied. (Right) Contact angles (computed) of a sessile droplet of HFE-7100 of a contact radius 1 mm on a solid substrate with a global superheat of 1 K at 1 atm as a function of the solid-to-liquid thermal conductivity ratio. The three groups of curves (upper, middle and lower) correspond, respectively, to three different values of the kinetic resistance to evaporation (see e.g. [2] for its expression): zero kinetic resistance, a non-zero one with a so-called accommodation coefficient equal to unity (ideal case), and the one equal to 0.5. Within each group, the solid (blue), dashed (red) and dot-dashed (green) curves correspond, respectively, to calculations carried out in framework of the distinguished case I (valid for not too large ratios), the distinguished case II (valid for sufficiently large ratios), and a completely isothermal substrate (valid in the limit of infinite thermal conductivity).

**Acknowledgements**

Support from BELSPO and ESA PRODEX projects and from F.R.S.—FNRS is gratefully acknowledged.

**References**

- [1] S.S. Sadhal, M.S. Plesset, *J. Heat Transfer*, 101 (1979) 48.
- [2] P. Colinet, A. Rednikov, in *Droplet Wetting and Evaporation*, D. Brutin (Ed.), Springer-Verlag, 2015.

**Modification of wetting properties of phenothiazines water solutions exposed to laser radiation in hypergravity conditions**

*M.L.Pascu\**, A. Simon, T. Tozar, A. Stoicu National Institute for Lasers, Plasma and Radiation Physics, 409 Atomistilor Street, 077125 Magurele, Romania, [Mihai.pascu@infpr.ro](mailto:Mihai.pascu@infpr.ro)

Since multiple drug resistance evolved continuously, the interest in developing new strategies to fight it has significantly increased. Therefore, it became crucial to discover new medicines or to improve the action of the existing ones. The employment of UV laser beams provides a new platform for these requirements, by inducing structural changes at molecular level of photosensitive non-antibiotics. A proposed method consists in the exposure of medicine solutions to laser radiation, obtaining in this way new photoproducts with possible antimicrobial activities. This is the case of phenothiazines, reported in this paper.

The aim of the experiments is to investigate the interaction of non-irradiated and laser irradiated medicine solutions with different target surfaces under hypergravity conditions, by generating pendant droplets and measuring the contact angles of sessile drops formed at liquid-solid-air interface. In biomedical applications the wetting processes play a decisive role; for this reason the wettability of target surfaces and the accumulation of medicine solutions in them is studied at different hypergravity levels. Impregnation of these surfaces with such solutions is important in developing new delivery procedures of medicines to target tissues. On the other hand, it has been evidenced that several bacteria can survive and are able to proliferate at high g-levels, thus threatening spacecraft's walls and components. The wettability of such surfaces by non-antibiotic solutions was also studied under the effect of increased gravity. This should be investigated since the use of medicines is always made after they transit hypergravity conditions at launching and landing. During the flight the medicines may be used in microgravity conditions, but even then, they are in a shape resulting after crossing hypergravity conditions.

In Figure 1 are given, as an example, the values of contact angles of chlorpromazine (CPZ) 2mg/ml water solutions at hypergravity level 2g with activated charcoal, when samples are presented as 3.1 µl droplets which contain unirradiated solution or solution exposed to 266 nm laser beam. The measurements are made in real time, in the first 400 ms after droplet generation.

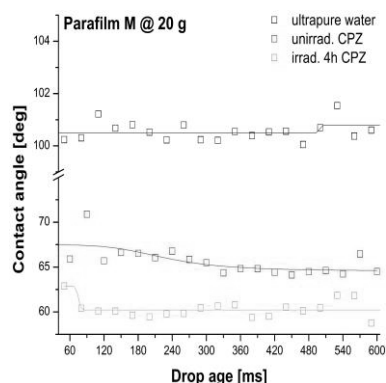


**Figure 1.** Contact angles evolution of CPZ at 2g on activated charcoal, function of droplet's age.

One may observe that the contact angles values for 4 hours irradiated CPZ are intermediate between those of pure water and unexposed CPZ water solution. Modifications of the values of contact angles on cotton, parafilm and even Aluminum when the same kind of solutions are placed in hypergravity conditions between 2g and 20g are also evidenced.

**Acknowledgements**

This work was supported by ANCSI through project number NUCLEU project PN1647/2016 and by the COST Action MP1106 "Smart and green interfaces - from single bubbles and drops to industrial, environmental and biomedical applications (SGI).

**Effect of Silver Nanoparticles on the Wetting and the Evaporation of Water Sessile Droplets for Different Substrates**

*L. Perrin<sup>1</sup>, A. Pajor-Swierzy<sup>2</sup>, R.G. Rubio<sup>3</sup>, F. Ortega<sup>1</sup>, S. Magdassi<sup>2</sup>, M.G. Velarde<sup>3</sup>. <sup>(1)</sup> Department of Chemistry, University Complutense of Madrid, Madrid, Spain, lperrin@ucm.es. <sup>(2)</sup> Casali Center for applied Chemistry, Hebrew University of Jerusalem, Israel. <sup>(3)</sup> Jerusalem, Pluridisciplinar Institut, University Complutense of Madrid, Madrid, Spain.*

The evaporation of drop on surfaces is present in many industrial and medical applications, e.g. printed electronics, spraying of pesticides, spray cooling, DNA mapping, etc. Despite this strong interest, the dynamics of evaporation of complex liquid mixtures and suspensions remains not fully understood. Indeed, one of the issues not included in the current theoretical descriptions is the adsorption of surfactants and/or particles at the liquid/vapor and liquid/solid interfaces during the evaporation process.

The lifetime of a sessile droplet occurs in several steps. It starts with a stage of spreading followed by three different stages of evaporation. A first stage, where the contact line remains constant with a contact angle that decreases from an advancing to a receding contact angle. Then a second stage of evaporation where the contact line reduces with constant contact angle, and finally a third stage where these parameters decrease simultaneously until the droplet completely disappears.

In this work the effect of hydrophobized silver nanoparticles on the wetting and evaporation of water sessile droplets has been studied in the ambient conditions of temperature and relative humidity. A droplet of complex liquid was deposited on a substrate and the evolution of contact line, height and contact angle were simultaneously determined using to a droplet shape analyzer. Special care was taken regarding the initial maximum volume of the droplet to ensure that the effect of gravity was negligible so that the droplet has a spherical cap shape. The values of the advancing and receding contact angles for several particle suspensions on different substrates were obtained. Also, the mixtures of the particles and a surfactant were studied. Mixtures of particles and surfactants are important for ink-jet printing. The experimental results were compared with the predictions of the theory of S. Semenov et al. [1]. Surprisingly good agreement was found for the results regarding the first stage of evaporation.

**Acknowledgements**

The study has been prepared in the framework Marie Curie Initial Training Network "Complex Wetting Phenomena" (CoWet).

**References**

[1] S. Semenov, V.M. Starov, R.G. Rubio, H. Agogo, M.G. Velarde, Evaporation of water sessile droplet: Universal behaviour in presence of contact angle hysteresis. *Colloids and Surfaces A: Physicochem. Eng. Aspects* 2011, 391, 135-144.

## HALL A - ADSORPTION ON SURFACES (2)

	<i>Hall A: Adsorption on surfaces (2)</i> <i>(Chair: V. Starov)</i>	<i>Hall B: Thermal processes</i> <i>(Chair: D. Brutin)</i>
<i>15:00-15:15</i>	<b>Mickael Antoni</b> Mass transfer and microstructures formation at water paraffin oil interfaces	<b>Khalili Sadaghiani Abdolali</b> Flow boiling on microstructured aluminum surfaces in high aspect ratio microchannel
<i>15:15-15:30</i>	<b>Basarova Pavlina</b> Atypical behaviour of aqueous solutions of short-chain alcohols in multi-phase systems	<b>M.C. Vlachou</b> Flow boiling incipience in macro-channels: Working conditions that maximize heat removal
<i>15:30-15:45</i>	<b>Ritu Ritu</b> Investigating the mass transfer and microstructures formation at liquid/liquid interfaces using FT-IR imaging spectroscopy	<b>Motezakker Ahmad Reza</b> Nucleate Pool Boiling Heat Transfer on pHEMA Coated Surfaces

## Mass Transfer And Microstructures Formation At Water Paraffin Oil Interfaces

M. Schmitt, R. Ritu, R. Denoyel, M. Antoni, Aix-Marseille Université, UMR/CNRS 7246 MADIREL, Centre Scientifique de St. Jérôme, 13397 – Marseille Cedex 20, m.antoni@univ-amu.fr

SPAN80 is a hydrophobic surfactant commonly used for the stabilization of emulsions. When SPAN80 is added to water in paraffin oil emulsions, the continuous paraffin oil phase becomes opaque over time indicating the occurrence of micrometer sized objects. Optical microscopy observations suggest that a self-emulsifying process promotes the appearance of small water droplets. Once created, these latter are transported into paraffin oil and contribute to the increasing opaqueness of the emulsions.

This work aims to better understand this phenomenon by investigating the exchanges taking place in the neighborhood of water/paraffin oil interfaces. A simplified system consisting of a water drop pendant at the end of a capillary tip in SPAN80 loaded paraffin oil is studied in controlled temperature conditions. The darkening of the drop with time is evidenced as illustrated in the figure below. This phenomenon is the consequence of the appearance of water micro-droplets at the interface. They progressively cover the complete interface and finally generate densely packed microstructures. The kinetics of this process strongly depends on the concentration of SPAN80 and temperature.

Long term evolution shows the increasing roughness with the formation of micro-droplets aggregates in the neighborhood of the water/paraffin oil interfaces (see arrow in the figure (d)). As time runs, the drop becomes elongated indicating a decrease in interfacial tension and an increase in the volume of the micro-droplets that are closest to the interface. The precise reason of this swelling is not yet clear. It probably implies classical self-emulsifying mechanisms at very low interfacial tensions. The aggregates slowly drift along the interface towards the bottom of the droplet from which they finally detach.

Self-emulsifying mechanisms triggered by SPAN80 exhibit two main phases: First, the formation of interfacial microstructures consisting in water micro-droplets. These micro-droplets will, in a second phase, aggregate and drift away from the interface. This phenomenon will progressively remove water from the pendant drop that, at the end of the process, shows up as a hollow vesicle.

The mass transfer effects investigated here might help to understand changes in the structure of emulsified suspensions [1, 2].

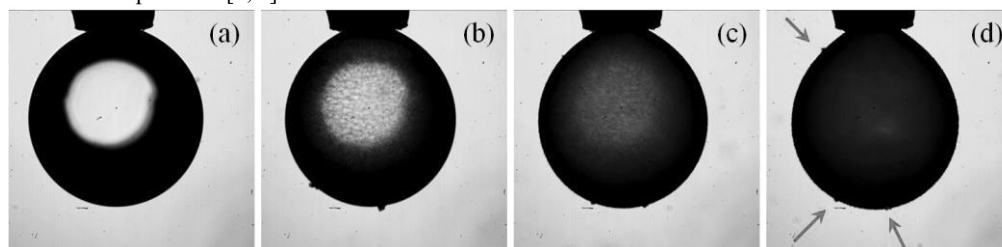


**Figure 1.** Pendant HPLC-grade water drop at  $t=0$  s (a), 2000 s (b), 4000s (c) and 8000 s (d). The continuous phase is paraffin oil with  $[\text{SPAN80}] = 2$  g/L. Temperature is set to  $T=35$  °C. Small aggregates are evidenced with arrows in (d).

#### Acknowledgements

This work was partially supported by ESA MAP-FASES, CNES and GdR-CNRS MFA.

#### References

- [1] Schmitt, M., Limage, S., Grigoriev, D. O., Krägel, J., Dutschk, V., Vincent-Bonnieu, S., Miller, R., Antoni, M., "Transition from Spherical to Irregular Dispersed Phase in Water/Oil Emulsions", *Langmuir* (2014), 30(16) , 45994604
- [2] Schmitt-Rozières, M.; Krägel, J.; Grigoriev, D. O.; Liggieri, L.; Miller, R.; Vincent-Bonnieu, S.; Antoni, M. "From Spherical to Polymorphous Dispersed Phase Transition in Water/Oil Emulsions", *Langmuir* 2009, 25 (8), 4266–4270

### Atypical Behaviour of Aqueous Solutions of Short-chain Alcohols in Multi-phase Systems

*P. Basařová<sup>1</sup>, T. Váchová<sup>1</sup>, S. Orvalho<sup>2</sup>. (1) UCT Prague, Technická 3, Prague, Czech Rep. pavlina.basaroval@vscht.cz. (2) ICPF CAS, Rozvojová 6, Prague, Czech Rep.*

The aqueous solutions of simple alcohols, as methanol, ethanol and propanol, are used in many industrial, biological, pharmaceutical and daily processes. We meet with them so often that we do not realize their atypical properties. Relatively well-known is the volume reduction of the mixture in comparison to the volume in the “pure” alcohol or water states. From the chemical-engineering point of view, the maximum in viscosity–composition dependence and lower wettability in comparison to common liquids have a much greater significance. This unusual behaviour is caused by the solution microstructure. It was found that simple alcohols are micro heterogeneous since they tend to develop distinct local microstructures consisting both of alcohol and water molecules. The existence of this molecular organization has been proved by several independent methods including popular molecular dynamic simulations. The basic conception is that the hydrogen-bonded chains which dominate the structure of pure alcohols are shortened and terminated by hydrogen bonds to water molecules. Adjacent chains then form composite chains via bridging water molecules. The scheme of such arrangement is illustrated in Fig. 1. These structures can have an effect on the interfacial properties of liquid mixtures and may cause unpredictable anomalies in the behaviour of systems where the surface phenomena play an important role. The typical examples are the motion of dispersed fluid particles (bubbles, drops) through the carrying bulk liquid, hydrodynamic interactions between such particles (coalescence and breakup), behaviour of fluid particles at rigid surfaces (adhesion). Such situations commonly occur in many important technological processes and equipment (fermenters, adsorption columns, waste water treatment, flotation, etc.), which presents strong motivation for the research.

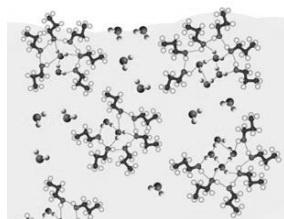


**Figure 1.** Simplified two-dimensional diagrams of the types of structures observed in the solution of propanol in water. Oxygen atoms are highlighted in red, carbon in black.

The microstructure influences the volumetric properties of solutions, which is reflected, among other things, by the density and viscosity values. This is very important fact because the short chain alcohols are applied as solvents and co-solvents. While the change of solution density is not very significant in comparison with an ideal mixture, the viscosity–composition maximum is remarkable. For example, the solution of ethanol with molar concentration 20% has almost three times higher dynamic viscosity than pure components and their ideal mixture. Therefore, a strong decrease in bubble terminal rising velocity can be expected. The gas phase velocity belongs to the most important parameters for the bubble column design and directly affects the gas holdup and flow regimes in sparged equipments. Besides the bubble velocity, the rate of the film drainage at bubble coalescence will be affected too, with impact on the bubble size distribution. The bubble size determines the rise velocity and the interface area for transport phenomena.

The lecture will present a new project and also its first results (Atypical wetting behaviour of alcohol–water mixtures on hydrophobic surfaces, *Colloids and Surfaces A: Physicochem. Eng. Aspects* 489 (2016) 200–206).

#### **Acknowledgements**

This work was supported by the Ministry of Education, Youth and Sports (project LD 13025). Support from COST action MP1106 is also gratefully acknowledged.

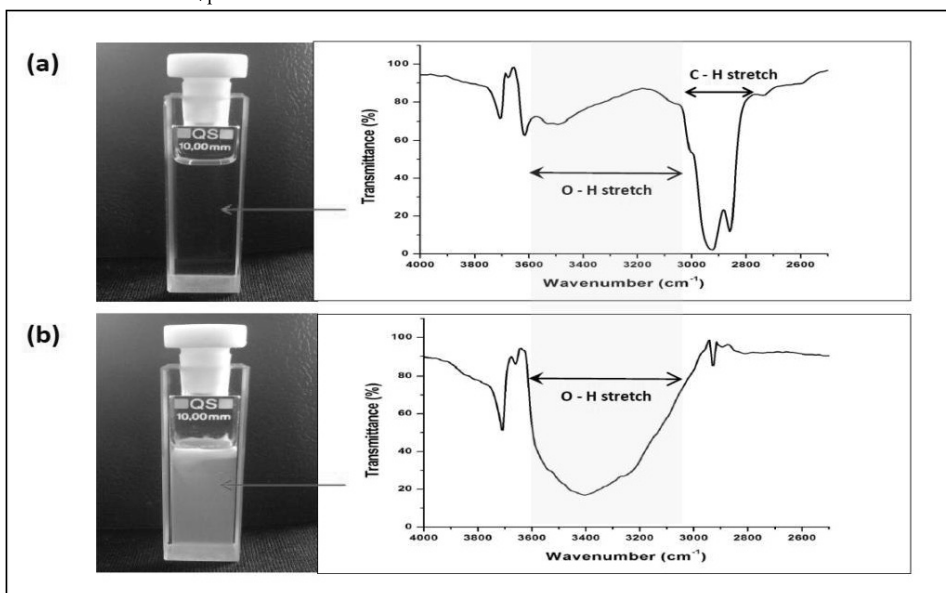
**Investigating The Mass Transfer And Microstructures Formation At Liquid/Liquid Interfaces Using FT-IR Imaging Spectroscopy**

*R. Ritu, M. Schmitt, R. Denoyel, M. Antoni, Aix-Marseille Université, UMR/CNRS 7246 MADIREL, Centre Scientifique de St. Jérôme, 13397 – Marseille Cedex 20, m.antoni@univ-amu.fr*

SPAN 80, a lipophilic surfactant is commonly used for the stabilization of emulsions. When SPAN 80 is introduced to water in paraffin oil emulsions, the continuous paraffin oil phase becomes opaque over time indicating the occurrence of micrometer-sized objects. Microscopy observations suggest that a self-emulsifying process promotes the appearance of small water droplets at the interface [1, 2]. Once created, these latter are transported into paraffin oil and contribute to the increasing opaqueness of the emulsions.

This study focuses on the investigation of this phenomenon, replacing paraffin oil by CCl<sub>4</sub>. In order to better understand this interfacial phenomenon, FT-IR imaging spectroscopy has been applied. This analytical technique provides information about the identification and concentration of compounds and their distribution in the accessible field of view (FOV) but requires the use of IR transparent solvents. This is the reason why CCl<sub>4</sub> is used. A Focal Plane Array (FPA) detector allows for the simultaneous acquisition of 128 x 128 numbers of spatially resolved spectra, as each pixel provides an independent infrared spectrum. It gives access to a 2.5 mm x 2.5 mm FOV in one single scan with the spatial resolution of 20µm and time resolution of about 1 minute.

Spontaneous emulsification at the water/CCl<sub>4</sub> interface is observed optically. Small water droplets are produced and protrude into the organic phase and make the CCl<sub>4</sub> phase opaque. This is illustrated in the figures. Figure (a) shows the configuration of the SPAN 80 loaded CCl<sub>4</sub> in a quartz cuvette in the absence of water. Figure (b) shows the mass transfer into CCl<sub>4</sub> after one day when water is initially introduced in the cuvette. The spectra correspond to the FT-IR signal obtained at the location given by the arrow. In order to monitor this process, we followed the evolution of the depth of the O-H stretching band (3200-3500 cm<sup>-1</sup>) over time (see spectra). As time elapses, this band becomes more pronounced that could be seen as an increase in the amount of water in the CCl<sub>4</sub> phase.



Left column: cuvette with CCl<sub>4</sub> and SPAN80 (1g/L). (a) without water, (b) with water. Right column shows the spectra.

**References**

- [1] H. Gonzalez-Ochoa, J. L. Arauz-Lara, "Spontaneous two-dimensional spherical colloidal structures", *Langmuir* 23 (2007) 5289-5291.
- [2] J. Santana-Solano, C. M. Quezada, S. Ozuna-Chacon, J. L. Arauz-Lara, "Spontaneous emulsification at the water/oil interface", *Colloids Surf. A*, 399 (2012) 78-82.



**Flow Boiling On Microstructured Aluminum Surfaces In High Aspect Ratio Microchannel**

*A.K.Sadaghiani<sup>1</sup>, Y. Sisman<sup>1</sup>, T.Karabacak<sup>2</sup>, A.Kosar<sup>1</sup>. (1) Sabanci University, Istanbul, Turkey akhailisadaghiani@sabanciuniv.edu. (2) University of Arkansas at Little Rock, AR, USA.*

It is known that the surface morphology has a considerable effect on bubble departure diameter and frequency in boiling. Boiling heat transfer on enhanced surfaces is one of the most popular alternatives for reaching high heat flux removal rates from confined spaces or small areas in various applications such as compact heat exchangers, cooling of small electric devices and engine cooling systems [1]. In this regard, the assessment of the effect of surface characteristics on nucleate boiling and boiling inception is vital. A number of studies have revealed the significant effect of surface characteristics on boiling heat transfer [2]. In this work, the effect of surface roughness on flow boiling in microchannels with high aspect ratios was investigated. Aluminum surfaces with 1.08, 1.4, and 4.2 μm roughnesses with different contact angles were examined. Table 1 summarizes the surface characteristics of surfaces.

**Table 1.** Surface characteristics of different samples

Sandpaper grit	Sandpaper size	Roughness (Ra) ± 5%	Contact Angle θ
Bare	NA	1.08 μm	93.3
#36	560 μm	4.2 μm	31.5
#1000	10 μm	1.4 μm	22.25

Experiments were conducted using deionized water as the working fluid in a microchannel with a length of 14 cm, a width of 1.5 cm, and a depth of 500 μm. The working fluid was pumped using a micro-gear pump with at different mass fluxes of 50 and 125 kg/m<sup>2</sup>.s. Figure 1 and 2 show the obtained heat transfer coefficients, and related flow visualization for different surfaces, respectively. As seen, the number of nucleation sites increases with surface roughness. #1000 grit size surface shows enhancement in heat transfer coefficient. This is mainly due to higher number of active nucleation sites [3]. Furthermore; surface with #36 grit size shows no enhancement in heat transfer coefficient. Although according to the nucleate boiling images shown in Figure 2, #36 surface has higher nucleation site in comparison to the base surface, due to lower contact angle it shows no considerable enhancement in nucleate boiling region.

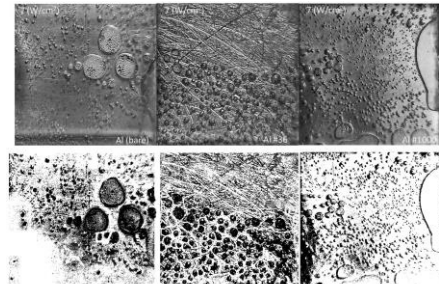
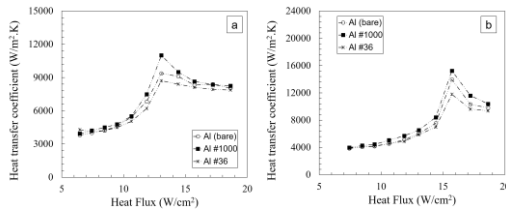


**Figure 1.** Heat transfer coefficients a) G=50 b) G=125 kg/m<sup>2</sup>.s **Figure 2.** Flow visualization images

The effect of surface roughness becomes more dominant as the flow rate increases. Furthermore, the plates with the grit of #36 do not provide any significant enhancement, while the plate of higher grit count leads to higher heat transfer coefficient.

**Acknowledgements**

The authors thank SUNUM (Sabanci University Nanotechnology Research and Applications Center) and the Center for Integrative Nanotechnology Sciences at UALR.

**References**

[1] Torregrosa, A., Broatch, A., Olmeda, P., Comejo, O., Experiments on subcooled flow boiling in IC engine-like conditions at low flow velocities, *Experimental Thermal and Fluid Science*, vol. 52, no. pp. 347-354, 2014.  
 [2] Jo, H., Ahn, H.S., Kang, S., Kim, M.H., A study of nucleate boiling heat transfer on hydrophilic, hydrophobic and heterogeneous wetting surfaces, *International Journal of Heat and Mass Transfer*, vol. 54, no. 25, pp. 5643-5652, 2011.

**Flow boiling incipience in macro-channels:  
Working conditions that maximize heat removal**

*M.C. Vlachou\**, J.S. Lioumbas, T.D. Karapantsios. Division of Chemical Technology, Aristotle University of Thessaloniki, 54124 Thessaloniki, Greece, \*marvlach@gmail.com

**Flow boiling** is listed as one of the most efficient ways of cooling, because it takes advantage of both the refrigerant’s latent heat of vaporization and the inertial forces of the forced flow to carry away large amounts of heat flux. During the **heat exchange process** of flow boiling, several parameters contribute to the heat transfer equilibrium result (the final heat can be removed from each system); surface tension, gravitational force, interfacial shear stress. **Working conditions** of the system (mass flux, heat flux, channel’s size & orientation) define the final influence of those parameters, the dominant heat transfer mechanism and consequently can lead to the **optimization**.

In this study work is focused to investigate the effect of working conditions (table 1) on boiling curve, heat transfer coefficient and bubble dynamics in order to maximize the efficiency of heat removal.

**Table 1.** Working conditions

Parameter	Value/ Range
Working fluid	Water
Temperature @ inlet	30 °C
Channel’s height	3 & 10 mm
Orientation	Horizontal & Vertical
Mass flux	330 – 830 kg/m <sup>2</sup> s
Heat flux	300 – 1000 kW/m <sup>2</sup>

Experiments are conducted with water as the working fluid. A flow boiling device with a macro-channel with variable height (3& 10mm) is used to conduct experiments. Simultaneous monitoring of temperature and bubble dynamics allows correlating boiling regimes with heat transfer results and evaluate the efficiency of each working condition. Bulk liquid’s temperature, flow rate, pressure drop along the channel and void fraction at the exit of the text section are also measured.

From the obtained results it is seen that the channel of 3mm height becomes more efficient after a certain wall superheat for horizontal case (figure1), which increases with increasing flow rate. Vertical channel’s behavior is to the same direction. An insight of the bubble dynamics is going to provide more information for assessing the flow boiling heat transfer mechanisms and the two phase heat transfer coefficient.

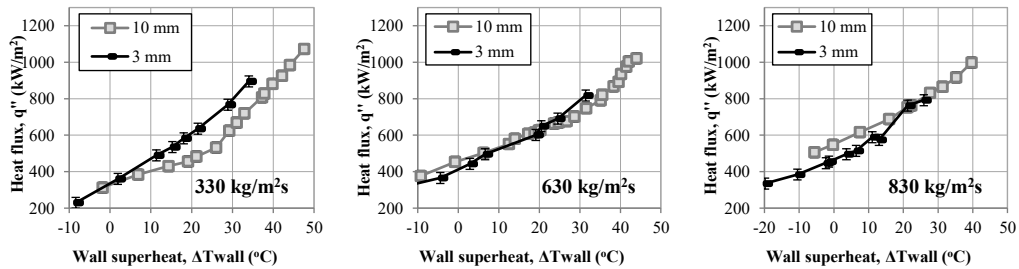


**Figure 1.** Effect of channel’s height on boiling curve for horizontal channel at three different mass fluxes.

**Acknowledgements**

The work is performed with the support of (1) “Highly efficient flow boiling macro-structured/ macro-porous channels” funded by the European Space Agency (Co. No. 4000106405/12/NL/PA) (2) IKY Fellowships of excellence for postgraduate studies in Greece – SIEMENS program. The work is performed under the umbrella of COST Action MP1106.

**Nucleate Pool Boiling Heat Transfer on pHEMA Coated Surfaces**

*A. Motezakker<sup>1</sup>, A.K.Sadaghian<sup>1</sup>, G. Ozaydin Ince<sup>1</sup>, A. Kosar<sup>1</sup> Sabanci University, Istanbul, Turkey  
ahmadrezam@sabanciuniv.edu.*

Boiling heat transfer has numerous applications such as cooling systems, refrigeration and power plants. In recent years, many studies have been done to analyze the physics of bubble creation and improving the whole mechanism of pool boiling with increasing bubble nucleation sites. Many kinds of enhanced surfaces have been used by investigators to increase nucleation bubble sites such as nanostructured and micro structured surfaces [1]. Many of investigators have used nanoporous surfaces to show their effects on heat transfer mechanisms. Due to the porous structure of pHEMA surface, it has been recently used in boiling experiments [2]. For example, the effect of pHEMA coated surfaces on flow boiling in a high ratio rectangular microchannel was investigated in the literature [3].

The effect of surface porosity on nucleate pool boiling is investigated in this study using pHEMA coated silicon plates with 4×4 cm<sup>2</sup> dimensions. The obtained results were compared with the bare silicon surfaces. Bubbles were visualized using a high speed camera. The setup consists of different components such as glass block, holder plates, cartridge heaters, thermocouples, gasket sealers and a condenser.

Obtained heat transfer coefficients for bare silicon and pHEMA nano-porous surfaces are shown in Figure 1. Enhancement of heat transfer coefficients on pHEMA surfaces can be seen in comparison with bare silicon wafer. Due to the porosity of pHEMA coated surface, the number of active nucleation sites and the bubble departure frequency are increased, which leads to enhancement in heat transfer.

The enhancement in heat transfer with a nano-porous surface may be attributed to the combined effects of the interaction among active nucleation sites, the increase in bubble generation frequency, the increase in bubble interactions, and the thin-film evaporation effect. This was also reported by Chen and Peterson [20]. Interaction among nucleation sites, bubble interaction near the departure point, and bubble movements on the heating surface due to nucleation sites are shown in Figure 2.

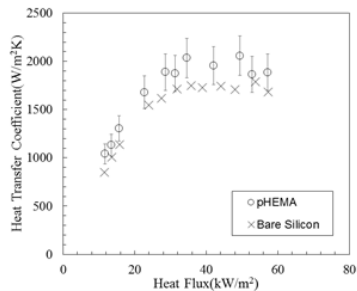


**Figure 1.** Obtained heat transfer coefficients.

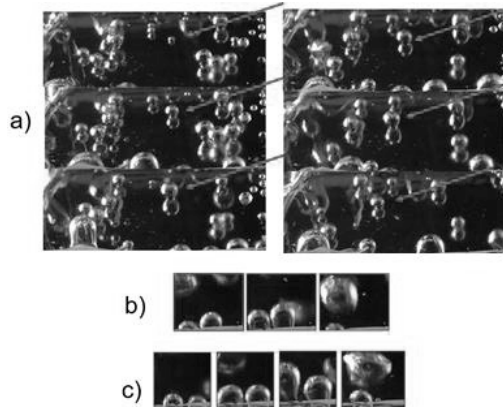


**Figure 2.** a) Bubble movement on porous surface b) Bubble coalescence during the departure on porous surface c) Bubble movement on the porous surface during the departure process

**References**

- [1] H. Kubo, H. Takamatsu, H. Honda, Effects of size and number density of micro-reentrant cavities on boiling heat transfer from a silicon chip immersed in degassed and gas-dissolved FC-72, *Journal of Enhanced Heat Transfer*, 6(2-4) (1999).
- [2] A. Kaya, G. Ozaydin-Ince, M. Sezen, Boiling heat transfer enhancement in mini/microtubes via polyhydroxyethylmethacrylate (pHEMA) coatings on inner microtube walls at high mass fluxes, *Journal of Micromechanics and Microengineering*, 23(11) (2013) 115017.
- [3] A.K. Sadaghiani, Y. Şişman, G.Ö. Ince, A. Koşar, An Experimental Study on Flow Boiling Characteristics of pHEMA Nano-Coated Surfaces in a Microchannel, in: *ASME 2016 5th International Conference on Micro/Nanoscale Heat and Mass Transfer*, American Society of Mechanical Engineers, 2016, pp. V002T008A002-V002T008A002



---

SECTION

# 6

---

POSTER PRESENTATIONS

1 <sup>st</sup> DAY .....	98
Session 1 .....	98
3 <sup>rd</sup> DAY .....	124
Session 2 .....	124

## POSTER PRESENTATIONS - 1<sup>st</sup> DAY

Wednesday, May 4th, 2016 (16:00-17:00)

Europe Foyer: Poster session 1

- 1 Investigating the Physical-Chemistry of Adsorption Layers, Liquid Films, Foams and Emulsions by Microgravity Experiments  
*L. Liggieri, F. Ravera, E. Santini, M. Ferrari, S. Llamas, P. Pandolfini, G. Loglio, R. Miller, J. Kraegel, A. Javadi, M. Karbaschi, V. Kovalchuk, B. Noskov, L. Cristofolini, D. Orsi, D. Clausse, I. Pezron, T. Karapantsios, J. Ferri, Y. Yamashita, M. Schmitt, M. Antoni.*
- 2 A Front-Tracking Method for Direct Numerical Simulation of Evaporation Process in a Multiphase System  
*M. Milieška, R. Kěželis*
- 3 Influence of enzymatic hydrolysis on dilatational properties of pumpkin (*Cucurbita pepo* sp.) seed protein isolate  
*S. Bučko, J. Katona, L. Petrović, R. Miller, N. Mucic*
- 4 Biodegradable aqueous foams based on xanthan and gellan gums  
*M. Krzanl, E. Jarek, H. Petkova, E. Santini, V. Ungalanthan, M. Lofti, A. Javadi, E. Mileva, P. Warszynski, R. Todorov, F. Ravera, L. Liggieri, R. Miller, D. Exerowa*
- 5 Influence of n-alkanol chain length on local and terminal velocities of rising bubbles  
*M. Krzan*
- 6 Kinetics of bubble coalescence at surfaces of different liquids –influence of external disturbances and size of the liquid films formed  
*A. Wiertel, J. Zawala, K. Malysa*
- 7 Influence of enzymatic hydrolysis on functional properties of pumpkin (*Cucurbita pepo* sp.) seed protein isolate  
*S. Bučko, J. Katona, Lj. Popović, L. Petrović, J. Milinković*
- 8 Heat Transfer Coefficient Of An Oscillating Meniscus  
*I. Malavasi, L. Pietrasanta, D. Fioriti, M. Mamei, N. Miche, M. Marengo*
- 9 Interfacial slow dynamics from the micro- to the nanoscale by a combination of real and momentum  
*D. Orsi, L. Liggieri, F. Ravera, L. Cristofolini*
- 10 Comparative Framework for Binder Formulation Development for Inkjet-based Three Dimensional Metal Printing  
*J.K. Ferri, A.D.Cramer, S. Buczek*
- 11 Highly subcooled flow boiling in macro-channels: Effect of channel's height and orientation  
*M.C. Vlachou, J.S. Lioumbas, T.D. Karapantsios*
- 12 Study of coarsening and coalescence for dry foams in 2D  
*A. Cagna, C. Honorez, W. Drenckhan*
- 13 Experimental Determination of Thin Film Drainage Around Single Foam Bubbles  
*A.T. Zamanis, M. Kostoglou, S.P. Evgenidis, T.D. Karapantsios*
- 14 Dynamics of adsorption of ionic surfactants at the water/air interface with hexane vapour in the gas phase  
*T.Kairaliyeva, R. A. Campbell, N. Mucic, A. Javadi, J. Krägel, E.V. Aksenenko, V.B. Fainerman, S.A. Aidarova, R. Miller*
- 15 Determination and comparison of size and stability of Nanobubbles produced by two different generators  
*E.D.Michailidi, R.I.Kosheleva, A.C.Mitropoulos*
- 16 Flow boiling of self-wetting 1- butanol/water mixture in a square microchannel  
*P. Vasileiadou, Khellil Sefiane, T.G. Karayiannis*

## EUROPE FOYER - SESSION 1

- 17 VOC free nanoemulsions of aminopropylaminoethylpolysiloxane prepared by phase inversion emulsification with C13 ethoxylated surfactants of various HLB  
*C. G. Koukiotis, G. Kokkinos, T. D. Karapantsios*
- 18 Study of Void Fraction Fluctuations Dependence on Bubble Size through Experimental and Simulated Electrical Signal Analysis  
*S. Evgenidis, M. Kostoglou, T. Karapantsios*
- 19 Velocity of rising air bubbles in aqueous beta-lactoglobulin solutions at different pH and salt concentrations  
*V. Ulaganathan, G. Gochev, C. Gehin-Delval, D.Z. Gunes, M.E. Leser, R. Miller*
- 20 Application of Electrical Resistance Tomography and Differential Pressure Method for Low Void Fraction Values Determination in Bubbly Flow of Sub-millimeter Bubbles  
*S. Evgenidis, P. Zikou, T. Karapantsios*
- 21 Removal of polycyclic aromatic hydrocarbons in aqueous solution by electrochemical oxidation  
*M. Brienza, G. Gallios, E. Vardaka, I. Voinovschi, D. Kupka, M. Vaclavikova*
- 22 Self-assembly by multi-drop evaporation of carbon-nanotube and graphene-oxide-platelets droplets on a glass substrate  
*C.S. Iorio, C. Minetti, Hatim Machraft*
- 23 Confined tube flow of elastic low viscosity emulsions  
*S. Caserta, V. Preziosi, G. Tomaiuolo, S. Guido*

**Investigating the Physical-Chemistry of Adsorption Layers, Liquid Films, Foams and Emulsions by Microgravity Experiments**

**L. Liggieri<sup>1</sup>, F. Ravera<sup>1</sup>, E. Santini<sup>1</sup>, M. Ferrari, S. Llamas<sup>1</sup>, P. Pandolfini<sup>1</sup>, G. Loglio<sup>1</sup>, R. Miller<sup>2</sup>, J. Kraegel<sup>2</sup>, A. Javadi<sup>2</sup>, M. Karbaschi<sup>2</sup>, V. Kovalchuk<sup>3</sup>, B. Noskov<sup>4</sup>, L. Cristofolini<sup>5</sup>, D. Orsi<sup>5</sup>, D. Clausse<sup>6</sup>, I. Pezron<sup>6</sup>, T. Karapantsios<sup>7</sup>, J. Ferr<sup>8</sup>, Y. Yamashita<sup>9</sup>, M. Schmitt<sup>10</sup>, M. Antoni<sup>10</sup>.**  
 (1) CNR-Istituto per l'Energetica e le Interfasi, Genova, Italy; [Liggieri@ge.ieni.cnr.it](mailto:Liggieri@ge.ieni.cnr.it). (2) Max-Planck Inst. für Kolloid und Grenzflächenforschung, Potsdam/Golm, Germany. (3) Institute of Bio-Colloid Chemistry, Kiev, Ukraine. (4) St. Petersburg State University, Dept. of Colloid Chemistry, Russian Federation. (5) Università di Parma, Dipartimento di Fisica e Scienze della Terra, Italy. (6) Université de Technologie de Compiègne, France. (7) School of Chemistry, Aristotle University of Thessaloniki, Greece. (8) Lafayette College, Easton PA, USA. (9) Faculty of Pharmacy Chiba Institute of Science, Japan. (10) Aix-Marseille Université, CNRS MADIREL – France.

Adsorption layers at liquid interfaces are essential constituents in nature and technologies. Emulsions and foams are paradigmatic examples of how the properties of these adsorption layers influence the behavior of complex liquid systems.

During the last years we have conceived, proposed and run a set of benchmark microgravity experiments to investigate the relationships between the features of emulsions and foams (foamability, stability, etc.) and the physical-chemistry of interfacial layers and liquid films.

Here we summarize and review the concepts and results of previous microgravity experiments and introduce the basic ideas concerned with new instrumentation and investigations that have been already approved by the European Space Agency and that will be realized during the next few years.

Because of the vast utilization of emulsions and foams in products and technologies, these studies have relevant transversal spin-offs in different fields (oil industry, chemical technologies, waste treatment, paints, foods, biotechnologies, cosmetics and pharmaceuticals, capsules and nanostructured materials,...).

**Acknowledgements**

This research was carried under the umbrella of COST Actions MP1106 and supported by the European Space Agency projects "Particle Stabilized Emulsions-PASTA", "Fundamental and Applied Studies in Emulsion Stability – FASES" and "Soft Matter Dynamics".



## Zirconia/ Polyaniline Nanocomposite: Synthesis, Characterization and Applicability as Photocatalyst

M.I. Čomor, M.V. Carević, N.D. Abazović, M.B. Radoičić, T.D. Savić, Vinča Institute of Nuclear Sciences, University of Belgrade, P.O. Box 522, Belgrade, Serbia, mirjanac@vinca.rs.

In recent years, nanocomposites of conductive polymers and inorganic particles have attracted more and more attention, since they have interesting physical properties and many potential applications. The physical and chemical properties of composites may be tuned by selecting the types of the polymers and the inorganic nanoparticles. For example, composites of conductive polyaniline (PANI) and nanocrystalline metal oxide ( $\text{TiO}_2$ ,  $\text{ZrO}_2$ , ...) combine the merits of both PANI and metal oxide particles, having potential applications in conductive coating, charge storage, electrocatalysis, electrochromic devices, photovoltaic cells and as photocatalysts for degradation of pollutants.

Following very successful combination of  $\text{TiO}_2$  and PANI for application as photocatalysts [1], we used similar method to synthesize and probe  $\text{ZrO}_2$ /PANI nanocomposites. Briefly, zirconia nanoparticles, synthesized hydrothermally in alkaline solution, using  $\text{ZrOCl}_2$  as precursor, were mixed with aqueous solution of appropriate concentration aniline and ammonium peroxydisulfate as oxidant, without addition of acid. The reaction mixture was stirred for 20 days at room temperature. The precipitates were then collected, washed and dried. We synthesized samples with initial  $[\text{ZrO}_2]/[\text{ANI}]$  mole ratios of 50, 100 and 150 designated as ZP-50, ZP-100 and ZP-150.

Detailed characterization of the ZP nanocomposites showed that zirconia maintained its initial monoclinic crystalline structure; TEM measurements revealed that bare zirconia nanoparticles have about 20- 40 nm in diameter; after formation of nanocomposite- layer of PANI can be seen, Figure 1. Obtained nanocomposites were probed as photocatalysts for degradation of trichlorophenol (TCP) using simulated solar light (Osram Vitalux lamp).

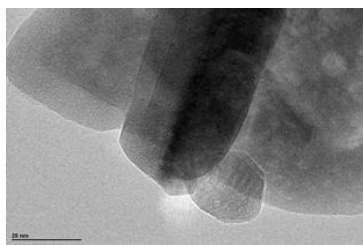


Figure 1. Typical TEM image of ZP-100 nanoparticles, bar is 20 nm.

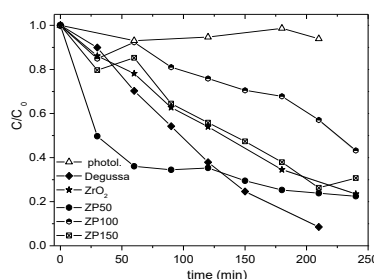


Figure 2. Kinetic curves of the photolysis and photocatalytic degradation of TCP using bare  $\text{ZrO}_2$  and ZP nanocomposites as well as Degussa (for comparison).

All examined powders can be used for photodegradation of TCP, when simulated. Solar light is used, as can be seen in Fig. 2. The best photocatalytic activity showed ZP-50 nanocomposite with the highest amount of PANI compared to zirconia, 60% of TCP was degraded after 1 hour. Its activity is even better than activity of Degussa, commercial  $\text{TiO}_2$  powder, which is not easy to achieve. We hope that this type of nanocomposites will prove to be excellent choice of GREEN, regarding process of synthesis and physico-chemical properties, materials for solving of environmental pollution problems.

### Acknowledgements

Financial support for this study was granted by The Ministry of Education, Science and Technological Development of The Republic of Serbia, Project: ON172056 and COST action MP1106.

### References

[1] M.B. Radoičić, Z.V. Šaponjić, I.A. Janković, G. Ćirić-Marjanović, S.P. Ahrenkiel, M.I. Čomor, *Applied Catalysis B: Environmental*, 136-137 (2013) 133.

**Influence of enzymatic hydrolysis on dilatational properties of Pumpkin (*Cucurbita pepo* sp.) seed protein isolate**

*S. Bučko<sup>1</sup>, J. Katona<sup>1</sup>, L. Petrović<sup>1</sup>, R. Miller<sup>2</sup>, N. Mucic<sup>2</sup>. (1) Faculty of Technology, University of Novi Sad, Bulevar Cara Lazara 1, 21000 Novi Sad, Serbia, (2)Max Planck Institute of Colloids and Interfaces, Am Mühlenberg 1, 14476 Potsdam–Golm, Germany, sandranj@uns.ac.rs.*

Pumpkin (*Cucurbita pepo* sp.) seeds are rich source of both, oil and proteins. Once the oil has been extracted, high quantities (>60 %) of proteins concentrate in an oil cake, a by-product of the oil extraction [1]. Pumpkin seed proteins are desirable ingredient in food and pharmaceutical products vastly for their pharmacological activities and high biological balance while their functional properties are still being underestimated due to their globular structure [2]. Namely, proteins with rigid, globular structure are considered to have inferior functionality to proteins with more flexible structure, therefore, the aim of this work was to investigate whether the alteration of pumpkin seed protein structure by enzymatic hydrolysis influences pumpkin seed protein isolate's (PSPI) interfacial properties, i.e. interfacial pressure, dilatational elasticity and dilatational viscosity. Investigation on dilatational properties of interfaces between PSPI or pumpkin seed protein hydrolysate (PSPH) solution and medium chain triglyceride oil was conducted under different experimental conditions of pH (3 and 5), protein solution concentration,  $c_{sol}$  (0.0008–0.8 g/100 cm<sup>3</sup>), ionic strength,  $I_c$  (0–1 mol/dm<sup>3</sup> NaCl) and oscillation frequency,  $\nu$  (0.01–0.2 1/s). Both PSPI and PSPH were found to adsorb at the interface since they increase interfacial pressure as their concentration increases, regardless of pH and  $I_c$ . Elastic component is dominant at all interfaces formed by PSPI and PSPH but interfaces with the highest dilatational elasticity are formed by PSPH, at pH 3 at the highest  $c_{sol}$  and at pH 5 at  $c_{sol}$ =0.008g/100 cm<sup>3</sup>. Increase in  $I_c$  to 1 mol/dm<sup>3</sup> NaCl had significant influence only on PSPI at pH 3 where it resulted in drop in interfacial pressure and dilatational elasticity.

Despite the fact that PSPI had higher interfacial pressure and dilatational elasticity ( $c_{sol}$ <0.8g/100 cm<sup>3</sup>) than PSPH at pH 3, the results indicate that enzymatic hydrolysis mitigated the influence of environmental conditions, pH and  $I_c$ , on interfacial properties of PSPI.

**Acknowledgements**

This work was financed by Ministry of Education, Science and Technological Development of Republic of Serbia, Grant No III 46010. It is done within COST CM1101 and MP1106 action framework.

**References**

- [1] Ž. Vaštag, Lj. Popović, S. Popović, V. Krimer, D. Peričin, Food Chemistry, 124 (2011) 1316.
- [2] S. Bučko, J. Katona, Lj. Popović, Ž. Vaštag, L. Petrović, M. Vučinić–Vasić, LWT– Food Science and Technology, 64 (2015) 609.

---

**Biodegradable aqueous foams based on xanthan and gellan gums**

---

*M. Krzan<sup>1</sup>, E. Jarek<sup>1</sup>, H. Petkova<sup>2</sup>, E. Santini<sup>3</sup>, V. Ungalantha<sup>4</sup>, M. Lofti<sup>4</sup>, A. Javadi<sup>4</sup>, E. Mileva<sup>2</sup>, P. Warszyński<sup>1</sup>, R. Todorov<sup>2</sup>, F. Ravera<sup>3</sup>, L. Liggieri<sup>3</sup>, R. Miller<sup>4</sup>, D. Exerowa<sup>2</sup>. (1) J. Haber Institute of Catalysis and Surface Chemistry PAS, Cracow, Poland nckrzan@cyf-kr.edu.pl, (2) Institute of Physical Chemistry BAS, "Acad. G. Bonchev" str. 11, Sofia 1113, Bulgaria; (3) Istituto per l' Energetica e le Interfasi, Consiglio Nazionale delle Ricerche, Genoa, Italy (4) Max Planck Institute for Colloid and Surface Chemistry, Golm/Potsdam, Germany*

The study of biosurfactant properties in relation to the stability of foams and emulsions is a very promising topic for a large number of applications especially as concern the replacement of chemically synthesised surfactants in industrial products.

Aqueous foams are intrinsically unstable and extremely complex systems with a cellular internal structure, consisting of polydisperse gas bubbles separated by thin liquid films. Foam evolution and its transient stability are functions of drainage and rupture of liquid films between air bubbles. The rate of foam drainage depends also on the surface rheological properties of the adsorption layers at the liquid interfaces.

Our aim was to develop a new bio-inspired, easy degradable, biopolymer based aqueous foams for various, industrial and biomedical application. We already proved that the particle as a component blocked the drainage of the liquid and foam coarsening enhancing the foam stability and surface elasticity. In the case of the chitosan foams we found that even the addition of hydrophilic nanoparticles into the chitosan solutions significantly increase the foam stability. We explained it by the partial hydrophobization of particles by the polycation (chitosan at pH below 4.5) which favors their transfer to the liquid/air interfaces making them good foam stabilizers.

In our present research we used the xanthan gum and gellan gum as a main ingredients of foaming solutions. We studied the single polysaccharide solutions and mixtures of them. The solutions and mixtures were enriched by trace concentrations of additional ingredients, as synthetic surfactants or colloidal/solid particles.

To optimize the polysaccharide solution composition for obtaining the most stable biofoams formulations the dynamic and equilibrium surface tensions together with the foamability measurements are performed.

It was found that the addition of synthetic surfactant strongly increases the surface activity of the mixture and results in the formation of stable, but thin foam layer. Similar effect has been obtained for mixture of polysaccharide solution and cationic synthetic surfactant with colloid or solid hydrophilic particles, probably due to partial hydrophobization of the particles. However in this case the effect was connected with the increasing of the solution surface elasticity.

It was prove that various polysaccharides could be used as a main compounds of the foaming mixtures. It could be estimated that in near future similar formulations will be used as a replacements of presently used synthetic surfactants based foaming formulations. This work is part of a wider study aimed at the development of new biocompatible, easy degradable, foams to be used as healing carriers in various pharmaceutical and biomedical fields.

**Acknowledgements**

Financial support from Polish National Scientific Centre (grant no. 2011/01/ST8/03717) is gratefully acknowledged. Part of this work has been also supported by the research and/or staff mobility actions COST MP1106, COST CM1101 and European Union Erasmus+ program (project number: 2014-1-PL01-KA103-000225).

## Influence of n-alkanol Chain Length on Local and Terminal Velocities of Rising Bubbles

*M. Krzan* J. Haber Institute of Catalysis and Surface Chemistry PAS, Cracow, Poland, [nekrzan@cyf-kr.edu.pl](mailto:nekrzan@cyf-kr.edu.pl)

Motion of the rising bubbles is a complex problem since it involves interaction between buoyancy force (added mass impact), drag and lift coefficients (state of the bubble interface and behaviour of the liquid). In water devoid of surfactants, the bubble surface is fully mobile, and therefore the bubble local velocity is higher than that of solid sphere of identical diameter and density. In contrary, when the bubble rise in the surface-active agents solutions the uneven distribution of surfactant molecules over its surface is induced as a result of a viscous drag exerted by fluid on the moving bubble interface. Adsorption coverage is lowered on the upstream part, while an accumulation of adsorbed molecules of surface active substance takes place at the rear part of the bubble. This gradient of the surface concentration can reduce interfacial mobility and consequently lower velocity of the bubble. However, majority of the existing experimental data describes only impact of the high concentration and adsorption coverage of surfactants on terminal velocity of the bubbles.

The paper presents results of determination of initial acceleration, profiles of the local velocities, values of maximum and terminal velocities, size and shape variations of the bubbles rising in solutions of n-alkanols homologous series (C2-C10). Results are shown for bubbles in the size range 1.3 to 1.5 mm and the bubble Reynolds numbers range up to roughly 600 (in water). Dimensions and deformation of bubbles were studied as well. Influence of solution concentration and n-alkanol chain length on timescale of establishment of a steady state, uneven distribution of the surfactant molecules over the bubble surface, was also evaluated.

Profiles of local velocities of bubbles in pure water and the n-alkanols solutions of different concentration were determined in a function of distance from the capillary orifice (inner diameter 0.075mm) on which the bubbles were formed. Motion of the bubbles was monitored in a glass square tube (4x4cm) by the special robotic station under the control of ImageJ freeware program. The data were recorded using the Moticam digital camera. Bubbles were formed at the capillary orifice (0.07 mm diameter) with the help of high precision peristaltic pump. Variations of the bubble velocities and bubble size and deformations with solution concentration were automatically analysed by the ImageJ digital image analysis program.

It was confirmed that after detachment from the capillary the bubbles accelerated rapidly, but initial acceleration was lowered in n-alkanol solutions. Profiles of the bubble local velocity showed a strong dependence on n-alkanol concentration, as expected. The values of the terminal velocity diminished drastically with increasing solution concentration, from the value of 35 cm/s in water down to about 15 cm/s in the high concentrations of n-alkanols studied. Presence of contaminations of higher surface active affected significantly the local velocity profiles in n-alkanol solutions. Interesting differences in profiles of the bubble local velocity, related to the n-alkanol chain length, were observed. Namely, in solutions of alkanols with  $C \leq 4$ , i.e., of lower surface activity, the bubbles always attained a plateau value of terminal velocity immediately after the acceleration stage. In the case low concentrations of n-alkanols with  $C \geq 5$  the accelerating bubbles were reaching a maximum velocity and next a deceleration stage was observed prior attaining the terminal velocity. The degree of deformation (ratio between horizontal and vertical diameter) also varied with solution concentration. It was equal 1.5 in water and decreased to the value about 1.03-1.5 in the cases of high concentration solutions studied. The effects of the adsorption rates on the behaviour of the bubble motion were also investigated and discussed for all studied surfactant concentrations. Numerical calculation of degree of adsorption coverages at surface of departing bubbles shows that value of adsorption coverage enough to fully retarded the bubble motion varied with a surface activity of the solute and decreased from a 40% in case of n-butanol, through 22% in n-pentanol, 10% in n-hexanol to only 4% in n-nonanol solutions. It could be conclude that the degree of the adsorption coverages diminish with the increasing of n-alkanol surface activity. Similarly, the observed differences in profiles of the bubble local velocity also can be related with the variation of studied compound surface activity.

### **Acknowledgements**

Financial support from Polish National Scientific Centre (grant no. 2011/01/ST8/03717) is gratefully acknowledged. Part of this work has been also supported by the research and/or staff mobility actions COST MP1106, COST CM1101 and European Union Erasmus+ program (project number: 2014-1-PL01-KA103-000225).

### Kinetics of bubble coalescence at surfaces of different liquids – influence of external disturbances and size of the liquid films formed

A. Wiertel<sup>1</sup>, J. Zawala<sup>1</sup>, K. Malysa<sup>1</sup>. (1) Jerzy Haber ICSC PAS, ul. Niezapominajek 8, Krakow, Poland, ncwiete@cyfronet.pl

The coalescence of air bubbles is the phenomenon occurring always where suitable degree of dispersion of an air phase in a liquid phase is desired. For example it affects the rate of formation and stability of foams, due to the fact that the foam layer is formed only, if the number of bubble arriving at the solution surface exceeds the number of rupturing ones. Moreover, the coalescence of air bubbles plays important role in processes carried out in bubble columns, gas strippers, distillation towers, direct-contact evaporators, flotation cells and stirred aerated tanks. Thus, knowledge of a degree of gas phase dispersion and kinetics of the bubbles coalescence is of crucial importance from the practical point of view. This is straightforwardly related to deep understanding of coalescence phenomenon, which is complex and whose mechanisms are still not fully understood.

We report here the experiments on kinetics of collision and bouncing of an air bubble at free surface of pure liquids (without addition of any surface-active substances), namely distilled water and silicone oil of kinematic viscosity equal to 0.65cSt. Influence of external disturbances on the bubble collision and bouncing courses is analysed on the basis of measurements carried out for the stagnant and vibrating (with controlled acceleration, i.e. amplitude and frequency), water/air and silicone oil/air interfaces. For stagnant interfaces it was found that the coalescence time ( $t_c$ ) was increasing with the bubble radius ( $R_b$ ). For example for water, when the  $R_b$  increased from 0.51 to 0.82 mm, the  $t_c$  increased from 25 to 74 ms. Similar trend was observed for the oil surface. This prolongation was due to a higher impact velocity (kinetic energy during collision) of larger bubbles. Higher impact velocity caused larger bubble deformation and higher tendency of the bubble to rebound from liquid/gas interface due to larger size of the liquid film formed. For vibrated liquid/gas interfaces it was shown that the bubble coalescence time could be prolonged significantly if the threshold value of vibrations acceleration is applied – it was a consequence of significant prolongation of the bubble bouncing time. This was due to the fact that the energy dissipated during the collision was re-supplied via interface vibrations with a properly adjusted acceleration. The analysis of the bubble deformation degree showed that this effect is related to constant bubble deformation, which causes constant radius of the liquid film, large enough to prevent the draining film from reaching the critical thickness of rupture at the moment of collision. It was found that higher acceleration should be applied to the system to prolong the  $t_c$  of the bubble of higher  $R_b$ . Moreover, it was found that, in the case of identical  $R_b$ , higher vibration acceleration had to be applied to prolong the  $t_c$ , for water comparing to the silicone oil (see Figure 1). This effect was attributed to difference in the surface tension of both pure liquids studied. The surface tension of the oil is ca. 4.5 times smaller than water; i.e. the bubble shape is much more deformable in oil. The results obtained prove that mechanism of the bubble bouncing from various interfaces depends on interrelation between rates of two simultaneously going processes: (i) exchange between kinetic and surface energies of the system and (ii) drainage of the liquid film separating the interacting interfaces.

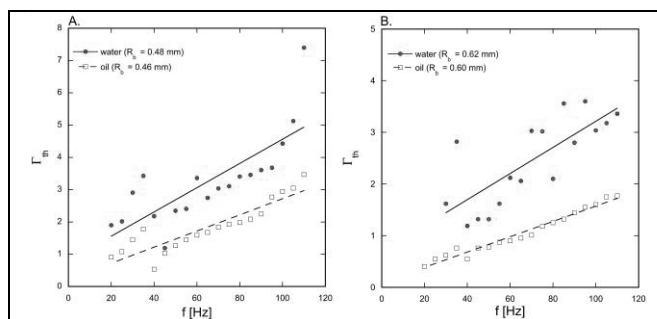


Figure 1. Values of the threshold acceleration as a function of frequency of the surface vibration.

#### Acknowledgements

The study is related to the activity of the European network action COST MP1106: “Smart and green interfaces - from single bubbles and drops to industrial, environmental and biomedical applications”. Financial support from the National Science Centre Research Grant No. 2013/09/D/ST4/03785 is acknowledged with gratitude.

**Influence of enzymatic hydrolysis on functional properties of pumpkin (*Cucurbita pepo* sp.) seed protein isolate**

S. Bučko<sup>1</sup>, J. Katona<sup>1</sup>, Lj. Popović<sup>1</sup>, L. Petrović<sup>1</sup>, J. Milinković<sup>1</sup>. (1) Faculty of Technology, University of Novi Sad, Bulevar cara Lazara 1, 21000 Novi Sad, Serbia, sandranj@uns.ac.rs.

Pumpkin (*Cucurbita pepo* sp.) seed proteins can be obtained from an oil cake, a by-product of the oil extraction, where protein content can be as high as 63.5 %. Main protein fraction of pumpkin seed proteins is presented by 12S globulins – cucurbitins, which are followed by 2S albumins. Together, cucurbitins and 2S albumins, make 59 % of total crude protein content in pumpkin seed proteins [1]. Large molecular weight and size, as well as poor solubility in water are some of the reasons why these proteins are still underutilized as functional ingredients in food products [2]. The aim of this study was to investigate the influence of molecular weight reduction, by means of enzymatic hydrolysis, on functional properties of pumpkin seed protein isolate (PSPI) under different environmental conditions of pH (3–8) and ionic strength (0–1 mol/dm<sup>3</sup> NaCl). Solubility, zeta potential and emulsifying properties of PSPI and two hydrolysates, H1–hydrolysed by alcalase and H2–hydrolysed by pepsin, were investigated. Zeta potential of PSPI and H1 exhibited similar patterns, with isoelectric point (pI) between pH 4 and pH 5, while in case of H2 negative charge prevailed at pH>6. Enzymatic hydrolysis increased solubility of PSPI throughout the whole range of pH tested, but especially at pH close to pI. Addition of NaCl caused both decrease and increase in solubility of PSPI, H1 and H2 depending on pH of the solution. Emulsifying properties of three proteins were investigated by characterization of mean droplet diameter of emulsions with 20 % of sunflower oil in protein solution prepared at different environmental conditions of pH (3, 5 and 8) and ionic strength (0 and 0.5 mol/dm<sup>3</sup> NaCl) and at different emulsifying conditions, i.e. protein concentration (1 and 1.5 g/100 cm<sup>3</sup>) and homogenization rate (10000 and 24000 rpm). PSPI failed to stabilize emulsion at pI, regardless of ionic strength, and at pH 3 when 0.5 mol/dm<sup>3</sup> NaCl was added, while both H1 and H2 successfully stabilized emulsions no matter of pH and ionic strength. Increase in protein concentration had little influence on mean droplet diameter, but increase in homogenization rate brought about reduction in emulsions' mean droplet diameter.

**Acknowledgements**

This work was financed by Ministry of Education, Science and Technological Development of Republic of Serbia, Grant No III 46010. It is done within COST CM1101 and MP1106 action framework.

**References**

- [1] S. Bučko, J. Katona, Lj. Popović, Ž. Vaštag, L. Petrović, M. Vučinić–Vasić, LWT– Food Science and Technology, 64 (2015) 609.
- [2] L. Day, Trends in Food Science & Technology 32 (2013) 25.

## Heat Transfer Coefficient Of An Oscillating Meniscus

*I. Malavasi<sup>1</sup>, L. Pietrasanta<sup>2</sup>, D. Fioriti<sup>3</sup>, M. Mameli<sup>3</sup>, N. Miche<sup>2</sup>, M. Marengo<sup>1,3</sup>. (1) Department of Engineering and Applied Sciences, University of Bergamo, Viale Marconi 5, 24044 Dalmine, Italy; ileana.malavasi@unibg.it. (2) School of Computing, Engineering and Mathematics, University of Brighton, Lewes Road, BN24GJ Brighton, UK. (3) University of Pisa — DESTEC, Largo L. Lazzarino 1, 56122 Pisa, Italy.*

The recent marked increase in power dissipation of electronic devices has drawn a great deal of attention for developing highly efficient passive heat transport devices (more than 100 W/cm<sup>2</sup>). For this purpose heat pipes (HP) are used. Heat transport tubes, using the oscillating flow due to the self-excited oscillation caused by evaporation and condensation of the working fluid, are capable of realizing high heat transport performance. This type of HP is referred to as pulsating heat pipe (PHP). A PHP consists of a simple capillary tube, with no wick structure, bent into many turns, and partially filled with a working fluid. A PHP is governed by complex internal thermo-hydrodynamic transport phenomena. Research on PHP has received substantial attention in the recent past, due to its potential applications in many passive heat transport situations [1,2]. At present there are no theoretical models or correlations available that can predict the PHP behaviour. This prevents the widespread use of PHPs in industrial applications. Comprehensive and reliable mathematical design tools can only be formulated if the nuances of its operating principles are well understood, which, at present, remain rather inadequate. In this context, this work is focused on understanding the simplest possible PHP structure, consisting of one liquid plug and one vapour bubble, also termed as a ‘unit-cell’. This research aims at studying in detail the thermo-fluid-dynamic behaviour of two-phase oscillating flows in a unit-cell mini-tube. The unit-cell is a closed-end straight microchannel, as shown in Figure 1, evacuated and partially filled with a working fluid (deionised water). The heat load is provided by a wire heater coiled on 50mm of the first end of the tube. The heat sink is provided by a water-cooling system; a finned condenser is mounted coaxially with the latter end of the capillary tube for an extent of 100mm. A set of micro-thermocouples has been mounted radially on the capillary tube in the evaporator section at two different depth: the wall thermocouples at 0.5mm from the inner wall while the fluid thermocouples are mounted reaching the main longitudinal axe of the capillary, deep in the fluid flow. The evaporator and the condenser section are embedded in a vacuum chamber, to minimise the convective dispersion toward the environment. The fluid motion can be thermally activated, typical of PHP, where oscillation parameters (frequencies and amplitudes) are not known a priori, and mechanically by means a motion control unit where additional oscillation parameters can be imposed. Parametric investigations as well as simultaneous flowing measurements aiming at the thermal characterization of a liquid/vapour meniscus oscillating in a capillary tube are performed under a definite range of power input. The effect of flow oscillation on the local two phase HTC is then investigated by measuring the instantaneous wall-to-fluid temperature difference, the heat flux level as well as the meniscus oscillation global amplitudes and frequencies.

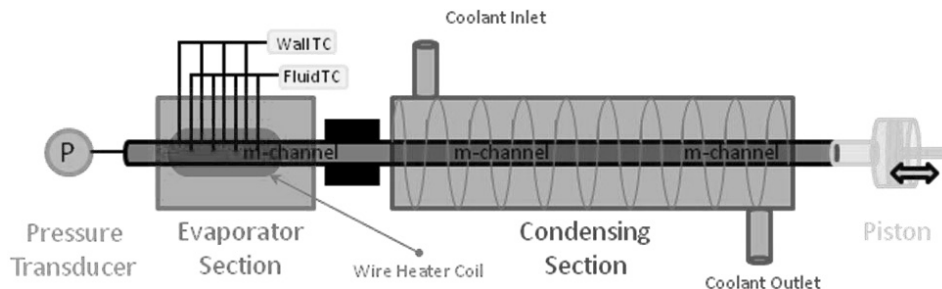


Figure 1. Test cell sketch.

#### Acknowledgements

The authors acknowledge the European Cooperation in Science and Technology — MPNS COST Action MP1106 “Smart and green interfaces — from single bubbles and drops to industrial, environmental and biomedical applications” led by Prof. T. Karapantsios.

#### References

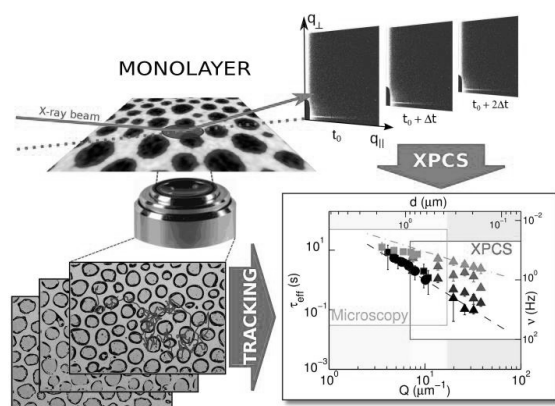
- [1] Y. Zhang, A. Faghri, International Journal of Heat and Mass Transfer, 45 (2002) 755.
- [2] S. Khandekar, V. Silwal, A. Bhatnagar, P. Sharma, Heat Pipe Science and Technology, 1(3) (2010) 279.

**Interfacial Slow Dynamics From The Micro- To The Nanoscale By A Combination Of Real And Momentum Space Techniques**

*Davide Orsi<sup>1\*</sup>, Libero Liggieri<sup>2</sup>, Francesca Ravera<sup>2</sup>, Luigi Cristofolini<sup>1,2,1</sup> - Dipartimento di Fisica e Scienze della Terra, Università degli Studi di Parma, Parma, Italy. 2- Consiglio Nazionale delle Ricerche - Istituto per l'Energetica e le Interfasi, U.O.S. Genova, Genova (Italy). \* Corresponding author: [davide.orsi@unipr.it](mailto:davide.orsi@unipr.it)*

Techniques operating in the momentum space, such as X-ray Photon Correlation Spectroscopy (XPCS), Dynamic Light Scattering or Digital Fourier Microscopy are used to study the microscopic dynamics in arrested systems. Experimental results have to be interpreted through a model, to compensate for the lack of a direct visual inspection in the system common to most cases: the choice of the model is a crucial point. For Brownian diffusion, correlation functions (CF) have simple exponential form with relaxation time  $\tau \sim Q^{-2}$ ; here, macroscopic mechanical properties and microscopic fluctuations are connected via Stokes-Einstein relations. However, this simple picture fails in arrested systems. For instance, polymeric layers or 2D gel systems [1] yield CF with compressed exponential form and  $\tau \sim Q^{-1}$  where defining diffusion coefficients is not trivial. Even more exotic scenarios have been observed e.g. in rejuvenated laponite and methylcellulose gels, in which stretched exponential CF are found with  $\tau \sim Q^{-1}$ . Many of these dynamical features are interpreted postulating either intermittent rearrangements, or random relaxations of stress fields, which however eluded so far any direct observation in real systems.

We characterize the dynamics of 2D Langmuir layers through a combination of real and momentum spaces techniques, namely microscopy tracking and Grazing Incidence XPCS. This combined approach extends the spatial range of investigation beyond the limits of each technique, to reach an extension of over two orders of magnitude, from 80nm up to tens of microns. We apply this to study the arrest dynamics of mixed Langmuir layers of phospholipids and silica nanoparticles: we are able to clearly distinguish different dynamical regimes and assign the dynamics observed in Q-space to diffusive motions and/or intermittent rearrangements observed in real space [2,3].



**References**

- [1] D. Orsi et al. Phys. Rev. E **89**, 042308 (2014)
- [2] D. Orsi, et al., Scientific Reports, **5**, 19730 (2015)
- [3] D. Orsi, et al., submitted (2016)



---

**Comparative Framework for Binder Formulation Development for Inkjet-based Three Dimensional Metal Printing**

---

*J.K. Ferri<sup>1,2</sup>, A.D.Cramer<sup>2</sup>, S. Buczek<sup>2</sup>. (1) Lafayette College, Department of Chemical Engineering, Easton, Pennsylvania, USA. ferrij@lafayette.edu (2) Additive Manufacturing Institute, Lafayette College, Easton, Pennsylvania, USA.*

Additive manufacturing technologies have the ability to revolutionize traditional manufacturing methods, especially with regards to metal and ceramic production. Additive manufacturing techniques lend to greater design flexibility, decreased waste, faster turnaround time for customized parts, and a reduced need for skilled users. Lafayette College's Additive Manufacturing Institute (AMI) utilizes an ExOne R-1 inkjet 3D metal printer for development. The inkjet process uses a binder to *glue* metal particles together during the print process, which is important as the binder dictates different properties of the printed part, such as feature resolution and green state part strength.

The binder formulation can be tuned to adjust these properties, however it is important to understand the impact it will have on its ability to be printed. The inverse Ohnesorge number ( $Z$ ) relates thermophysical properties to ink jettability. We investigated the relationship between polymer concentration ( $C_p$ ) in a binder and its thermophysical properties, ultimately seeking the impact on binder jettability. An increase in polymer concentration led to a reduction in the  $Z$  value; at an approximate polymer concentration of 5wt% the binder formulation is below the limit of the jettable range.

***Acknowledgements***

The authors gratefully acknowledge support from the IDEAL Center for Innovation and the ExOne Company.

**Highly subcooled flow boiling in macro-channels:  
Effect of channel's height and orientation**

M.C. Vlachou\*, J.S. Lioumbas, T.D. Karapantsios. Division of Chemical Technology, Aristotle University of Thessaloniki, 54124 Thessaloniki, Greece, \*marvlach@gmail.com

When it comes to thermal management systems, **flow boiling** yields the most attraction. This is because it can remove high heat loads via the fluid's phase change, while the formed bubbles are sheared off the hot surface via inertial forces. The present work focuses on the investigation of a specific range of experimental parameters that refer to extreme conditions such as the fast cooling of very hot walls, e.g. walls exposed to gas flames. Parameters under investigation are (a) high subcooling level and (b) high mass flux.

This study addresses the effect of **channel's height and orientation** on the removed heat flux and the heat transfer coefficient. Experiments are conducted with water as the working fluid. A device (figure 1) has been constructed with a macro-channel with variable height (3& 10mm), which permits simultaneous monitoring of the heated surface temperature and bubble dynamics in order to correlate boiling regimes with heat transfer results. Other measurements that take place include: bulk liquid's temperature & flow rate, pressure drop along the channel and void fraction at the exit of the test section via a patented custom-made non-intrusive impedance technique (IVED).

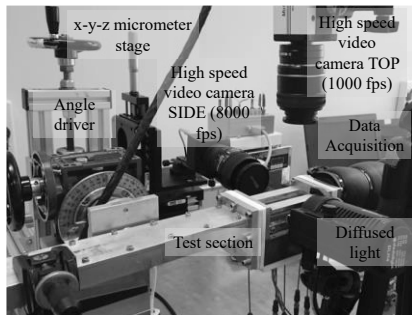


Figure 1. Experimental device.

From the so far obtained results (figure 2) it is seen that vertical orientation enhances heat removal for the same working conditions compared to the horizontal for both channels, which is in accordance with pertinent literature [1, 2]. An insight of the bubble dynamics is going to provide more information for assessing the flow boiling heat transfer mechanisms and the two phase heat transfer coefficient.

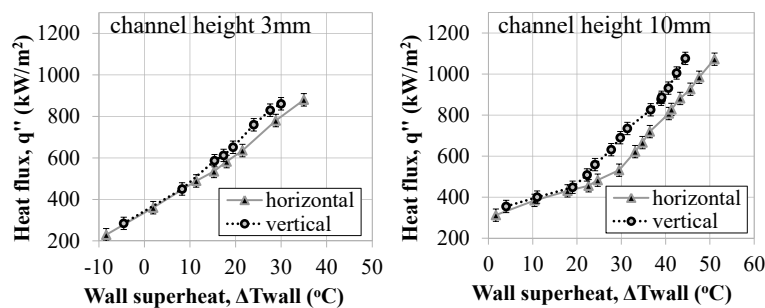


Figure 2. Effect of orientation on the boiling curve for small and large channel and mass flux 330 kg/m<sup>2</sup>s.

**Acknowledgements**

The work is performed with the support of (1) "Highly efficient flow boiling macro-structured/ macro-porous channels" funded by the European Space Agency (Co. No. 4000106405/12/NL/PA) (2) IKY Fellowships of excellence for postgraduate studies in Greece – SIEMENS program. The work is performed under the umbrella of COST Action MP1106.

**References**

- [1] M. A. Akhavan-Behabadi, M. Esmailpour, *International Communications in Heat and Mass Transfer*, 55 (2014) 8.
- [2] A. Kundu, R. Kumar, A. Gupta, *International Journal of Refrigeration*, 45 (2014) 1.

---

**Study of Coarsening and Coalescence for Dry Foams in 2D**

---

*A. Cagna a, C. Honorez a, b & W. Drenckhan b. aTECLIS, Longessaigne, France bLPS, Orsay, France, alain.cagna@teclis.fr*

Just after its generation a liquid foam undergoes three important ageing processes: drainage, coarsening and coalescence. It is very complicated to study simultaneously these three phenomena since they are tightly coupled. An elegant solution to this problem is to use 2D foams which consist of a monolayer of bubbles trapped between two plates (figure 1). These have the advantage of providing direct access to visualization, hence providing the information on which process occurs during the foam life (1, 2). For example, coarsening is simple to observe: Von Neuman demonstrated that the time evolution of 2D bubbles depends only on the number of their sides: the evolution of the area  $A$  as a function of time of a bubble of  $n$  sides is  $dA/dt \propto (n - 6)$ . It means that bubbles with  $n > 6$  grow, bubbles with  $n < 6$  shrink and the area of hexagonal bubbles ( $n = 6$ ) is constant. The coalescence is related to the disappearance of the bubbles, if a bubble disappears even though its area is not equal to zero so the foam is coalescing. However, the coarsening is also occurring during the coalescence phenomenon. These two processes may be simultaneous, so it is necessary to separate them to have a better understanding of foam life.

We used a 2D cell ("Hele Shaw" configuration) adapted on a Foamscan to generate and study the coarsening and the coalescence of liquid foams obtained with different surfactant concentrations and different liquid fractions. The foam height was measured and analyzed through the Foamscan software and the geometrical and topological aspects of the bubbles were studied by the dedicated CSA software. The analysis allows to investigate the influence of the physical parameters and the formulation of foams on the competition between coarsening and coalescence.

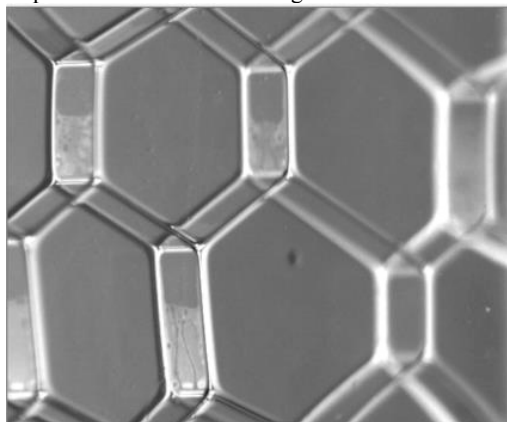


**Figure 1:** Monolayer of bubbles trapped between two glass plates

#### *References*

- [1]. Saint-Jalmes A. *Soft Matter*. 2006;2(10):836-49.
- [2]. Saulnier L, et al. *Colloids and Surfaces A: Physicochemical & Engineering Aspects*. 2015(0).

Experimental Determination of Thin Film Drainage Around Single Foam Bubbles

A.T. Zamanis, M. Kostoglou, S.P. Evgenidis, T.D. Karapantsios., Division of Chemical Technology, Department of Chemistry, Aristotle University of Thessaloniki, Univ. Box 116, 54124 Thessaloniki, GREECE. E-mail: azamanis@chem.auth.gr, agzamanis@yahoo.gr

This work aims to present the first steps of the development of an electrical resistance technique coupled with pressure and optical measurements capable of measuring the drainage of thin films around a single bubble. A small bubble is initially created inside a vertical liquid bridge whose ends are in contact with two metallic rods which act as sensing electrodes. The bubble is then expanded inside the bridge up to the point that a thin film forms between the bubble and the outer surface of the bridge. Pressure and optical measurements serve as indicators of the shape and size of the bubble and the liquid bridge. Two modes of operation are examined (Figure 1). The first mode calls for the bubble steadily increasing in size until film rupture while the liquid in the bridge remains constant. In the second mode it is the liquid of the bridge that is withdrawn until film rupture while the bubble is maintained constant. In both modes the increasing electrical resistance during film thinning is recorded. The liquids that used in both modes are water, water/SDS (50ppm), water/ethanol (0.3%, v/v) and water/SDS/ethanol (50ppm SDS +0.3%, v/v ethanol). The diameter of electrodes was 3.12 mm and the initial volume of liquid bridge was 20 $\mu$ l. In the first mode reconnection of liquid bridge under certain conditions is observed. In the second mode where different drainage rates applied (water: 1.132 mm<sup>3</sup>/s, water/SDS: 1.655 mm<sup>3</sup>/s, water/ethanol: 0.454 mm<sup>3</sup>/s, water/SDS/ethanol: 0.465 mm<sup>3</sup>/s) the liquid bridge is destroyed through neck or film rupture depending on the conditions.

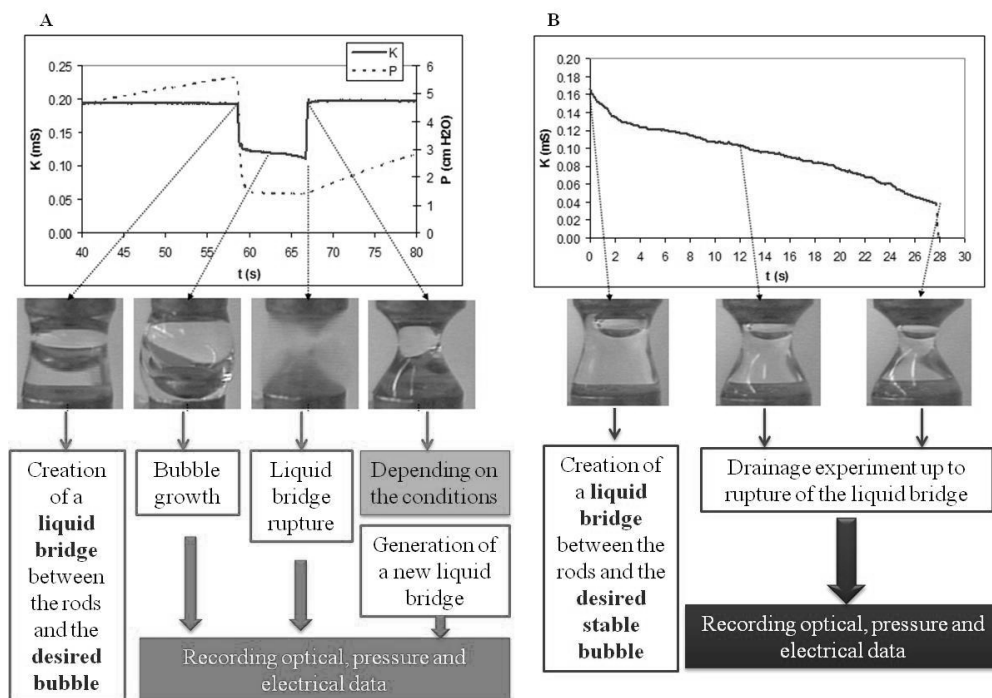


Figure 1. Plots of electrical conductivity of liquid frige versus time during (A) bubble growth (first mode) and (B) drainage (second mode).

### Dynamics of Adsorption of Ionic Surfactants at the Water/Air Interface with Hexane Vapour in the Gas Phase

**T. Kairaliyeva<sup>1,2</sup>, R. A. Campbell<sup>3</sup>, N. Mucic<sup>1</sup>, A. Javadi<sup>1,4</sup>, J. Krägel<sup>1</sup>, E.V. Aksenenko<sup>5</sup>, V.B. Fainerman<sup>6</sup>, S.A. Aidarova<sup>2</sup> and R. Miller**  
 (1) Max Planck Institute of Colloids and Interfaces, Potsdam, Germany, [Talmira.Kairaliyeva@mpikg.mpg.de](mailto:Talmira.Kairaliyeva@mpikg.mpg.de). (2) Kazakh National Technical University after K.I. Satpaev, Almaty, Kazakhstan. (3) Institute Laue-Langevin, Grenoble, France. (4) Chemical Engineering Department, University of Tehran, Tehran, Iran. (5) Institute of Colloid Chemistry and Chemistry of Water, Kiev, Ukraine. (6) Medical University Donetsk, Donetsk, Ukraine

Although a great deal of research has been conducted in the area of fluid mechanics, the complete dynamics of such flows are not yet fully understood due to their complex interphase coupling, whereby different phases may strongly affect one another. Fluid interfaces are omnipresent in most modern technologies and their quantitative characterization is essential for the optimum use of such technologies [1].

Historically, the adsorption of surfactants at water/oil interfaces was described by models developed for the water/air interface. However, the presence of an oil phase leads to significant interactions between the hydrophobic chains of the surfactant molecules and the molecules of the oil phase [2].

On the basis of experimental data for the homologous series of alkyltrimethyl ammonium bromides ( $C_n$ TAB) the equilibrium surface tension isotherms at the aqueous solution/alkane interface are discussed. A model assuming a competitive adsorption of alkane and  $C_n$ TAB molecules at the interface can describe the experimental data quantitatively, as demonstrated in [3]. The same thermodynamic model describes also the adsorption behaviour of  $C_n$ TAB molecules at the interface between the aqueous surfactant solutions and an alkane saturated air phase. The alkane molecules co-adsorb from the vapour phase and also compete with the  $C_n$ TAB molecules, depending on the alkane chain length [4]. Also the dynamic properties of  $C_n$ TAB adsorption layers at the interface to an alkane bulk phase or vapour phase are strongly influenced by the co-adsorption of the alkane molecules [5]. Also FIGARO experiments with neutron reflections were made at the Institut Laue Langevin Grenoble, France. The results shown in Figs. 1 and 2 are obtained from experiments for aqueous  $C_{16}$ TAB solutions at the water/hexane vapour interface.

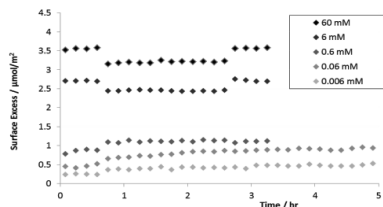


Figure 1. Adsorption of  $C_{16}$ TAB

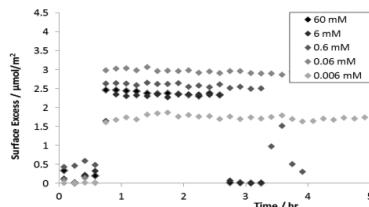


Figure 2. Adsorption of hexane.

#### References

- [1] M. Tacihi Rahni, M. Karbaschi, and R. Miller, "Computational Methods for Complex Liquid-Fluid Interfaces", in "Progress in Colloid and Interface Science", Vol. 5, CRC Press, Taylor & Francis Group.
- [2] V.B. Fainerman, N. Mucic, V. Pradines, E.V. Aksenenko and R. Miller, Adsorption of alkyltrimethylammonium bromides at water/alkane interfaces – competitive adsorption of alkanes and surfactants, *Langmuir*, 29 (2013) 13783–13789
- [3] V.B. Fainerman, E.V. Aksenenko, N. Mucic, A. Javadi and R. Miller, Thermodynamics of adsorption of ionic surfactants at water/alkane interfaces, *Soft Matter*, 10 (2014) 6873-6887.
- [4] N. Mucic, N. Moradi, A. Javadi, E.V. Aksenenko, V.B. Fainerman and R. Miller, Mixed adsorption layers at the aqueous  $C_n$ TAB solution / hexane vapor interface, *Colloids Surfaces A*, 442 (2014) 50-55.
- [5] N. Mucic, N.M. Kovalchuk, V. Pradines, A. Javadi, E.V. Aksenenko, J. Krägel and R. Miller, Dynamic properties of  $C_n$ TAB adsorption layers at the water/oil interface, *Colloids Surfaces A*, 441 (2014) 825-830.

**Determination and Comparison of Size and Stability of Nanobubbles Produced by Two Different Generators**

*E.D.Michailidi<sup>1</sup>, R.I.Kosheleva<sup>1</sup>, A.C.Mitropoulos<sup>1</sup> Hephæstus Advanced Laboratory, Eastern Macedonia & Thrace Institute of Technology, St.Lucas, Kavala, Greece, [elisavet.michailidi@gmail.com](mailto:elisavet.michailidi@gmail.com).*

Nanobubbles (NB) are nanoscopic gas cavities in liquids with  $d < 1\mu\text{m}$ . They have attracted the attention of the scientific community due to the fact that despite their small size they demonstrate an extended lifetime; other physicochemical properties have been investigated too [1]. The present research examines the size distribution and stability of NB produced by a specially designed apparatus [2] with two different heads; one with a porous plug and another with a nozzle. Size distribution is determined by dynamic light scattering (DLS), while stability from  $\zeta$ -potential measurements. Nanobubbles are produced within aqueous solutions of deionized water. For the case of porous plug head, the mixture of gas and water is forced through a porous medium of random packing while for the case of nozzle the mixture is forced through an orifice acquiring high velocity. The introduced gas is high purity  $\text{O}_2$ . The production conditions of pressure and temperature are 24 bar and 40 °C respectively. The samples were collected after 45 minutes of operation.

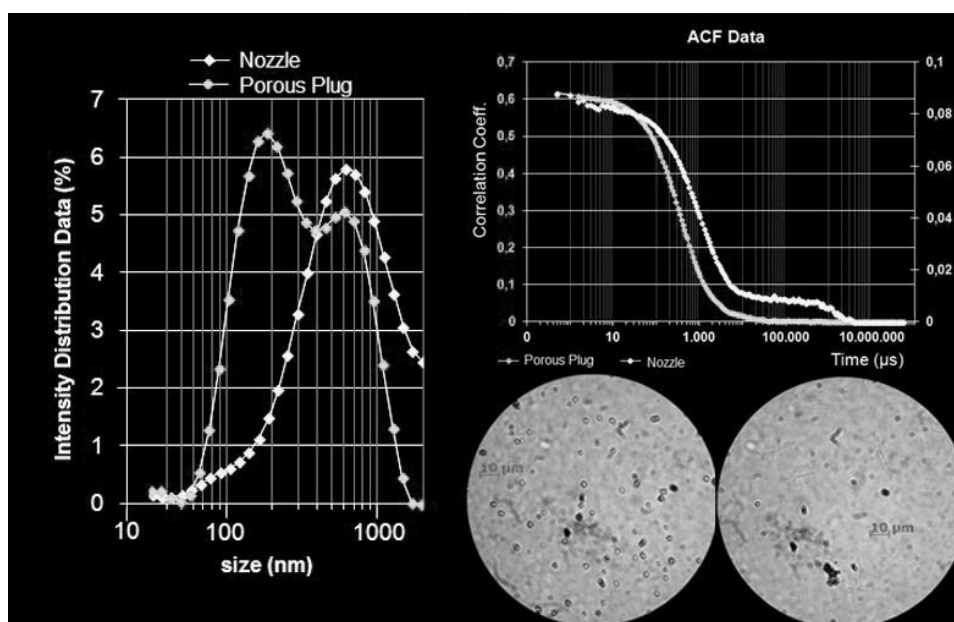


**Figure 1.** NB; lLeft: DLS; right up: ACF; right down microscopy (analysis: 10μm, left: porous plug, right: nozzle).

Comparing the results of DLS for both methods (i.e. porous plug and nozzle) it can be seen that the size of NB from porous plug generator is smaller (164 nm) than those produced by the nozzle (824 nm), fact also shown from auto-correlation function (ACF) decay time. However, the nozzle performs more uniform distribution compared to the porous plug; where two peaks are observed, except the main peak at 164nm there is an additional one at 531nm corresponding to lower intensity. Zeta-potential measurements were also carried out. For the porous plug  $\zeta = -9.83\text{mV}$ , whereas for nozzle  $\zeta = -17.1\text{mV}$ ; the stability is better for the later than the former. The negative sign represents the negatively charged NB, where repulsive forces prevent coalescence [3]. Yet, the microscopy shows that the concentration from the porous plug is much higher than that of the generator nozzle. To conclude, the examination of size distribution and stability reveals that the head of the generator plays an important role in the production of NB. Further investigation is underway.

**References**

- [1] K. Ohgaki, N. Khanh, Y. Joden, A. Tsuji & T. Nakagawa, *Chemical Engineering Science*, 65 (2010), 1296.
- [2] A. Mitropoulos & G. Bomis, Device for generating and handling nanobubbles, EP 2995369A1/16-3-2016.
- [3] M. Takahashi, *The Journal of Physical Chemistry B*, 109 (2005) 21858.

## Flow Boiling of Self-Rewetting 1- Butanol/Water Mixture in a Square Microchannel

*P. Vasileiadou<sup>1</sup>, Khellil Sefiane<sup>1</sup>, T.G. Karayiannis<sup>2</sup>* (1) School of Engineering, University of Edinburgh, The King's Buildings, Mayfield Road, Edinburgh EH93JL, UK, [p.vasileiadou@ed.ac.uk](mailto:p.vasileiadou@ed.ac.uk). (2) College of Engineering, Design and Physical Sciences, Brunel University, London, Uxbridge UB8 3PH, UK

The progress over the past few decades in microelectronics has led to the requirement for more effective cooling techniques. Two-phase flow heat transfer with phase change is a promising way of cooling as it allows for high heat transfer coefficients and uniform temperatures. One of the factors that affect the heat transfer performance is the cooling fluid used and hence, its selection is of paramount importance to ensure heat transfer enhancement [1]. Refrigerants were the most commonly used fluids in the past, however their environmental impact has come to light and alternative fluids have been under investigation. The use of mixtures is one such alternative to refrigerants and thus, several studies have been conducted on them.

In this study, a 5% v/v butanol/water mixture and its pure components (deionised water, butanol) were used as working fluids and their heat transfer behavior was examined. The experiments were conducted with a 5mm inner hydraulic diameter square borosilicate glass channel at a vertical orientation. The channel was covered with a thin layer of tantalum (metal), which allowed it to conduct electricity while remaining transparent and hence, it could be used as a resistive heater. Three heat fluxes were examined in this experiment ( $2.8\text{kW/m}^2$ ,  $4.2\text{kW/m}^2$  and  $6.1\text{kW/m}^2$ ) and the liquids were induced in the system subcooled at three mass fluxes:  $0.33\text{kg/m}^2\text{s}$ ,  $0.66\text{kg/m}^2\text{s}$  and  $1.00\text{kg/m}^2\text{s}$ , and were heated up to saturation and boiling. The experiments were run in an enclosed environment with a controlled temperature of  $40^\circ\text{C}$  in order for the heat losses to be minimized. For each experiment, high speed imaging was obtained in order to identify the flow boiling patterns. The channel wall temperature was measured along with the pressure drop across the channel and the local heat transfer coefficients ( $h_L$ ) over time were calculated along the length of the channel (Figure 1).

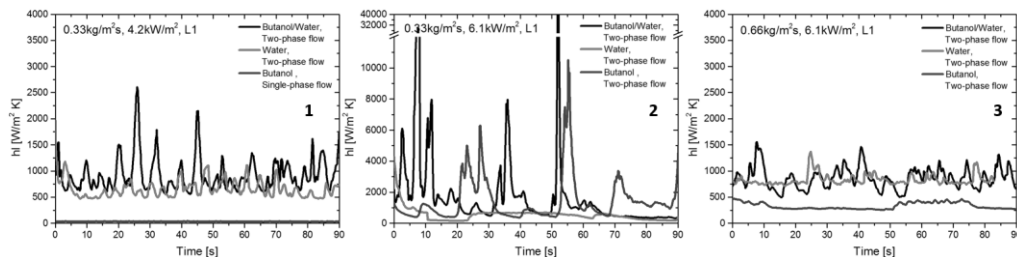


**Figure 1.** Local heat transfer coefficient,  $h_L$ , over time for 5% v/v butanol/water mixture, butanol and water at the highest point of the channel (L1) at mass flux  $G=0.33\text{kg/m}^2\text{s}$  and heat flux (1)  $q=4.2\text{kW/m}^2$ , (2)  $q=6.1\text{kW/m}^2$  and at (3)  $G=0.66\text{kg/m}^2\text{s}$  and  $q=6.1\text{kW/m}^2$

The boiling regimes observed using high speed visualization for all the fluids were: bubble, slug and elongated slug/annular flow. Furthermore, the channel wall temperature was found to fluctuate over time with two-phase flow, which was attributed solely to boiling within the channel. Recoiling and rewetting were observed for all the fluids but a periodic pattern was observed for the butanol/water mixture. Moreover, the channel wall temperature was found to be lower for the butanol/water mixture comparing to those of pure butanol and water. In conclusion, the mixture showed an enhancement in heat transfer comparing to its pure components. Heat transfer coefficients were found to increase with increasing heat flux and the periodicity of the heat transfer coefficient fluctuations for the mixture suggested more consistent heat transfer over a longer period of time.

### Acknowledgements

This research was supported by the UK Engineering and Physical Sciences Research Council (EPSRC).

### References

[1] Duursma, G., Sefiane, K., Dehaene, A., Harmand, S., & Wang, Y. 2014 Flow and Heat Transfer of Single- and Two-Phase Boiling of Nanofluids in Microchannels. *Heat Transfer Engineering*, 36(14-15), 1252–1265.

**VOC Free Nanoemulsions Of Aminopropylaminoethyl Polysiloxane Prepared By Phase Inversion Emulsification With C13 Ethoxylated Surfactants Of Various HLB**

*Christos G. Koukiotis<sup>1,2</sup>, Giannis Kokkinos<sup>1</sup>, Thodoris D. Karapantsios<sup>1</sup>. (1) Department of Chemical Technology, Department of Chemistry, Aristotle University of Thessaloniki, Thessaloniki, Greece, koukiotis@gmail.com (2) LOUFAKIS CHEMICALS SA, Industrial Area of Thessaloniki, Thessaloniki, Greece.*

There is an increasing interest in the formation of nanoemulsions for foodstuff [1], cosmetics[2], pharmaceutical products[3] (e.g., for drug delivery systems) and other industries due to the advantages compared to macro-emulsions, like the small droplet size, higher stability and optical transparency.

In our work we study the emulsification of TSF4708 (aminopropylaminoethyl polysiloxane) by using phase inversion emulsification technic and C13 ethoxylated surfactants of various HLB.

Our emulsions were of zero VOC as we prepared them by avoiding the use of any co-solvent. Using C13 ethoxylated surfactants of HLB 11-13 we got transparent nanoemulsion of very low particle size (fig. 1). Dynamic surface measurements of the nanoemulsions (fig. 2) shows that nanoemulsion with C13 ethoxylated with HLB=11 (Lutensol TO6) presents also the lower dynamic surface tension.

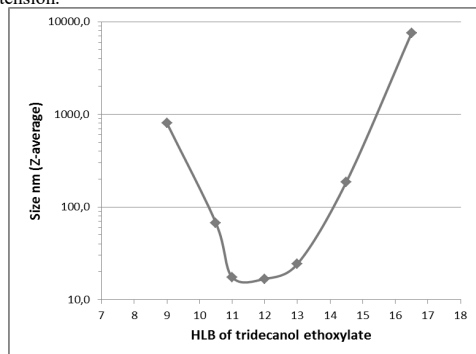


Figure 1. Particle size of polysiloxane emulsion by DLS vs the HLB of the used C13 ethoxylated surfactant.

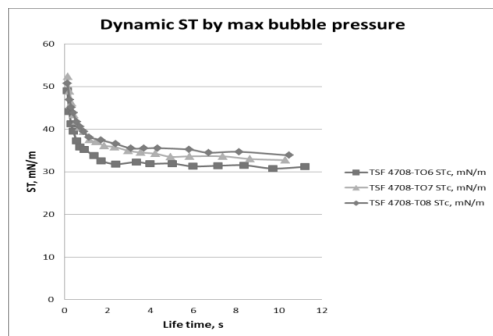


Figure 2. Dynamic surface tension of nanoemulsions by max bubble pressure.

**Acknowledgements**

Financial support by the European Space Agency through the project FASES (Fundamental and Applied Studies of Emulsion Stability) is gratefully acknowledged.

**References**

- [1] Silva, H., Cerqueira, M., & Vicente, A. (2012). Food and Bioprocess Technology, 5(3), 854-867.
- [2] Miller, D. J., Henning, T., & Grünbein, W. (2001). Colloids and Surfaces A: Physicochemical and Engineering Aspects, 183–185(0), 681-688
- [3] Anton, N., Benoit, J.-P., & Saulnier, P. (2008). Journal of Controlled Release, 128(3), 185-199



## Study of Void Fraction Fluctuations Dependence on Bubble Size through Experimental and Simulated Electrical Signal Analysis

S. Evgenidis<sup>1</sup>, M. Kostoglou<sup>1</sup>, T. Karapantsios<sup>1</sup>.


(1) Aristotle University of Thessaloniki, Department of Chemical Technology, School of Chemistry, Univ. Box 116, 54124, Thessaloniki, Greece, [sevgenid@chem.auth.gr](mailto:sevgenid@chem.auth.gr).

This work studies the effect of bubble size on void fraction fluctuations analyzing experimental and simulated electrical signals for the case of bubbly flow. Bubble size is known to affect seriously the average void fraction in bubbly flows where buoyant velocities vary considerably with bubble size. On the contrary, there is no systematic literature report about bubble size effects on the intensity and frequency of void fraction fluctuations around the average void fraction. Experiments are conducted in co-current upward dispersed bubble flow inside a 21 mm tube, while bubble sizes and gas/liquid velocities resemble conditions of Decompression Sickness (DCS) in the bloodstream of human vena cava. A patented electrical impedance spectroscopy technique [1] is employed along with non-intrusive ring electrodes to register void fraction fluctuations down to  $10^{-5}$ . Bubble sizes are estimated from high resolution optical images. It is found that the intensity and frequency of void fraction fluctuations vary appreciably with bubble size when keeping constant the gas and liquid flow rates. Moreover, these variations are not random but scale with bubble size. As a first step to quantify this effect, an empirical expression is derived that relates bubble size to statistical properties of void fraction [2]. Analysis of simulated electrical signals confirms the dependence of void fraction fluctuations on bubble size and also facilitates the assessment of information provided by the aforementioned empirical equation.

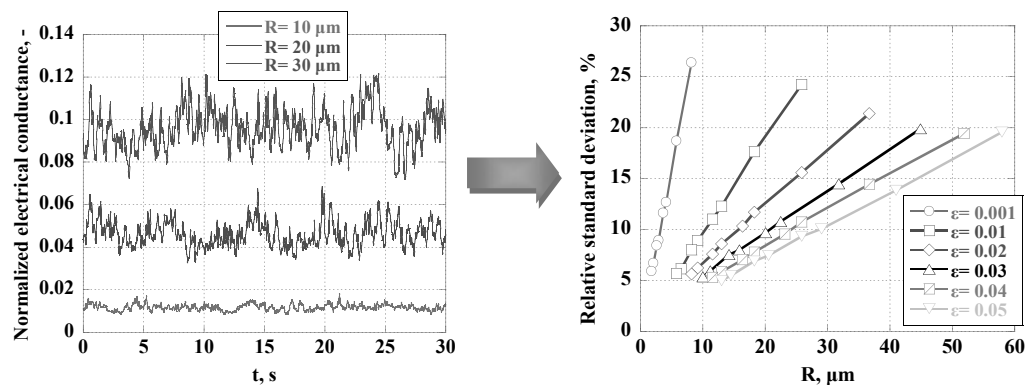


**Figure 1.** Bubble size effect on relative standard deviation of electrical signals for varying void fraction ( $\epsilon$ ) values.

### Acknowledgements

This study was funded by  (GSTP Project: In-Vivo Embolic Detector, I-VED - Contract No.: 4000101764 and MAP Project: Convective boiling and condensation local analysis and modelling of dynamics and transfers, MANBO – Contract No.: 4200020289) and carried out under the umbrella of COST Action MP1106: ‘Smart and green interfaces— from single bubbles and drops to industrial, environmental and biomedical applications’. The view expressed herein can in no way be taken to reflect the official opinion of the European Space Agency.

### References

- [1] T. D. Karapantsios, S. P. Evgenidis, K. Zacharias, T. Mesimeris, *European Patent Office*, 3005942 A1 (2015).
- [2] S. P. Evgenidis, T. D. Karapantsios, *International Journal of Multiphase Flow*, 75 (2015) 163.

---

**Velocity Of Rising Air Bubbles In Aqueous Beta-Lactoglobulin Solutions At Different Ph And Salt Concentrations**

---

*V. Ulaganathan<sup>1</sup>, G. Gochev<sup>1,2</sup>, C. Gehin-Delval<sup>3</sup>, D.Z. Gunes<sup>3</sup> M.E. Leser<sup>3</sup> and R. Miller<sup>1</sup> (1) Max-Planck-Institute for Colloid and Interface Science, D-14476 Golm, Germany, [vamseekrishna.ulaganathan@mpikg.mpg.de](mailto:vamseekrishna.ulaganathan@mpikg.mpg.de) (2) Institute of Physical Chemistry, Bulgarian Academy of Sciences, 1113 Sofia, Bulgaria. (3) Nestlé Research Center, CH-1000 Lausanne 26, Switzerland*

The local velocity profile (LVP) of a rising bubble can serve as a fingerprint for the dynamic behavior of the adsorption/desorption processes going on at a solution/air interface. Bubbles of air in pure water show a LVP with a range of acceleration and leveling off after a certain distance of the bubble movement. In solutions of surface active compounds at sufficiently high bulk concentrations, however, the bubble surface becomes very rigid due to the fast established adsorption layer and the observed terminal velocity is much lower as measured for a completely free and therefore mobile bubble surface. At intermediate concentrations a transition between the two extreme cases of the LVP are observed with a maximum velocity value the location of which is shifting to shorter distances with increasing bulk concentrations [1]. The LVP of bubbles in aqueous  $\beta$  lactoglobulin (BLG) solutions proves to be extremely sensitive for the adsorption of proteins at very low bulk concentrations. In addition, it can show that the pH and ionic strength of the aqueous solution has a strong impact on the surface properties of BLG at the solution/air interface. This behavior is in line with experimental results at the surface of air bubbles at rest in BLG solutions [2].

It is observed that the time for establishing an immobile rigid surface layer at the rising bubble surface becomes shorter with increasing pH. A peculiar behavior is observed at the isoelectric point (IEP) where the LVPs show irregularities. Under dynamic conditions BLG has not its highest surface active at the IEP [3].

**Acknowledgements**

PhD grant (VU) from Nestle Research Centre, Lausanne, Switzerland is gratefully acknowledged.

**References**

- [1] S.S. Dukhin, V.I. Kovalchuk, G.G. Gochev, M. Lotfi, M. Krzan, K. Malysa and R. Miller, Dynamics of Rear Stagnant Cap Formation at the Surface of Spherical Bubbles Rising in Surfactant Solutions at large Reynolds Numbers Under Conditions of Small Marangoni Number and Slow Sorption Kinetics, *Adv. Colloid Interfaces Sci.*, doi:10.1016/j.cis.2014.10.002.
- [2]. V. Ulaganathan, I. Retzlaf, J.Y. Won, G. Gochev, C. Gehin-Delval, M.E. Leser, B.A. Noskov and R. Miller,  $\beta$ -Lactoglobulin Adsorption Layers at the Water/Air Surface: 1. Adsorption Kinetics and Surface Pressure Isotherm: Effect of pH and Ionic Strength, submitted to *Colloids Surfaces A*
- [3]. V. Ulaganathan, G. Gochev, C. Gehin-Delval, M.E. Leser and R. Miller Effect of pH and salt concentration on rising air bubbles in  $\beta$ -lactoglobulin solutions, submitted to *Colloids Surfaces A*

## Application of Electrical Resistance Tomography and Differential Pressure Method for Low Void Fraction Values Determination in Bubbly Flow of Sub-millimeter Bubbles

S. Evgenidis<sup>1</sup>, P. Zikou<sup>1</sup>, T. Karapantsios<sup>1</sup>.

(1) Aristotle University of Thessaloniki, Department of Chemical Technology, School of Chemistry, Univ. Box 116, 54124, Thessaloniki, Greece, sevgenid@chem.auth.gr.

This work investigates experimentally the variation of void fraction with respect to gas/liquid flow properties and bubble size in a dispersed bubbly flow resembling Decompression Sickness conditions in humans' bloodstream. Decompression Sickness (DCS) is a clinical syndrome caused by rapid reduction of environmental pressure in the body that results in formation of bubbles within body tissues, creating symptoms of variable severity that range from joint pain to permanent deficits or even death.


Experiments are conducted in a co-current upward dispersed bubbly flow inside a 21 mm tube. Water and blood simulant are used as test liquids with velocity from ~3 to ~30 cm/s. Bubble sizes are controlled using prescribed surfactant (SDS) concentrations and range from ~50 to ~800  $\mu\text{m}$ . The resulting void fraction values range from 0.001 to 0.1. Void fraction is measured at three axial locations of the flow employing: a) three similar Electrical Resistance Tomography (ERT) probes (*P2000*, *ITS*), each consisting of 16 flush-mounted plate electrodes (2mm x 2mm) made of stainless steel and b) three ultra-sensitive differential pressure ( $\Delta P$ ) sensors (*DP 15*, *Validyne*) combined with a proper signal demodulator (*CD280*, *Validyne*) and a 16-bit data acquisition card (*DAQPad-6015*, *National Instruments*). Bubble sizes are estimated from high resolution optical images.

Results obtained demonstrate that ERT and  $\Delta P$  void fraction measurements are in accepted agreement for all experimental conditions. Void fraction seems to be axially uniform along the vertical pipe as results from ERT measurements at three axial locations combined with local and global  $\Delta P$  measurements. Moreover, void fraction increases with increasing gas superficial velocity and decreasing liquid superficial velocity or average bubble size.

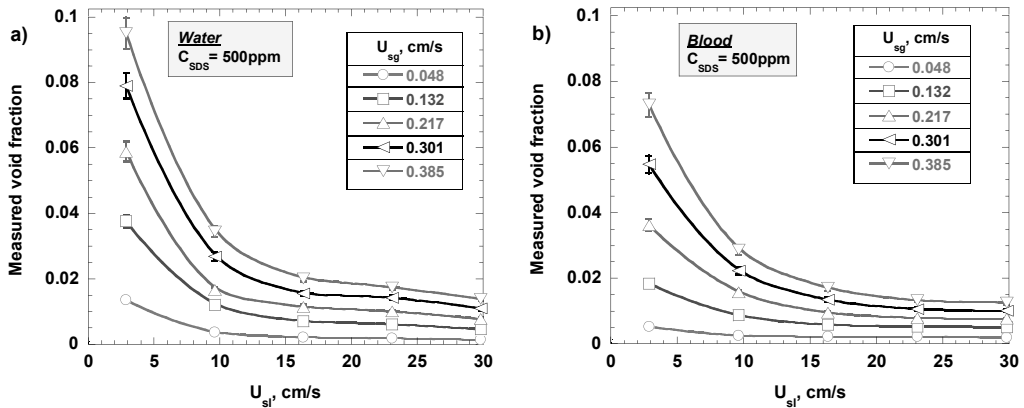


**Figure 1.** Effect of superficial liquid velocity ( $U_{sl}$ ) and superficial gas velocity ( $U_{sg}$ ) on measured void fraction for  $C_{sds} = 500$  ppm in (a) Water and (b) Blood.

### Acknowledgements

This study was funded by  (GSTP Project: In-Vivo Embolic Detector, I-VED - Contract No.: 4000101764 and MAP Project: Convective boiling and condensation local analysis and modelling of dynamics and transfers, MANBO – Contract No.: 4200020289) and carried out under the umbrella of COST Action MP1106: ‘Smart and green interfaces— from single bubbles and drops to industrial, environmental and biomedical applications’. The view expressed herein can in no way be taken to reflect the official opinion of the European Space Agency.

**Removal Of Polycyclic Aromatic Hydrocarbons In Aqueous Solution  
By Electrochemical Oxidation**

*G. Gallios<sup>1</sup>, E. Vardaka<sup>1</sup>, I. Voinovschi<sup>1</sup>, M. Brienza<sup>1</sup>, D. Kupka<sup>2</sup>, M. Vaclavikova<sup>2</sup> (1) Aristotle University, Thessaloniki, Greece, (2) Institute of Geotechnics, Slovak Academy of Sciences, Watsonova 45, 04001 Kosice, Slovakia, monica.brienza@unibas.it*

Electrochemical oxidation is a promising technology for the treatment of polluted water. In recent years, the presence and concentration of polycyclic aromatic hydrocarbons (PAHs) in the environment have been reported in several parts of the world. The accumulation and persistence of PAHs in the environment can produce harmful effects; in both aquatic and terrestrial ecosystems due to their highly carcinogenic, mutagenic properties [1-3]. Additionally, PAHs are persistent organic pollutants due to their chemical stability and resistance to biodegradation. The objective of this study was to evaluate the ability of electrochemical oxidation to remove PAHs from polluted water using titanium-based dimensionally stable anode (DSA). Anthracene has been used as model compound since it is found in high concentrations in contaminated environmental samples. The experiments were carried out in a laboratory scale electrolytic cell made of Plexiglas (active volume 500 mL), using one anode and two cathodes. The pH was not controlled. Parameters such as addition of small quantity of electrolytes and current density were examined. Small initial concentrations of anthracene (1mg L<sup>-1</sup>) were used at room temperature. The treated contaminated solutions were analysed by HPLC. Complete degradation of the target PAH was achieved in 10 minutes. The process was studied further up to 120 min, where complete degradation of the PAH was achieved. Intermediate products were detected in HPLC after a few minutes of treatment. So, the next step will be to identify the possible structures of metabolites that can be formed during this electrochemical oxidation. Concluding, the preliminary experiments have shown that electrochemical oxidation with DSA anode has a great potential in the treatment of wastewaters contaminated with PAHs.

**Keywords:** *Electrochemical oxidation, PAHs, Anthracene, degradation, polyaromatic hydrocarbons*

**Acknowledgements**

The financial support of this research provided by the following projects: People Programme (Marie Curie Actions) of the European Union's Seventh Framework Programme FP7/2007-2013/ under REA grant agreement n°612250 (project WaSClean FP7-People-2013-IAAP) as well as Slovak R&D Agency project No APVV-10-0252-WATRIP and NATO SPS Multi-Year Project EAP.SFPP 984403.

**References**

- [1] F. Busetti, A. Heitz, M. Cuomo, S. Badoer, P. Traverso, *J Chromatogr A* 1102 (2006)104
- [2] E. Manoli, C. Samara, *Environ Pollut* 151 (2008) 477
- [3] CA Menzie, BB Potocki, J Santodonato. *Environ Sci Technol* 26 (1992)1278

## Self-Assembly By Multi-Drop Evaporation Of Carbon-Nanotube And Graphene-Oxide-Platelets Droplets On A Glass Substrate

C.S. Iorio<sup>1</sup>, C. Minetti<sup>1</sup>, Hatim Machrafi<sup>1,2</sup> (1) Service Chimie-Physique, Université Libre de Bruxelles, Brussels, Belgium, [ciorio@ulb.ac.be](mailto:ciorio@ulb.ac.be), (2) Thermodynamics of Irreversible Phenomena, Université de Liège, Liège, Belgium.

Self-assembly has many advantages and applications. It is applied in the medical sector [1]. It can also be used for energy storage [2] or in membrane technology [3]. Here we focus on the procedure of creating complicated structures. We propose to do this by depositing droplets containing nanoparticles and let them evaporate. The Marangoni motion in the droplet that is triggered by the evaporation makes the nanoparticles follow a certain pattern. We have performed a theoretical study on the instability onset [4] and the purpose here is to use the Marangoni convection to assemble the nanoparticles. Then another drop is deposited on the same spot, which evaporates. This is repeated for a third time. In this way a certain structure is obtained. We use two nanofluids: a 2g/l solution of graphene-oxide (GO) platelets dispersed in water and a 1g/l solution of single-walled carbon (SWC) nanotubes dispersed in water. Figure 1 shows a schematic view of the procedure: (a) we deposit three droplets next to each other; (b) after evaporation, the nanoparticles stick to the glass substrate; we add another droplet only in the middle and at the right of the substrate; (c) after evaporation, a thicker deposition is obtained on middle and the right side of the substrate; we add again another droplet, but only at the right; (d) after evaporation, the right side shows an even thicker deposition.



**Figure 1.** Schematic representation of the self-assembly.

Figure 2 shows preliminary results of SEM images of the self-assembled structures of the SWC solution for one, two and three evaporated drops, respectively.

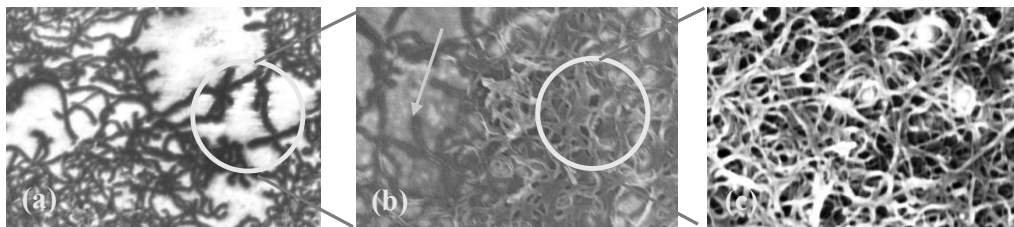


**Figure 2.** SEM images (100.000 x) of the self-assembly of SWC nanotubes after evaporation of 1 drop (a), two drops (b) and three drops (c).

Figure 2(a) shows that after evaporation of one drop, no clear structure is identifiable. Figure 2(b) shows nicely the difference: the arrow shows the background (from a zoom of Figure 2(a)), while the circle shows the second layer of SWC nanotubes. Not only a second layer is constructed, but a higher density is obtained as well. It seems that the first layer acts as a kind of coating that change the contact angle and increases the adherence of the glass substrate. In Figure 2(c), it can be seen that the third evaporated drop already causes a self-assembled dense structure. So the density increases more than linearly after each evaporated drop.

### References

- [1] L.J. Ke, G.Z. Gao, Y. Shen, J.W. Zhou and P.F. Rao, *Nanoscale Research Letters* **10**, 449 (2015).
- [2] C.C.B. Bufon, J.D.C. González, D.J. Thurmer, D. Grimm, M. Bauer and O.G. Schmidt, *Nano Letters* **10**, 2506 (2010).
- [3] J. Ding, X. Li, X. Wang, J. Zhang, D. Yu and B. Qiu, *Nanoscale Research Letters* **10**, 493 (2015)
- [4] H. Machrafi, A. Rednikov, P. Colinet and P. C. Dauby, *Physical Review E* **91**, 053018 (2015).

**Confined tube flow of elastic low viscosity emulsions.**

*S. Caserta<sup>1,2</sup>, V. Preziosi<sup>1</sup>, G. Tomaiuolo<sup>1</sup>, S. Guido<sup>1,2</sup>* (1) Department of Chemical, Materials and Industrial Production Engineering, University of Naples Federico II, P.zza Tecchio 80, 80125, Naples, Italy; [sergio.caserta@unina.it](mailto:sergio.caserta@unina.it) (2) Consorzio Interuniversitario Nazionale per la Scienza e Tecnologia dei Materiali INSTM, Napoli, Italy.

Despite the extensive literature available on the topic, liquid-liquid mixing is still one of the most difficult and least understood mixing problems, especially when one of the two phases shows a non-Newtonian behavior. Non-Newtonian fluid flows at the microscale are complex to describe mathematically due to their shear rate dependent viscosity and their elastic behavior, which are greatly enhanced given the typically small residence times. Since non-Newtonian fluids can have elastic behavior and at the same time exhibit nonlinear viscous effects like shear-thinning of the viscosity, it is particularly difficult to study viscoelastic flows in isolation from other effects. A case of special interest arises when some elasticity is introduced by adding small concentrations of high-molecular weight components to the continuous phase (thus making a so called Boger fluid). Such fluids are particularly important because their viscosity behavior is nearly constant with the shear rate even showing significant elastic stresses, thus making them suitable to enable elastic effects to be probed separately from viscous ones. In this work, we focus on the effect of matrix elasticity of low viscosity oil/water emulsions in a confined flow apparatus. Newtonian silicone oil is used as the dispersed phase, while three different water-based solutions are used as the continuous phase, i.e. a Newtonian and two elastic non-Newtonian fluids (Boger fluids), respectively. A direct comparison of the fluid dynamic behavior of Boger fluids compared to the one of Newtonian fluids, at the same Reynolds number, allowed us to isolate the influence of matrix elasticity on emulsion morphology.

In all the experiments, a droplet-free layer can be observed close to the wall, since larger droplets accumulate toward the channel axis, while smaller droplets are marginated in an intermediate region. The droplet-free layer is tunable with fluid elasticity, and it could be exploited as a mechanism to separate the two emulsion phases in a flow device. The results could be relevant for the design of mixers and emulsification systems based on confined flow, where the formation of a droplet-free layer at the wall is usually overlooked.

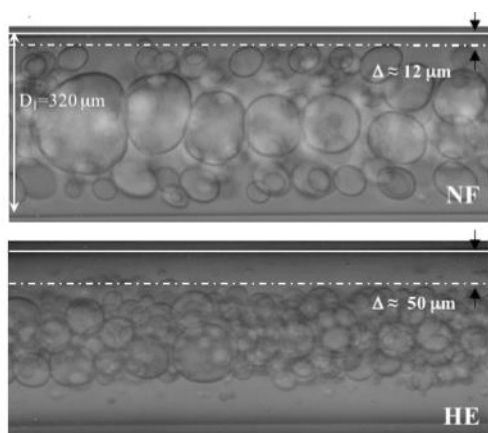


**Figure 1.** Wall depletion layer of Newtonian (upper) and Elastic (lower) fluids as continuous phases, droplets are Newtonian Silicon Oils in both cases. The total flow rate is 30 ml/h, capillary internal diameter is 320  $\mu\text{m}$ .

**References**

- [1] D.F. James, *Annual Review of Fluid Mechanics*, 41 (2009) 129.
- [2] J.R. Stokes, *Journal of Fluid Mechanics*, 429 (2001) 67.
- [3] J.R. Stokes, *Journal of Fluid Mechanics*, 429 (2001) 117.
- [4] V. Preziosi, G. Tomaiuolo, M. Fenizia, S. Caserta, S. Guido, *Journal of Rheology*, (2016) in press.

**EUROPE FOYER - SESSION 1**

## POSTER PRESENTATIONS - 3<sup>rd</sup> DAY

Friday, May 6th, 2016 (15:45-17:00)

Europe Foyer: Poster session 2

- 1 The Visualization of Multiphase Plasma Jet During Plasma Processing of Dispersed and Solid Ceramics Materials  
*R. Keželis, M. Milieška, V. Grigaitienė, M. Aikas*
- 2 The Numerical And Experimental Research Of Dynamic And Thermal Properties of In-flight Particles In Plasma-chemical Reactor  
*M. Milieška, R. Keželis*
- 3 Definition of Fundamental Parameters for Modelling of a New Thin-film Photocatalytic Reactor to Remove Sulfamethoxazole Antibiotic  
*C.B. Ozkal, Z. Frontistis, D. Mantzavinos, S. Meric*
- 4 Photocatalytic hydrogen evolution from water by cadmium based photocatalyst  
*M. Ersoz, E. Aslan, I. Hatay Patir, M. Kus*
- 5 Room-temperature Ferromagnetism in Hydrothermally Synthesized Mn<sup>2+</sup> Doped Titania Nanotubes  
*Z. Šaponjić, M. Vranješ, J. Kuljanin Jakovljević, N. Abazović, Z. Konstantinović, A. Pomar, M. Stoiljković, M. Čomor, A. Pavlović*
- 6 Zirconia/ Polyaniline Nanocomposite: Synthesis, Characterization and Applicability as Photocatalyst  
*M.I. Čomor, M.V. Carević, N.D. Abazović, M.B. Radoičić, T.D. Savić*
- 7 Dynamic Surface Activity of the Pulmonary Surfactant (PS) – Graphene Oxide (GO) System  
*T. R. Sosnowski, M. Mazurkiewicz-Pawlicka, A. Malolepszy, L. Stobiński*
- 8 Mass Recovery Kinetics of Heated Carbonated Glass Fabric in Atmosphere with Different Humidity and CO<sub>2</sub> Concentration  
*G. Bajars, E. Pentjuss, A. Lulis, J. Gabrusenoks, J. Balodis*
- 9 Investigation of Electrophoretically Deposited Metal Oxide and Reduced Graphene Oxide Composite as Anode Materials for High Performance Lithium Ion Batteries  
*G. Bajars, K. Kaprans, J. Mateuss, A. Dorondo, G. Kucinskis, J. Kleperis*
- 10 Superabsorbent conducting hydrogel composites produced from Semi-IPN poly(acrylamide-co-maleic acid) with pH sensitivity for Methylene Blue dye removal  
*S. Meriç, B. Tasdelen, D. İz. Çifçi*
- 11 Silver Loss From Potable Water Consumed In The International Space Station  
*M. Petala, V. Tsiridis, I. Mintsouli, E. Darakas, M. Kostoglou, S. Sotiropoulos, T. D. Karapantsios*
- 12 Crystal growth of biological macromolecules using ultrasonic irradiation  
*E.D. Chrysina, A. Derpogosian, A. Papagiannopoulos, S. Pispas, P. Zoumpoulakis, G. Heropoulos*
- 13 Theoretical considerations and analysis of experiment for a bubble growing on a hot plate during decompression in microgravity  
*M. Kostoglou, T.D. Karapantsios, A. Nedou*
- 14 Amphiphobic coatings for protection in seawater environment  
*F. Cirisano, M. Ferrari, A. Benedetti, L. Liggieri, F. Ravera, E. Santini*
- 15 Hierarchically macro/mesoporous TiO<sub>2</sub> monoliths derived from particle laden foam  
*D. Zabiegaj, M. T. Buscaglia, V. Buscaglia, E. Santini, M. Ferrari, L. Liggieri, F. Ravera*
- 16 Fluorine-free Oleophobic coatings deposition and characterization for application in housekeeping  
*A. Plomaritis, I. Tucker, T. D. Karapantsios*



## EUROPE FOYER - SESSION 2

- 17 Fluorapatitenanopowdersynthesed by surfactant-assisted microwave method under isothermal condition  
*V. Stanić, B. K. Adnadjević, S. I. Dimitrijević, M. N. Mitrić, B. Jokić, B. B. Zmejkovski, V. Živković-Radovanović*
- 18 Surface Contribution to Lithium Storage in Anatase TiO<sub>2</sub> Nanotube Arrays  
*N. Cvjetičanin, M. Bratić, D. Jugović, M. Mitrić*
- 19 A prototype carousel-type device for studying boiling in porous matrix at microgravity conditions  
*J. Lioumbas, T. D. Karapantsios*
- 20 Pre-processing Based Approach to Study the Water-Biofilm-Pipe Interface  
*E. Ramos-Martínez, M. Herrera, J. Izquierdo, R. Pérez-García, M. Petala, E. Darakas, V. Tsiridis*
- 21 Development of New Device for Measuring the Thermal Conductivity of Polymeric nanocomposite Materials  
*M. Gannoum, M. Kostoglou, R. Gonzalez-Cinca, T. D. Karapantsios*
- 22 Micro-structured Porous Surfaces for Highly Efficient Flow Boiling Applications  
*C. Argiropoulos, S. Sklari, M. Kostoglou, T. Karapantsios*
- 23 BaTi<sub>1-x</sub>Sn<sub>x</sub>O<sub>3</sub> (x = 0, 0.05 and 0.1) ceramics with improved dielectric properties obtained by sintering in different atmospheres (air and Ar)  
*A. Garaj, S. Marković, N. Cvjetičanin*
- 24 Adsorption in conjunction with SAXS under the influence of a rotational field  
*R.I. kosheleva, E.P. Favvas, T.D Karapantsios, A.Ch. Mitropoulos*

## The Visualization And Numerical And Experimental Investigation Of Multiphase Plasma Jet During Plasma Processing Of Dispersed And Solid Ceramics Materials

R. Kėželis<sup>1</sup>, M. Miliška<sup>1</sup>, V. Grigaitienė<sup>1</sup>, M. Aikas<sup>1</sup>. (1) Lithuanian energy institute, Breslaujos str. 3, Kaunas, Lithuania, [romualdas.kezelis@lei.lt](mailto:romualdas.kezelis@lei.lt).

In connection with the rising demand of high quality thermal insulation materials working at high temperatures the new methods of their manufacture are sought. One of such methods at present time is plasma technology having good prospects. This technology enables joining together the processes of melting of raw material and manufacture of material required (high temperature insulation fiber, nano-dispersed particles or spherical ceramic granules) forming a single process, using kinetic energy of high temperature flow generated by the plasma torch [1,2]. The deciding factor determining the final product properties and efficient use of the plasma technology for manufacture of materials mentioned above are heat transfer from the plasma jet to ceramics particles injected in plasma jet and reactor surfaces.

This study discuss the the results of analytical and experimental investigations to analysing the behaviour of interaction of solid material, dispersed particles, granules, also melted and concentrated ceramic material domains with plasma jet.

The specific equipment, consisting of plasma torch and plasma jet reactor for hard ceramic powder melting and conversion of the melt into fibre was constructed. The main operating parameters of plasma torch are: power supply ( $P$ ) – 70–120 kW, arc current ( $I$ ) – 150–300 A, arc voltage ( $U$ ) – 250–400 V, total air flow rate ( $G$ ) – 15-30 g·s<sup>-1</sup>, the average outlet temperature ( $T$ ) – 2800–3800 K, average outlet velocity ( $v$ ) – 650–1250 m·s<sup>-1</sup>.

For investigations plasma chemical reactor was used. It was built of several separate sections 0.015 m of diameter. The first section was 0.01 m of length and others – 0.005 m. During experiments the length of reactor was changed from 0.15 up to 0.3 m. The exhaust diameter of the last section varied from 0.001 to 0.015 m. This allowed changing outlet high temperature jet velocity to obtain better melting regime. All sections of the reactor as well as plasma torch were cooled by water. The zeolites powder, 60 – 120 μm in size, and glass strips were used during experiments. Plasma torch, generating non-equilibrium plasma jet at atmospheric pressure and auxiliaries used for high temperature jet generation as well as plasma chemical reactor are described in details elsewhere in [3,4].

The interaction of plasma jet and hard ceramic particles were numerically investigated by means of “Fluent” and “Jets&Poudres” software improved and applied to model for specific plasma jet [5]. It was found that flow velocity and temperature relief determines the increasing of particles velocity and temperature near the substratum surface placed in the distance of  $x/d=12$ . The maximal velocity of particles slightly exceeds the mean plasma jet velocity.

The investigation of formation of multi-phase flow parameters has been performed experimentally. A high-speed RedLake MotionPro video camera was used for instantaneous imaging of plasma spray process. Observations by camera suggest that multiphase jet in exhaust plasma chemical reactor nozzle consists of melted domains, solid grains of different sizes and fiber filaments.

Performed experimental and analytical studies showed that process of plasma melting and conversion of melt into fibre depend on following main factors: i) plasma generator characteristics and operating regime; ii) plasma flow formation, characteristics and its interaction with walls of the reactor; iii) plasma forming gas and powder injection approach and place; iv) powder composition, size and fraction, its injection rate parameters; v) initial domain formation, splat layering and process of spray pyrolysis. The obtained fiber yield was about 80%.

### Acknowledgements

The study is related to the activity of the European Cooperation in Science and Technology action COST MP1106 “Smart and Green Interfaces – from single bubbles and drops to industrial, environmental and biomedical applications (SGI)”.

### References

- [1] G.C. Wei, P.F Becher. *Am. Ceram. Soc. Bull.* 65 (1985) 298. [2] F.B. Yeh. *Heat and mass transfer*, 49 (2006) 297.
- [3] V. Valinčius, V. Krušinskaitė, P. Valatkevičius, V. Valinčiūtė. *Plasma sources science and technology*, 13 (2004) 199. [4] V. Valinčiūtė, R Kėželis, V. Valinčius. *Advances in heat transfer; Proceedings of the Baltic heat transfer conference 2*, 2007, 580. [5] Y.P. Wan, J.R. Fincke, S. Sampath, V. Prasad, J. Herman. *Heat Mass Transfer*; 45 (2002) 1007.

---

**The Numerical And Experimental Research Of Dynamic And Thermal Properties of In-flight Particles In Plasma-chemical Reactor**

---

M. Milieška<sup>1</sup>, R. Keželis<sup>1</sup>. (1) Lithuanian energy institute, Breslaujos str. 3, Kaunas, Lithuania, [mindaugas.milieska@lei.lt](mailto:mindaugas.milieska@lei.lt)

---

The most common thermal plasma application is plasma spraying technique where the small particles are injected into the plasma jet, heated, melted and partially evaporated when they hit a substrate thus forming a coating [1].

As the plasma spraying is the mostly studied thermal plasma application it is nearly impossible to consider the entire body of literature on the subject which covers a lot of aspects influencing the properties of deposited coatings [2]. However, the fiber formation using plasma technology lacks the scientific focus despite the process of fiber formation is quite similar to plasma spraying.

The plasma fibrillation technology enables to join the processes of raw material melting, melt homogenization and formation of ceramic fiber, nano-dispersed particles or spherical ceramic granules. In the case of the plasma fibrillation technology the plasma torch forms the plasma jet which enters the reactor channel and mixes with injected dispersive (50-100  $\mu\text{m}$  in diameter) particles. The melted particles stick to the reactor walls and flows to the exit of the reactor. The kinetic energy of the plasma jet at the outflow of the reactor drags the small drops of the melt, stretches them and forms the 10  $\mu\text{m}$  thickness and 0.3 m length fibers.

The present study presents the results of analytical and experimental investigation on the behavior of  $\text{Al}_2\text{O}_3$  particles (50-100  $\mu\text{m}$  in size) injected in plasma jet generated by DC plasma torch. The interaction of plasma jet and hard ceramic particles were investigated experimentally and numerically.

Experimentally the velocity of particles leaving the reactor was measured by means of LaVision ParticleMaster shadow laser imaging system. For this purpose, the parameters of plasma-chemical reactor were selected to avoid the particle melting.

The parameters of plasma torch during the experiments were: power – 53-68 kW; plasma forming air flow rate –  $27\text{-}32 \cdot 10^{-3}$  kg/s; dispersive particle rate up to  $6 \cdot 10^{-3}$  kg/s. The length of the reactor was 0.29 m and the inner diameter – 0.015 m. At these plasma reactor parameters the temperature and velocity of plasma flow at the outlet of the reactor were 1250-1330 K and 610-760 m/s, respectively.

The measured velocities of dispersive particles at the outlet of the reactor reaches 300 m/s of the smallest, 60  $\mu\text{m}$  in diameter, particles. The largest particles of 100  $\mu\text{m}$  in diameter reaches up to 150 m/s velocity.

The velocity and temperature of the particles (60-100  $\mu\text{m}$  in diameter) were simulated numerically using the methodology found in the scientific literature [2-5]. It was calculated that at the selected plasma reactor parameters the velocity and temperature of the used  $\text{Al}_2\text{O}_3$  particles should be between 170-350 m/s and 650-800 K, respectively.

The calculated and measured values correlate very well. The small difference between the calculated and measured values can be explained by the fact that the numerical simulation doesn't include the particle interaction between reactor walls and each other.

#### Acknowledgements

The study is related to the activity of the European Cooperation in Science and Technology action COST MP1106 "Smart and Green Interfaces – from single bubbles and drops to industrial, environmental and biomedical applications (SGI)".

#### References

- [1] A. Vardelle, C. Moreau, N.J. Themelis, C. Chazelas. *Plasma Chem Plasma Process*, 35 (2015) 491.
- [2] C. Tendero, Ch. Tixier, P. Tristant, J. Desmaison, P. Leprince, *Spectrochim Acta Part B*, 61 (2006) 2.
- [3] P.V. Ananthapadmanabhan, T.K. Thiyagarajan, K.P. Sreekumar, N. Venkatramani, *Scripta Mater*, 20 (2004) 145.
- [4] G. Shanmugavelayutham, V. Salvarajan, T.K. Thiyagarajan, P.V.A. Padmanabhan, K.P. Sreekumar, R.U. Satpute, *Curr Appl Phys*, 6 (2006) 41.
- [5] T. Zhang, D.T. Gawne, B. Liu, *Surf Coat Technol*, 132 (2000) 233.

## Definition of Fundamental Parameters for Modelling of a New Thin-film Photocatalytic Reactor to Remove Sulfamethoxazole Antibiotic

C.B. OZKAL<sup>1\*</sup>, Z. FRONTISTIS<sup>2</sup>, D. MANTZAVINOS<sup>2</sup>, S. MERIC<sup>1\*</sup> (1) Çorlu Engineering Faculty, Environmental Engineering Department, Namık Kemal University, Çorlu 59860, Tekirdag, Turkey, [cbozkal@nku.edu.tr](mailto:cbozkal@nku.edu.tr); [smeric@nku.edu.tr](mailto:smeric@nku.edu.tr)

This study is designed to statistically evaluate experimental data using a factorial design approach with the intent of providing a mathematical model that takes into account the parameters influencing the efficiency of photocatalytic (PC) degradation of Sulfamethoxazole (SMX) antibiotic at immobilized thin-film (TF) system.

Determination of the parameters were based on experimental justification of the literature findings reported so far. Experiments were carried out at the flat plate reactor designed with specific intent to provide replicable experimental conditions, with intent to fulfill the modeling [1,2]. The reactor was operated in recycling batch conditions. Antibiotic degradation was monitored by HPLC analysis while the degradation products of concern were specified by LC/MS-MS analysis [2]. Pre-liminary experimentation on the optimization and validation of studied conditions by means of replicability and stability was followed regarding different initial antibiotic concentration, UV energy levels, irradiated surface area, water matrix (ultrapure and secondary treated wastewater) and time intervals as model parameters. The independent variables are given in two levels of values, to be high and low (+ and -). A full of 2<sup>5</sup> experimental designs was performed carrying out 32 experiments randomly. For further evaluation and to assess the significance of the main effects and the interaction effects of parameters, Lenth's method was used.

The reproducibility and obtained responses under different flow and hydraulic conditions in terms of PC degradation rates are promising for future study and in accordance with the mathematical modelling and actualising scale-up purposes [2,3,4]. The classification and election of standardized effects to be considered in the model equation is performed with a PARETO analysis (Figure 1) [3,4]. The accuracy of the obtained model for estimating experimental results of any condition is statistically evaluated with a probability distribution function that can be seen in Figure 1-b. And the model provided valid outputs even for the scenario with different antibiotics. TF photocatalysis is found to be eligible for PC degradation of different antibiotics.

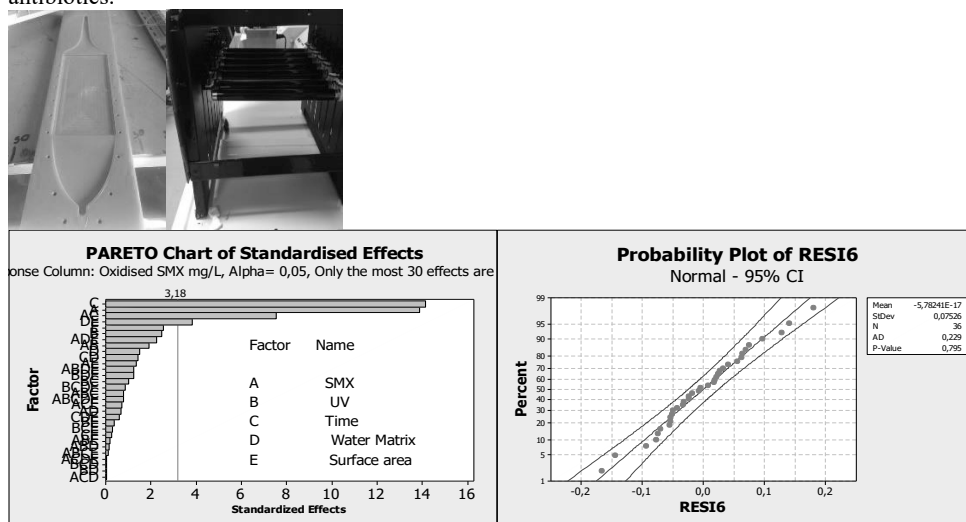


Figure 1. The view of TF\_PC reactor and PARETO Chart and Normal Probability distribution of experimental and modelling results.

### Acknowledgements

This STSM is performed and funded within context of COST MP1106 and NKUBAP.00.17.DR.14.01 projects.

### References

- [1] D. Fatta-Kassinos, M. L. Vasquez, K. Kümmere, *Chemosphere*, 85(5), (2011). 693-709.
- [2] M. Vezzoli, W. N. Martens, J. M. Bell, *Applied Catalysis A: General*, 404(1), (2011) 155-163.
- [3] I. Michael, Z. Frontistis, D. Fatta-Kassinos, *Comprehensive Analytical Chemistry*, 62, (2013) 345-407.
- [4] N. Miranda-García, M. I. Maldonado, J. M. Coronado, S. Malato, *Catalysis Today*, 151(1) (2010) 107-113.[6] Z. Frontistis, E. Hapeshi, D. Fatta-Kassinos, D. Mantzavinos, *Photochem. Photobiol. Sci* 14, (2015). 528.

---

**Photocatalytic Hydrogen Evolution From Water By Cadmium Based Photocatalyst**

---

*Emre Aslan<sup>1</sup>, Imren Hatay Patir<sup>1</sup>, Mahmut Kus<sup>2,3</sup>, Mustafa Ersoz<sup>1,3</sup>,(1) Selcuk University, Faculty of Science, Department of Chemistry, 42075 Konya, Turkey ,(2) Selcuk University, Faculty of Engineering, Department of Chemical Engineering, 42075, Konya, Turkey(3)Selcuk University, Advanced Technology Research and Application Center, 42075, Konya, Turkey, merso@selcuk.edu.tr*

Alternative energy sources have great attention due to the running out of conventional fossil fuels. Photocatalytic H<sub>2</sub> production from water splitting using semiconductor photocatalysts has drawn considerable attention as a promising way of resolving global energy and environmental problems. The development of visible-light driven photocatalysts is indispensable for the utilization of the main part of the solar spectrum, which is of great importance for the practical application of the semiconductor photocatalytic system [1,2].

In this study, oleic acid (OA) capped CdS, CdSe and alloyed CdS<sub>0.75</sub>Se<sub>0.25</sub> nanocrystals were synthesized by two-phase approach, which is a non-injection method for the synthesis of such alloys that can be conducted in one step, in one pot and at low temperature and pressure. Photocatalytic activities of OA capped nanocrystals have been investigated in the Na<sub>2</sub>S/Na<sub>2</sub>SO<sub>3</sub> solution for the hydrogen evolution. The results showed that CdSeS alloys show better activity than CdSe and CdS nanocrystals [3]. Other types of nanocrystals, which are 3-mercaptopropionic acid (MPA) capped CdS, CdTe and alloyed CdTeS nanocrystals, were synthesized by hydrothermal method at low temperature and pressure. Photocatalytic hydrogen evolution with MPA capped nanocrystals have been studied under visible-light irradiation in the aqueous solution by using at the pH 4.65 ascorbic acid and Co<sup>2+</sup> solution as the sacrificial electron donor and the artificial catalyst, respectively [4]. Significantly, the photocatalytic hydrogen evolution proceeds for longer than 24h and 12h for OA capped nanocrystals and MPA capped nanocrystals, respectively, without any noticeable decrease in the activity.

**Acknowledgements**

The authors would like to thank TUBITAK (The Scientific and Technological Research Council of Turkey) (211T185), the COST Action (MP1106) and TUBA (Turkish Academy of Sciences) for supporting this work.

**References**

- [1] X. Zong, J. Han, G. Ma, H. Yan, G. Wu, C. Li, 2011, *J. Phys. Chem. C*, 115, 12202–12208.
- [2] F. A. Frame, E. C. Carroll, D. S. Larsen, M. Sarahan, N. D. Browning, F. E. Osterloh, 2008, *Chem. Commun.*, 2206–2208.
- [3] E. Aslan, O. Birinci, A. Aljabour, F. Ozel, I. Akin, I. Hatay Patir, M. Kus, M. Ersoz, 2014, *ChemPhysChem*, 15, 2668–2671.
- [4] C. Baslak, E. Aslan, I. Hatay Patir, M. Kus, M. Ersoz, *International Journal of Hydrogen Energy*, under review

**Room-temperature Ferromagnetism in Hydrothermally Synthesized Mn<sup>2+</sup> Doped Titania Nanotubes**

Z. Šaponjić<sup>1</sup>, M. Vranješ<sup>1</sup>, J. Kuljanin Jakovljević<sup>1</sup>, N. Abazović<sup>1</sup>, Z. Konstantinović<sup>2</sup>, A. Pomar<sup>3</sup>, M. Stojković<sup>1</sup>, M. Čomor<sup>1</sup>, A. Pavlović<sup>1</sup>. (1) Vinča Institute of Nuclear Science, University of Belgrade, P.O. Box 522, 11001, Belgrade, Serbia, (2) Center for Solid State Physics and New Materials, Institute of Physics Belgrade, University of Belgrade, Pregrevica 118, 11080 Belgrade, Serbia. (3) Institut de Ciència de Materials de Barcelona, CSIC, Campus UAB, 08193 Bellaterra, Spain. (4) Faculty of Agriculture, University of Belgrade, Zemun, Serbia, saponjic@vinca.rs.

The ability to control the spin of electrons in addition to their charge in diluted magnetic semiconductors would expand their applications in conventional electronic devices. The term diluted magnetic semiconductor (DMS) refers to a non-magnetic semiconductor material where the host cations are replaced with magnetic impurities up to a few atomic percent. Traditionally, DMSs were mostly based on II-VI or III-V compounds. Those materials were unattractive for practical electronic applications, since ferromagnetism has been achievable far below room temperature [1]. Recently, oxide based DMS materials have attracted considerable attention due to the reports of ferromagnetism at room temperature in several systems and, hence, their potential application in emerging field of thin-film magneto-optic and spin-electronic devices [2].

Hydrothermal synthetic route for preparation of 0.01-0.017 at% Mn<sup>2+</sup> doped titania nanotubes which showed room temperature ferromagnetism is reported in this work. Dispersions of Mn<sup>2+</sup> doped TiO<sub>2</sub> nanoparticles were used, as precursors. Morphologies of Mn<sup>2+</sup> doped TiO<sub>2</sub> nanocrystals and resulted Mn<sup>2+</sup> doped titania nanotubes were characterized by transmission electron microscopy. Precursor Mn<sup>2+</sup> doped TiO<sub>2</sub> nanoparticles have polyagonal shape and dimension of about 5nm, while the Mn<sup>2+</sup> doped nanotubes have outer diameter of about 10nm while the length varies widely even reaching hundred nanometers independently of dopant concentration.

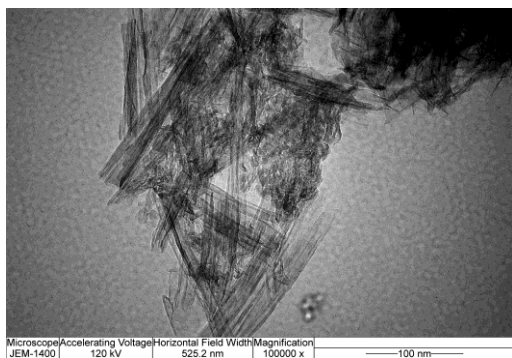


**Figure 1.** TEM image of 0.017 at% Mn<sup>2+</sup> doped titania nanotubes

X-ray diffraction (XRD) analysis of precursor Mn<sup>2+</sup> doped TiO<sub>2</sub> nanoparticles, for all dopant concentrations, confirmed anatase crystal structure while the XRD analysis of resultant Mn<sup>2+</sup> doped titania nanotubes indicated changes in crystalline structure i.e. in addition to anatase crystalline phase of TiO<sub>2</sub>, the appearance of titanate crystalline form observed, also. This finding is in agreement with crystalline form of undoped titania nanotubes. Reflection spectra of Mn<sup>2+</sup> doped titania nanotubes revealed their slightly altered optical properties in comparison to undoped TiO<sub>2</sub> nanoparticles. Room temperature ferromagnetic ordering with saturation magnetic moment which decreases with increasing concentration of dopant ions was observed for all measured films made of Mn<sup>2+</sup> doped titania nanotubes.

**References**

- [1] R. Janisch, P. Gopal and N. A. Spaldin, *J. Phys.: Condens. Matter.* 17 (2005) 657.
- [2] Y. Kim, J. H. Park, B. G. Park, H. J. Noh, S. J. Oh, J. S. Yang, D. H. Kim, S. D. Bu, T. W. Noh, H. J. Lin, H. H. Hsieh and C. T. Chen, *Phys. Rev. Lett.* 90 (2003) 017401.

## Zirconia/ Polyaniline Nanocomposite: Synthesis, Characterization and Applicability as Photocatalyst

M.I. Čomor, M.V. Carević, N.D. Abazović, M.B. Radoičić, T.D. Savić, Vinča Institute of Nuclear Sciences, University of Belgrade, P.O. Box 522, Belgrade, Serbia, mirjanac@vinca.rs.

In recent years, nanocomposites of conductive polymers and inorganic particles have attracted more and more attention, since they have interesting physical properties and many potential applications. The physical and chemical properties of composites may be tuned by selecting the types of the polymers and the inorganic nanoparticles. For example, composites of conductive polyaniline (PANI) and nanocrystalline metal oxide ( $\text{TiO}_2$ ,  $\text{ZrO}_2$ , ...) combine the merits of both PANI and metal oxide particles, having potential applications in conductive coating, charge storage, electrocatalysis, electrochromic devices, photovoltaic cells and as photocatalysts for degradation of pollutants.

Following very successful combination of  $\text{TiO}_2$  and PANI for application as photocatalysts [1], we used similar method to synthesize and probe  $\text{ZrO}_2$ /PANI nanocomposites. Briefly, zirconia nanoparticles, synthesized hydrothermally in alkaline solution, using  $\text{ZrOCl}_2$  as precursor, were mixed with aqueous solution of appropriate concentration aniline and ammonium peroxydisulfate as oxidant, without addition of acid. The reaction mixture was stirred for 20 days at room temperature. The precipitates were then collected, washed and dried. We synthesized samples with initial  $[\text{ZrO}_2]/[\text{ANI}]$  mole ratios of 50, 100 and 150 designated as ZP-50, ZP-100 and ZP-150.

Detailed characterization of the ZP nanocomposites showed that zirconia maintained its initial monoclinic crystalline structure; TEM measurements revealed that bare zirconia nanoparticles have about 20- 40 nm in diameter; after formation of nanocomposite- layer of PANI can be seen, Figure 1. Obtained nanocomposites were probed as photocatalysts for degradation of trichlorophenol (TCP) using simulated solar light (Osram Vitalux lamp).

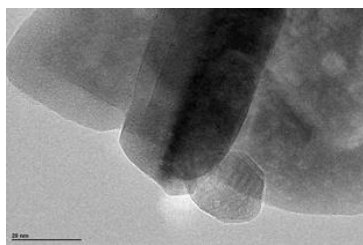


Figure 1. Typical TEM image of ZP-100 nanoparticles, bar is 20 nm.

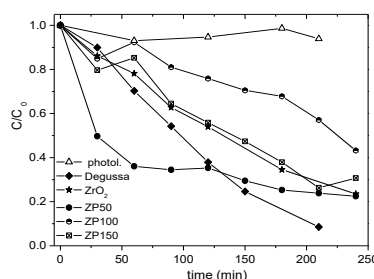


Figure 2. Kinetic curves of the photolysis and photocatalytic degradation of TCP using bare  $\text{ZrO}_2$  and ZP nanocomposites as well as Degussa (for comparison).

All examined powders can be used for photodegradation of TCP, when simulated. Solar light is used, as can be seen in Fig. 2. The best photocatalytic activity showed ZP-50 nanocomposite with the highest amount of PANI compared to zirconia, 60% of TCP was degraded after 1 hour. Its activity is even better than activity of Degussa, commercial  $\text{TiO}_2$  powder, which is not easy to achieve. We hope that this type of nanocomposites will prove to be excellent choice of GREEN, regarding process of synthesis and physico-chemical properties, materials for solving of environmental pollution problems.

### Acknowledgements

Financial support for this study was granted by The Ministry of Education, Science and Technological Development of The Republic of Serbia, Project: ON172056 and COST action MP1106.

### References

[1] M.B. Radoičić, Z.V. Šaponjić, I.A. Janković, G. Ćirić-Marjanović, S.P. Ahrenkiel, M.I. Čomor, *Applied Catalysis B: Environmental*, 136-137 (2013) 133.

## Dynamic Surface Activity of the Pulmonary Surfactant (PS) – Graphene Oxide (GO) System

T. R. Sosnowski, M. Mazurkiewicz-Pawlicka, A. Małolepszy, L. Stobiński, Faculty of Chemical and Process Engineering, Warsaw University of Technology, Waryńskiego 1, Warsaw, Poland, t.sosnowski@ichp.pw.edu.pl.

Pulmonary surfactant (PS) constitutes the first barrier between inhaled air and the liquid which covers the lung tissue. Contaminants contained influence the surface properties of the innate biosurfactant, disturbing the mechanical and hydrodynamic phenomena in the respiratory system. If contamination is formed by condensed matter, the properties of such micro- or nanoparticles may be modified by contact with surfactant constituents, resulting in altered bioavailability (i.e. toxic potential) of inhaled materials [1,2]. Graphene-derived nanoparticles are promising material in various applications so they can be more often found in laboratories and industrial workplaces. Therefore, it is also possible that they can be inhaled and have impact on health via direct interactions with PS.

In this work we study the effect of graphene oxide (GO) on animal-derived PS by studying interfacial dynamics with the oscillating drop method.

GO nanoflakes were obtained in the Graphene Laboratory of WUT by modified Hummers method. Chemical composition and structure of obtained material were analyzed by selected microscopic and spectroscopic techniques [3]. GO particles were resuspended in water and mixed with Curosurf® (Chiesi, Italy) used as the realistic model of PS. The final suspensions contained 13 mg/ml of phospholipids and 0.1 mg/ml of GO. Static adsorption and drop oscillation measurements were done with PAT-1M tensiometer (Sinterface, Germany). The experiments were done at physiologically-relevant conditions:  $T=36.6\pm 0.2^{\circ}\text{C}$ , oscillation frequency 0.125-0.5 Hz, and 10% surface area change.

Determined surface tension hysteresis loop was slightly modified by GO nanoflakes (Figure 1), presence of which reduced the maximum and the minimum surface tension in the cycle, suggesting a possible synergetic nanoparticles effect on sorption kinetics of PS components at the air/water interface. Adsorption studies indicated that GO nanoflakes themselves have some surface activity. The apparent surface visco-elastic parameters of both systems (PS and PS+GO) are similar under tested dynamic conditions. Our result suggest therefore that GO does not impair the native activity of PS in a way previously reported for other nanoparticles [4].

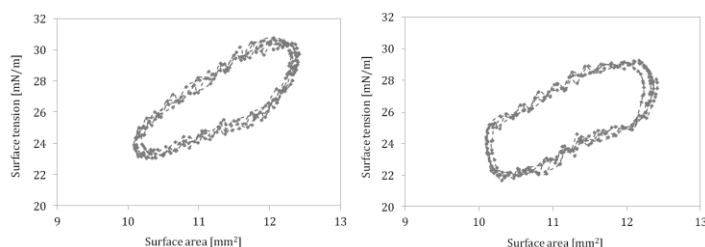


Figure 1. Surface tension hysteresis during oscillation of pure PS (left) and PS-GO suspension (right).

### Acknowledgements

Work supported by National Centre for Science of Poland – grant No. 2014/13/B/ST8/00808. Work done under umbrella of the COST Action MP1106.

### References

- [1] T.R. Sosnowski, *J. Nanosci. Nanotechnol.* 15 (2015) 3476.
- [2] T.R. Sosnowski, *Curr. Pharm. Des.* (2016) - doi: 10.2174/1381612822666160128145644
- [3] L. Stobiński, B. Lesiak, A. Małolepszy, M. Mazurkiewicz, et al., *J. Electr. Spectr. Rel. Phenom.* 195 (2014), 145.
- [4] D. Kondej, T.R. Sosnowski, *Env. Sci. Pollut. Res.* 23 (2016) 4660.



### Mass Recovery Kinetics of Heated Carbonated Glass Fabric in Atmosphere with Different Humidity and CO<sub>2</sub> Concentration

G. Bajars, E. Pentjuss, A. Lūsis, J. Gabrusenoks, J. Balodis. Institute of Solid State Physics, University of Latvia, Kengaraga street 8, Riga, Latvia, gunars.bajars@lu.lv.

The Na-Al-Si glass fabric fibers contain Na<sup>+</sup> ions that diffuse to its surface and together with CO<sub>2</sub> and H<sub>2</sub>O from atmosphere during long term storing create here the hydrated carbonate shell [1-3]. Heating of fabric may lead to inverse process – decomposition of hydrated carbonates with evolving of CO<sub>2</sub> and H<sub>2</sub>O and mass loss. The previous investigation of mass recovery kinetics in room atmosphere of fabric samples heated at different temperatures showed that during the first 0,25 h after sample heating the recovery of its mass (or relative mass) in all tested cases follows ( $R^2 > 0,99$ ) the regression (1) [3]

$$A(t) = A_1(1 - \exp(-t/t_1)) + A_2(1 - \exp(-t/t_2)). \quad (1)$$

In (1)  $A_1$  and  $A_2$  are mass (or relative mass) constants,  $t_1$  and  $t_2$  - time constants. Experiments showed, that  $A_1 \ll A_2$  and  $t_1 \ll t_2$ . However there is given only possible proposal how to explain the meaning of these constants. Only room mass recovery atmosphere was investigated in a relative narrow interval of time (0-2400 h) [3].

To solve these tasks in addition there are used artificially increased CO<sub>2</sub> concentration (up to 1500-2000 ppm) and relative humidity (RH) (up to 70 %) in mass recovery atmosphere. The mass recovery process was studied up to 8000 h and more.

The unleached samples of K-glass fabric with initial composition of (18-22)Na<sub>2</sub>O-(3-5)Al<sub>2</sub>O<sub>3</sub>-(73-79)SiO<sub>2</sub> from JSC Valmiera Glass were used in experiments. The threads of fabric consist of 600 elementary glass fibers with diameter of 6 μm. Thermogravimetric analysis showed that in long term (years) stored fabric the shell of elementary fiber mainly consists of trona (Na<sub>3</sub>H(CO<sub>3</sub>)<sub>2</sub>·2H<sub>2</sub>O) having beginning of decomposition at about 57 °C. SEM images show that the shell contains the differently sized (mainly below 1 μm) ordered crystals and free space between them, so that crystals here have free access to surrounding atmosphere. The fabric samples were heated before mass recovery process in region of 40 to 160 (200) °C by step of 5 °C. Condition  $t_1 \ll t_2$  allows to separate surely both mass increasing process described by parts of regression (1).

Experiments of mass recovery in different atmospheres showed that the first part of regression (1) characterizes the mass increase of shells by absorption of CO<sub>2</sub> and second one - H<sub>2</sub>O. The constants  $A_1$  and  $A_2$  characterize CO<sub>2</sub> and H<sub>2</sub>O mass absorption limits (maximal, equilibrium or saturated states) when  $t \rightarrow \infty$ . Because constant  $t_1 \ll t_2$  CO<sub>2</sub> mass reaches its saturated state at the beginning of 0.25 h interval, but H<sub>2</sub>O mass does not reach it till the end of this interval, and out of the interval begins to fall below the values predicted by relation (1). It indicates to appearance of some reordering in crystals of carbonated shell that reduces water absorption limit. The values of  $A_1$  and  $A_2$  depend on previous sample heating temperature and mass recovery atmosphere constituents. The increase of heating temperature over 57 °C leads to sharp increase of  $A_1$  and  $A_2$  that is associated with evolving of CO<sub>2</sub> and H<sub>2</sub>O during previous heating. Value  $A_1$  has a sharp (at about 70 °C) and  $A_2$  has a wide and structured maximum, extended up to about 160 °C. Both of them have correlation with its time constants relations vs heating temperature as it suggests the interpretation of time constants. It may occur in the decomposed surface layer of trona crystals. Obviously direct water crystallization begins as second fast mass increase. In this case the owned mass is stable after artificial RH lowering in atmosphere. There is necessary an additional research to explain obtained results.

#### Acknowledgements

The financial support of Latvian State Research Program IMIS2 is greatly acknowledged. Presenting author G. Bajars acknowledges a financial support from COST action MP 1106.

#### References

- [1] B.W. Veal, D.J. Lam, D.P. Karim, *Nuclear Technology*, 51 (1980)136.
- [2] I.S.T. Tsong, C.A. Houser, W.B. White, G.L. Power, S.S.C. Tong, *Non-Cryst.Solids*, 38-39 (1980) 649.
- [3] E. Pentjuss, A. Lūsis, G. Bajars, J. Gabrusenoks, *IOP Conf. Series: Materials Science and Engineering*, 49 (2013) 012044.

**Investigation of Electrophoretically Deposited Metal Oxide and Reduced Graphene Oxide Composite as Anode Materials for High Performance Lithium Ion Batteries**

**G Bajars<sup>1</sup>, K. Kaprans<sup>1</sup>, J. Mateuss<sup>2</sup>, A. Dorondo<sup>1</sup>, G. Kucinskis<sup>1</sup>, J. Kleperis<sup>1</sup>.** (1) Institute of Solid State Physics, University of Latvia, Kengaraga street 8, Riga, Latvia, gunars.bajars@lu.lv. (2) Faculty of Physics and Mathematics, University of Latvia, Zellu street 8, Riga, Latvia.

Graphite as anode material for lithium ion batteries (LIBs) has good electrochemical properties as well as charge/discharge performance. However, it has a low theoretical capacity about 372 mAhg<sup>-1</sup> compared with graphene - 970 mAhg<sup>-1</sup> [1]. Graphene, a crystalline form of carbon, has attracted tremendous scientific interest in both the fundamental and the applied area since it was discovered [2]. Additionally a lot of metal oxides have been studied as different anode for lithium ion batteries mostly due to their high lithium storage ability [1].

Two metal oxides, Fe<sub>2</sub>O<sub>3</sub> and TiO<sub>2</sub>, combined with reduced graphene oxide (rGO), were studied as anode material for LIBs. Electrophoretic deposition (EPD) method to obtain thin metal oxide/graphene oxide (MO/GO) films on stainless steel substrate was developed in current research. EPD technique has many advantages in the preparation of thin films from suspensions, such as high deposition rate and throughput, good uniformity, controlled thickness of the obtained films and no need of binders.

Thin films of composite anode material were deposited from water suspensions under potentiostatic mode. Thermal reduction of as-deposited films was performed by heating at 500 °C and 700 °C in argon/hydrogen flow. The morphology and structure of the electrophoretically prepared MO/rGO thin films were examined by scanning electron microscopy, Raman spectroscopy and X-ray diffraction analysis. Electrochemical measurements were carried out in two electrode electrochemical cell with lithium foil as the counter and reference electrode and LiPF<sub>6</sub> in ethylene carbonate and dimethyl carbonate mixture (volume ratio 1:1) as an electrolyte.

Specimens reduced at 700 °C showed the following specific capacities: TiO<sub>2</sub>/rGO - 116 mAh·g<sup>-1</sup> at 20 mA·g<sup>-1</sup> current, Fe<sub>2</sub>O<sub>3</sub>/rGO - 39 mAh·g<sup>-1</sup> at 30 mA·g<sup>-1</sup>, and TiO<sub>2</sub>/Fe<sub>2</sub>O<sub>3</sub>/rGO - 93 mAh·g<sup>-1</sup> at 50 mA·g<sup>-1</sup> current. Higher specific capacities were obtained for specimens reduced at 500 °C: TiO<sub>2</sub>/rGO - 775 mAh·g<sup>-1</sup> at 125 mA·g<sup>-1</sup> current, Fe<sub>2</sub>O<sub>3</sub>/rGO - 232 mAh·g<sup>-1</sup> at 1000 mA·g<sup>-1</sup>, and TiO<sub>2</sub>/Fe<sub>2</sub>O<sub>3</sub>/rGO - 985 mAh·g<sup>-1</sup> at 110 mA·g<sup>-1</sup> current. Obtained results obviously show that composites with TiO<sub>2</sub> predominantly in anatase form exhibit higher specific capacities than those predominantly in rutile form.

Besides the highest capacity TiO<sub>2</sub>/Fe<sub>2</sub>O<sub>3</sub>/rGO composite showed excellent cycling ability maintaining almost 100 % specific capacity after 100 charge/discharge cycles. It means that TiO<sub>2</sub>/Fe<sub>2</sub>O<sub>3</sub>/rGO composite exhibits a great potential for application as an anode material in LIBs.

**Acknowledgements**

The financial support of Latvian Council of Science Cooperation Project No 666/2014 is greatly acknowledged. Presenting author G. Bajars acknowledges a financial support from COST action MP 1106.

**References**

- [1] G. Wanga, T. Liua, Y. Luoa, Y. Zhaob, *Journal of Alloys and Compounds*, 509 (2011) 216–220.
- [2] B. Banov, L. Ljutzkanov, I. Dimitrov, A. Trifonova, H. Vasilchina, A. Aleksandrova, A. Mochilov, B.T. Hang, S. Okada, J.I. Yamaki, J. Nanosci. *Nanotechnol.* 8 (2008) 591–594.

### Superabsorbent conducting hydrogel composites produced from Semi-IPN poly(acrylamide-co-maleic acid) with pH sensitivity for Methylene Blue dye removal

Belül Tasdelen<sup>1\*</sup>, Deniz İzlen Çiğçi<sup>2</sup>, Sureyya Meriç<sup>2\*</sup>. (1) Department of Biomedical Engineering Çorlu Faculty of Engineering, Namık Kemal University, Çorlu 59860- Tekirdağ, Turkey (2) Department of Environmental Engineering, Çorlu Faculty of Engineering, Namık Kemal University, Çorlu 59860- Tekirdağ, Turkey. (\*):btesdelen@nku.edu.tr; dicitci@nku.edu.tr; smeric@nku.edu.tr

Hydrogels which have sensitivity of pH, temperature and conductivity are used different scientific area such as biosensor and pharmaceutical [1]. In environmental applications, hydrogels are the most alternative material used to adsorb and remove of dyes and metal from wastewater especially textile wastewater. However, main characteristic feature of textile wastewater is that it has high conductivity about 13-15 mS/cm [2]. Polyaniline is a higher conductivity polymer and can be used to preparation of conductive hydrogel [3].

In this work, semi-IPN poly(acrylamide-co-maleic acid)/polyaniline composite hydrogel was successfully synthesized by two-steps gamma radiation induced polymerization in aqueous solution. First, acrylamide (AAm)/maleic acid (MA) copolymeric hydrogels were prepared by irradiation of the ternary mixtures of acrylamide/MA/water by  $\gamma$ -rays at ambient temperature. Then, the networks were semi-interpenetrated (s-IPN) with linear conducting polymer, polyaniline (PANI) under  $\gamma$ -irradiation at room temperature. Preparation of hydrogel is given in Fig. 1.

To study the batch adsorption of MB, hydrogels by amounts of 1 g/L were placed in aqueous solutions of MB. A range of 10-150 mg/L MB initial concentrations were tested at room temperature for adsorption at 24 h adsorption time. Supernatant samples were submitted to absorbance readings at 664 nm wavelength to determine concentration of MB while hydrogels were precipitated at the bottom of the beakers. The amount of adsorption per unit mass of hydrogels was calculated according to Tasdelen et al. [4].

In this study, we proposed a novel alternative method to incorporate a conductive linear polymer (PANI) inside a network of pH-sensitive hydrogel under  $\gamma$ -irradiation at room temperature. SEM scanning of hydrogels are given in Figure 1. s-IPN poly(AAm-co-MA)/PANI hydrogels possessed a high electrical conductivity. In addition, the composite hydrogel with good conductive properties also displayed unique pH-sensitivity. The s-IPN hydrogel systems were employed for swelling and diffusion experiments in water and aqueous solutions of the Methylene Blue (MB) as a model drug in at room temperature were investigated and high adsorption capacity was shown in both hydrogel. The drug uptake and release properties of s-IPN poly(AAm-co-MA)/PANI composite hydrogels were also studied. The incorporation of MA and aniline lead to an increase in electrostatic interaction between charge sites on carboxylate ions and cationic MB molecules.

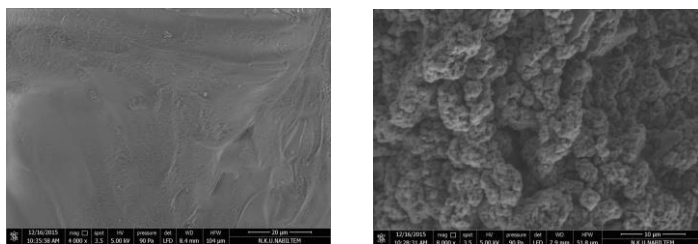


Figure 1: Scanning electron micrographs of the composite hydrogels a)poly(AAm-co-MA) b) poly(AAm-co-MA)/PANI hydrogels.

#### Acknowledgements

This work has been done under the umbrella of COST Action MP1106. The authors acknowledge Namık Kemal University Scientific Research Projects (NKUBAP.00.17.AR.14.14) for funding.

#### References

- [1] K. Sharma, B.S. Kaith, V. Kumar, S. Kalia, V. Kumar, H.C. Swart, *Geoderma*, 232-234 (2014) 45.
- [2] S. Meriç, H. Selçuk, V. Belgiorno, *Water Research*, 39(6) 2005 1147.
- [3] Q. Tang, J. Wu, H. Sun, S. Fan, D. Hu, J. Lin, *Carbohydrate Polymers*, 73(3) (2008) 473.
- [4] B. Taşdelen, A.E. Osmanioglu, E. Kam, *Polymer Bulletin*, 70 (2013) 3041.

**Silver Loss From Potable Water Consumed In The International Space Station**

*M. Petala<sup>1</sup>, V. Tsiridis<sup>1</sup>, I. Mintsouli<sup>2</sup>, E. Darakas<sup>1</sup>, M. Kostoglou<sup>2</sup>, S. Sotiropoulos<sup>2</sup>, Th. Karapantsios<sup>2</sup>*  
 (1) Department of Civil Engineering, Aristotle University of Thessaloniki, Thessaloniki, 54124, Greece, petala@civil.auth.gr; (2) Department of Chemistry, Aristotle University of Thessaloniki, Thessaloniki, 54124, Greece.

The availability of potable water, both in terms of quality and quantity is essential for the International Space Station (ISS) crew. Potable water is produced on ground and is transported to the ISS. During each launching/transportation campaign, water quality complies either to Russian or US standards [1]. The disinfection agent is silver for the Russian type of water and iodine for the US type of water. So far, silver loss from potable water has been confirmed throughout the campaigns and thus, health issues arise concerning the safe and durable storage of potable water supplies in future (long term) missions [2,3].

The aim of this study is to evaluate the behaviour of the disinfectant agent, silver, with various metallic and polymeric wetted materials used throughout the process of water preparation and storage. Silver ions were added into Russian type water electrolytically, so as to reach a silver ions' concentration equal to either 10 or 0.5 mg Ag<sup>+</sup>/L. Afterwards, water was brought in contact with various surfaces at surface (S) to volume (V) ratio equal to 5.0 cm<sup>-1</sup> and temperature 30°C, and was stored either for 7d (water with high Ag concentration) or 28 d (water containing low Ag concentration). At the end of the storage period all wetted surfaces were leached, in order to examine the deposition of Ag onto the surfaces.

Silver losses from water containing 10 mg Ag<sup>+</sup>/L varied from 7.4% up to 96.8%, while silver losses from water containing 0.5 mg Ag<sup>+</sup>/L varied between 62.5% to 100%. Leaching of wetted materials verified the deposition of silver onto their surface, while the Ag mass balance closed reasonably, above 90%, in all cases. Results show that silver deposits on stainless steel (SS) surfaces even when a passivation layer protects the metallic surface. Extensive SEM and high resolution XPS analysis reveals that silver deposits uniformly across the SS surface to a depth larger than 3 nm. Moreover, evidence is provided that silver deposits in its metallic form on all stainless steel surfaces, in line with a galvanic deposition mechanism.

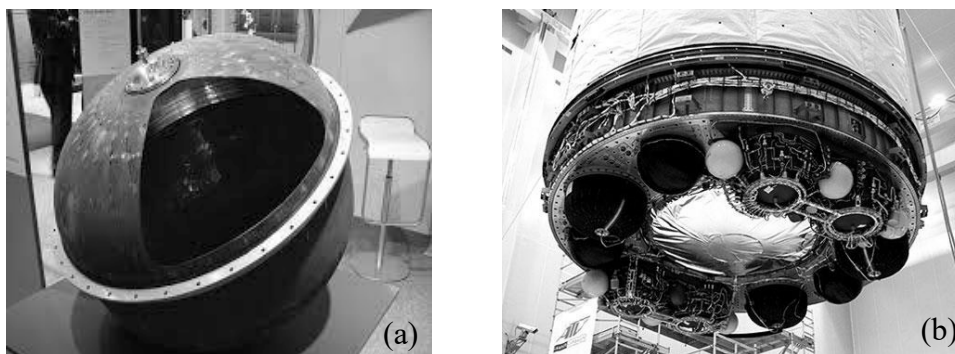


**Figure 1.** (a) ATV potable water tank and (b) water tanks installation on the Jules Verne ATV (Source: ESA).

**Acknowledgements**

This study was carried under the program “Biocide Management for Long Term Water Storage” funded by ESA (Co. No. 4000109529/13/NL/CP). The view expressed herein can in no way be taken to reflect the official opinion of the European Space Agency. This work is conducted under the umbrella of the COSTMP1106 Action: Smart and Green Interfaces—from single bubbles and drops to industrial, environmental, and biomedical applications.

**References**

- [1] P. Rebeyre, *TEC-MMG/2010/29*, July 2012a.
- [2] P. Rebeyre, *TEC-MMG/2012/324*, October 2012b.
- [3] N.M. Adam, *SAE INTERNATIONAL TECHNICAL PAPER SERIES*, 2009-01-2459, 2009.

---

**Crystal Growth Of Biological Macromolecules Using Ultrasonic Irradiation**


---

*A. Derpogiosian<sup>1</sup>, A. Papagiannopoulos<sup>2</sup>, S. Pispas<sup>2</sup>, P. Zoumpoulakis<sup>1</sup>, G. Heropoulos<sup>1</sup>, E.D. Chrysina<sup>1</sup>. (1) Institute of Biology, Medicinal Chemistry & Biotechnology (2) Theoretical & Physical Chemistry Institute, National Hellenic Research Foundation, 48, Vas. Constantinou Ave., Athens, Greece, [echrysina@eie.gr](mailto:echrysina@eie.gr), [gherop@eie.gr](mailto:gherop@eie.gr)*

Knowledge of the three dimensional structure of biological macromolecules is of key importance in order to understand and modulate their function, especially when these are involved in industrial processes. To this end, a number of tools have been developed including X-ray crystallography, Nuclear Magnetic Resonance spectroscopy (NMR), Electron Microscopy (EM) and Small Angle X-ray scattering (SAXS). X-ray crystallography remains the most powerful method as reflected in the number of protein structures deposited annually with the «Protein Data Bank, [www.rcsb.org](http://www.rcsb.org)». Crystal growth though is not at all trivial and still remains a bottleneck. Researchers, until present, have given emphasis on the factors affecting crystallization such as ionic strength, temperature, organic solvents and use of additives to promote ordered precipitation. Efforts have also been directed towards miniaturization of the sample volumes used, employing robotic equipment and reducing the overall cost of protein production/consumption for screening a broad range of crystallization conditions. Previous studies have shown that use of external fields such as ultrasound [1-2] could be beneficial and promotes the nucleation stage accelerating protein crystallization. Our work focuses on the investigation of ultrasonic irradiation on protein samples and its effect on crystal growth using hen egg white lysozyme (HEWL). The oligomeric state and the hydrodynamic radius of the protein solutions were thoroughly investigated employing dynamic light scattering prior to crystallization and the samples were irradiated using different time frames. For this purpose multi angle DLS coupled with a water bath tank (Branson 1520, Branson) and our in house robotic crystallization facility (OryxNano, Douglas Instruments, UK) were employed. The results showed that ultrasound acted as a nucleation promoter affecting the kinetics of nucleation and crystal growth (Figure 1).

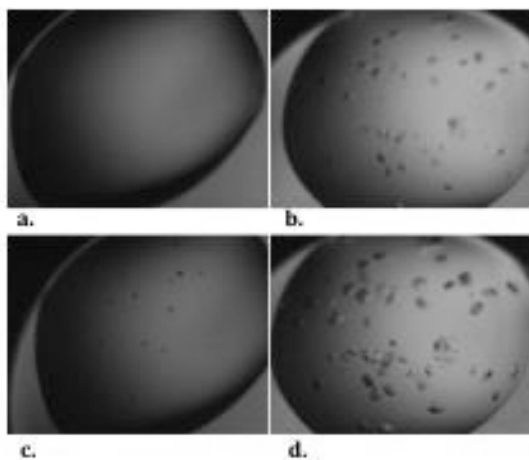


**Figure 1.** Crystallization trials using HEWL. Drops with protein crystallization solution after 60 and 90 min used as control, are shown in (a) and (c), respectively, while drops from irradiated samples are presented in (b), (d) for the corresponding time.

#### **Acknowledgements**

This work has been supported by the European Community's Seventh Framework Programme (FP7/2007-2013) under ARCADE (grant agreement FP7-REGPOT-2009-1-No 245866).

#### **References**

- [1] K. Kakinouchi, H. Adachi, H. Matsumura, T. Inoue, S. Murakami, Y. Mori, Y. Koga, K. Takano, S. Kanaya *J. Cryst. Growth*, 292 (2006) 437.
- [2] R. Crespo, P.M. Martins, L. Gales, F. Rocha, A.M. Damas *J. Appl. Cryst.*, 43 (2010) 1419.

**Theoretical Considerations and Analysis of Experiment for a Bubble Growing on a Hot Plate During Decompression in Microgravity**

*M. Kostoglou, T.D. Karapantsios, A. Nedou Division of Chemical Technology, Department of Chemistry, Aristotle University, Univ. Box 116, 541 24 Thessaloniki, Greece, email address: kostoglou@chem.auth.gr*

The focus of the present work is the modeling of bubble growth on a hot plate during decompression (depressurization) of a volatile liquid at temperatures close to saturation and in the presence of dissolved gas [1]. In particular, this work presents an organized attempt to analyze data obtained from an experiment under microgravity conditions. In this respect, a bubble growth mathematical model is developed and solved at three stages, all realistic under certain conditions but of increasing physical and mathematical complexity: At the first stage, the temperature variation both in time and space is ignored leading to a new semi-analytical solution for the bubble growth problem [2]. At the second stage, the assumption of spatial uniformity of temperature is relaxed and instead a steady linear temperature profile is assumed in the liquid surrounding the bubble from base to apex. The semi-analytical solution is extended to account for the two-dimensionality of the problem [3]. As the predictions of the above models are not in agreement with the experimental data, at the third stage an inverse heat transfer problem is set up. The third stage model considers an arbitrary average bubble temperature time profile and it is solved numerically using a specifically designed numerical technique. The unknown bubble temperature temporal profile is estimated by matching theoretical and experimental bubble growth curves. A discussion follows on the physical mechanisms that may explain the evolution of th

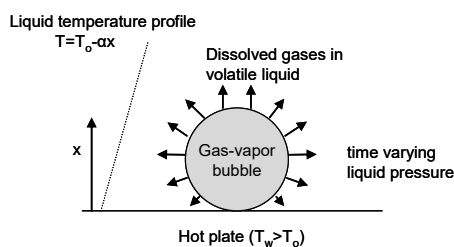


**Figure 1.** A schematic of the bubble growing in a steady linear temperature profile.

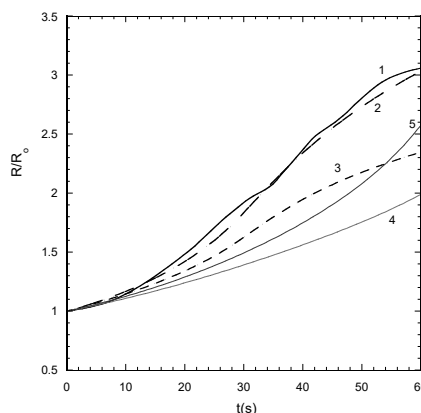


**Figure 2.** Bubble radius evolution curves: (1) Experimental (2) Variable vapor pressure (3) Variable vapour pressure with no mass transfer contribution (4) Vapor pressure 1 bar (5) Vapor pressure 1.1 bar.

**Acknowledgements**

The authors would like to acknowledge the European Space Agency (ESA) for the financial support in this project. The work was performed under the umbrella of COST actions MP1106 and MP1305.

**References**

- [1] O. Kannengieser, C. Colin, W. Bergez, *Microgravity Science and Technology*, 22 (2010) 447.
- [2] N. Divinisi, T. Karapantsios, R. de Briyini, M. Kostoglou, V. Bontozoglou, J. Legros, *AIChE Journal* 52 (2006) 3029.

**Amphiphobic Coatings For Protection In Seawater Environment**

---

*Francesca Cirisano, Michele Ferrari, Alessandro Benedetti, Libero Liggieri, Francesca Ravera, Eva Santini CNR – Istituto per l' Energetica e le Interfasi, 16149 Genova, Italy Corresponding author: m.ferrari@ge.ieni.cnr.it*

In the marine field the use of highly hydro and oleophobic (amphiphobic) materials is relatively young and not very explored. Amphiphobic materials created for marine applications could be an innovative solution where technological and ecological aspects allow to be merged, taking into account the limitations imposed by international laws in terms of environmental protection. In particular, in this work a coating with amphiphobic/superamphiphobic behaviour for marine applications has been characterized and tested in both laboratory and field conditions, since investigations in real seawater are crucial to evaluate the behaviour of SH/SO surfaces because of a complexity not reproducible in laboratory. Because of the real conditions where the surface can operate, preliminary tests of wearing, thermal stress and durability have been also performed in order to study amphiphobic systems for different applications related to the marine environment.

**Hierarchically Macro/Mesoporous TiO<sub>2</sub> Monoliths Derived From Particle Laden Foam**

*D. Zabiegaj, M. T. Buscaglia, V. Buscaglia, E. Santini, M. Ferrari, L. Liggieri, F. Ravera, CNR-Institute for Energetics and Interphases, via De Marini 6, 16149 Genoa (I); zabiegaj@ge.ieni.cnr.it*

The utilization of nanoparticles/nanopowders is relevant in the field of tailoring and fabrication of high specific surface area materials for gas adsorption, filtering, catalysis or other industrial applications.

In the method proposed here particle stabilized wet foams are used as templates for the gel-casting process. In details, polymerization occurs between organic Poly(vinyl alcohol) and cross-linker DHF, previously dissolved in the liquid phase, providing a solid foam structure with particles mainly distributed at the surface of the cells. A further thermal treatment at high temperature (1000-1200 °C) allows the complete removal of organic components and the proper sintering of these porous materials.

This work pointed out that the morphology of the final samples obtained strongly depends on the composition of the adsorption layers stabilizing the precursor foams. A systematic characterization of the surface properties of TiO<sub>2</sub> particle dispersions in presence of short chain ionic surfactants, crossed with the analysis of the bulk dispersion by Dynamic Light Scattering (DLS) and  $\zeta$ -potential measurements, has been carried out [1]. The obtained results help to select the best conditions in which the transfer of particles to the liquid-air interfaces is favoured, providing stable foams, suitable for solidification [2,3], Figure 1.

The final samples are characterized, from the morphological and textural point of view, via SEM analysis and by nitrogen adsorption isotherms (BET). The crystalline structure of materials has been analyzed by X-ray diffraction method (XRD).

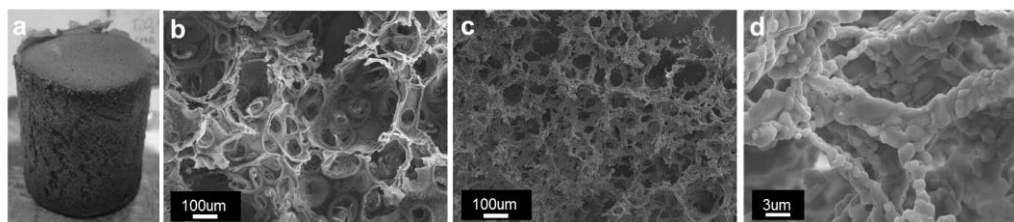


**Figure 1.** Solid foam obtained from 5wt% TiO<sub>2</sub> dispersion, contained 5e-3M CTAB and 3,9wt% PVA: green body foam (a, b) and after sintering at 1200°C (c-general structure, d- foam cells).

**References**

- [1] D. Zabiegaj et al, J. Nanoscience and Nanotechnology, 15 (2015) 3618-3625
- [2] D. Zabiegaj et al, Colloids and Surfaces: A 438 (2013) 132-140
- [3] D. Zabiegaj et al, Colloids and Surfaces: A 473 (2015) 24-31



---

**Fluorine-Free Oleophobic Coatings Deposition And Characterization  
For Application In Housekeeping.**

---

*A. Plomaritis<sup>a,b</sup>, I. Tucker<sup>a</sup>, T. D. Karapantsios<sup>b</sup>, a Unilever Research & Development Port Sunlight, Quarry Rd East, Bebington, Wirral CH63 3JW, Merseyside, UK, Thanasis.plomaritis@unilever.com, b Department of Chemical Technology, School of Chemistry, Aristotle University of Thessaloniki, P.O. Box 54124, Thessaloniki, Greece*

The detergents technologies have evolved dramatically over the past years; hence the large manufacturers are looking to impart special specifications to their products. Making their products capable of providing secondary cleaning benefits is one of the fields that large manufacturers are seriously interested in. In other words, they want cleaned surfaces to either acquire dirt repellence properties after the first use of the detergent or for every next time less effort be needed to get this surface cleaned.

In order to get these qualities to cleaned surfaces, a thin transparent film needs to stay onto the surface after the cleaning process. The way hydrophobicity or hydrophilicity affects the process is very well studied because these properties define how easily the aqueous solution of the detergent wets and spreads over the surface.

Based on the above, a study about the controlled creation of an oleophobic film onto surfaces is underway to test how this affects the adhesion of dirt onto these surfaces. The work involves study of the chemistry, topography and electric charge of surfaces commonly encountered in home environment. The chemistry and electric charge of surfaces are critical parameters which determine how easily a film is adsorbed on surfaces and also dictate the appropriate film properties for successful adsorption.

**Fluorapatite Nanopowder Synthesed By Surfactant-Assisted Microwave Method Under Isothermal Condition**

*Vojislav Stanić, Borivoje K. Adnadjević, Suzana I. Dimitrijević, Miodrag N. Mitrić, Bojan Jokić, Bojana B. Zmejovski, Vukosava Živković-Radovanić, University of Belgrade, 11000 Belgrade, Serbia, vojvo@vin.bg.ac.rs.*

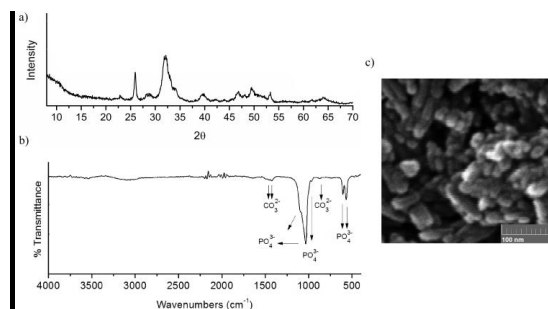
Biomaterials based on hydroxyapatite are commercially available for the repair and reconstruction of bone tissue defects. Implant-associated infections are significant surgical problems and usually require removal [1]. Fluorapatite (FAP;  $\text{Ca}_{10}(\text{PO}_4)_6\text{F}_2$ ) is considered as a potential biomaterial for bone repair due to bioactive, biocompatible and antibacterial activity[2, 3]. In vitro studies have showed that the cytotoxic, genotoxic and mutagenic effects of fluorapatite biomaterials have no effect or are negligible [4].

The surfactant-assisted synthesis of fluorapatite nanopowder was conducted using a microwave reactor (Discover, CEM Corp., Matthews, North Carolina, US) supplied with a programmed temperature control system. The reaction was carried out in a microwave field of 2.45 GHz, maintaining the desired temperatures at 60 °C. Two solutions were made, the first of Brij 35 and  $\text{Ca}(\text{CH}_3\text{COO})_2\cdot\text{H}_2\text{O}$  and the other of  $(\text{NH}_4)_2\text{HPO}_4$  and NaF. The pH of both solutions was maintained at pH ~10 by the  $\text{NH}_4\text{OH}$  solution before mixing. The synthesis process in the microwave field lasted 5 minutes. The precipitate thus obtained was filtered by a vacuum filtration, then dried at 105 °C, and finally grained in a mortar.

The synthesized powder sample was analysed by X-ray diffractometer (XRD, Philips PW 1050), Nicolet 6700 FTIR spectrophotometer and the field-emission scanning electron microscope (FESEM, TESCANMira3 XMU).

The XRD pattern of synthesized fluorapatite powder is presented in Figure 1a. The positions of its X-ray diffraction peaks were in accordance with ASTM data and fluorapatite (Card 15-0876). The diffraction peaks of synthesized sample were broad, indicating the obtained products have low crystallinity and that crystallites were nanosized. There are no other characteristic peaks of impurities, such as CaO and other calcium phosphates. The FTIR spectra of the sample (Figure 1b) displayed typical absorbance bands for phosphate groups. The presence of weak bands at  $870\text{ cm}^{-1}$  and  $1430\text{ cm}^{-1}$  are ascribed to  $\text{CO}_3^{2-}$  ions, which indicate to a B-type substitution where some  $\text{CO}_3^{2-}$  groups are within  $\text{PO}_4^{3-}$  sites of the apatite lattice.

The FESEM micrograph of the FAP particles is presented in Figure 1c. The particles have a nano-size character and an irregular rod-like morphology. The average length of particles is about 50 nm and they have about 15–25 nm in diameter.



## Surface Contribution to Lithium Storage in Anatase TiO<sub>2</sub> Nanotube Arrays

*N. Cvjetičanin<sup>1</sup>, M. Bratić<sup>2</sup>, D. Jugović<sup>3</sup>, M. Mitrić<sup>4</sup>. (1) Faculty of Physical Chemistry, Studentski trg 12-16, Belgrade, Serbia, [nikola.cvj@ffh.bg.ac.rs](mailto:nikola.cvj@ffh.bg.ac.rs) (2) Vinca Institute of Nuclear Sciences (lab.040), Belgrade, Serbia (3) Institute of Technical Sciences of SASA, Knez Mihailova 35/IV, Belgrade, Serbia, (4) Vinca Institute of Nuclear Sciences (lab.020), Belgrade, Serbia.*

Anodically grown TiO<sub>2</sub> nanotubes (NTs) have attracted much attention in the last two decades because they have a wide range of applications which are mostly based on semiconductive but also on potential biomedical properties of TiO<sub>2</sub>. These applications include photocatalysis, electrochromic devices, solar cells, hydrogen storage, sensing applications, biomedical coatings, drug delivery and payload release systems [1,2]. The insertion of lithium ion into TiO<sub>2</sub> nanotube arrays (NTAs) is interesting from two points of view: (1) improvement of photoelectrochemical performance of NTs as the consequence of change of electronic structure upon Li<sup>+</sup> insertion and (2) potential application of NTs as anode for lithium ion batteries (LIBs). [3,4].

In this study the electrochemical anodization of Ti-foil in the solution of NH<sub>4</sub>F in glycerol was performed at 20, 30, 45 and 60 volts for 6 hours. The inner diameter of obtained NTs increases from 60 to 110-140 nm with increasing voltage up to 45 V, while the thickness of nanotube walls remains approximately the same. At 60 V the morphology of NTs is significantly changed because several NTs are merged into one whose inner diameter tapers as it goes to the top and becomes elliptical and 200-400 nm wide. All Ti-foils covered with TiO<sub>2</sub> NTs were annealed for 3 hours in air at 400 °C to convert TiO<sub>2</sub> from amorphous to crystal anatase form. The insertion/deinsertion of Li-ion was investigated by exposing Ti/TiO<sub>2</sub>-NTs electrodes of the same geometrical surface area to the 1M solution of LiClO<sub>4</sub> in propylene carbonate (PC). The cyclic voltammetry experiments, for all anatase TiO<sub>2</sub> NTs electrodes, were recorded at scan rates 1 to 20 mV s<sup>-1</sup> in the potential range from 3 to 1 V vs. Li/Li<sup>+</sup>. At all scan rates, for all NTAs, Ti<sup>4+</sup>/Ti<sup>3+</sup> redox peaks appear designating very fast insertion/deinsertion kinetics. However, even at the lowest scan rate of 1 mV·s<sup>-1</sup> redox peak-to-peak separation, which amounts 0.46-0.48 V is significantly larger from the Nernstian. The absence of better reversibility may be attributed to slow electron transport through semiconducting TiO<sub>2</sub> NTs. The galvanostatic cycling was performed by using the same current density 50 μA·cm<sup>-2</sup> (geometric surface area) for all Ti/TiO<sub>2</sub>-NTs electrodes. The galvanostatic charge/discharge (lithium extraction/lithium insertion) areal capacity of NTAs, increases by increasing anodization voltage. The discharge capacity retention after 50 cycles is excellent for NTs obtained at 20, 30 and 45 V, while for NTs obtained at 60V capacity fading during discharge can be observed. The voltage profiles for 50th cycle for all anodization voltages show two regions. The region where the voltage is constant reflects equilibrium between two phases: Li-poor Li<sub>0.026</sub>TiO<sub>2</sub> and Li-rich Li<sub>0.52</sub>TiO<sub>2</sub> [5,6]. The region with inclined voltage profile designates the existence of surface storage mechanism [6,7]. The ratio of capacities of inclined and flat part during discharge (lithium insertion) is approximately 0.75 for NTs obtained at 20, 30 and 45 V. It increases to 1.07 for those synthesized at 60 V. These results show that storage capacity larger than the maximum capacity of bulk anatase, which corresponds to composition Li<sub>0.5</sub>TiO<sub>2</sub>, may be significantly increased by using TiO<sub>2</sub> NTAs due to the surface storage of lithium ion. Discharge capacity retention of TiO<sub>2</sub> NTAs is much better comparing to TiO<sub>2</sub> nanoparticles which may have very large contribution of surface storage capacity [7].

### Acknowledgements

The Ministry of Education and Science of the Republic of Serbia provided financial support under grants nos III 450014 and III 45004.

### References

- [1] X. Chen and S. S. Mao, Chem. Rev 107 (2007) 2891
- [2] P. Roy, S. Berger, P. Schmuki, Angew. Chem. Int. Ed. 50 (2011) 2904
- [3] B. H. Meekins, P.V. Kamat, ASC Nano 3(11) (2009) 3437
- [4] Q. L. Wu, J. Li, R. Deshpande, N. Subramanian, S. E. Rankin, F. Yang, Y.-T. Cheng, J. Phys. Chem. C 116 (2012) 18669
- [5] M. Wagemaker, G.J. Kearley, A.A. van Well, H. Mutka, F.M. Mulder, J. Am. Chem. Soc. 125 (2003) 840
- [6] M. Wagemaker, F. M. Mulder, Acc. Chem. Res. 46 (2013) 1206
- [7] C. Jiang, M. Wei, Z. Qi, T. Kudo, I. Honma, H. Zhou, J. Power Sources 166 (2007) 239

## A Prototype Carousel-Type Device For Studying Boiling In Porous Matrix At Microgravity Conditions

J.S. Lioumbas\*, T.D. Karapantsios. Division of Chemical Technology, Aristotle University of Thessaloniki, 54124 Thessaloniki, Greece, \*lioumbas@gmail.com

This work investigates the influence of microgravity conditions on heat and mass transfer phenomena over and below the surface of an initially fully saturated with water, porous matrix (porous), when this is immersed in hot immiscible fluid (hot oil). The motivation behind this work is two-fold. First to examine the potential of wetted porous media as protective walls against fire indoor incidents where intense thermal loads are present. Second, to investigate that process of food frying excluding the complication induced by the continuous changing of the natural product characteristics (i.e. matrix shrinkage and pores collapse). This is achieved by replacing the natural product with a porous simulant (i.e. glass based porous matrix). Regardless the type of porous material, boiling in porous media includes the following phenomena:

- A. Temperature increase of the porous matrix (thermalization) leading to water phase change and vapor formation inside the pores.
- B. Vapor transportation from the vapor formation spots inside the pores toward the porous matrix interface.
- C. Bubbles growth and detachment from porous matrix–oil interface.

The significant role of the buoyancy forces on the above phenomena has been recently proved [1, 2] after performing frying experiments at increased gravitational acceleration levels (i.e. from 1 to 9g). Experiments in the absence of gravitational acceleration will further elucidate the role of inertia on bubble dynamics (growth, detachment, departure) during boiling in porous media. For this reason, we designed and built a prototype carousel-type experimental apparatus (Fig. 1). To simplify the geometry of the system, the porous matrix has only one surface exposed to hot oil, the others being thermally insulated. Therefore, the hot oil triggers boiling solely over the exposed porous surface.

The experiment is scheduled to fly at 64th ESA Parabolic Flight Campaign. Analysis of the acquired data is expected to reveal how the process of boiling in porous media is affected by the absence of gravity. To our knowledge this is the first experiment on boiling in porous media performed at weightlessness.

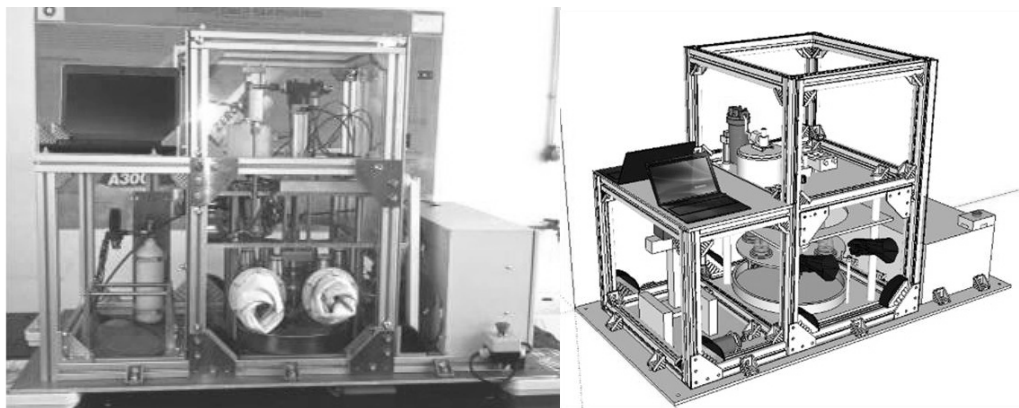


Figure 1. Experimental device.

### Acknowledgements

The present activity was carried out with ESA funding (contracts: No.: 22470/09/NL/Cbi, CCN1 & BOILING: Multi scale Analysis of Boiling, No.: AO-2004-111) and under the umbrella of COST Action MP1106: 'Smart and green interfaces – from single bubbles and drops to industrial, environmental and biomedical applications'.

### References

- [1] Lioumbas, J.S., Karapantsios, T.D. Effect of increased gravitational acceleration in potato deep-fat frying. Food Research International, 55, pp. 110-118 (2014).
- [2] Lioumbas, J.S., Krause, J. & Karapantsios, T.D. "Hypergravity to explore the role of buoyancy in boiling in porous media", Microgravity Science and Technology, vol. 25, no. 1, pp. 17-25 (2013).

## Pre-processing Based Approach to Study the Water-Biofilm-Pipe Interface

**E. Ramos-Martínez<sup>1</sup>**, M. Herrera<sup>2</sup>, J. Izquierdo<sup>1</sup>, R. Pérez-García<sup>1</sup>, M. Petala<sup>3</sup>, E. Darakas<sup>3</sup>, V. Tsiridis<sup>3</sup>. (1) Universitat Politècnica de Valencia, C. de Vera s/n, Valencia, Spain, [evarama@upv.es](mailto:evarama@upv.es). (2) University of Bath, Claverton Down Rd, Bath, United Kingdom. (3) Aristotle University of Thessaloniki, University Campus, Thessaloniki, Greece.

Water quality deterioration resulted from drinking water distribution systems' (DWDSs) biofilms pollution have attracted wide concern. Besides the health risk that biofilms involve, due to their role as a pathogen shelter, a number of problems associated with biofilm development in DWDSs can be identified [1]. Biofilms in DWDSs are affected by not only biological factors but also interaction of various physico-chemical and hydraulics factors. However, due to their complexity most of the studies are carried out under simplified conditions. Generally, the effect that just one or two variables have on biofilm is studied. Our proposal is based on the combination of various existing data sets from similar studies to conduct a meta-data analysis of biofilm development. Data acquisition has been carried out through an exhaustive search and an intensive networking. All the information has been pre-processed and homogenised through suitable approaches to outlier detection (Local Outlier Factor) [2], selection of variables, and handling missing data (Multivariate Imputation by Chained Equations) [3]. A complete and extensive database is obtained (284 cases with 15 variables). Different analyses have been carried out on the data set to help understand all the aspects influencing the water-biofilm-pipe interface in DWDSs. The target attribute "Biofilm" is the outcome that we study. When studying its relation with the rest of the variables (Figure 1) it is observed that the devices that physically less resemble pipes have higher biofilm development. The same trend is found when analysing the duct's shape, which is important when extrapolating data obtained from bench top scale studies. Regarding pipe material, no big differences are observed among the different materials. However, the biofilm average values found in iron based pipes tend to be the highest ones, a fact that could be taken into account when designing DWDSs. In the case of the continuous attributes (Figure 1b), when testing the free chlorine residual the linear regression line (red) does not present any clear slope. The Locally Weighted Scatterplot Smoothing (LOWESS) line [4] presents a trend toward lower biofilm development when increasing the free chlorine concentration. It suggests that, although influential, it is not as relevant as expected and there are other important factors to take into account when studying the biofilm layer growth in DWDSs. Results of our study are promising as regards the development of management strategies about mitigating the negative effects of biofilms in WDSs.

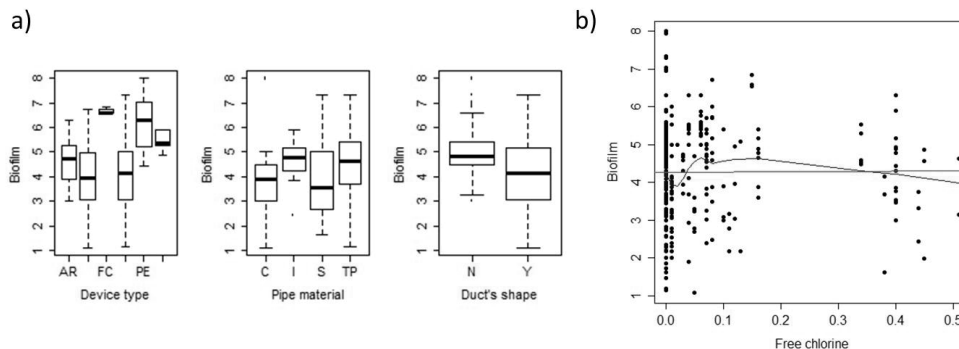


**Figure 1.** Biofilm development regarding some of the studied variables

### Acknowledgements

We want to express our gratitude to the research grant (FPI), Ministerio de Economía (ref.: BES-2010-039145), Spain.

### References

- [1] E. Ramos-Martínez, *PhD thesis*, Universitat Politècnica de Valencia, 2016.
- [2] H.P. Kriegel, M. M. Breunig, R. T. Ng, J. Sander. *Proc. of the 2000 ACM SIGMOD Int. Conf. on Manag. of Data*, Dallas, TX, USA, 2000, 93-94.
- [3] S. van Buuren, K. Groothuis-Oudshoorn. *Journal of Statistical Software*, 45(2011), 3.
- [4] W. S. Cleveland. *J. of the American Statist. Assoc.*, 74, (1979), 829-836.

### Development of New Device for Measuring the Thermal Conductivity of Polymeric nanocomposite Materials

*M. Gannoum<sup>1,2</sup>, M. Kostoglou<sup>1</sup>, R. Gonzalez-Cinca<sup>2</sup>, T. D. Karapantsios<sup>1</sup>. (1) Division of Chemical Technology, Department of Chemistry, Aristotle University of Thessaloniki, University Box 116, 541 24 Thessaloniki, Greece, [mike198687@hotmail.com](mailto:mike198687@hotmail.com). (2) Polytechnic University of Catalonia, Castelldefels School of Telecommunication and Aerospace Engineering, EETAC, Esteve Terradas, 7, 08860 Castelldefels - Spain*

This work presents a miniaturized version of a previously designed device<sup>[1][2]</sup> capable of measuring the thermal conductivity of polymeric nanocomposite materials. The new device (Figure 1) is based on two cylindrical tanks containing cold and hot liquid, respectively, each of them wetting one side of a disc-shaped polymeric sample. The new device uses much smaller size samples (diameter  $d=2.7\text{cm}$ , thickness  $\delta=3\text{mm}$ ) in comparison with the previous design sample size ( $d=15\text{cm}$ ,  $\delta=3\text{mm}$ ), which ensures sample integrity/rigidity and saves material which in the case of nanoadditives may be expensive or scarce. In addition, the device is affordable and portable without compromising the operation convenience and precision/accuracy. The device is based on the hot/cold tank principle, which is simple and easy to operate, is non-destructive to the sample, is safe to use and thermal conductivity is estimated through a simple mathematical model. The technique relies on recording the temperature evolution of a fluid in two separate tanks exchanging heat to each other. One tank contains a hot fluid ( $45\text{-}55^\circ\text{C}$ ), and the other a cold fluid (room temperature), while heat is being transferred through a sample placed in between the tanks.

Teflon samples are used first for the validation of the device's capacity, with the acquired results of thermal conductivity being in good agreement with literature values and also with measurements of the previous version of the device. Next, samples of polymeric nanocomposites of different nano additives concentrations are measured. Results demonstrate that the thermal conductivity of two types of epoxy resins (EPON828,827) increases with the addition of different concentrations of nano additives such as; Alumina ( $\text{Al}_2\text{O}_3$ ), Boron nitride (BN), Silicone Carbide (SiC), Organoclay nanomere (I.30E), carbon nanotubes (CNT's) and different Silicone dioxide ( $\text{SiO}_2$ ) additives. It is found that some additives such as Alumina yield observable impact on the thermal conductivity of the epoxy resin whereas others such as multi-walled carbon nanotubes (MWCNT's) give a noticeable effect only at the higher examined concentrations. In the absence of additives, no impact on the epoxy resin thermal conductivity is observed when cured by different curing agents such as D2000, D230 and IPD. On the contrary, in the presence of additives, a clear effect of the curing agents D2000, D230 on the thermal conductivity of epoxy resin is observed. The significance of the nanocomposites curing process and the impact of achieving good degree of dispersion of the nanoadditives in the polymeric matrix is discussed.



**Figure 1.** Schematic of the new miniaturized device

#### Acknowledgements

This study was co-funded by European Union- European Regional Development Fund and Greek Ministry of Education/GGET-EYDE-ETAK through program ESPA 2007-2013 / EPAN II / Action "SYNERGASIA-II" (project 11SYN-5-10).

#### References

- [1] A. Plomaritis, M. Kostoglou, J. Lioumbas, T.D. Karapantsios, P. Xidas, K. Triantafyllidis, D., Bikiaris "Innovative device for measuring the thermal conductivity of polymeric materials of high heterogeneity and uneven surface", 10th Hellenic Polymer Society Conference, Patras (Greece), December 4-6, (2014).
- [2] Plomaritis, A., "Innovative Hot/Cold tank device for the measurement of thermal conductivity of polymeric materials", Master Thesis (in Greek), Faculty of Chemistry, Department of Chemical Technology, Aristotle University of Thessaloniki, (2014)

---

**Micro-structured Porous Surfaces for Highly Efficient Flow Boiling Applications**

---

*C. Argiropoulos<sup>1</sup>, S. Sklari<sup>2</sup>, M. Kostoglou<sup>1</sup>, T. Karapantsios<sup>1</sup>. (1) Aristotle University of Thessaloniki, Thessaloniki 54124 Aristotle University of Thessaloniki, Thessaloniki, Greece, argiropoulosc@gmail.com. (2) Center for research and Technology, 6<sup>th</sup> km Charilaou-Thermi Rd P.O. Box 60361 GR 57001 Thermi, Thessaloniki, Greece*

An effort is being carried out to produce innovative micro-structured porous surfaces offering high density nucleation sites and controlled wettability that aim at improving the convective boiling heat transfer in flow boiling applications. Thin, copper mesh sheets, a commercial product employed in electromagnetic shielding applications, has been chosen as base material from which the surfaces are constructed. Due to their rigid structure, these copper sheets can be easily adjusted over smooth surfaces giving shape to forms of single or multilayer micro-structured porous surfaces. Those structures are meant to promote bubble dynamics and modify the heat transfer mechanisms in the micro-scale level, increasing heat transfer efficiency and thus paving the way for more compact and efficient heat exchanging devices. In this work we present a variation of laboratory techniques that have been explored so far to produce suitable micro-structured surfaces while simultaneously discuss the significance of each technique in terms of convenience, handling and efficiency. These techniques aim to reduce the thermal contact resistance between the heating element and the porous layer and include among others fixing of the mesh over the surface in a way that a uniform contact between the peaks of the mesh structure is maintained. In order to further minimize the thermal contact resistance, flame torching, low temperature soldering and high temperature sintering attempts of the mesh sheets over the smooth substrate have also been performed. High – temperature sintering of the copper meshes over smooth copper surface is proving to be a straightforward and efficient way to produce reliable boiling surfaces with minimal thermal contact resistance.

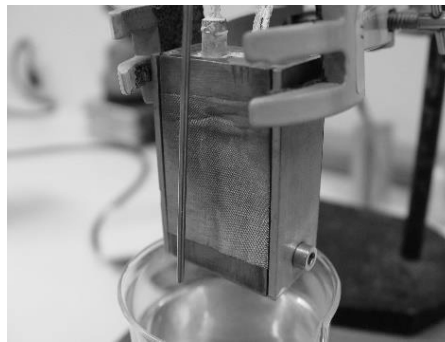


**Figure 1.** Fixed copper mesh over copper surface,

**Acknowledgements**

This work is performed with the support of (1) “Highly efficient flow boiling macro-structured/ macro porous channels” funded by the European Space Agency (Co. No. 4000106405/12/NL/PA), (2) “Multiphase Analysis of Boiling” (MANOB, MAP Project AO-2004-111 Co. No. 4200020289). The work is performed under the umbrella of COST Actions MP1106 and MP1305

**BaTi<sub>1-x</sub>Sn<sub>x</sub>O<sub>3</sub> (x = 0, 0.05 and 0.1) ceramics with improved dielectric properties obtained by sintering in different atmospheres (air and Ar)**

*Andrej Garaj<sup>1</sup>, Smilja Marković<sup>2</sup>, Nikola Cvjetičanin<sup>1</sup>, <sup>1</sup>Faculty of Physical Chemistry, University of Belgrade, Belgrade, Serbia, garaj.andrej@gmail.com, <sup>2</sup>Institute of Technical Sciences of SASA, Belgrade, Serbia*

Barium titanate (BaTiO<sub>3</sub>) ceramics has found its application in semiconductor industry. The reason for this is its dielectric and ferroelectric properties. Electrical properties, such as magnitude of relative dielectric permittivity and Curie temperature, of these barium titanate – based materials can be adjusted in two ways varying the sintering conditions and/or by doping with various cations. In this research we synthesized barium titanate-stannate (BTS; BaTi<sub>1-x</sub>Sn<sub>x</sub>O<sub>3</sub>) powders by solidstate reaction technique (with x=0, 0.05 and 0.1; denoted BT, BTS5 and BTS10, respectively) in order to examine the influence of the sintering atmosphere (air and argon) on the dielectric properties of BTS. The powders were uniaxially pressed (P = 240MPa) into cylindrical compacts (Ø 6 mm and h ≈ 2 mm) and sintered in SETSYS TMA (Setaram Instrumentation, Caluire, France) by heating rate of 10 °/min up to 1420 °C and with dwell time of 2 hours. In order to examine the influence of the sintering atmosphere two sets of experiments were performed: (1) in air, and (2) in Ar. The electrical measurements were made in cooling from 160 to 20 °C in air, at 1 kHz using a Wayne Kerr Universal Bridge B224. The microstructure and crystal structure of BTS ceramics were studied by SEM-EDS methods and by X-ray diffractometry and Raman spectroscopy at room temperature. On the basis of the obtained data it can be seen that due to the sintering of these materials in argon atmosphere leads to a significant increase in the value of the dielectric permittivity.



### Adsorption in conjunction with SAXS under the influence of a rotational field

**R.I. kosheleva<sup>1</sup>**, E.P. Favvas<sup>2</sup>, T.D Karapantsios<sup>3</sup>, A.Ch. Mitropoulos<sup>1</sup>. (1) Eastern Macedonia & Thrace Institute of Technology, St. Lucas, Kavala, Greece, rakosel87@hotmail.com, (2) National Centre for Scientific Research "Demokritos", St. Paraskevi, Athens, Greece, (3) Aristotle University of Thessaloniki, Dpt. of Chemistry, Univ. Box 116, 54124 Thessaloniki, Greece

The adsorption mechanism of gases and vapors on porous materials is paramount in many aspects such as gas separation process, hydrogen storage, catalysis etc. Although numerous studies have been done towards this direction, the present study is the first one that introduces rotational field as an additional parameter. Small Angle X-Ray Scattering (SAXS) measurements were conducted and analyzed for both static and rotating conditions. The rotation of the sample was achieved by a special rotating cell with a rotation frequency of 2150rpm.

To provide a comparison between the two conditions (static and rotation) for SAXS measurements, a contrast matching technique was applied. Vycor7930 was used as the adsorbent and CH<sub>2</sub>Br<sub>2</sub> as adsorbate having the same electron density with the solid [1, 2]. Pores are partially filled at relative pressure of 0,4. Results obtained from SAXS measurements are presented in Figure 1.

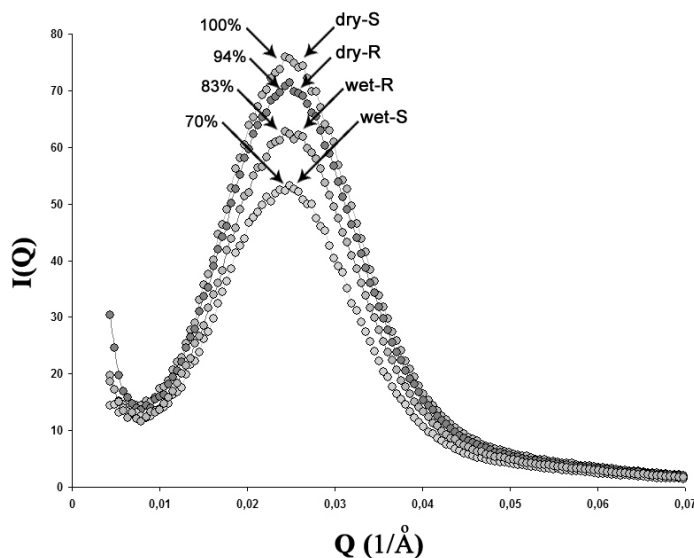


**Figure 1:** SAXS spectra on four sample cases: dry-S (static); dry-R (rotating); wet-S and wet-R. The available free space is also shown. Although dry-S is higher than dry-R, wet-S is lower than wet-R; indicating adsorbate contraction.

Vycor main peak is located as expected at  $Q=0.0248\text{\AA}^{-1}$  corresponding to a Bragg spacing of  $\sim 250\text{\AA}$ . Rotation increases the adsorption capacity of the porous matrix by  $\sim 13\%$ . Fractal analysis shows that fractal dimension of  $D_{\text{wet-S}}=2.25$  while  $D_{\text{wet-R}}=2.37$  corresponding to the value of dry-S. Although dry-R spectrum is somehow lower than dry-S;  $D_{\text{wet-S}} < D_{\text{dry-R}}=2.34$ ; i.e. the situation for wet samples is the opposite. The result confirms that rotation leads to adsorbate contraction; that is, more free space is gained. At the innermost part of the spectrum dry-R shows an increase in  $I(Q)$  while the main peak is about 6% lower. The innermost increase may be due to rotating blade effect, whereas the peak decrease may be due to rotation that blurs the scatterers. Further investigation is underway.

#### References

- [1] A. Ch. Mitropoulos, *Journal of Colloid and Interface Science*, 336 (2009) 679.  
[2] A. Ch. Mitropoulos *et al.*, *Sci.Rep.* 5, 1-12 (2015).



SMART &  
GREEN  
INTERFACES

*CONFERENCE  
PROGRAM AND  
BOOK OF ABSTRACTS*  
*4 - 6 May, 2016* *Athens, Greece*

